EVALUATION OF A NOVEL IMMUNOTHERAPEUTIC AS A TREATMENT OPTION FOR GULF WAR ILLNESS USING PRECLINICAL MODELS OF THE DISEASE

by

JESSICA MICHELLE CARPENTER

(Under the Direction of Nikolay M. Filipov)

ABSTRACT

Gulf War Illness (GWI), a chronic, multisymptomatic disease including neurological and immune system deficits, affects a third of the military personnel deployed during the 1990-1991 Gulf War. In-theater overexposures to neurotoxicants, such as pesticides, prophylactic pyridostigmine bromide (PB) pills, and in some veterans, chemical nerve agents are implicated in GWI pathogenesis. Unfortunately, GWI therapeutics are limited and manage individual or a few symptoms. As GWI veterans age, a rise in symptom severity and risk of age-related co-morbidities are of concern. Thus, understanding the progressive pathobiology of GWI and developing efficacious treatments is imperative. This dissertation sought to investigate GWI-specific progressive neurological and pathological effects within two, chemically distinct rodent models of the disease and evaluate the efficacy of the immunotherapeutic, Lacto-N-fucopentaose III (LNFPIII). The GWI models utilized herein included the 1) PB + the pyrethroid insecticide permethrin (10 days; PB/PM model), and 2) PB + the insect repellent DEET + stress (corticosterone) + the nerve agent surrogate diisopropylfluorophosphate (DFP) (15

days; PB/DEET/CORT/DFP model). Acutely, both models produced widespread brain monoaminergic disbalance and hippocampal neuroinflammation with these effects more pronounced in the PB/PM and PB/DEET/CORT/DFP model, respectively. LNFPIII co-administration restored this acute neurochemical dyshomeostasis and neuroinflammation. Long-term investigations with these models (6-10 months post GWI exposures) produced deficits in motor, mood, and cognitive functions, hippocampal neuroinflammation, and hippocampal synaptic plasticity. Delayed LNFPIII treatment (4-6 months post GWI exposure) ameliorated behavioral abnormalities (e.g., motor and cognitive function), alleviated hippocampal neuroinflammation, and enhanced hippocampal synaptic plasticity. Additionally, PB/PM exposure induced acute and lasting changes in the gut microbiota and inflammation; these effects were improved by LNFPIII. Further, structural brain alterations were characterized longitudinally (12 months) in both models. Both models led to enlarged ventricles and reductions in global brain and hippocampal volumes. However, model-specific alterations included reductions in cortical and brainstem volumes in the PB/PM and PB/DEET/CORT/DFP model, respectively. Collectively, these findings addressed substantial knowledge gaps in GWI preclinical research by characterizing the complex pathology and behavioral phenotypes produced by two, chemically distinct preclinical GWI models at varying stages of life and emphasized the potential for LNFPIII as a promising therapeutic for GWI pathology.

INDEX WORDS: Gulf War Illness, LNFPIII, Pesticides, Behavior, Neuroinflammation, Microbiome, Magnetic Resonance Imaging

EVALUATION OF A NOVEL IMMUNOTHERAPEUTIC AS A TREATMENT OPTION FOR GULF WAR ILLNESS USING PRECLINICAL MODELS OF THE DISEASE

by

JESSICA MICHELLE CARPENTER

B.A., The University of Mississippi, 2014

A Dissertation Submitted to the Graduate Faculty of The University of Georgia in Partial Fulfillment of the Requirements for the Degree

DOCTOR OF PHILOSOPHY

ATHENS, GEORGIA

2022

EVALUATION OF A NOVEL IMMUNOTHERAPEUTIC AS A TREATMENT OPTION FOR GULF WAR ILLNESS USING PRECLINICAL MODELS OF THE DISEASE

by

JESSICA MICHELLE CARPENTER

Major Professor:	Nikolay M. Filipov
Committee:	Donald A. Harn
	Jae-Kyung Lee
	John J. Wagner

Electronic Version Approved:

Ron Walcott
Vice Provost for Graduate Education and Dean of the Graduate School
The University of Georgia
May 2022

DEDICATION

I would like to dedicate this work to my family and friends who have provided their unwavering support as I pursued this dream. There are no words or actions big enough to thank you for the continuous love and encouragement over the past 6 years, but I am truly grateful for each of you that have been alongside me on this journey.

To Mom, Dad, and John -

None of this would have been possible without your constant reassurances that I am capable of achieving my dreams. Thank you for believing in me.

To Ollie and Otto-

Woof, woof!

ACKNOWLEDGEMENTS

First and foremost, I would like to express my sincere gratitude to my mentor and major advisor, Dr. Nikolay Filipov, for his incredible patience and unwavering support over the past few years. I am extremely grateful for the opportunity to be a part of your lab. Your dedication to mentorship and teaching has aided tremendously in my development as a scientist. Thank you for always encouraging me to aim higher.

I would also like to acknowledge to my graduate committee, Dr. Donald Harn, Dr. Jamise Lee, and Dr. John Wagner for their guidance, support, and recommendations throughout my graduate career. I extend a special thanks to those that have aided in the studies presented in this dissertation, in particular, Dr. Kyle Brown, Dr. Collin Preston, Dr. Ryan Mote, Danielle Ludwig, and Alexandria Goodyear. Min, Hannah, Rachael, Kelly, and Christian- I am not only deeply grateful for your friendship, but also your constructive and valuable insights into this work. In addition, I am thankful for the University of Georgia's Neuroscience and Athens community that have provided support and friendships to me throughout my time here.

Finally, thank you to my former mentor Dr. Kenneth Sufka, for motivating me to pursue this doctorate degree. I appreciate your unfaltering encouragement and continuous dedication to my scientific career.

TABLE OF CONTENTS

Page

LIST OF TABLES

Page

LIST OF FIGURES

Page

CHAPTER 1

INTRODUCTION AND LITERATURE REVIEW

1.1 The Persian Gulf War

The 1990-1991 Persian Gulf War (GW) began when growing disputes over oil pricing and production culminated with the Iraqi invasion and occupation of Kuwait on August 2, 1990. As a result, the United Nations sanctioned a quick response, and a military coalition comprised of 34 countries assembled (Operation Desert Shield) in the Persian Gulf in opposition to this invasion. This included military presence from the United States (approximately 700,000 personnel), Saudi Arabia, the United Kingdom, United Arab Emirates, Kuwait, Bahrain, Oman, Qatar, Pakistan, Canada, France, and Australia. Failure of diplomacy aimed at peaceful withdrawal of the Iraqi troops from Kuwait led to the initiation of a 6-week air campaign on Iraqi forces in January 1991 known as Operation Desert Storm. This air assault culminated into 4 days of ground combat before a ceasefire was declared on February 28, 1991. The majority of troops returned home by July 1991 (White et al., 2016).

Although the GW was a relatively short war, with few in-theater injuries and death, it has become to be known for the chronic adverse health effects that affect veterans from the war. Within a year of returning home, GW soldiers began experiencing and reporting unexplained, chronic health symptoms (White et al., 2016). These symptoms appeared to affect many, but not all GW veterans and collectively became known as Gulf War Illness

(GWI) after several epidemiological studies in the late 1990s (Doebbeling et al., 2000; Fukuda et al., 1998; Gray et al., 1999; Hyams and Roswell, 1998; Kroenke et al., 1998).

1.2 Gulf War Illness (GWI) Case Definitions

Thirty years have passed since the 1990-1991 Gulf War, but approximately 30% of the 700,000 United States military personnel that served during the GW continue to suffer from GWI. GWI is characterized by a myriad of diverse symptoms that cannot be accounted for by an existing medical diagnosis; these symptoms include fatigue, headache, cognition and memory problems, widespread pain, dermatological conditions, gastrointestinal issues, and respiratory dysfunction (White et al., 2016). Epidemiological studies indicate that GWI affects Army and Marine veterans at higher rates than those in the Navy or Air Force and enlisted personnel more than officers; furthermore, the prevalence of GWI is higher in veterans that served in forward areas during the GW (Binns et al., 2008).

Early GWI studies evaluated the multitude of symptoms experienced by GWI veterans primarily through self-reported questionnaires and surveys (for review, Barret et al., 2002; White et al., 2016). However, a need for GWI diagnostic criteria emerged because of the multifaceted and heterogenous symptomology experienced by veterans that significantly overlaps with other diseases. As a result, multiple case definitions for GWI were put forward based on the symptoms GW veterans self-reported. These included the early Haley syndrome criteria (Haley et al., 1997), followed by the Center for Disease Control (CDC; formerly Chronic Multisymptom Illness (CMI)) definition (Fukuda et al., 1998), and the Kansas case definition (Steele, 2000); the latter two were recommended for

clinical and research use, respectively, in 2014 (IOM, 2014; White et al., 2016), and are still in use, with some refinement, today (Cohen et al., 2021).

1.2.1 The Haley Syndromes Criteria

The Haley syndromes were formed by using factor analysis of standardized symptom questionnaires from GW veterans; as a result, 3 syndromes emerged. These included 1) impaired cognition (i.e., problems in attention, memory, reasoning, insomnia, depression, daytime sleepiness, and headaches); 2) confusion-ataxia (i.e., problems in thinking, disorientation, balance, vertigo, and impotence); and 3) arthromyoneuropathy (i.e., characterized by joint and muscle pain, muscle fatigue, difficulty lifting, and extremity paresthesia) (Haley et al., 1997; IOM, 2014). These criteria allow for specific, but very narrow, characterization of GWI.. Consequently, this definition limits and underestimates the occurrence of GWI in veterans (IOM, 2014; White et al., 2016), which is why the other two definitions are now favored and accepted.

1.2.2 The Center for Disease Control (CDC) case definition

To meet the criteria for the CDC definition, GW veterans must experience at least one symptom in two or more of the following three categories for more than 6 months: 1) fatigue, 2) cognitive and mood dysfunction (i.e., feeling depressed, anxious or moody, difficultly concentrating and remembering, trouble finding words, difficulty sleeping), and 3) musculoskeletal pain (i.e., joint pain, stiffness, or muscle pain) (Fukuda et al., 1998). The CDC definition is recommended for clinical use, but for research purposes, is considered overly inclusive with some bias towards increased GWI prevalence (IOM, 2014; Ribeiro and Deshpande, 2021).

1.2.3 The Kansas case definition

The Kansas case criteria state that GWI veterans must have multiple and/or moderate to severe chronic symptoms in at least three of the six following domains: 1) fatigue/sleep problems (i.e., feeling unwell after exercise, not rested after sleep, or difficulty falling/staying asleep), 2) neurologic/cognitive/mood symptoms (i.e., difficulty remembering information, feeling irritable, depression, olfactory sensitivity, blurred vision, light sensitivity, headaches, feeling faint, or numbness/tingling in extremities), 3) somatic pain (i.e., joint, muscle), 4) gastrointestinal symptoms (i.e., diarrhea, nausea, or abdominal pain/cramping), 5) respiratory symptoms (i.e., difficulty breathing, frequent cough, or wheezing), and 6) skin abnormalities (i.e., rash) (Gifford et al., 2021; Steele, 2000). Per this case definition, symptoms must have appeared and persisted for at least 6 months after the GW and excludes veterans who were prior diagnosed with medical or psychiatric conditions (i.e., cancer, heart disease, multiple sclerosis, stroke, traumatic brain injury, bipolar disorder, etc.) (Gifford et al., 2021; Steele, 2000). The Kansas definition is recommended for clinical research and has a consistent prevalence rate; however, it excludes GW veterans with multiple co-morbidities from being diagnosed with GWI (Gifford et al., 2021; IOM, 2014; Steele, 2000).

1.2.4 GWI Common Data Elements (CDEs)

Recently, a collaboration of GWI veterans, advocates, clinicians, scientists, and investigators worked to develop Common Data Elements (CDEs) to standardize data collected across GWI research (Cohen et al., 2021). This working group was divided into two subgroups (symptoms and systems assessment) to review tools within specific domains and the applicability of the instruments/forms for GWI research. For example, the

symptoms working group evaluated CDEs in domains including: 1) baseline/covariate information; 2) fatigue; 3) post-exertional malaise; 4) pain; 5) sleep; and 6) quality of life/functional status/activity/exercise challenge studies. The systems assessment working group reviewed the following domains: 1) neurologic/neuropsychological/neuro imaging; 2) autonomic; 3) endocrine/neuroendocrine; 4) immune; and 5) biomarkers. Both groups evaluated deployment exposures and GWI risk factors; this culminated into 12 total CDE domains (Cohen 2021).

Next, the group classified assessment tools for GWI and determined CDE standards classifications; these CDE tools were classified as core, supplemental-highly recommended, supplemental, or exploratory. For example, the group recommended the CDC (Fukuda et al., 1998) and the Kansas (Steele, 2000) GWI case definitions and the Veterans RAND Short Form 36 item Health Survey (VR-36) as core data elements in all GWI studies. Further, for each of the 12 CDE domains, a number of recommended tools for future studies that were based on these classifications was provided (Cohen et al., 2021). The CDEs provide a way for GWI research to be systemically collected, analyzed, and shared, which will improve GWI investigations for a clearer understanding of this disease pathology.

1.3 Clinical Presentation of GWI Symptoms and Pathologies

Multiple clinical studies have conducted neuropsychological evaluations in veterans with GWI and consistently report higher levels of deficits within this group. The clinical neuropsychological testing battery used in these studies include motor, attention, and executive function tasks. GWI veterans performed worse in tasks of motor skills including lower reaction speed and grip strength across several studies with different

cohorts (Anger et al., 1999; Axelrod and Milner, 1997; Hom et al., 1997; Proctor et al., 2006; Toomey et al., 2009). Cognitive performance was also impaired, i.e., GWI veterans exhibited lower abilities in abstract reasoning, problem solving, attention, and learning/memory compared to controls (Goldstein et al., 1996; Hom et al., 1997; Janulewicz et al., 2017; Toomey et al., 2009). GWI veterans also report higher rates of mood dysfunction (e.g., anxiety and depression) (Binder et al., 1999; Hom et al., 1997; Lindem et al., 2003; Sillanpaa et al., 1997). Studies determined that these mood deficits could impact the reporting of other symptoms (i.e., cognitive and memory complaints), as well as the results of tests in neuropsychological domains such as sustained attention, motor coordination, and executive functioning (Binder et al., 1999; Lindem et al., 2003; Sillanpaa et al., 1997).

Numerous clinical imaging investigations have revealed alterations in GWI veteran brain structure and function compared to veteran controls. Structural MRI studies consistently report reduced white and gray matter volume in multiple cortical and subcortical areas (hippocampus, hypothalamus, brainstem, cerebellum) in GWI veterans (Chao, 2020; Chao et al., 2011; Chao et al., 2015; Christova et al., 2017; James et al., 2017; Rayhan et al., 2013; Van Riper et al., 2017; Zhang et al., 2020; Zhang et al., 2021). Functional MRI (fMRI) studies have detected significant signal changes (activity) in regions governing cognitive, memory, motor and mood function such as the prefrontal, somatosensory, and motor cortices (Gopinath et al., 2012; Wylie et al., 2019), as well as the thalamus, caudate, and hippocampus (Calley et al., 2010; Cooper et al., 2016; Li et al., 2011). Additionally, an early study detected neuronal loss in the basal ganglia with corresponding dopamine dysfunction (Haley et al., 2000). The aberrations observed in

these areas are consistent with reported symptomology by veterans and correlate strongly with performance deficits in working memory, attention, and motor tasks as well as with mood impairments, pain, and sleep quality (Calley et al., 2010; Chao, 2020; Clarke et al., 2019; Hubbard et al., 2014; Washington et al., 2020; Zhang et al., 2021).

Chronic pain is another consistently reported symptom in clinical questionnaires by veterans with GWI (Cook et al., 2010; Gopinath et al., 2012; Kearney et al., 2016; Rayhan et al., 2013; Stimpson et al., 2006; Thomas et al., 2006; Van Riper et al., 2017). This pain presents in two forms, predominantly as somatic (in tissues, such as skin, muscles, and joints), but also visceral (Van Riper et al., 2017; Zhou et al., 2018). Apart from self-reports, few clinical studies have investigated chronic pain in a GWI context (Cook et al., 2010; Zhou et al., 2018). Interestingly, it has been shown that physical exertion promotes hyperalgesic pain responses in GWI veterans with somatic pain (Cook et al., 2010), suggesting that silent symptomology might be uncovered by certain stimuli. A recent study also found that GWI veterans with chronic musculoskeletal pain, require a greater amount of neural resources for cognitive performance under experimental pain stimulus (Lindheimer et al., 2021).

Accumulating evidence also points to immune system dysregulation, in particular, inflammation as a key GWI pathological signature (Alshelh et al., 2020; Broderick et al., 2013; Broderick et al., 2011; Khaiboullina et al., 2015; Parkitny, L. et al., 2015). Clinically, GWI veterans present with higher blood levels of the acute phase protein C-reactive protein (CRP) and increased lymphocytes, monocytes, neutrophiles and platelet counts compared to controls (Johnson et al., 2016). Peripheral increases in circulating inflammatory cytokines are also apparent in GWI veterans (Broderick et al., 2013; Broderick et al., 2018;

Broderick et al., 2011; Khaiboullina et al., 2015; Parkitny et al., 2015). Such include higher serum levels of IL-7, IL-4, TNF-α, IL-13, and IL-17F (Khaiboullina et al., 2015). Interestingly, physical exertion applied to veterans with GWI increased inflammatory NF-kB pathway activity and cytokine levels (IL-6, IL-5, and TNF-α) (Broderick et al., 2013; Broderick et al., 2018), while it decreased the anti-inflammatory cytokine IL-10 (Broderick et al., 2013). Further, daily immune profiling (25 days) found that in GWI veterans, higher daily fatigue scores were associated with increases in proinflammatory IL-1β and IL-15 (Parkitny et al., 2015).

Due to the innate difficulties in assessing the neuroimmune state in the brain of living GWI veterans, the majority of these data relied on peripheral measures of inflammation; however, recent clinical studies have begun to overcome these difficulties using sophisticated methods (Alshelh et al., 2020; Cheng et al., 2020). For example, increases in *in vivo* imaging of TSPO, a protein upregulated in activated microglia and astrocytes and an index of neuroinflammation, were observed in several brain cortical regions of GWI veterans, including the precuneus, prefrontal, primary motor, and somatosensory areas (Alshelh et al., 2020). Additionally, a MRI study evaluated microstructural brain changes using neurite density imaging (NDI) and found that the NDI correlated with peripheral upregulation of TNF receptor I and II in the blood of GWI veterans (Cheng et al., 2020). The latter suggests that the data on immune dysregulation in the periphery can be used as a proxy for the brain to some extent.

Veterans with GWI also experience many GI symptoms, such as nausea, diarrhea, and abdominal pain/cramps (Dunphy et al., 2003; Koch and Emory, 2005; Zhou et al., 2018). Recent evidence suggests that the enteric microbiome may play a significant role in

GWI symptomology, but clinical studies remain limited. One study found that enteric dysbiosis occurs within GWI, as several beneficial bacterial families *(Lachnospiraceae, Bifidobacterium, and Roseburia)* were significantly decreased in GWI veterans (Janulewicz et al., 2019). This has led to multiple preclinical investigations of the gut microbiome in GWI models discussed later (Kimono et al., 2020; Seth et al., 2018).

1.4 Etiological Factors of GWI

Several etiological factors have been investigated with some of them implicated in the GWI pathogenesis. Precise etiology of GWI is still unknown but is largely attributed to war-time chemical overexposures (White et al., 2016). Deployment related overexposures include insecticides and pesticides, a nerve agent prophylactic, and chemical warfare agents in addition to war-related psychological and environmental stressors. Further, combinations of these overexposures are thought to culminate in the symptom presentation of GWI. In fact, multiple GWI clinical studies have found relationships between GW deployment-related exposures and reported symptomology (Janulewicz et al., 2017; Proctor et al., 2006; Proctor et al., 1998; Toomey et al., 2009; Zundel et al., 2019).

Pesticide exposures were widespread among troops during the GW; it is estimated that soldiers were exposed to over 35 different types of insecticides and pesticides (Binns et al., 2008). These include insect repellents, organochlorine, pyrethroid, organophosphate, and carbamate pesticides (Binns et al., 2008). While guidelines for use of these compounds in military settings were in place, there were many reports of misuse among troops (Binns et al., 2008; National Academies of Sciences and Medicine, 2016) which further increased overexposure potential.

The insect repellent, *N,N*-Diethyl-*m*-toluamide (DEET), is an aromatic amide that repels a wide range of insects (Binns et al., 2008). During the GW, three different DEET products of various concentrations were supplied in cream (33%), liquid (33%) and stick (75%) formulations that could be applied to the skin (Binns et al., 2008). Lindane powder, an organochlorine compound, was primarily used as a delousing agent for processing Iraqi prisoners of war with minimal use by the soldiers (Binns et al., 2008). Permethrin (PM) is a synthetic pyrethroid that acts as a repellent and insecticide against pests such as mosquitos, biting flies, ticks and mites (Fricker et al., 2000). It was supplied to troops as a 0.5% spray to apply to uniforms and bed netting. The proposed application was once every 6 weeks as it has been shown to retain its potency for an extended period after application, but suspected usage is much higher (Fricker et al., 2000). Carbamate pesticides used during the GW include bendiocarb and propoxur, which were sprayed on surfaces to kill pests (Binns et al., 2008). Several different organophosphate pesticides were used during the GW and included chlorpyrifos, diazinon, and malathion at different concentrations as fumigating agents in the living quarters (Binns et al., 2008). Other organophosphates included dichlorvos pest strips that were supplied for personal use to the military population (Binns et al., 2008).

These compounds have different mechanisms of action and effect multiple signaling systems. In particular, pyrethroids, such as permethrin, alter the kinetics of the voltage-sensitive sodium channels, leading to a transient increase in sodium permeability and resulting hyperexcitability (Soderlund et al., 2002). Organophosphates bind to and inhibit the normal action of acetylcholinesterase (AChE). Inhibition of AChE leads to an excessive accumulation of acetylcholine (ACh) in synapses of nerve and/or muscle cells

followed by increased binding of ACh on receiving cells. Depending on the organophosphate type, dose, duration, and exposure frequency, toxicity symptoms can range from mild to severe muscle contractions, impaired cognition, dizziness, shortness of breath, and vomiting; severe toxicity results in respiratory failure and death (Cecchine et al., 2000). Insect repellents, DEET in particular, have been shown to have weak AChE activity and can block sodium and potassium channels; these processes can lead to, respectively, neurotoxicity and numbing sensations in humans (Swale et al., 2014). DEET is able to remain in deeper skin layers for an extended amount of time, and it also enhances the dermal absorption of other compounds (Binns et al., 2008).

Additionally, chemical warfare attacks (i.e., exposure to nerve agents, such as sarin) were a concern for military forces during the GW (White et al., 2016). Nerve agents, such as sarin or cyclosarin, are irreversible AChE inhibitors that lead to buildup of ACh. Therefore, use of the reversible AChE inhibitor pyridostigmine bromide (PB) as prophylactic to the possible exposure to nerve agents was recommended and PB tablets distributed. By temporarily binding to AChE, PB protected soldiers from potential subsequent exposure to irreversible AChE nerve agents. It is estimated that approximately 250,000 personnel consumed at least some PB during the GW (Golomb, 2008). PB was supplied in a 21-tablet blister pack and was recommended to be taken at the regimen of one 30 mg PB tablet every 8 hours (Binns et al., 2008). However, because of the self-administration of PB, it is suspected that consumption exceeded the daily recommendation. Thus, the veteran's exposure levels to PB are unknown, with few documented health records, but there is a strong correlation between PB intake and GWI symptoms (Binns et al., 2008).

A small subset of deployed soldiers was accidentally exposed to sarin and cyclosarin during the destruction of an Iraqi munitions storage site in Khamisiyah, Iraq following the GW cease fire. Modelling of the sarin plume suggested that over 100,000 soldiers could have been exposed to potentially toxic levels of nerve agents over the course of four days in March of 1991. There are no accurate estimates for the levels of sarin/cyclosarin exposure, but it is assumed that no troops were in the vicinity of where the exposures would have been most pronounced and potentially lethal (Fricker et al., 2000). Instead, most exposed soldiers were estimated to be in the low-level hazard zone, away from the munition site demolition. Regardless, exposure to low-levels of sarin produces symptoms that are consistent with symptoms experienced by GWI veterans. Excessive exposure to any of these compounds (pesticides, nerve agents, PB) leads to some level of neurotoxicity and could underlie the chronic health effects present in GWI veterans. Multiple investigations have identified overlap of these exposures in GWI veterans, but the precise levels in which GWI veterans were exposed to these chemical mixtures in theater remain unknown (Fricker et al., 2000; White et al., 2016).

Other contributing factors considered in the etiology of GWI include psychological stress, Kuwaiti oil well fires, vaccines, and depleted uranium (Binns et al., 2008). Initially, psychological stress, particularly post-traumatic stress disorder (PTSD), was debated as a significant causative factor of GWI (Binns et al., 2008). However, studies indicate that approximately 35% of GWI veterans suffer from PTSD (Ford et al., 2001; Jeffrey et al., 2021; Weiner et al., 2011), and this comorbidity exacerbates, but does not explain, GWI clinical symptoms (Carrera et al., 2021). Conclusions on the long term effects of the Kuwaiti oil well fires were mixed initially and are still debatable, albeit recent studies

suggest that exposed personnel were at higher risk for GWI and brain cancer (Barth et al., 2009; Steele et al., 2012). Studies linking vaccines to GWI symptom development are limited, but evidence from the majority of studies suggests that there are no associations between GWI and the vaccines received prior to and during the GW (Binns et al., 2008; Steele et al., 2012; White et al., 2016). Depleted uranium (DU) was used during the GW in dense armor-piercing weapons as well as in tank armor. Upon hard impact, DU combusts and oxidizes, allowing for ingestion or retention of DU particles or shrapnel, respectively (Binns et al., 2008). Studies investigating the role of DU in GWI pathogenesis were also debated for years, but recent evidence suggests that even the highest exposure levels of DU do not contribute to GWI (Parrish and Haley, 2021).

Overall, a consensus for the etiological factors influencing GWI symptomology is attributed to chemical overexposures (i.e., pesticides, PB, and nerve agents) during the war (White et al., 2016). Studies have demonstrated the correlation between GW deployment related exposures as well as combinational exposures (e.g., pesticides and PB) and reported symptomology (Boyd et al., 2003; Fricker et al., 2000; Janulewicz et al., 2017; Proctor et al., 2006; Proctor et al., 1998; Steele et al., 2012; Toomey et al., 2009; Zundel et al., 2019). Other possible etiological factors, such as the Kuwaiti oil fires, DU, and vaccines are not viewed as substantially contributing to the development GWI. Although these all might have increased some symptoms, such as respiratory symptoms in some troops with close proximity to the Kuwaiti oil fires, they have not demonstrated the persisting and multi-symptom effects like chemical overexposures.

1.5 GWI Preclinical Investigations

Current GWI preclinical research focuses on utilizing various paradigms of GW relevant chemical overexposures to elucidate the mechanisms underlying GWI. This line of research follows the assumption, supported by etiological/epidemiological data reviewed earlier, that the main GWI etiological factors involve varying, overlapping chemical overexposures and, in some instances, stress. Researchers have used GWI animal models (both mouse and rat) incorporating multiple pesticides, chemical warfare agents (surrogates), prophylactics, and stress in various combinations and through multiple exposure routes (i.e., dermal, oral, intraperitoneal) to mimic in theater exposures and recapitulate GWI symptomology (for review, (Dickey et al., 2021; Ribeiro and Deshpande, 2021; White et al., 2016). This has provided translational value as GWI pathophysiology has been recapitulated in several of these animal models as evidenced by aberrations in behavioral performance (i.e., cognitive, motor, mood dysfunction, and pain) and numerous biological parameters (i.e., gut dysbiosis, elevated oxidative stress, glial activation, neurochemical alterations, chronic neuroinflammation, and leaky blood-brain barrier) (for review, (Dickey et al., 2021; Ribeiro and Deshpande, 2021; White et al., 2016). Further, preclinical models have been used to evaluate potential treatment interventions for GWI.

1.5.1 Animal Models

Established rodent models of GWI have clinical translational potential and follow various combinations of GW chemical agent exposures (i.e., carbamate, pesticides, and nerve agents) with and without stress. One of the first models for exploring GWI neurotoxicant exposures involved investigating the effects of DEET, PM, and PB, alone and in combination over the course of 45 days in rats (Abou-Donia et al., 2004; Abou-

Donia et al., 2001). A similar model evaluated the effects of PM and DEET alone and in combination for 60 days in rats (Abdel-Rahman et al., 2001). This model was expanded to incorporate PB, PM, DEET and daily restraint stress in rats and has been used in multiple settings (Abdel-Rahman et al., 2004; Abdel-Rahman et al., 2002; Hattiangady et al., 2014; Madhu et al., 2019; Megahed et al., 2014; Parihar et al., 2013; Shetty et al., 2017); additionally this model has been used in mice (Abdullah et al., 2012). Further, models have incorporated additional exposures, particularly organophosphates such as the pesticide chlorpyrifos (CPF). Such models include exposures to PB, PM, and CPF (Nutter and Cooper, 2014; Nutter et al., 2013; Nutter et al., 2015), plus the addition of DEET (Cooper et al., 2018; Flunker et al., 2017).

Recent preclinical research has incorporated the use of nerve agent surrogates such as DFP, an organophosphate with similar chemical structure to sarin, to account for the subset of soldiers that were accidentally exposed to nerve agents during the GW. There are various models that use DFP as a sarin surrogate. One DFP based model utilizes a low dose exposure to DFP over the course of 5 days (Phillips and Deshpande, 2016, 2018; Ribeiro et al., 2020). Similar models use even lower doses but extend the exposure period (Naughton et al., 2018). Another model that mimics GWI symptomology is the PB/DEET/CORT/DFP model (O'Callaghan et al., 2015); interestingly, this initial study found that CORT/DFP exposure alone was sufficient to elicit a GWI neuroinflammatory phenotype, thus current studies focus on this exposure paradigm (Ashbrook et al., 2018; Gao et al., 2020; Jones et al., 2020; Koo et al., 2018; Locker et al., 2017). A detailed discussion of the two GWI animal models (O'Callaghan et al., 2015; Zakirova et al., 2015) utilized in this dissertation is provided next.

1.5.2 Pyridostigmine Bromide and Permethrin (PB/PM) Mouse Model

One established GWI model involves short-term (10 days) exposure to the nerve agent prophylactic, PB, and the insecticide, PM, in mice. As discussed previously, actual veteran exposure rates to PB and PM remain unknown; however, given the short duration of ground conflict, this model mimics GW chemical exposures that have been associated with increased GWI prevalence (Ribeiro and Deshpande, 2021; Steele et al., 2012). The PB/PM model has been well characterized from acute to chronic timepoints post GW chemical exposure. Further, it has been used to evaluate various potential treatments for GWI. In separate studies, no significant behavioral phenotypes or neuroinflammation were present at 8-18 days post-exposure (Abdullah et al., 2011; Zakirova et al., 2015). However, anxiety-like behavior appeared at 30 days post-exposure (Abdullah et al., 2011), and aberrations in cognition, memory, lipid metabolism, and glial activation were present at 5 months post-PB/PM, a translationally-relevant time point (Abdullah et al., 2011; Zakirova et al., 2015). At 10-15 months post GWI exposures, cognitive dysfunction, depressive-like behaviors, and neuroinflammation were apparent (Abdullah et al., 2016; Joshi et al., 2018; Zakirova et al., 2016), and persisted to 22.5 months post-PB/PM exposure (Zakirova et al., 2016). Not only has this model elucidated highly translational GWI-relevant longitudinal changes across the mouse lifespan but has also identified therapeutic targets for the biological mechanisms for GWI pathobiology. Studies investigating proteomic, lipidomic and metabolomic changes in the brain revealed alterations in lipid metabolism, cellular bioenergetics, peroxisomes, lysosomes, and mitochondria (Abdullah et al., 2011; Abdullah et al., 2012; Abdullah et al., 2016; Abdullah et al., 2013). An additional study determined that a PM metabolite, 3-phenoxybenzoic acid (3-PBA), stimulates the adaptive immune

response in the brain and periphery, leading to increases in blood-brain-barrier disruption, neuroinflammation, and monocyte infiltration into the brain (Joshi et al., 2019). Further, PB/PM exposure elicited long-term effects on gut health and microbiota. Specifically, PB/PM treatment produced, leaky gut, and TLR-4 activation as well as increases in the abundances of bacteria belonging to *Lachnospiraceae* and *Ruminococcaceae* families and the genus *Allobaculum* (Alhasson et al., 2017).

1.5.3 Pyridostigmine Bromide, DEET, Corticosterone and Diisopropylfluorophosphate (PB/DEET/CORT/DFP) Mouse Model

Another established and well characterized GWI model utilizes exposure to GW agents such as PB, the insect repellent DEET, corticosterone (CORT) to emulate war-related stress and diisopropylfluorophosphate (DFP), an organophosphate with similar structure to the nerve agent sarin (O'Callaghan et al., 2015). The treatment paradigm follows a 14 day exposure to PB/DEET followed by CORT administration via drinking water during days 7-14, and a single exposure to DFP on day 15 (O'Callaghan et al., 2015). Acutely, at 6 h post-PB/DEET/CORT/DFP, widespread neuroinflammation was apparent in multiple brain areas including the prefrontal cortex, hippocampus, and striatum as increases in mRNA levels of inflammatory TNF-α and IL-1β. At this early timepoint, no evidence of neurodegeneration was apparent (O'Callaghan et al., 2015).

1.5.4 Behavioral deficits reminiscent of GWI in preclinical models

Behavioral alterations in preclinical models mirror the GWI veteran symptomology, and present as mood alterations, learning/memory impairments, and motor deficits. While these models produce similar GWI effects, it is important to note that the

chemical exposure type, dose, and time post exposure all play a role in symptom presentation and severity.

Mood alterations in GWI models present primarily as increases in anxiety and depression, an effect that corresponds to the GWI veteran population symptomology (Janulewicz et al., 2017). Anxiety-like behaviors were present in multiple models of varying chemical treatments (Carreras et al., 2018; Phillips and Deshpande, 2016; Zhu et al., 2020), particularly those that also included a stress component (Abdullah et al., 2012; Parihar et al., 2013). GWI chemical exposures have also led to increases in depressive-like behaviors (Hattiangady et al., 2014; Phillips and Deshpande, 2016, 2018; Ribeiro et al., 2020; Zhu et al., 2020).

Cognitive and memory problems remain a complaint in GWI veterans, and several GWI animal models recapitulate such effects in tests of learning and memory (Janulewicz et al., 2017). In multiple GWI models, rodents exposed to GWI chemicals have short- and long-term memory impairments (Hattiangady et al., 2014; Madhu et al., 2019; Parihar et al., 2013; Phillips and Deshpande, 2016). Motor deficits have also been observed in preclinical GWI models. These present as sensorimotor deficits (Abdullah et al., 2012), as well as alterations in locomotor function (Hoy et al., 2000a; Hoy et al., 2000b) that, in some models, may be pain-related (Cooper et al., 2018; Flunker et al., 2017). Regarding pain, a primary complaint among GWI veterans, research is limited, but preclinical studies indicate that physical exertion increases pain response to innocuous stimulation (Nizamutdinov et al., 2018). Moreover, biological studies have shown that GWI chemicals exposure led to alterations in nociceptor K_v and Na_v channels in the dorsal root ganglia and muscle leading to maladaptive excitatory transmission. Further, it increased resting times

and decreased locomotion behaviorally, suggesting an increased pain state (Cooper et al., 2018; Flunker et al., 2017; Nutter and Cooper, 2014; Nutter et al., 2015).

Neurochemical disbalance may also play a pathogenic role in GWI, as neurochemicals, such as monoamines, regulate behavior (Belujon and Grace, 2017; Ferrari and Tarelli, 2011; Korte-Bouws et al., 2018; Willard et al., 2015). Studies investigating neurochemical changes have largely focused on AChE inhibition and cholinergic activation due to the mechanism of action of GWI chemicals such as PB, sarin, or its surrogate, DFP (Abdel-Rahman et al., 2002; Miller et al., 2018; Ojo et al., 2014; Zakirova et al., 2015). Additionally, studies have also shown decreases in inhibitory GABAergic activity in areas maintaining cognition (Carreras et al., 2018; Megahed et al., 2014).

1.5.5 Neuroimmune and Gastrointestinal dysfunction in GWI models

Of note, in recent years, GWI animal models have provided evidence of (neuro)immune dysfunction that may exacerbate many of the symptoms GWI veterans face. Data show that post exposure to various GW chemical combinations, increases in neuroinflammation and gliosis are present throughout the brain (Carreras et al., 2018; Michalovicz et al., 2020; Michalovicz et al., 2019; Miller et al., 2018; O'Callaghan et al., 2015; Parihar et al., 2013; Zakirova et al., 2016; Zakirova et al., 2017; Zakirova et al., 2015). GWI models consistently show robust glial activation in the brain, particularly the hippocampus and cortex, of both microglia, the brain's resident immune cell, and astrocytes (Abdel-Rahman et al., 2002; Abdullah et al., 2012; Carreras et al., 2018; Madhu et al., 2019). Interestingly, one MRI study found that there were morphological and connectively changes in glia that corresponded to elevations in inflammatory cytokines post GWI exposure (Koo et al., 2018). These increases in brain and spinal cord

inflammatory markers include TNF-α, IL-6, IL-1β, and HMGB1 and have been consistent across GWI models (Carreras et al., 2018; Lacagnina et al., 2021; Madhu et al., 2019; Michalovicz et al., 2019; O'Callaghan et al., 2015; Parihar et al., 2013). Further, it has been shown in multiple studies that GWI chemicals reduce hippocampal neurogenesis and neuronal integrity (Abdel-Rahman et al., 2001, 2002; Megahed et al., 2014; Ojo et al., 2014; Parihar et al., 2013; Phillips and Deshpande, 2016) and increase oxidative stress in the brain (Shetty et al., 2017).

Recent studies of various of GW chemical combinations have highlighted the role of the gut-brain-immune axis in GWI. As discussed earlier, exposure to PB/PM led to increases in gut permeability, TLR-4 activation, and the abundances of the *Firmicutes* and *Tenericutes* phylums and the genus *Allobaculum* (Alhasson et al., 2017). An additional study with these chemicals found that long-term effects included altered abundance of gut commensal bacteria like *Akkermansia* in addition to neuroinflammation and loss of neuronal plasticity (Kimono et al., 2020). Further, a separate GWI mouse model found that butyrate priming resulted in a slight increase in the abundance of beneficial bacteria with the genera *Bifidobacterium*, *Lactobacillus*, and *Roseburia*, as well as in recovery from leaky gut syndrome and other metabolic indicators (Seth et al., 2018).

1.6 State of Treatment Modalities for GWI

1.6.1 Clinical Therapeutic Interventions

Curative treatment modalities do not exist for GWI veterans, in part due to the heterogeneous presentation of disease symptomology (DDGWIRP, 2018). Thus, to date, only symptomatic treatments are available. Numerous clinical therapeutic interventions have been explored including cognitive behavioral therapy (Chao et al., 2021; Donta et al.,

2003; Mathersul et al., 2020), mindfulness-based stress reduction (Kearney et al., 2016), dietary changes (Holton et al., 2020; Holton et al., 2021), and various pharmacological treatments and supplements (Baraniuk et al., 2013; Donovan et al., 2021; Donta et al., 2004; Golier et al., 2016; Golomb et al., 2014; Helmer et al., 2020; Holodniy and Kaiser, 2019). GWI veterans undergoing cognitive behavioral therapy (CBT) have shown improvements in overall GWI symptom severity, as well as individual measures of cognition, mood, fatigue, pain, and sleep quality (Chao et al., 2021; Donta et al., 2003; Kearney et al., 2016; Mathersul et al., 2020). Further beneficial effects were seen when CBT was used in conjunction with other treatment modalities, such as exercise (Donta et al., 2003) and mindfulness based stress reduction (Kearney et al., 2016). The low glutamate diet eliminates dietary amino acids that can contribute to long-term excitotoxicity, while also increasing micronutrients and antioxidants that counteract oxidative stress and excitotoxicity (Holton et al., 2020; Holton et al., 2021). In a clinical trial, this dietary change led to a reduction of GWI symptoms, particularly pain and fatigue (Holton et al., 2020). A follow-up study concluded that this diet reduced inflammatory cytokines such as TNF-α, IL-1β, and IL-6 in GWI veterans (Holton et al., 2021). Pharmacological interventions have proved useful for management of some symptoms as well. For example, carnosine treatment improved diarrhea as well as cognitive symptoms in GWI veterans (Baraniuk et al., 2013) and coenzyme Q10 treatment improved physical function and GWI symptom complaints (Golomb et al., 2014). Recently, botanical treatments including curcumin, maritime pine, stinging nettle, and resveratrol have also been shown to improve some GWI symptoms (Donovan et al., 2021; Hodgin et al., 2021; Younger et al., 2021).

1.6.2 Preclinical Therapeutic Interventions

Although these therapies have provided some symptoms benefits, they have limited efficacy in resolving the underlying causes of GWI (Dickey et al., 2021). Thus, one aim of preclinical GWI research is focused on major, disease-modifying therapeutic targets. Considering immune dysfunction in GWI, recent preclinical studies have explored the efficacy of several treatment compounds that have shown promising results. For example, curcumin, found in turmeric, has antioxidant, anti-inflammatory, neurogenic and mood enhancing properties; when administered to rats post-exposure to GWI chemicals, improvements in cognition and mood were present, in conjunction with increases in neurogenesis and reductions in glial activation markers in the hippocampus (Kodali et al., 2018). Oleoylethanolamide (OEA) treatment, a naturally occurring lipid that has antioxidant/anti-inflammatory effects in the brain, improved behavioral measures of memory and mood, reduced neuroinflammation, and diminished levels of very-long-chain fatty acids in a GWI model (Joshi et al., 2018). Additionally, monosodium luminol, a treatment for oxidative stress, has shown promising effects by reducing inflammation, improving cognitive and mood function, and modulating glial activation (Shetty et al., 2020). Other pharmacological treatments for GWI have been explored including the antidepressant ketamine and has demonstrated significant improvement in mood measures such as anxiety and depression (Ribeiro et al., 2020; Zhu et al., 2020).

1.6.3 Lacto-N-fucopentaose III

In addition to anti-inflammatory treatments, broader immunomodulatory therapies may also be an advantageous treatment option for GWI. Lacto-N-fucopentaose III (LNFPIII) is a Lewis(X)-containing immunomodulatory glycan found in human breast

milk and on parasitic helminths that, to date, has had no documented adverse effects (Atochina et al., 2008; Bhargava et al., 2012; Srivastava et al., 2014; Tundup et al., 2015; Zhu et al., 2012). When conjugated to a dextran carrier, LNFPIII activates CD14/TLR-4 signaling for extracellular signal-regulated kinase (ERK)-dependent production of anti-inflammatory mediators to skew the inflammatory balance of the innate immune system in an anti-inflammatory direction (Atochina et al., 2008; Bhargava et al., 2012; Srivastava et al., 2014; Tundup et al., 2015; Zhu et al., 2012). One study utilizing LNFPIII in experimental autoimmune encephalomyelitis (EAE), an animal model of Multiple Sclerosis, found that this treatment significantly reduced the severity of EAE. Specifically, LNFPIII treatment decreased neuroinflammation, alternatively activated macrophages and monocytes, and skewed the peripheral immune response toward a Th2 dominant profile (Zhu et al., 2012). Further, LNFPIII has been shown to increase the production of the anti-inflammatory cytokine, IL-10, and decrease inflammation in a study of diet-induced obesity (Bhargava et al., 2012). These data highlight the value of evaluating LNFPIII in GWI models, as GWI has been demonstrated to have an underlying immune component in its etiology.

1.7 Direction of Dissertation

The effects observed within the PB/PM and PB/DEET/CORT/DFP GW exposure paradigms (O'Callaghan et al., 2015; Zakirova et al., 2015) align with ongoing GWI symptomology and provide a platform for future translational studies investigating treatments. However, while the PB/PM model has been well characterized in certain biological and behavioral measures across the murine lifespan, the PB/DEET/CORT/DFP has not been extensively evaluated past an acute timepoint. This leaves a substantial

knowledge gap for this highly relevant treatment exposure paradigm and warrants investigation, both acutely and chronically. Moreover, both models lack relevant information regarding the biological (i.e., alterations in neurochemistry, neuro-inflammation, brain structure, and gut microbiome) and behavioral consequences of these GW treatment exposures both acutely and longitudinally. Additionally, therapeutic evaluations in these models are sparse or none. However, LNFPIII has been shown to have many beneficial effects in other treatment scenarios, especially in reducing inflammation in a mouse encephalitis model. Earlier data with these GWI models have shown increases in neuroinflammation (e.g., inflammatory markers and gliosis) (O'Callaghan et al., 2015; Zakirova et al., 2015), thus LNFPIII might be a worthy candidate as a therapeutic for GWI. Thus, this dissertation aims to address each of these knowledge gaps and is discussed next (summary Figure 1).

Chapter Two focuses on the acute effects of PB/PM and PB/DEET/CORT/DFP exposures on brain neurochemistry as well as the neuroinflammatory phenotype present 6 h post GW chemicals treatment cessation. These acute effects within chemical exposures have yet to be characterized and may contribute to persisting alterations in the central nervous system (CNS) that could impact behavior later on. Similarities and differences between the two models at this early time point will be evaluated and, additionally, the effects of daily co-treatment of LNFPIII in both of these models will be evaluated for modulation of GWI induced effects.

Further, while the PB/PM model has been characterized behaviorally throughout the mouse's lifespan, translational treatment evaluations with it have been limited. Chapter Three will determine the efficacy of LNFPIII treatment when given months after PB/PM

exposure termination. Additionally, a battery of behavioral tests and neurobiological evaluations will be performed 6-8 months and 9 months, respectively, post PB/PM exposure. These long term timepoints have yet to be characterized within this model.

Recently, it was demonstrated that PB/PM exposure produce acute changes in the gut microbiome of mice (Alhasson et al., 2017), however the chronic effects of GWI exposures on the microbiome and gut health are unknown. Thus, Chapter Four will address this discrepancy by evaluating the gut microbiota within the PB/PM model. Additionally, gut health will be evaluated by examining gut inflammation. The effects of delayed LNFPIII treatment after PB/PM exposure on these parameters will also be investigated.

To date, only the acute neuroinflammatory profile has been characterized in the PB/DEET/CORT/DFP model (O'Callaghan et al., 2015). Chapter Five aims to characterize the long-term behavioral and neurobiological alterations of the PB/DEET/CORT/DFP model 8-10 post GW chemicals exposure. Further, similar to Chapter Three, the efficacy of LNFPIII treatment when started 7 months post GW chemicals exposure will be determined.

Numerous clinical imaging studies have revealed alterations in GWI veteran brain structure and function compared to veteran controls (Chao, 2020; Chao et al., 2011; Chao et al., 2015; Christova et al., 2017; Gopinath et al., 2012; James et al., 2017; Rayhan et al., 2013; Van Riper et al., 2017; Wylie et al., 2019; Zhang et al., 2020; Zhang et al., 2021). However, these studies in the preclinical setting have been limited (Koo et al., 2018), but could provide crucial translational insights into the progression of GWI. Thus, Chapter Six assesses the longitudinal structural brain alterations following GW chemicals exposures in both the PB/PM and PB/DEET/CORT/DFP models.

Persistent hippocampal aberrations, such as increases in gliosis and cell loss, have been observed post GW chemicals exposure (Joshi et al., 2018; Megahed et al., 2014; Parihar et al., 2013; Wang et al., 2020). However, electrophysiological studies investigating hippocampal synaptic plasticity and transmission within GWI models are absent. Appendices A and B include data on the acute and persisting effects of PB/PM and PB/DEET/CORT/DFP exposures on synaptic plasticity and inflammatory markers in the hippocampus.

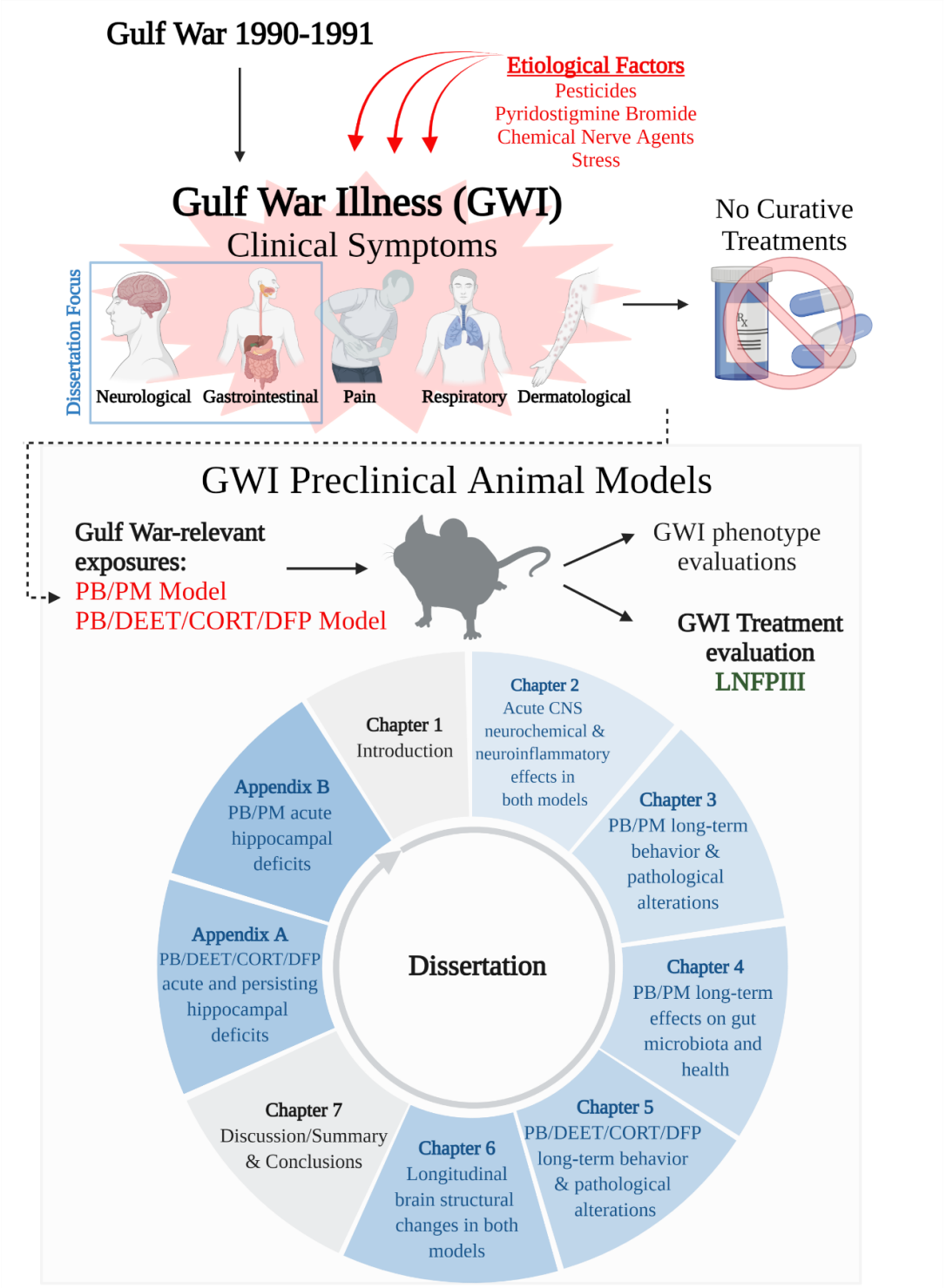

Figure 1.1 Summary Figure of GWI Etiology, Symptoms, and Direction of Dissertation

References

Abdel-Rahman, A., Abou-Donia, S.M., El-Masry, E.M., Shetty, A.K., Abou-Donia, M.B., 2004. Stress and Combined Exposure to Low Doses of Pyridostigmine Bromide, DEET, and Permethrin Produce Neurochemical and Neuropathological Alterations in Cerebral Cortex, Hippocampus, and Cerebellum. Journal of Toxicology and Environmental Health, Part A 67(2), 163-192.

Abdel-Rahman, A., Shetty, A.K., Abou-Donia, M.B., 2001. Subchronic Dermal Application of N,N-Diethyl m-Toluamide (DEET) and Permethrin to Adult Rats, Alone or in Combination, Causes Diffuse Neuronal Cell Death and Cytoskeletal Abnormalities in the Cerebral Cortex and the Hippocampus, and Purkinje Neuron Loss in the Cerebellum. Experimental Neurology 172(1), 153-171.

Abdel-Rahman, A., Shetty, A.K., Abou-Donia, M.B., 2002. Disruption of the Blood–Brain Barrier and Neuronal Cell Death in Cingulate Cortex, Dentate Gyrus, Thalamus, and Hypothalamus in a Rat Model of Gulf-War Syndrome. Neurobiology of Disease 10(3), 306-326.

Abdullah, L., Crynen, G., Reed, J., Bishop, A., Phillips, J., Ferguson, S., Mouzon, B., Mullan, M., Mathura, V., Mullan, M., Ait-Ghezala, G., Crawford, F., 2011. Proteomic CNS profile of delayed cognitive impairment in mice exposed to Gulf War agents. Neuromolecular Med 13(4), 275-288.

Abdullah, L., Evans, J.E., Bishop, A., Reed, J.M., Crynen, G., Phillips, J., Pelot, R., Mullan, M.A., Ferro, A., Mullan, C.M., Mullan, M.J., Ait-Ghezala, G., Crawford, F.C., 2012. Lipidomic profiling of phosphocholine-containing brain lipids in mice with sensorimotor deficits and anxiety-like features after exposure to Gulf War agents. Neuromolecular medicine 14, 349-361.

Abdullah, L., Evans, J.E., Joshi, U., Crynen, G., Reed, J., Mouzon, B., Baumann, S., Montague, H., Zakirova, Z., Emmerich, T., Bachmeier, C., Klimas, N., Sullivan, K., Mullan, M., Ait-Ghezala, G., Crawford, F., 2016. Translational potential of

long-term decreases in mitochondrial lipids in a mouse model of Gulf War Illness. Toxicology 372, 22-33.

Abdullah, L., Evans, J.E., Montague, H., Reed, J.M., Moser, A., Crynen, G., Gonzalez, A., Zakirova, Z., Ross, I., Mullan, C., 2013. Chronic elevation of phosphocholine containing lipids in mice exposed to Gulf War agents pyridostigmine bromide and permethrin. Neurotoxicology and Teratology 40, 74-84.

Abou-Donia, M.B., Dechkovskaia, A.M., Goldstein, L.B., Abdel-Rahman, A., Bullman, S.L., Khan, W.A., 2004. Co-exposure to pyridostigmine bromide, DEET, and/or permethrin causes sensorimotor deficit and alterations in brain acetylcholinesterase activity. Pharmacology Biochemistry and Behavior 77(2), 253-262.

Abou-Donia, M.B., Goldstein, L.B., Jones, K.H., Abdel-Rahman, A.A., Damodaran, T.V., Dechkovskaia, A.M., Bullman, S.L., Amir, B.E., Khan, W.A., 2001. Locomotor and Sensorimotor Performance Deficit in Rats following Exposure to Pyridostigmine Bromide, DEET, and Permethrin, Alone and in Combination. Toxicological Sciences 60(2), 305-314.

Alhasson, F., Das, S., Seth, R., Dattaroy, D., Chandrashekaran, V., Ryan, C.N., Chan, L.S., Testerman, T., Burch, J., Hofseth, L.J., Horner, R., Nagarkatti, M., Nagarkatti, P., Lasley, S.M., Chatterjee, S., 2017. Altered gut microbiome in a mouse model of Gulf War Illness causes neuroinflammation and intestinal injury via leaky gut and TLR4 activation. PLoS One 12(3), e0172914.

Alshelh, Z., Albrecht, D.S., Bergan, C., Akeju, O., Clauw, D.J., Conboy, L., Edwards, R.R., Kim, M., Lee, Y.C., Protsenko, E., Napadow, V., Sullivan, K., Loggia, M.L., 2020. In-vivo imaging of neuroinflammation in veterans with Gulf War illness. Brain, Behavior, and Immunity 87, 498-507.

Anger, W., Storzbach, D., Binder, L., Campbell, K., Rohlman, D., McCauley, L., 1999. Evidence of cognitive deficits in Persian Gulf War veterans: interim report from a population-based study. J Int Neuropsychol Soc 5, 203-212.

Ashbrook, D.G., Hing, B., Michalovicz, L.T., Kelly, K.A., Miller, J.V., de Vega, W.C., Miller, D.B., Broderick, G., O'Callaghan, J.P., McGowan, P.O., 2018. Epigenetic impacts of stress priming of the neuroinflammatory response to sarin surrogate in mice: a model of Gulf War illness. Journal of Neuroinflammation 15(1), 86.

Atochina, O., Da'dara, A.A., Walker, M., Harn, D.A., 2008. The immunomodulatory glycan LNFPIII initiates alternative activation of murine macrophages in vivo. Immunology 125(1), 111-121.

Axelrod, B.N., Milner, I.B., 1997. Neuropsychological findings in a sample of Operation Desert Storm veterans. J Neuropsychiatry Clin Neurosci 9(1), 23-28.

Baraniuk, J.N., El-Amin, S., Corey, R., Rayhan, R., Timbol, C., 2013. Carnosine treatment for gulf war illness: a randomized controlled trial. Glob J Health Sci 5(3), 69-81.

Barth, S.K., Kang, H.K., Bullman, T.A., Wallin, M.T., 2009. Neurological mortality among US veterans of the Persian Gulf War: 13-year follow-up. American journal of industrial medicine 52(9), 663-670.

Belujon, P., Grace, A.A., 2017. Dopamine System Dysregulation in Major Depressive Disorders. Int J Neuropsychopharmacol 20(12), 1036-1046.

Bhargava, P., Li, C., Stanya, K.J., Jacobi, D., Dai, L., Liu, S., Gangl, M.R., Harn, D.A., Lee, C.H., 2012. Immunomodulatory glycan LNFPIII alleviates hepatosteatosis and insulin resistance through direct and indirect control of metabolic pathways. Nat Med 18(11), 1665-1672.

Binder, L.M., Storzbach, D., Anger, W.K., Campbell, K.A., Rohlman, D.S., of the Portland Environmental, O.M., Center, H.R., 1999. Subjective Cognitive Complaints, Affective Distress, and Objective Cognitive Performance in Persian Gulf War Veterans. Archives of Clinical Neuropsychology 14(6), 531-536.

Binns, J.H., Barlow, C., Bloom, F.E., Clauw, D.J., Golomb, B.A., Graves, J.C., Hardie, A., Knox, M.L., Meggs, W.J., Nettleman, M.D., 2008. Gulf war illness and the health

of gulf war veterans. DEPARTMENT OF VETERANS AFFAIRS WASHINGTON DC RESEARCH ADVISORY COMMITTEE ON ….

Boyd, K.C., Hallman, W.K., Wartenberg, D., Fiedler, N., Brewer, N.T., Kipen, H.M., 2003. Reported Exposures, Stressors, and Life Events Among Gulf War Registry Veterans. Journal of Occupational and Environmental Medicine 45(12), 1247-1256.

Broderick, G., Ben-Hamo, R., Vashishtha, S., Efroni, S., Nathanson, L., Barnes, Z., Fletcher, M.A., Klimas, N., 2013. Altered immune pathway activity under exercise challenge in Gulf War Illness: An exploratory analysis. Brain, Behavior, and Immunity 28, 159-169.

Broderick, G., Fletcher, M.A., Gallagher, M., Barnes, Z., Vernon, S.D., Klimas, N.G., 2018. Exploring the Diagnostic Potential of Immune Biomarker Co-expression in Gulf War Illness, in: Yan, Q. (Ed.) Psychoneuroimmunology: Methods and Protocols. Springer New York, New York, NY, pp. 101-120.

Broderick, G., Kreitz, A., Fuite, J., Fletcher, M.A., Vernon, S.D., Klimas, N., 2011. A pilot study of immune network remodeling under challenge in Gulf War Illness. Brain, Behavior, and Immunity 25(2), 302-313.

Calley, C.S., Kraut, M.A., Spence, J.S., Briggs, R.W., Haley, R.W., Hart, J., 2010. The neuroanatomic correlates of semantic memory deficits in patients with Gulf War illnesses: a pilot study. Brain Imaging and Behavior 4(3), 248-255.

Carrera Arias, F.J., Aenlle, K., Abreu, M., Holschbach, M.A., Michalovicz, L.T., Kelly, K.A., Klimas, N., O'Callaghan, J.P., Craddock, T.J.A., 2021. Modeling Neuroimmune Interactions in Human Subjects and Animal Models to Predict Subtype-Specific Multidrug Treatments for Gulf War Illness. Int J Mol Sci 22(16), 8546.

Carreras, I., Aytan, N., Mellott, T., Choi, J.K., Lehar, M., Crabtree, L., Leite-Morris, K., Jenkins, B.G., Blusztajn, J.K., Dedeoglu, A., 2018. Anxiety, neuroinflammation,

cholinergic and GABAergic abnormalities are early markers of Gulf War illness in a mouse model of the disease. Brain Res 1681, 34-43.

Cecchine, G., Golomb, B.A., Hilborne, L.H., Spektor, D.M., Anthony, C.R., 2000. A Review of the Scientific Literature as it Pertains to Gulf War Illnesses: Volume 8: Pesticides. RAND Corporation.

Chao, L.L., 2020. The Prevalence of Mild Cognitive Impairment in a Convenience Sample of 202 Gulf War Veterans. International Journal of Environmental Research and Public Health 17(19), 7158.

Chao, L.L., Abadjian, L., Hlavin, J., Meyerhoff, D.J., Weiner, M.W., 2011. Effects of low-level sarin and cyclosarin exposure and Gulf War Illness on Brain Structure and Function: A study at 4T. NeuroToxicology 32(6), 814-822.

Chao, L.L., Kanady, J.C., Crocker, N., Straus, L.D., Hlavin, J., Metzler, T.J., Maguen, S., Neylan, T.C., 2021. Cognitive behavioral therapy for insomnia in veterans with gulf war illness: Results from a randomized controlled trial. Life Sciences 279, 119147.

Chao, L.L., Zhang, Y., Buckley, S., 2015. Effects of low-level sarin and cyclosarin exposure on white matter integrity in Gulf War Veterans. Neurotoxicology 48, 239-248.

Cheng, C.-H., Koo, B.-B., Calderazzo, S., Quinn, E., Aenlle, K., Steele, L., Klimas, N., Krengel, M., Janulewicz, P., Toomey, R., Michalovicz, L.T., Kelly, K.A., Heeren, T., Little, D., O'Callaghan, J.P., Sullivan, K., 2020. Alterations in high-order diffusion imaging in veterans with Gulf War Illness is associated with chemical weapons exposure and mild traumatic brain injury. Brain, behavior, and immunity 89, 281-290.

Christova, P., James, L.M., Engdahl, B.E., Lewis, S.M., Carpenter, A.F., Georgopoulos, A.P., 2017. Subcortical brain atrophy in Gulf War Illness. Exp Brain Res 235(9), 2777-2786.

Clarke, T., Jamieson, J.D., Malone, P., Rayhan, R.U., Washington, S., VanMeter, J.W., Baraniuk, J.N., 2019. Connectivity differences between Gulf War Illness (GWI) phenotypes during a test of attention. PLoS One 14(12), e0226481-e0226481.

Cohen, D.E., Sullivan, K.A., McNeil, R.B., Klimas, N.G., McNeil, R., Ashford, W., Bested, A., Bunker, J., Cheema, A., Cohen, D., Cook, D., Cournoyer, J., Craddock, T., Golier, J., Hardie, A., Helmer, D., Lindheimer, J.B., Lloyd, P.J., Kerr, K., Krengel, M., Nadkarni, S., Nugent, S., Paris, B., Reinhard, M., Rumm, P., Schneiderman, A., Sims, K.J., Steele, L., Turner, M., Sullivan, K., Abdullah, L., Abreu, M., Abu-Donia, M., Aenlle, K., Arocho, J., Balbin, E., Baraniuk, J., Block, K., Block, M., DeBeer, B., Engdahl, B., Filipov, N., Fletcher, M.A., Kalasinsky, V., Kokkotou, E., Lidie, K., Little, D., Loging, W., Morris, M., Nathanson, L., Nichols, M.D., Pasinetti, G., Shungu, D., Waziry, P., VanLeeuwen, J., Younger, J., Klimas, N., 2021. A common language for Gulf War Illness (GWI) research studies: GWI common data elements. Life Sciences, 119818.

Cook, D.B., Stegner, A.J., Ellingson, L.D., 2010. Exercise Alters Pain Sensitivity in Gulf War Veterans with Chronic Musculoskeletal Pain. The Journal of Pain 11(8), 764-772.

Cooper, B.Y., Flunker, L.D., Johnson, R.D., Nutter, T.J., 2018. Behavioral, cellular and molecular maladaptations covary with exposure to pyridostigmine bromide in a rat model of gulf war illness pain. Toxicology and Applied Pharmacology 352, 119-131.

Cooper, C.M., Briggs, R.W., Farris, E.A., Bartlett, J., Haley, R.W., Odegard, T.N., 2016. Memory and functional brain differences in a national sample of U.S. veterans with Gulf War Illness. Psychiatry Research: Neuroimaging 250, 33-41.

DDGWIRP, 2018. The Gulf War Illness Landscape in: Programs, D.o.D.C.D.M.R. (Ed.).

Dickey, B., Madhu, L.N., Shetty, A.K., 2021. Gulf War Illness: Mechanisms Underlying Brain Dysfunction and Promising Therapeutic Strategies. Pharmacology & Therapeutics 220, 107716.

Doebbeling, B.N., Clarke, W.R., Watson, D., Torner, J.C., Woolson, R.F., Voelker, M.D., Barrett, D.H., Schwartz, D.A., 2000. Is there a Persian Gulf War syndrome? Evidence from a large population-based survey of veterans and nondeployed controls. The American Journal of Medicine 108(9), 695-704.

Donovan, E.K., Kekes-Szabo, S., Lin, J.C., Massey, R.L., Cobb, J.D., Hodgin, K.S., Ness, T.J., Hangee-Bauer, C., Younger, J.W., 2021. A Placebo-Controlled, Pseudo-Randomized, Crossover Trial of Botanical Agents for Gulf War Illness: Curcumin (Curcuma longa), Boswellia (Boswellia serrata), and French Maritime Pine Bark (Pinus pinaster). International Journal of Environmental Research and Public Health 18(5), 2468.

Donta, S.T., Clauw, D.J., Engel, J., Charles C., Guarino, P., Peduzzi, P., Williams, D.A., Skinner, J.S., Barkhuizen, A., Taylor, T., Kazis, L.E., Sogg, S., Hunt, S.C., Dougherty, C.M., Richardson, R.D., Kunkel, C., Rodriguez, W., Alicea, E., Chiliade, P., Ryan, M., Gray, G.C., Lutwick, L., Norwood, D., Smith, S., Everson, M., Blackburn, W., Martin, W., Griffiss, J.M., Cooper, R., Renner, E., Schmitt, J., McMurtry, C., Thakore, M., Mori, D., Kerns, R., Park, M., Pullman-Mooar, S., Bernstein, J., Hershberger, P., Salisbury, D.C., Feussner, J.R., Group, f.t.V.C.S.S., 2003. Cognitive Behavioral Therapy and Aerobic Exercise for Gulf War Veterans' IllnessesA Randomized Controlled Trial. JAMA 289(11), 1396-1404.

Donta, S.T., Engel, C.C., Jr., Collins, J.F., Baseman, J.B., Dever, L.L., Taylor, T., Boardman, K.D., Kazis, L.E., Martin, S.E., Horney, R.A., Wiseman, A.L., Kernodle, D.S., Smith, R.P., Baltch, A.L., Handanos, C., Catto, B., Montalvo, L., Everson, M., Blackburn, W., Thakore, M., Brown, S.T., Lutwick, L., Norwood, D., Bernstein, J., Bacheller, C., Ribner, B., Church, L.W., Wilson, K.H., Guduru, P., Cooper, R., Lentino, J., Hamill, R.J., Gorin, A.B., Gordan, V., Wagner, D., Robinson, C., DeJace, P., Greenfield, R., Beck, L., Bittner, M., Schumacher, H.R.,

Silverblatt, F., Schmitt, J., Wong, E., Ryan, M.A., Figueroa, J., Nice, C., Feussner, J.R., Group, V.A.C., 2004. Benefits and harms of doxycycline treatment for Gulf War veterans' illnesses: a randomized, double-blind, placebo-controlled trial. Ann Intern Med 141(2), 85-94.

Dunphy, R.C., Bridgewater, L., Price, D.D., Robinson, M.E., Zeilman, C.J., III, Verne, N.G., 2003. Visceral and cutaneous hypersensitivity in Persian Gulf war veterans with chronic gastrointestinal symptoms. PAIN 102(1).

Ferrari, C.C., Tarelli, R., 2011. Parkinson's disease and systemic inflammation. Parkinsons Dis 2011, 436813.

Flunker, L.K., Nutter, T.J., Johnson, R.D., Cooper, B.Y., 2017. DEET potentiates the development and persistence of anticholinesterase dependent chronic pain signs in a rat model of Gulf War Illness pain. Toxicology and Applied Pharmacology 316, 48-62.

Ford, J.D., Campbell, K.A., Storzbach, D., Binder, L.M., Anger, W.K., Rohlman, D.S., 2001. Posttraumatic Stress Symptomatology Is Associated With Unexplained Illness Attributed to Persian Gulf War Military Service. Psychosomatic Medicine 63(5).

Fricker, R.D., Reardon, E., Spektor, D.M., Cotton, S.K., Hawes-Dawson, J., Pace, J.E., Hosek, S.D., 2000. Pesticide Use During the Gulf War: A Survey of Gulf War Veterans. RAND Corporation.

Fukuda, K., Nisenbaum, R., Stewart, G., Thompson, W.W., Robin, L., Washko, R.M., Noah, D.L., Barrett, D.H., Randall, B., Herwaldt, B.L., Mawle, A.C., Reeves, W.C., 1998. Chronic Multisymptom Illness Affecting Air Force Veterans of the Gulf War. JAMA 280(11), 981-988.

Gao, J., Xu, F., Starlard-Davenport, A., Miller, D.B., O'Callaghan, J.P., Jones, B.C., Lu, L., 2020. Exploring the Role of Chemokine Receptor 6 (Ccr6) in the BXD Mouse Model of Gulf War Illness. Frontiers in Neuroscience 14(818).

Gifford, E.J., Vahey, J., Hauser, E.R., Sims, K.J., Efird, J.T., Dursa, E.K., Steele, L., Helmer, D.A., Provenzale, D., 2021. Gulf War illness in the Gulf War Era Cohort and Biorepository: The Kansas and Centers for Disease Control definitions. Life Sciences 278, 119454.

Goldstein, G., Beers, S.R., Morrow, L.A., Shemansky, W.J., Steinhauer, S.R., 1996. A preliminary neuropsychological study of Persian Gulf veterans. Journal of the International Neuropsychological Society 2(4), 368-371.

Golier, J.A., Caramanica, K., Michaelides, A.C., Makotkine, I., Schmeidler, J., Harvey, P.D., Yehuda, R., 2016. A randomized, double-blind, placebo-controlled, crossover trial of mifepristone in Gulf War veterans with chronic multisymptom illness. Psychoneuroendocrinology 64, 22-30.

Golomb, B.A., 2008. Acetylcholinesterase inhibitors and Gulf War illnesses. Proceedings of the National Academy of Sciences 105(11), 4295.

Golomb, B.A., Allison, M., Koperski, S., Koslik, H.J., Devaraj, S., Ritchie, J.B., 2014. Coenzyme Q10 benefits symptoms in Gulf War veterans: results of a randomized double-blind study. Neural Comput 26(11), 2594-2651.

Gopinath, K., Gandhi, P., Goyal, A., Jiang, L., Fang, Y., Ouyang, L., Ganji, S., Buhner, D., Ringe, W., Spence, J., Biggs, M., Briggs, R., Haley, R., 2012. FMRI reveals abnormal central processing of sensory and pain stimuli in ill Gulf War veterans. Neurotoxicology 33(3), 261-271.

Gray, G.C., Kaiser, K.S., Hawksworth, A.W., Hall, F.W., Barrett-Connor, E., 1999. Increased postwar symptoms and psychological morbidity among U.S. Navy Gulf War veterans. The American journal of tropical medicine and hygiene Am J Trop Med Hyg Am. J. Trop. Med. Hyg. 60(5), 758-766.

Haley, R.W., Fleckenstein, J.L., Marshall, W.W., McDonald, G.G., Kramer, G.L., Petty, F., 2000. Effect of Basal Ganglia Injury on Central Dopamine Activity in Gulf War

Syndrome: Correlation of Proton Magnetic Resonance Spectroscopy and Plasma Homovanillic Acid Levels. Archives of Neurology 57(9), 1280-1285.

Haley, R.W., Kurt, T.L., Hom, J., 1997. Is there a Gulf War Syndrome? Searching for syndromes by factor analysis of symptoms. Jama 277(3), 215-222.

Hattiangady, B., Mishra, V., Kodali, M., Shuai, B., Rao, X., Shetty, A.K., 2014. Object location and object recognition memory impairments, motivation deficits and depression in a model of Gulf War illness. Front Behav Neurosci 8, 78.

Helmer, D.A., Van Doren, W.W., Litke, D.R., Tseng, C.L., Ho, L., Osinubi, O., Pasinetti, G.M., 2020. Safety, Tolerability and Efficacy of Dietary Supplementation with Concord Grape Juice in Gulf War Veterans with Gulf War Illness: A Phase I/IIA, Randomized, Double-Blind, Placebo-Controlled Trial. Int J Environ Res Public Health 17(10).

Hodgin, K.S., Donovan, E.K., Kekes-Szabo, S., Lin, J.C., Feick, J., Massey, R.L., Ness, T.J., Younger, J.W., 2021. A Placebo-Controlled, Pseudo-Randomized, Crossover Trial of Botanical Agents for Gulf War Illness: Resveratrol (Polygonum cuspidatum), Luteolin, and Fisetin (Rhus succedanea). International Journal of Environmental Research and Public Health 18(5), 2483.

Holodniy, M., Kaiser, J.D., 2019. Treatment for Gulf War Illness (GWI) with KPAX002 (methylphenidate hydrochloride + GWI nutrient formula) in subjects meeting the Kansas case definition: A prospective, open-label trial. Journal of Psychiatric Research 118, 14-20.

Holton, K.F., Kirkland, A.E., Baron, M., Ramachandra, S.S., Langan, M.T., Brandley, E.T., Baraniuk, J.N., 2020. The Low Glutamate Diet Effectively Improves Pain and Other Symptoms of Gulf War Illness. Int J Environ Res Public Health 12(9), 2593.

Holton, K.F., Ramachandra, S.S., Murray, S.L., Baron, M., Baraniuk, J.N., 2021. Effect of the low glutamate diet on inflammatory cytokines in veterans with Gulf War Illness (GWI): A pilot study. Life Sciences 280, 119637.

Hom, J., Haley, R.W., Kurt, T.L., 1997. Neuropsychological correlates of Gulf War syndrome. Archives of Clinical Neuropsychology 12(6), 531-544.

Hoy, J.B., Cornell, J.A., Karlix, J.L., Schmidt, C.J., Tebbett, I.R., van Haaren, F., 2000a. Interactions of pyridostigmine bromide, DEET and permethrin alter locomotor behavior of rats. Vet Hum Toxicol 42(2), 65-71.

Hoy, J.B., Cornell, J.A., Karlix, J.L., Tebbett, I.R., van Haaren, F., 2000b. Repeated coadministrations of pyridostigmine bromide, DEET, and permethrin alter locomotor behavior of rats. Vet Hum Toxicol 42(2), 72-76.

Hubbard, N.A., Hutchison, J.L., Motes, M.A., Shokri-Kojori, E., Bennett, I.J., Brigante, R.M., Haley, R.W., Rypma, B., 2014. Central Executive Dysfunction and Deferred Prefrontal Processing in Veterans with Gulf War Illness. Clin Psychol Sci 2(3), 319-327.

Hyams, K.C., Roswell, R.H., 1998. Resolving the Gulf War Syndrome Question. American Journal of Epidemiology 148(4), 339-342.

IOM, 2014. Chronic Multisymptom Illness in Gulf War Veterans: Case Definitions Reexamined. The National Academies Press, Washington, DC.

James, L.M., Christova, P., Engdahl, B.E., Lewis, S.M., Carpenter, A.F., Georgopoulos, A.P., 2017. Human Leukocyte Antigen (HLA) and Gulf War Illness (GWI): HLA-DRB1*13:02 Spares Subcortical Atrophy in Gulf War Veterans. EBioMedicine 26, 126-131.

Janulewicz, P.A., Krengel, M.H., Maule, A., White, R.F., Cirillo, J., Sisson, E., Heeren, T., Sullivan, K., 2017. Neuropsychological characteristics of Gulf War illness: A meta-analysis. PLoS One 12(5), e0177121-e0177121.

Janulewicz, P.A., Seth, R.K., Carlson, J.M., Ajama, J., Quinn, E., Heeren, T., Klimas, N., Lasley, S.M., Horner, R.D., Sullivan, K., Chatterjee, S., 2019. The Gut-

Microbiome in Gulf War Veterans: A Preliminary Report. International Journal of Environmental Research and Public Health 16(19), 3751.

Jeffrey, M., Collado, F., Kibler, J., DeLucia, C., Messer, S., Klimas, N., Craddock, T.J.A., 2021. Post-traumatic stress impact on health outcomes in Gulf War Illness. BMC Psychol 9(1), 57-57.

Johnson, G.J., Slater, B.C., Leis, L.A., Rector, T.S., Bach, R.R., 2016. Blood Biomarkers of Chronic Inflammation in Gulf War Illness. PLoS One 11(6), e0157855.

Jones, B.C., Miller, D.B., Lu, L., Zhao, W., Ashbrook, D.G., Xu, F., Mulligan, M.K., Williams, R.W., Zhuang, D., Torres-Rojas, C., O'Callaghan, J.P., 2020. Modeling the Genetic Basis of Individual Differences in Susceptibility to Gulf War Illness. Brain Sciences 10(3), 143.

Joshi, U., Evans, J.E., Joseph, R., Emmerich, T., Saltiel, N., Lungmus, C., Oberlin, S., Langlois, H., Ojo, J., Mouzon, B., 2018. Oleoylethanolamide treatment reduces neurobehavioral deficits and brain pathology in a mouse model of Gulf War Illness. Sci Rep 8(1), 12921.

Joshi, U., Pearson, A., Evans, J.E., Langlois, H., Saltiel, N., Ojo, J., Klimas, N., Sullivan, K., Keegan, A.P., Oberlin, S., 2019. A permethrin metabolite is associated with adaptive immune responses in Gulf War Illness. Brain, Behavior, and Immunity(81), 545-559.

Kearney, D.J., Simpson, T.L., Malte, C.A., Felleman, B., Martinez, M.E., Hunt, S.C., 2016. Mindfulness-based Stress Reduction in Addition to Usual Care Is Associated with Improvements in Pain, Fatigue, and Cognitive Failures Among Veterans with Gulf War Illness. Am J Med 129(2), 204-214.

Khaiboullina, S.F., DeMeirleir, K.L., Rawat, S., Berk, G.S., Gaynor-Berk, R.S., Mijatovic, T., Blatt, N., Rizvanov, A.A., Young, S.G., Lombardi, V.C., 2015. Cytokine expression provides clues to the pathophysiology of Gulf War illness and myalgic encephalomyelitis. Cytokine 72(1), 1-8.

Kimono, D., Bose, D., Seth, R.K., Mondal, A., Saha, P., Janulewicz, P., Sullivan, K., Lasley, S., Horner, R., Klimas, N., Chatterjee, S., 2020. Host Akkermansia muciniphila Abundance Correlates With Gulf War Illness Symptom Persistence via NLRP3-Mediated Neuroinflammation and Decreased Brain-Derived Neurotrophic Factor. Neuroscience Insights 15, 2633105520942480.

Koch, T.R., Emory, T.S., 2005. Evaluation of Chronic Gastrointestinal Symptoms following Persian Gulf War Exposure. Military Medicine 170(8), 696-700.

Kodali, M., Hattiangady, B., Shetty, G., Bates, A., Shuai, B., Shetty, A., 2018. Curcumin treatment leads to better cognitive and mood function in a model of Gulf War Illness with enhanced neurogenesis, and alleviation of inflammation and mitochondrial dysfunction in the hippocampus. Brain, Behavior, and Immunity 69, 499-514.

Koo, B.-B., Michalovicz, L.T., Calderazzo, S., Kelly, K.A., Sullivan, K., Killiany, R.J., O'Callaghan, J.P., 2018. Corticosterone potentiates DFP-induced neuroinflammation and affects high-order diffusion imaging in a rat model of Gulf War Illness. Brain, behavior, and immunity 67, 42-46.

Korte-Bouws, G.A.H., van Heesch, F., Westphal, K.G.C., Ankersmit, L.M.J., van Oosten, E.M., Gunturkun, O., Korte, S.M., 2018. Bacterial Lipopolysaccharide Increases Serotonin Metabolism in Both Medial Prefrontal Cortex and Nucleus Accumbens in Male Wild Type Rats, but Not in Serotonin Transporter Knockout Rats. Pharmaceuticals (Basel) 11(3), 66.

Kroenke, K., Koslowe, P., Roy, M., 1998. Symptoms in 18,495 Persian Gulf War Veterans: Latency of Onset and Lack of Association with Self-Reported Exposures. Journal of Occupational and Environmental Medicine 40(6).

Lacagnina, M.J., Li, J., Lorca, S., Rice, K.C., Sullivan, K., O'Callaghan, J.P., Grace, P.M., 2021. A role for neuroimmune signaling in a rat model of Gulf War Illness-related pain. Brain, Behavior, and Immunity 91, 418-428.

Li, X., Spence, J.S., Buhner, D.M., Hart, J., Jr., Cullum, C.M., Biggs, M.M., Hester, A.L., Odegard, T.N., Carmack, P.S., Briggs, R.W., Haley, R.W., 2011. Hippocampal dysfunction in Gulf War veterans: investigation with ASL perfusion MR imaging and physostigmine challenge. Radiology 261(1), 218-225.

Lindem, K., Proctor, S.P., Heeren, T., Krengel, M., Vasterling, J., Sutker, P.B., Wolfe, J., Keane, T.M., White, R.F., 2003. Neuropsychological Performance in Gulf War Era Veterans: Neuropsychological Symptom Reporting. Journal of Psychopathology & Behavioral Assessment 25(2), 121-127.

Lindheimer, J.B., Stegner, A.J., Van Riper, S.M., Ninneman, J.V., Ellingson, L.D., Cook, D.B., 2021. Nociceptive stress interferes with neural processing of cognitive stimuli in Gulf War Veterans with chronic musculoskeletal pain. Life Sciences 279, 119653.

Locker, A.R., Michalovicz, L.T., Kelly, K.A., Miller, J.V., Miller, D.B., O'Callaghan, J.P., 2017. Corticosterone primes the neuroinflammatory response to Gulf War Illness-relevant organophosphates independently of acetylcholinesterase inhibition. J Neurochem 142(3), 444-455.

Madhu, L.N., Attaluri, S., Kodali, M., Shuai, B., Upadhya, R., Gitai, D., Shetty, A.K., 2019. Neuroinflammation in Gulf War Illness is linked with HMGB1 and complement activation, which can be discerned from brain-derived extracellular vesicles in the blood. Brain, Behavior, and Immunity 81, 430-443.

Mathersul, D.C., Eising, C.M., DeSouza, D.D., Spiegel, D., Bayley, P.J., 2020. Brain and Physiological Markers of Autonomic Function Are Associated With Treatment-Related Improvements in Self-Reported Autonomic Dysfunction in Veterans With Gulf War Illness: An Exploratory Pilot Study. Glob Adv Health Med 9, 2164956120922812.

Megahed, T., Hattiangady, B., Shuai, B., Shetty, A.K., 2014. Parvalbumin and neuropeptide Y expressing hippocampal GABA-ergic inhibitory interneuron numbers decline in a model of Gulf War illness. Front Cell Neurosci 8, 447.

Michalovicz, L.T., Kelly, K.A., Sullivan, K., O'Callaghan, J.P., 2020. Acetylcholinesterase inhibitor exposures as an initiating factor in the development of Gulf War Illness, a chronic neuroimmune disorder in deployed veterans. Neuropharmacology 171, 108073.

Michalovicz, L.T., Locker, A.R., Kelly, K.A., Miller, J.V., Barnes, Z., Fletcher, M.A., Miller, D.B., Klimas, N.G., Morris, M., Lasley, S.M., O'Callaghan, J.P., 2019. Corticosterone and pyridostigmine/DEET exposure attenuate peripheral cytokine expression: Supporting a dominant role for neuroinflammation in a mouse model of Gulf War Illness. Neurotoxicology 70, 26-32.

Miller, J.V., LeBouf, R.F., Kelly, K.A., Michalovicz, L.T., Ranpara, A., Locker, A.R., Miller, D.B., O'Callaghan, J.P., 2018. The Neuroinflammatory Phenotype in a Mouse Model of Gulf War Illness is Unrelated to Brain Regional Levels of Acetylcholine as Measured by Quantitative HILIC-UPLC-MS/MS. Toxicological Sciences 165(2), 302-313.

National Academies of Sciences, E., Medicine, 2016. Gulf War and Health: Volume 10: Update of Health Effects of Serving in the Gulf War, 2016.

Naughton, S.X., Hernandez, C.M., Beck, W.D., Poddar, I., Yanasak, N., Lin, P.-C., Terry, A.V., 2018. Repeated exposures to diisopropylfluorophosphate result in structural disruptions of myelinated axons and persistent impairments of axonal transport in the brains of rats. Toxicology 406-407, 92-103.

Nizamutdinov, D., Mukherjee, S., Deng, C., Stauss, H.M., Shapiro, L.A., 2018. Gulf War agents pyridostigmine bromide and permethrin cause hypersensitive nociception that is restored after vagus nerve stimulation. Neurotoxicology 69, 93-96.

Nutter, T.J., Cooper, B.Y., 2014. Persistent modification of Nav1.9 following chronic exposure to insecticides and pyridostigmine bromide. Toxicology and Applied Pharmacology 277(3), 298-309.

Nutter, T.J., Jiang, N., Cooper, B.Y., 2013. Persistent Na+ and K+ channel dysfunctions after chronic exposure to insecticides and pyridostigmine bromide. NeuroToxicology 39, 72-83.

Nutter, T.J., Johnson, R.D., Cooper, B.Y., 2015. A delayed chronic pain like condition with decreased Kv channel activity in a rat model of Gulf War Illness pain syndrome. NeuroToxicology 51, 67-79.

O'Callaghan, J.P., Kelly, K.A., Locker, A.R., Miller, D.B., Lasley, S.M., 2015. Corticosterone primes the neuroinflammatory response to DFP in mice: potential animal model of Gulf War Illness. J Neurochem 133(5), 708-721.

Ojo, J.O., Abdullah, L., Evans, J., Reed, J.M., Montague, H., Mullan, M.J., Crawford, F.C., 2014. Exposure to an organophosphate pesticide, individually or in combination with other Gulf War agents, impairs synaptic integrity and neuronal differentiation, and is accompanied by subtle microvascular injury in a mouse model of Gulf War agent exposure. Neuropathology 34(2), 109-127.

Parihar, V.K., Hattiangady, B., Shuai, B., Shetty, A.K., 2013. Mood and memory deficits in a model of Gulf War illness are linked with reduced neurogenesis, partial neuron loss, and mild inflammation in the hippocampus. Neuropsychopharmacology 38(12), 2348-2362.

Parkitny, L., Middleton, S., Baker, K., Younger, J., 2015. Evidence for abnormal cytokine expression in Gulf War Illness: A preliminary analysis of daily immune monitoring data. BMC Immunol 16, 57-57.

Parkitny, L., Middleton, S., Baker, K., Younger, J., 2015. Evidence for abnormal cytokine expression in Gulf War Illness: A preliminary analysis of daily immune monitoring data. BMC Immunol 16, 57.

Parrish, R.R., Haley, R.W., 2021. Resolving whether inhalation of depleted uranium contributed to Gulf War Illness using high-sensitivity mass spectrometry. Sci Rep 11(1), 3218-3218.

Phillips, K.F., Deshpande, L.S., 2016. Repeated low-dose organophosphate DFP exposure leads to the development of depression and cognitive impairment in a rat model of Gulf War Illness. NeuroToxicology 52, 127-133.

Phillips, K.F., Deshpande, L.S., 2018. Chronic Neurological Morbidities and Elevated Hippocampal Calcium Levels in a DFP-Based Rat Model of Gulf War Illness. Military Medicine 183(suppl_1), 552-555.

Proctor, S.P., Heaton, K.J., Heeren, T., White, R.F., 2006. Effects of sarin and cyclosarin exposure during the 1991 Gulf War on neurobehavioral functioning in US army veterans. NeuroToxicology 27(6), 931-939.

Proctor, S.P., Heeren, T., White, R.F., Wolfe, J., Borgos, M.S., Davis, J.D., Pepper, L., Clapp, R., Sutker, P.B., Vasterling, J.J., Oznoff, D., 1998. Health status of Persian Gulf War veterans: self-reported symptoms, environmental exposures and the effect of stress. International Journal of Epidemiology 27(6), 1000-1010.

Rayhan, R.U., Stevens, B.W., Timbol, C.R., Adewuyi, O., Walitt, B., VanMeter, J.W., Baraniuk, J.N., 2013. Increased brain white matter axial diffusivity associated with fatigue, pain and hyperalgesia in Gulf War illness. PLoS One 8(3), e58493.

Ribeiro, A.C., Zhu, J., Kronfol, M.M., Jahr, F.M., Younis, R.M., Hawkins, E., McClay, J.L., Deshpande, L.S., 2020. Molecular mechanisms for the antidepressant-like effects of a low-dose ketamine treatment in a DFP-based rat model for Gulf War Illness. NeuroToxicology.

Ribeiro, A.C.R., Deshpande, L.S., 2021. A review of pre-clinical models for Gulf War Illness. Pharmacology & Therapeutics 228, 107936.

Seth, R.K., Kimono, D., Alhasson, F., Sarkar, S., Albadrani, M., Lasley, S.K., Horner, R., Janulewicz, P., Nagarkatti, M., Nagarkatti, P., Sullivan, K., Chatterjee, S., 2018. Increased butyrate priming in the gut stalls microbiome associated-gastrointestinal inflammation and hepatic metabolic reprogramming in a mouse model of Gulf War Illness. Toxicology and Applied Pharmacology 350, 64-77.

Shetty, A.K., Attaluri, S., Kodali, M., Shuai, B., Shetty, G.A., Upadhya, D., Hattiangady, B., Madhu, L.N., Upadhya, R., Bates, A., Rao, X., 2020. Monosodium luminol reinstates redox homeostasis, improves cognition, mood and neurogenesis, and alleviates neuro- and systemic inflammation in a model of Gulf War Illness. Redox Biology 28, 101389.

Shetty, G.A., Hattiangady, B., Upadhya, D., Bates, A., Attaluri, S., Shuai, B., Kodali, M., Shetty, A.K., 2017. Chronic Oxidative Stress, Mitochondrial Dysfunction, Nrf2 Activation and Inflammation in the Hippocampus Accompany Heightened Systemic Inflammation and Oxidative Stress in an Animal Model of Gulf War Illness. Frontiers in Molecular Neuroscience 10(182).

Sillanpaa, M.C., Agar, L.M., Milner, I.B., Podany, E.C., Axelrod, B.N., Brown, G.G., 1997. Gulf War veterans: a neuropsychological examination. J Clin Exp Neuropsychol 19(2), 211-219.

Soderlund, D.M., Clark, J.M., Sheets, L.P., Mullin, L.S., Piccirillo, V.J., Sargent, D., Stevens, J.T., Weiner, M.L., 2002. Mechanisms of pyrethroid neurotoxicity: implications for cumulative risk assessment. Toxicology 171(1), 3-59.

Srivastava, L., Tundup, S., Choi, B.S., Norberg, T., Harn, D., 2014. Immunomodulatory glycan lacto-N-fucopentaose III requires clathrin-mediated endocytosis to induce alternative activation of antigen-presenting cells. Infect Immun 82(5), 1891-1903.

Steele, L., 2000. Prevalence and Patterns of Gulf War Illness in Kansas Veterans: Association of Symptoms with Characteristics of Person, Place, and Time of Military Service. American Journal of Epidemiology 152(10), 992-1002.

Steele, L., Sastre, A., Gerkovich, M.M., Cook, M.R., 2012. Complex factors in the etiology of Gulf War illness: wartime exposures and risk factors in veteran subgroups. Environ Health Perspect 120(1), 112-118.

Stimpson, N.J., Unwin, C., Hull, L., David, T., Wessely, S., Lewis, G., 2006. Prevalence of reported pain, widespread pain, and pain symmetry in veterans of the Persian Gulf War (1990-1991): the use of pain manikins in Persian Gulf War health research. Mil Med 171(12), 1181-1186.

Swale, D.R., Sun, B., Tong, F., Bloomquist, J.R., 2014. Neurotoxicity and mode of action of N, N-diethyl-meta-toluamide (DEET). PLoS One 9(8), e103713-e103713.

Thomas, H.V., Stimpson, N.J., Weightman, A., Dunstan, F., Lewis, G., 2006. Pain in veterans of the Gulf War of 1991: a systematic review. BMC Musculoskeletal Disorders 7(1), 74.

Toomey, R., Alpern, R., Vasterling, J.J., Baker, D.G., Reda, D.J., Lyons, M.J., Henderson, W.G., Kang, H.K., Eisen, S.A., Murphy, F.M., 2009. Neuropsychological functioning of U.S. Gulf War veterans 10 years after the war. J Int Neuropsychol Soc 15(5), 717-729.

Tundup, S., Srivastava, L., Norberg, T., Watford, W., Harn, D., 2015. A Neoglycoconjugate Containing the Human Milk Sugar LNFPIII Drives Anti-Inflammatory Activation of Antigen Presenting Cells in a CD14 Dependent Pathway. PLoS One 10(9), e0137495.

Van Riper, S.M., Alexander, A.L., Koltyn, K.F., Stegner, A.J., Ellingson, L.D., Destiche, D.J., Dougherty, R.J., Lindheimer, J.B., Cook, D.B., 2017. Cerebral white matter structure is disrupted in Gulf War Veterans with chronic musculoskeletal pain. PAIN 158(12).

Wang, X., Xu, Z., Zhao, F., Lin, K.J., Foster, J.B., Xiao, T., Kung, N., Askwith, C.C., Bruno, J.P., Valentini, V., 2020. Restoring tripartite glutamatergic synapses: A

potential therapy for mood and cognitive deficits in Gulf War illness. Neurobiology of Stress, 100240.

Washington, S.D., Rayhan, R.U., Garner, R., Provenzano, D., Zajur, K., Addiego, F.M., VanMeter, J.W., Baraniuk, J.N., 2020. Exercise alters cerebellar and cortical activity related to working memory in phenotypes of Gulf War Illness. Brain Communications 2(1).

Weiner, M.W., Meyerhoff, D.J., Neylan, T.C., Hlavin, J., Ramage, E.R., McCoy, D., Studholme, C., Cardenas, V., Marmar, C., Truran, D., Chu, P.W., Kornak, J., Furlong, C.E., McCarthy, C., 2011. The relationship between Gulf War illness, brain N-acetylaspartate, and post-traumatic stress disorder. Military medicine 176(8), 896-902.

White, R.F., Steele, L., O'Callaghan, J.P., Sullivan, K., Binns, J.H., Golomb, B.A., Bloom, F.E., Bunker, J.A., Crawford, F., Graves, J.C., Hardie, A., Klimas, N., Knox, M., Meggs, W.J., Melling, J., Philbert, M.A., Grashow, R., 2016. Recent research on Gulf War illness and other health problems in veterans of the 1991 Gulf War: Effects of toxicant exposures during deployment. Cortex 74, 449-475.

Willard, A.M., Bouchard, R.S., Gittis, A.H., 2015. Differential degradation of motor deficits during gradual dopamine depletion with 6-hydroxydopamine in mice. Neuroscience 301, 254-267.

Wylie, G.R., Genova, H., Dobryakova, E., DeLuca, J., Chiaravalloti, N., Falvo, M., Cook, D., 2019. Fatigue in Gulf War Illness is associated with tonically high activation in the executive control network. Neuroimage Clin 21, 101641-101641.

Younger, J., Donovan, E.K., Hodgin, K.S., Ness, T.J., 2021. A Placebo-Controlled, Pseudo-Randomized, Crossover Trial of Botanical Agents for Gulf War Illness: Reishi Mushroom (Ganoderma lucidum), Stinging Nettle (Urtica dioica), and Epimedium (Epimedium sagittatum). International Journal of Environmental Research and Public Health 18(7), 3671.

Zakirova, Z., Crynen, G., Hassan, S., Abdullah, L., Horne, L., Mathura, V., Crawford, F., Ait-Ghezala, G., 2016. A Chronic Longitudinal Characterization of Neurobehavioral and Neuropathological Cognitive Impairment in a Mouse Model of Gulf War Agent Exposure. Front Integr Neurosci 9, 71-71.

Zakirova, Z., Reed, J., Crynen, G., Horne, L., Hassan, S., Mathura, V., Mullan, M., Crawford, F., Ait-Ghezala, G., 2017. Complementary proteomic approaches reveal mitochondrial dysfunction, immune and inflammatory dysregulation in a mouse model of Gulf War Illness. PROTEOMICS–Clinical Applications 11(9-10), 1600190.

Zakirova, Z., Tweed, M., Crynen, G., Reed, J., Abdullah, L., Nissanka, N., Mullan, M., Mullan, M.J., Mathura, V., Crawford, F., Ait-Ghezala, G., 2015. Gulf War agent exposure causes impairment of long-term memory formation and neuropathological changes in a mouse model of Gulf War Illness. PLoS One 10(3), e0119579-e0119579.

Zhang, Y., Avery, T., Vakhtin, A.A., Mathersul, D.C., Tranvinh, E., Wintermark, M., Massaband, P., Ashford, J.W., Bayley, P.J., Furst, A.J., 2020. Brainstem atrophy in Gulf War Illness. NeuroToxicology 78, 71-79.

Zhang, Y., Vakhtin, A.A., Dietch, J., Jennings, J.S., Yesavage, J.A., Clark, J.D., Bayley, P.J., Ashford, J.W., Furst, A.J., 2021. Brainstem damage is associated with poorer sleep quality and increased pain in gulf war illness veterans. Life Sciences 280, 119724.

Zhou, Q., Verne, M.L., Zhang, B., Verne, G.N., 2018. Evidence for Somatic Hypersensitivity in Veterans With Gulf War Illness and Gastrointestinal Symptoms. Clin J Pain 34(10), 944-949.

Zhu, B., Trikudanathan, S., Zozulya, A.L., Sandoval-Garcia, C., Kennedy, J.K., Atochina, O., Norberg, T., Castagner, B., Seeberger, P., Fabry, Z., Harn, D., Khoury, S.J.,

Guleria, I., 2012. Immune modulation by Lacto-N-fucopentaose III in experimental autoimmune encephalomyelitis. Clin Immunol 142(3), 351-361.

Zhu, J., Hawkins, E., Phillips, K., Deshpande, L.S., 2020. Assessment of Ketamine and its Enantiomers in an Organophosphate-Based Rat Model for Features of Gulf War Illness. International Journal of Environmental Research and Public Health 17(13), 4710.

Zundel, C.G., Krengel, M.H., Heeren, T., Yee, M.K., Grasso, C.M., Janulewicz Lloyd, P.A., Coughlin, S.S., Sullivan, K., 2019. Rates of Chronic Medical Conditions in 1991 Gulf War Veterans Compared to the General Population. Int J Environ Res Public Health 16(6).

CHAPTER 2

NEUROCHEMICAL AND NEUROINFLAMMATORY PERTURBATIONS IN TWO GULF WAR ILLNESS MODELS: MODULATION BY THE IMMUNOTHERAPEUTIC LNFPIII

Jessica M. Carpenter, Hannah E. Gordon, Helaina D. Ludwig, John J. Wagner, Donald A. Harn, Thomas Norberg, Nikolay M. Filipov
Published in Neurotoxicology 2020.
Reprinted here with the permission of publisher.

Abstract

Gulf War Illness (GWI) manifests a multitude of symptoms, including neurological and immunological, and approximately a third of the 1990-1991 Gulf War (GW) veterans suffer from it. This study sought to characterize the acute neurochemical (monoamine) and neuroinflammatory profiles of two established GWI animal models and examine the potential modulatory effects of the novel immunotherapeutic Lacto-N-fucopentaose III (LNFPIII). In Model 1, male C57BL/6J mice were treated for 10 days with pyridostigmine bromide (PB) and permethrin (PM). In Model 2, a separate cohort of mice were treated for 14 days with PB and N,N-Diethyl-methylbenzamide (DEET), plus corticosterone (CORT) via drinking water on days 8-14 and diisopropylfluorophosphate (DFP) on day 15. LNFPIII was administered concurrently after GWI chemicals treatments. Brain and spleen monoamines and hippocampal inflammatory marker expression were examined by, respectively, HPLC-ECD and qPCR, 6 h post treatment cessation. Serotonergic (5-HT) and dopaminergic (DA) dyshomeostasis caused by GWI chemicals was apparent in multiple brain regions, primarily in the nucleus accumbens (5-HT) and hippocampus (5-HT, DA) for both models. Splenic levels of 5-HT (both models) and norepinephrine (Model 2) were also disrupted by GWI chemicals. LNFPIII treatment prevented many of the GWI chemicals induced monoamine alterations. Hippocampal inflammatory cytokines were increased in both models, but the magnitude and spread of inflammation was greater in Model 2; LNFPIII was anti-inflammatory, mostly in the apparently milder Model 1. Overall, in both models, GWI chemicals led to monoamine disbalance and neuroinflammation. LNFPIII co-treatment prevented many of these disruptions in both models, which is indicative of its promise as a potential GWI therapeutic.

Abbreviations: AMY, amygdala; CORT, corticosterone; DEET, N,N-Diethyl-methylbenzamide; DFP, diisopropylfluorophosphate; dHip, dorsal hippocampus; GW, Gulf War; GWI, Gulf War Illness; HPLC-ECD, high performance liquid chromatography with electrochemical detection; IL, interleukin; LNFPIII, Lacto-N-fucopentaose III; NAc, nucleus accumbens; PB, pyridostigmine bromide; PFC, prefrontal cortex; PM, permethrin; qPCR, quantitative polymerase chain reaction; STR, striatum; vHip, ventral hippocampus; DA, dopamine; HVA, homovanillic acid; 5-HT, serotonin; 5-HIAA, 5-hydroxyindoleacetic acid; MHPG, 3-methoxy-4-hydroxyphenylglycol; NE, norepinephrine

Keywords: Gulf War Illness; LNFPIII; monoamines; neuroinflammation; pesticides

1. Introduction

Aberrant communication between the immune and the central nervous systems (CNS) has been implicated in the pathogenesis of various disease states. While controlled innate immune system activation and ensuing inflammation serve important protective and homeostatic functions in the body, if left unchecked, it can be detrimental (Karin et al., 2006). In the CNS, uncontrolled inflammation (neuroinflammation) can cause cognitive, memory, and mood deficits; it exacerbates, among others, Alzheimer's disease (AD), Multiple Sclerosis (MS), and Parkinson's disease (PD) pathologies (Capuron and Miller, 2011; Czirr and Wyss-Coray, 2012; Ferrari and Tarelli, 2011). Further, neuroinflammation can be initiated in the periphery and have destructive effects centrally. For example, peripheral inflammation exacerbated nigrostriatal degeneration and motor dysfunction in a PD model (Pott Godoy et al., 2010).

Recently, this neuroimmune crosstalk has been implicated in a complex multi-symptom disorder known as Gulf War Illness (GWI). GWI affects approximately 30% of the veterans from the 1990-1991 Gulf War (GW) and targets the immune, nervous, musculoskeletal, and gastrointestinal systems (DDGWIRP, 2018; White et al., 2016). Prominent symptoms of GWI include fatigue, impaired cognition, memory and motor function, and altered mood (White et al., 2016). The precise etiology of GWI remains undetermined, but suspected contributing factors, in combination with war theatre stress, include overexposures to chemicals, such as the nerve agent prophylactic pyridostigmine bromide (PB) and pesticides, like permethrin (PM), chlorpyrifos, and N-Diethyl-3-methylbenzamide (DEET). A subset of GW veterans were also exposed to the nerve agents sarin and cyclosarin (Boyd et al., 2003; Cherry et al., 2001; Steele et al., 2012; White et

al., 2016). Due to their association with GWI, these chemicals are referred to as GWI chemicals.

In addition to the cognition, memory, motor function and mood deficits exhibited by GWI veterans, structural abnormalities, such as reduced hippocampal volumes and increased diffusivity in white matter connections, are reported (Chao et al., 2010; Rayhan et al., 2013; Toomey et al., 2009; White et al., 2016). Accumulating clinical and experimental evidence suggests that at least some neurological GWI deficits might be associated with immune dysfunction. For example, several studies have shown that GWI veterans exhibit systemic inflammation compared to matched veteran controls (Broderick et al., 2013; Broderick et al., 2018; Parkitny et al., 2015). Many of these neurological and immunological deficits are recapitulated in animal models of GWI; data show that post exposure to GWI chemicals, neuronal dysfunction and increases in neuroinflammatory markers throughout the brain are present (Carreras et al., 2018; Miller et al., 2018; O'Callaghan et al., 2015; Parihar et al., 2013). Further, rodent behavioral data mirror GWI symptomology in terms of impaired cognition, memory and motor function, as well as increased anxiety and depressive-like behaviors (Abdullah et al., 2011; Carreras et al., 2018; Hattiangady et al., 2014; Parihar et al., 2013; Zakirova et al., 2015).

Many of the neurological and behavioral deficits associated with GWI could stem from neurotransmitter dysfunction. Affect disorders, including sickness behavior and depression, have been linked to serotonin (5-HT) and dopamine (DA) dysregulation (Belujon and Grace, 2017; Korte-Bouws et al., 2018). Dopaminergic dysfunction, especially in the basal ganglia, is implicated in motor function impairments (Ferrari and Tarelli, 2011; Willard et al., 2015). Further, multiple studies show that inflammation can

alter monoamine neurotransmitter balance and transmission in the brain, which subsequently influences behavior (Dunn, 2006). For example, inflammatory cytokine challenge alters central monoaminergic transmission, i.e., metabolism of 5-HT and norepinephrine (NE) is increased in response to IL-1 and DA homeostasis is disrupted by IFN-α (Dunn, 2006; Felger and Miller, 2012). In addition, peripheral monoamines can be immunomodulatory as the spleen, rich in 5-HT and NE, can modulate activation of T-cells and pro-inflammatory cytokines (Blandino et al., 2006; Wu et al., 2019).

While researchers have sifted through the immunological component of GWI, few have investigated the role neurotransmitters, monoamines in particular, play in GWI symptomology. Studies investigating neurochemical changes have largely focused on acetylcholinesterase (AChE) inhibition and cholinergic activation due to the mechanism of action of GWI chemicals such as PB, sarin, or its surrogate, DFP (Miller et al., 2018; Ojo et al., 2014; Zakirova et al., 2015). Others have found alterations in GABA-ergic activity in brain regions that regulate cognition (Carreras et al., 2018; Megahed et al., 2014). However, as indicated earlier, some of the neurological symptoms might be due to monoamine disbalance (Parihar et al., 2013; Zakirova et al., 2015).

Immunotherapies have shown promise in treating common neurological diseases such as PD, AD, and MS (Wisniewski and Goni, 2015; Zella et al., 2019; Ziemssen et al., 2016). Given that GWI has both immunological and neurological underpinnings, it is important to examine treatments that cater to both fields. Therapeutic intervention in GWI has been explored including trials with the antibiotic doxycycline, coenzyme Q10, and carnosine supplementation (Baraniuk et al., 2013; Donta et al., 2004; Golomb et al., 2014). However, like other GWI interventions, these treatments improved only some GWI

symptoms and might not be a desirable option for long term treatment (DDGWIRP, 2018). Moreover, while viable treatment options to veterans suffering from GWI would be the ultimate goal, testing of new therapeutics with a strong safety profile in an acute (exposure-related) paradigm is also important, but such testing has not been done.

Lacto-N-fucopentaose III (LNFPIII) is an immunomodulatory glycan found in human breast milk, and when conjugated to a dextran carrier, it utilizes CD14/TLR-4 signaling to activate ERK-dependent production of anti-inflammatory mediators (Tundup et al., 2015). As a result, the inflammatory balance of the innate immune system is skewed in an anti-inflammatory direction (Tundup et al., 2015). LNFPIII, being a component of human milk, provides insight into its safety profile; so far, there have been no reported adverse reactions to it (Atochina et al., 2008; Bhargava et al., 2012; Srivastava et al., 2014; Tundup et al., 2015; Zhu et al., 2012). Studies have demonstrated LNFPIII's ability to increase production of anti-inflammatory cytokines under chronic states of inflammation and to alternatively activate macrophages (Atochina et al., 2008; Bhargava et al., 2012; Srivastava et al., 2014). Further, in an animal model of MS, LNFPIII significantly reduced the severity of experimental autoimmune encephalomyelitis, in part by decreasing inflammation and infiltration of immune cells into the CNS (Zhu et al., 2012).

Given the lack of detailed neurochemical characterization of accepted models of GWI and the modulatory effects that inflammation plays on neurotransmitter homeostasis, the present study sought to characterize the acute neurochemical monoamine profiles in two established GWI animal models. In addition, we also aimed at further characterizing the hippocampal neuroinflammatory profiles of these two models, as this is a key structure associated with GWI-related cognitive dysfunction. Finally, we examined whether the

immunotherapeutic LNFPIII had any modulatory effects on the aforementioned parameters.

2. Materials and Methods

2.1 Materials

The following chemicals were used for animal treatments: pyridostigmine bromide (PB; Sigma Aldrich, St. Louis, MO), permethrin (PM; 29.5% cis/69.5% trans isomer; Chem Service Inc., West Chester, PA), diisopropylfluorophosphate (DFP; Sigma Aldrich), N-Diethyl-3-methylbenzamide (DEET; Sigma Aldrich), and corticosterone (CORT; Steraloids, Newport, RI). Lacto-N-fucopentaose III (LNFPIII) dextran conjugate was produced as previously described (Tundup et al., 2015). All additional chemicals and reagents used in this study, unless otherwise noted, were of analytical or higher grade and were obtained from Sigma Aldrich or Fisher Scientific (Hampton, NH).

2.2 Animals

Male C57BL/6J mice (8-9 weeks old; Jackson Laboratories, Bar Harbor, ME) were housed 4 per cage in an environmentally controlled room (22-24° C) and maintained on a 12 h light/dark cycle (0700-1900 lights on) for one week of acclimation and throughout the study. Mice were handled daily prior to the start of the study to minimize experimenter induced stress. Food and water were available *ad libitum*. All procedures were approved in advance by the University of Georgia Institutional Animal Care and Use Committee and were in accordance with the latest National Institutes of Health and ARRIVE guidelines.

2.3 GWI Models

The present study followed two established, chemically different GWI animal models as outlined in Figure 1 (O'Callaghan et al., 2015; Zakirova et al., 2015). Following

Zakirova et al. (2015), mice (N=24) were treated daily for 10 days with a combination of PB and PM (0.7 and 200 mg/kg, respectively) or DMSO vehicle IP, immediately followed by a SC injection of LNFPIII or dextran vehicle (both 35 μg/mouse) diluted in sterile saline. For this model, there were 4 treatment groups with 6 mice per group and were as follows: Vehicle-Vehicle (DMSO-Dextran), Vehicle-LNFPIII (DMSO-LNFPIII), PB/PM-Vehicle (PB/PM-Dextran), and PB/PM-LNFPIII. This model will be referred to as Model 1 throughout this manuscript (Fig. 1A).

A separate cohort of mice (N=26), following O'Callaghan et al. (2015), were treated for 14 days with a combination of PB and DEET (2 and 30 mg/kg, respectively; SC), or saline vehicle and immediately followed by LNFPIII or dextran vehicle (both 35 μg/mouse) diluted in sterile saline. On days 8-14, these mice were also administered CORT via drinking water (200 mg/L in 1.5% EtOH tap water) ad libitum; control mice were given the 1.5% EtOH vehicle water during this period. On day 15, mice received a single IP injection of DFP (3.75 mg/kg) or saline vehicle. Four treatment groups were as follows: Vehicle-Vehicle (Saline/water/saline-Dextran), Vehicle-LNFPIII (Saline/water/saline-LNFPIII), PB/DEET/CORT/DFP-Vehicle (PB/DEET/CORT/DFP-Dextran), and PB/DEET/CORT/DFP-LNFPIII. There were 6 mice per treatment group, except in the PB/DEET/CORT/DFP-Vehicle group in which there were 8. This model will be referred to as Model 2 throughout this manuscript (Fig. 1B).

2.4 Tissue Collection

Six hours after the last treatment, mice were euthanized, blood was collected, and organs (brain, inguinal lymph nodes, spleen, thymus, liver and kidney) were weighed and frozen on dry ice. For the brain only, a sagittal cut was made and one half was quickly

frozen on dry ice while the other half was immersed in 4% paraformaldehyde for fixation as in Krishna *et al.* (2016). All tissues were stored at -80° C until analysis.

2.5 Neurochemistry

Concentrations of brain and spleen monoamines and their metabolites were determined using high performance liquid chromatography with electrochemical detection (HPLC-ECD) as previously described (Coban and Filipov, 2007; Krishna et al., 2016). Briefly, brains were sectioned into 500-μm thick slices and micropunches (1.5 mm diameter) from the prefrontal cortex (PFC), nucleus accumbens (NAc), striatum (STR), amygdala (AMY), dorsal hippocampus (dHIP), and ventral hippocampus (vHIP) were homogenized in 100 μl of 0.2 N $HClO_4$. A small portion (average 6.2 mg weight) of the spleen was cut, weighed and homogenized in 200 μl of 0.2 N $HClO_4$. Samples were centrifuged (13,200 x G at 4° C for 10 min) and sample supernatant (20 μL) was injected into the HPLC-ECD for detection of: 1) norepinephrine (NE) and its metabolite 3-methoxy-4-hydroxyphenylglycol (MHPG); 2) dopamine (DA) and its metabolite homovanillic acid (HVA); 3) serotonin (5-HT) and its metabolite 5-hydroxyindoleacetic acid (5-HIAA). Prior to statistical analysis, neurotransmitters and metabolite levels were protein-normalized using the Bradford assay as previously described (Coban and Filipov, 2007; Krishna et al., 2016).

2.6 Real-time quantitative PCR (qPCR) for inflammatory markers

Total RNA from a single brain punch (1.5 mm diameter, 500 μm thick section, ventral hippocampus: vHip) was isolated by an E.Z.N.A total RNA isolation kit (Omega Bio-Tek, Norcross, GA) according to the manufacturer's directions. The RNA was quantified with a Take3 micro-volume plate and Epoch microplate spectrophotometer

(BioTek, Winooski, VT). Seventy-five ng RNA/sample was used to synthesize cDNA with a Maxima first strand cDNA synthesis kit for RT-qPCR (Thermo Scientific, Waltham, MA) and a Peltier thermal cycler (Bio-Rad, Hercules, CA; 10 min at 25°C, 15 min at 50°C, 5 min at 85°C). Using 1 or 2 ng of cDNA per sample, expression of various inflammatory genes (Supplementary Table 1) were determined by a qPCR with mouse-specific primers (RealTimePrimers, Elkins Park, PA) and Maxima SYBR Green/lowRox qPCR Master Mix (2x) (Thermo Scientific). Amplifications were performed on Mx3005P qPCR machine (Stratagene, San Diego, CA) and treatment differences were calculated as a fold change by the $^{\Delta\Delta}$ Ct method with 18S as the house keeping gene, as described previously (Krishna et al., 2016; Lin et al., 2013).

2.7 Statistical Analysis

Two-way analysis of variance (ANOVA) was used to determine main effects of treatments or treatment interactions with each GWI model analyzed separately. If a two-way ANOVA was significant ($p \leq 0.05$), treatment means were separated by Student-Newman-Keuls (SNK) *post hoc* test or pairwise comparisons (as appropriate). If normality failed, data were log transformed prior to statistical analyses, but the non-transformed values were used for graphical representation. Data were analyzed using SigmaPlot 12.5 (San Jose, CA), and graphs were generated using GraphPad Prism 5 (San Diego, CA).

3. Results

3.1 Brain Neurotransmitters

3.1.1 Serotonin (5-HT)

In the NAc, levels of the 5-HT metabolite 5-HIAA were increased in both models (Model 1, $p \leq 0.01$, Fig. 2b and Model 2, $p \leq 0.05$, Fig. 2b') by GWI chemicals. This was

accompanied by a numerical decrease of 5-HT in Model 1 (Fig. 2a) and significant decrease of 5-HT in Model 2 ($p \leq 0.05$, Fig 2a'). LNFPIII treatment did not have a significant effect on NAc 5-HIAA, but it did prevent the numerical/significant decreases of 5-HT caused by GWI chemicals in both models (Fig. 2a and 2a'). As a result, 5-HT turnover (5-HIAA/5-HT ratio) was increased by GWI chemicals significantly in both models (Fig. 2c, $p \leq 0.05$ and Fig. 2c', $p \leq 0.05$); this effect was numerically prevented by LNFPIII (Fig. 2c', $p = 0.06$).

Similarly, in the vHip, GWI chemicals increased levels of the 5-HT metabolite 5-HIAA in Model 1 ($p \leq 0.05$, Fig. 2e) and numerically in Model 2. This was accompanied by a concomitant increase in 5-HT by GWI chemicals significantly in Model 1 ($p \leq 0.05$, Fig. 2d) and trending in Model 2 ($p = 0.07$, Fig. 2d'). LNFPIII did not have an effect on the levels of 5-HIAA, however, it did prevent the increases in 5-HT in both models (Model 1, $p \leq 0.05$, Fig. 2d and Model 2, $p = 0.06$, Fig. 2d'). Due to the increases in both 5-HIAA and 5-HT, the 5-HIAA/5-HT ratio in the vHip was not affected by GWI chemicals (Fig. 2f and 2f').

Serotonergic effects of the GWI chemicals in other regions included the STR, AMY, and dHip. In particular, in Model 1 GWI chemicals increased levels of 5-HIAA in the STR, AMY, and dHip (p's ≤ 0.05, Table 1) and these effects were not present in Model 2 (Table 2). There was a trend ($p \leq 0.10$) for increases in 5-HT turnover by GWI chemicals in both models for the STR (data not shown) and in Model 2 for the AMY (data not shown). LNFPIII did not prevent GWI chemical effects on striatal 5-HIAA, but it did prevent the numerical decrease of STR 5-HT in Model 1 ($p = 0.06$, Table 1). As a result, LNFPIII

prevented the increase in STR turnover in Model 1 ($p \leq 0.05$), an effect not observed in Model 2 (data not shown).

3.1.2 Dopamine (DA)

In the vHip, numerical and trending increases in DA by GWI chemicals were present in Model 1 (Fig. 3c) and Model 2 ($p = 0.08$, Fig. 3c'), respectively. These effects were accompanied by increases in the DA metabolite HVA in Model 1 (Fig. 3d) and Model 2 ($p \leq 0.05$, Fig. 3d'). In Model 1, LNFPIII prevented the increase in vHip DA ($p \leq 0.05$, Fig. 3c) and the numerical increase in HVA. Interestingly, LNFPIII further increased levels of both DA (Fig. 3c') and HVA ($p \leq 0.05$, Fig. 3d') in Model 2, suggesting that the drive for GWI chemicals induced DA dyshomeostasis in the vHip and the modulatory effect of LNFPIII is model-specific.

In the dHip, trending decreases and significant increases of DA by GWI chemicals were apparent in Model 1 ($p = 0.10$, Table 1) and Model 2 ($p \leq 0.05$, Table 2), respectively. This was accompanied by increases of the DA metabolite HVA in both models, with Model 2's effects of HVA being significant ($p \leq 0.001$, Table 2). LNFPIII did not prevent the effects observed in Model 1. However, similar to the vHip, LNFPIII further increased HVA in Model 2 ($p \leq 0.05$, Table 2). As a result, trends ($p < 0.10$) for increased turnover (HVA/DA ratio) were apparent in both models (data not shown).

DA alterations by GWI chemicals were also observed in the PFC and STR in Model 1, NAc in Model 2, and AMY in both models. Increases in HVA by GWI chemicals were observed in the STR ($p \leq 0.05$, Table 1) and PFC (Table 1) in Model 1. This was accompanied by a numerical increase in DA in the PFC (Table 1) in Model 1. As a result of the increased HVA by GWI chemicals in the STR of Model 1, there was an increase in

turnover ($p \leq 0.001$, data not shown). Similar trending increases in turnover were apparent in the AMY ($p = 0.07$, data not shown) in Model 1 and NAc ($p = 0.09$, data not shown) in Model 2. LNFPIII did not modulate the increases in DA, HVA, or turnover in these regions, except for the PFC, in which LNFPIII prevented the numerical increases of DA and HVA in Model 1 (Table 1).

3.2 Spleen Neurotransmitters

In Model 1, a significant treatment interaction ($p \leq 0.05$, Table 3) was seen on splenic 5-HT; LNFPIII prevented the 5-HT increase by GWI chemicals, but also increased 5-HT on its own (Table 3). No significant differences in splenic 5-HIAA were present in this model. In Model 2, GWI chemicals significantly increased levels of 5-HT ($p \leq 0.01$, Table 3) and 5-HIAA ($p \leq 0.05$, Table 3). LNFPIII did not prevent the 5-HT or 5-HIAA effects in Model 2. Splenic 5-HT turnover remained unaffected by treatments in both models.

In Model 1, no significant alterations in splenic NE, its metabolite MHPG or NE turnover (MHPG/NE ratio) were present (Table 3). However, in Model 2, LNFPIII (trending, $p = 0.10$) increased NE in the presence of GWI chemicals (Table 3). GWI chemicals significantly increased MHPG ($p \leq 0.05$; Table 3) and LNFPIII also increased MHPG (trending, $p = 0.10$; Table 3). This increase in MHPG by GWI chemicals led to a trending increase in NE turnover ($p = 0.06$, data not shown) in Model 2.

3.3 Real-time qPCR for inflammatory markers in the vHip

In Model 1, PB/PM caused significant upregulation of IL-1β (Fig. 5a), CCL-2 (Fig. 4c), YM-1 (Fig. 4f) and F4/80 (Table 4; p's ≤ 0.05) in the vHip. Casp1 was also significantly increased ($p \leq 0.01$, Fig. 4d), and there was a numerical increase of TNFα (p

= 0.07, Table 4). In mice treated with LNFPIII, increases in Fizz1 (Table 4), Casp1 (Fig. 4d), and YM-1 (Fig. 4f) were prevented and there were similar trends for preventing the increases of IL-1β and CCL-2 (Fig. 4a and c). IL-18 was increased specifically by LNFPIII in the PB/PM + LNFPIII group ($p \leq 0.01$, Fig. 4e).

In Model 2, PB/DEET/CORT/DFP caused significant and robust upregulation of IL-1β (Fig. 4g), CCL-2 (Fig. 4i), YM-1 (Fig. 4l), and IL-6 (Fig. 4h) (p's ≤ 0.001). Trending increases by PB/DEET/CORT/DFP were apparent for TNFα ($p = 0.07$, Table 4) and HMBG1 ($p = 0.09$, Table 4). LNFPIII did not prevent these effects. However, in the presence of LNFPIII, the increases of F4/80 ($p= 0.09$, Table 4) and YM-1 ($p \leq 0.05$, Fig. 4l) by PB/DEET/CORT/DFP were lessened.

Here, we also examined the ratio between anti-inflammatory Arg1 and inflammatory NOS2 to determine the nitric oxide status (Rath et al., 2014). While there were no significant changes in either model for Arg1 or NOS2 hippocampal mRNAs (Table 4), PB/PM treatment caused a trending reduction in the Arg1/NOS2 ratio ($p = 0.06$, Table 4) that was unaffected by LNFPIII.

4. Discussion

It has been well documented that veterans with GWI experienced a myriad of chemical exposures during the 1990-1991 Gulf War. Thus, it is imperative to take advantage of models with similar chemical conditions to further understand the pathogenesis of GWI and identify possible therapeutic targets (White et al., 2016). Here, we utilized two chemically different GWI models (O'Callaghan et al., 2015; Zakirova et al., 2015)to further characterize the models' immediate monoamine profiles after GWI chemicals exposure, discern the neuroinflammatory environments, and examine how a

novel immunomodulatory treatment, LNFPIII, can modulate the aforementioned parameters. To characterize the neurochemical profiles of the two models utilized in this study, monoamines were examined from various brain regions and the spleen with the use of HPLC-ECD. Further, neuroinflammation was evaluated in the ventral hippocampus (vHip) with qPCR. Perturbations were evident in both models for monoamines, both centrally and peripherally, and for brain inflammatory markers. LNFPIII treatment modulated a number of these effects.

A number of behavioral symptoms experienced by GWI veterans could be explained, at least in part, by monoamine dyshomeostasis. Several reports have implicated alterations in cognition and memory, motor function, and mood in the pathology of GWI (Carreras et al., 2018; Parihar et al., 2013). Here, evidence for alterations in central levels of 5-HT, DA, as well as changes in inflammatory markers, could explain the some of the symptoms experienced by GWI veterans, especially if these perturbations are lasting and/or have lasting consequences.

Increased serotonin utilization was evident in multiple structures including the NAc, STR, AMY, dHip, and vHip. In both models, GWI chemicals led to increased metabolism of 5-HT in the NAc and vHip; these areas are highly innervated by serotoninergic projections that regulate affect, as well as memory (Hensler, 2006). LNFPIII modulated these serotoninergic effects in both models. For example, while in the NAc of both models increases in 5-HIAA were not modulated by LNFPIII, it prevented increases in 5-HT turnover by causing a compensatory increase in 5-HT, albeit to a lesser extent in Model 2. Similar effects on 5-HT were observed in the vHip. The less pronounced and subtle effects of LNFPIII in Model 2 could be attributed to the more impactful nature of

this model. Thus, a larger dose of the LNFPIII, as in previous studies using LNFPIII treatment (50 μg), could be entertained in future studies using Model 2 (Tundup et al., 2015; Zhu et al., 2012). Persistence of these acute effects by GWI chemicals exposure may lead to mood disturbances such as anxiety and depression, as well as influence fatigue, which all play part in GWI symptomology (DDGWIRP, 2018; Korte-Bouws et al., 2018; Pavese et al., 2010). Further, it has been shown that persistent alterations in 5-HT affect hippocampal neurogenesis; thus, the increases in hippocampal metabolism of 5-HT in both models observed here may impact learning, memory, and mood regulation in the long term (Alenina and Klempin, 2015; Sahay et al., 2011). By compensating for GWI chemicals effects on 5-HT homeostasis, LNFPIII might aid in mitigating some of these neurological deficits.

Dopamine dyshomeostasis was evident in both models within multiple brains regions (STR, AMY, vHip, and dHip), albeit to a different extent. These areas, all innervated by DA projections, regulate cognition, learning and memory, emotional processing and motor function (Belujon and Grace, 2017; Kempadoo et al., 2016; Willard et al., 2015). Here, GWI chemicals caused similar increases in DA utilization (turnover) in the dHip in both models. Model specific alterations of DA were also apparent in the STR, AMY, and vHip in Model 1 and NAc and vHip in Model 2. LNFPIII modulations of DA were apparent, but distinct, among the models. For example, in Model 1, LNFPIII prevented elevations in DA in the vHip. However, in Model 2, LNFPIII further increased DA. This suggests that the overlap of DA effects between the two models is brain region specific and that LNFPIII effects are both model- and brain region-specific. Persistent utilization of DA, especially in regions such as the hippocampus or striatum, may lead to

behavioral dysfunction. GWI veterans have shown deficits in tasks of memory and cognitive function compared to healthy controls, and many of these results have been recapitulated in animal studies (Abdullah et al., 2011; Anger et al., 1999; Hattiangady et al., 2014; Hubbard et al., 2014; Macht et al., 2019; Parihar et al., 2013; White et al., 2016; Zakirova et al., 2015). Dopamine release promotes learning and memory in the dorsal hippocampus; increased acute utilization of DA in the present study suggests decreased tissue reserve that could impact learning and memory where DA would be needed in the process (Kempadoo et al., 2016). Further, GWI veterans show deficits in psychomotor tasks (Anger et al., 1999; Proctor et al., 2006) that could be linked to increased utilization of DA by GWI chemicals in areas, such as the PFC and STR, in both models. The STR is a crucial area for regulation of movement and interestingly, stress (a major component of Model 2) has been implicated in disrupting striatal DA metabolism, resulting in motor deficits (Haber, 2016; Sudha and Pradhan, 1995).

In the periphery, increases in splenic 5-HT by GWI chemicals in both models were apparent with the effects in Model 1 prevented by LNFPIII. These serotonergic effects suggest GWI chemicals caused acute peripheral serotonin imbalance. Increased utilization of 5-HT plays a role in activating T-cells and modulates immune responses, i.e., cytokine release (Wu et al. 2018). To this end, peripheral increases in IL-6 and TNFα can mediate disturbances in mood, i.e., anxiety and depression (Wohleb et al., 2014; You et al., 2011). In addition, 5-HT alterations in the periphery might be reflective of the homeostasis of this neurotransmitter in the CNS (Herr et al., 2017). Perturbations in splenic norepinephrine were not apparent in Model 1. However, GWI chemicals in Model 2 elevated the NE metabolite MHPG and this effect was not prevented by LNFPIII resulting in an elevation

in NE turnover. This is most likely explained by this model's exposure to corticosterone, as stress has been shown to deplete NE in the spleen, in part by increasing its metabolism (Blandino et al., 2006; Kennedy et al., 2005). Further, this increased metabolism of NE in the spleen could lead to elevations in inflammatory mediators peripherally (Blandino et al., 2006) and could explain some of the central inflammation in this model.

Multiple GWI studies, including with one of the models utilized in the present study, have determined that systemic inflammation and widespread neuroinflammation, particularly within the hippocampus, is apparent post exposure to GWI chemicals (Broderick et al., 2013; Broderick et al., 2018; O'Callaghan et al., 2015; Parkitny et al., 2015). Here, we evaluated expression of various inflammatory genes in the vHip to compare to the previous research conducted (i.e., O'Callaghan et al. 2015), characterize neuroinflammation in Model 1 de novo, and determine if this coincides with the altered CNS monoamine neurochemistry.

In both models, increased levels of CCL-2, IL-1β, TNFα and YM-1 expression was apparent with the magnitude of the increase being greater in Model 2. Of note, IL-6 was not affected in Model 1, but was significantly upregulated in Model 2. The early effects on CCL-2, IL-1β and IL-6 seen in Model 2 mirror the inflammatory effects observed in a previous study with this model (O'Callaghan et al., 2015). Concomitant with the less robust acute neuroinflammation in Model 1, LNFPIII was an effective anti-inflammatory treatment in this model, but less so in Model 2. Of note, Casp1 was upregulated by GWI chemicals in Model 1, but not when LNFPIII was also present. The upregulation of Casp1, at least in Model 1, is suggestive of inflammasome activation, which could lead to increases in active IL-1β, as the mature form of IL-1β is dependent on Casp1 cleavage (Deng et al.,

2019; Dinarello et al., 2013). The fact that LNFPIII prevented this effect on Casp1 indicates that part of its protective effects is by preventing inflammasome activation. Interestingly, expression of IL-18 was increased by LNFPIII in the presence of GWI chemicals in Model 1. A recent study highlighted the synergistic role that IL-18 and IL-10 play in M2 macrophage polarization (Kobori et al., 2018), suggesting that the increases in brain IL-18 by LNFPIII might work in concert with Casp-1 inhibition to curb inflammation. F4/80, a marker of both M1 and M2 microglia (Greter et al., 2015), was upregulated by GWI chemicals in both models, but LNFPIII only dampened this increase in Model 2. Further, YM-1, a microglia M2 marker, was increased in both models. These increases in M2 microglia markers suggest an immune system attempt to rebalance the responses to GWI chemicals at this early time point (Ansari, 2015). Of note, the Arg1:NOS2 ratio was only marginally affected (decreased) by GWI treatment (Model 1) and LNFPIII did not modulate this ratio. This indicates that nitric oxide likely plays a secondary or minor role in the GWI chemicals induced neuroinflammation and its consequences. Overall, brain qPCR data suggest that (1) both models skew the innate immune system towards inflammation by targeting mostly inflammatory cytokines and less so nitric oxide balancing molecules and (2) the anti-inflammatory effects of LNFPIII in this context are cytokine-centered.

LNFPIII produces its anti-inflammatory effects by targeting the CD14/TLR-4 signaling to activate ERK dependent production of several anti-inflammatory mediators (Atochina et al., 2008; Srivastava et al., 2014; Tundup et al., 2015). The fact that LNFPIII modulated inflammatory effects primarily in Model 1, but not as well in the Model 2 could be attributed to the potent nature of this model (Locker et al., 2017; O'Callaghan et al.,

2015). The acute increases in inflammatory cytokines might be too strong to allow for LNFPIII to be potent anti-inflammatory in the short-term in Model 2 and a higher LNFPIII dose might be needed to combat the effects of DFP treatment (O'Callaghan et al., 2015). However, the level of inflammation/neuroinflammation by GWI is more subtle in Model 1 and data from this model suggests that LNFPIII, at the treatment level used here, might be effective if given in an acute GWI-exposure related scenario.

5. Summary/Conclusion

Overall, centrally, in both models, serotonergic and dopaminergic dyshomeostasis was present in multiple brain regions. However, the effects observed varied between models and was more pronounced in Model 1. Peripherally, splenic 5-HT and NE were altered by GWI chemicals, primarily in Model 2. Further, GWI chemicals in both models produced some shared (IL-1β, CCL-2, TNFα and YM-1) and model specific elevations in hippocampal inflammatory markers. LNFPIII treatment modulated many of these acute effects, especially in brain neurochemistry and neuroinflammation (Summary Fig. 5). Many of these acute effects post GWI chemicals treatment, if persistent in the long term, could mediate the symptoms GWI veterans currently experience. LNFPIII shows protective effects at this early time point in restoring neurochemical disbalance and neuroinflammation, highlighting its value as a promising therapeutic that should be further investigated in long term GWI studies after initial GWI chemicals exposure.

6. Acknowledgements/Conflicts of interest

The authors declare no conflicts of interest. This research was supported by Department of Defense grant number W81XWH-16-1-0586 to NMF. HEG's participation in this research was made possible by NIH grant T35OD010433.

7. References

Abdullah, L., Crynen, G., Reed, J., Bishop, A., Phillips, J., Ferguson, S., Mouzon, B., Mullan, M., Mathura, V., Mullan, M., Ait-Ghezala, G., Crawford, F., 2011. Proteomic CNS profile of delayed cognitive impairment in mice exposed to Gulf War agents. Neuromolecular Med 13(4), 275-288.

Alenina, N., Klempin, F., 2015. The role of serotonin in adult hippocampal neurogenesis. Behav Brain Res 277, 49-57.

Anger, W., Storzbach, D., Binder, L., Campbell, K., Rohlman, D., McCauley, L., 1999. Evidence of cognitive deficits in Persian Gulf War veterans: interim report from a population-based study. J Int Neuropsychol Soc 5, 203-212.

Ansari, M.A., 2015. Temporal profile of M1 and M2 responses in the hippocampus following early 24h of neurotrauma. J Neurol Sci 357(1-2), 41-49.

Atochina, O., Da'dara, A.A., Walker, M., Harn, D.A., 2008. The immunomodulatory glycan LNFPIII initiates alternative activation of murine macrophages in vivo. Immunology 125(1), 111-121.

Baraniuk, J.N., El-Amin, S., Corey, R., Rayhan, R., Timbol, C., 2013. Carnosine treatment for gulf war illness: a randomized controlled trial. Glob J Health Sci 5(3), 69-81.

Belujon, P., Grace, A.A., 2017. Dopamine System Dysregulation in Major Depressive Disorders. Int J Neuropsychopharmacol 20(12), 1036-1046.

Bhargava, P., Li, C., Stanya, K.J., Jacobi, D., Dai, L., Liu, S., Gangl, M.R., Harn, D.A., Lee, C.H., 2012. Immunomodulatory glycan LNFPIII alleviates hepatosteatosis and insulin resistance through direct and indirect control of metabolic pathways. Nat Med 18(11), 1665-1672.

Blandino, P., Jr., Barnum, C.J., Deak, T., 2006. The involvement of norepinephrine and microglia in hypothalamic and splenic IL-1beta responses to stress. J Neuroimmunol 173(1-2), 87-95.

Boyd, K.C., Hallman, W.K., Wartenberg, D., Fiedler, N., Brewer, N.T., Kipen, H.M., 2003. Reported Exposures, Stressors, and Life Events Among Gulf War Registry Veterans. Journal of Occupational and Environmental Medicine 45(12), 1247-1256.

Broderick, G., Ben-Hamo, R., Vashishtha, S., Efroni, S., Nathanson, L., Barnes, Z., Fletcher, M.A., Klimas, N., 2013. Altered immune pathway activity under exercise challenge in Gulf War Illness: an exploratory analysis. Brain Behav Immun 28, 159-169.

Broderick, G., Fletcher, M.A., Gallagher, M., Barnes, Z., Vernon, S.D., Klimas, N.G., 2018. Exploring the Diagnostic Potential of Immune Biomarker Co-expression in Gulf War Illness. Methods Mol Biol 1781, 101-120.

Capuron, L., Miller, A.H., 2011. Immune system to brain signaling: neuropsychopharmacological implications. Pharmacol Ther 130(2), 226-238.

Carreras, I., Aytan, N., Mellott, T., Choi, J.K., Lehar, M., Crabtree, L., Leite-Morris, K., Jenkins, B.G., Blusztajn, J.K., Dedeoglu, A., 2018. Anxiety, neuroinflammation, cholinergic and GABAergic abnormalities are early markers of Gulf War illness in a mouse model of the disease. Brain Res 1681, 34-43.

Chao, L.L., Rothlind, J.C., Cardenas, V.A., Meyerhoff, D.J., Weiner, M.W., 2010. Effects of low-level exposure to sarin and cyclosarin during the 1991 Gulf War on brain function and brain structure in US veterans. Neurotoxicology 31(5), 493-501.

Cherry, N., Creed, F., Silman, A., Dunn, G., Baxter, D., Smedley, J., Taylor, S., Macfarlane, G.J., 2001. Health and exposures of United Kingdom Gulf war veterans. Part II: The relation of health to exposure. Occup Environ Med 58(5), 299-306.

Coban, A., Filipov, N.M., 2007. Dopaminergic toxicity associated with oral exposure to the herbicide atrazine in juvenile male C57BL/6 mice. J Neurochem 100(5), 1177-1187.

Czirr, E., Wyss-Coray, T., 2012. The immunology of neurodegeneration. J Clin Invest 122(4), 1156-1163.

DDGWIRP, 2018. The Gulf War Illness Landscape in: Programs, D.o.D.C.D.M.R. (Ed.).

Deng, J., Yu, X.Q., Wang, P.H., 2019. Inflammasome activation and Th17 responses. Mol Immunol 107, 142-164.

Dinarello, C.A., Novick, D., Kim, S., Kaplanski, G., 2013. Interleukin-18 and IL-18 binding protein. Front Immunol 4, 289.

Donta, S.T., Engel, C.C., Jr., Collins, J.F., Baseman, J.B., Dever, L.L., Taylor, T., Boardman, K.D., Kazis, L.E., Martin, S.E., Horney, R.A., Wiseman, A.L., Kernodle, D.S., Smith, R.P., Baltch, A.L., Handanos, C., Catto, B., Montalvo, L., Everson, M., Blackburn, W., Thakore, M., Brown, S.T., Lutwick, L., Norwood, D., Bernstein, J., Bacheller, C., Ribner, B., Church, L.W., Wilson, K.H., Guduru, P., Cooper, R., Lentino, J., Hamill, R.J., Gorin, A.B., Gordan, V., Wagner, D., Robinson, C., DeJace, P., Greenfield, R., Beck, L., Bittner, M., Schumacher, H.R., Silverblatt, F., Schmitt, J., Wong, E., Ryan, M.A., Figueroa, J., Nice, C., Feussner, J.R., Group, V.A.C., 2004. Benefits and harms of doxycycline treatment for Gulf War veterans' illnesses: a randomized, double-blind, placebo-controlled trial. Ann Intern Med 141(2), 85-94.

Dunn, A.J., 2006. Effects of cytokines and infections on brain neurochemistry. Clin Neurosci Res 6(1-2), 52-68.

Felger, J.C., Miller, A.H., 2012. Cytokine effects on the basal ganglia and dopamine function: the subcortical source of inflammatory malaise. Front Neuroendocrinol 33(3), 315-327.

Ferrari, C.C., Tarelli, R., 2011. Parkinson's disease and systemic inflammation. Parkinsons Dis 2011, 436813.

Golomb, B.A., Allison, M., Koperski, S., Koslik, H.J., Devaraj, S., Ritchie, J.B., 2014. Coenzyme Q10 benefits symptoms in Gulf War veterans: results of a randomized double-blind study. Neural Comput 26(11), 2594-2651.

Greter, M., Lelios, I., Croxford, A.L., 2015. Microglia Versus Myeloid Cell Nomenclature during Brain Inflammation. Front Immunol 6, 249.

Haber, S.N., 2016. Corticostriatal circuitry. Dialogues Clin Neurosci 18(1), 7-21.

Hattiangady, B., Mishra, V., Kodali, M., Shuai, B., Rao, X., Shetty, A.K., 2014. Object location and object recognition memory impairments, motivation deficits and depression in a model of Gulf War illness. Front Behav Neurosci 8, 78.

Hensler, J.G., 2006. Serotonergic modulation of the limbic system. Neurosci Biobehav Rev 30(2), 203-214.

Herr, N., Bode, C., Duerschmied, D., 2017. The Effects of Serotonin in Immune Cells. Front Cardiovasc Med 4, 48-48.

Hubbard, N.A., Hutchison, J.L., Motes, M.A., Shokri-Kojori, E., Bennett, I.J., Brigante, R.M., Haley, R.W., Rypma, B., 2014. Central Executive Dysfunction and Deferred Prefrontal Processing in Veterans with Gulf War Illness. Clin Psychol Sci 2(3), 319-327.

Karin, M., Lawrence, T., Nizet, V., 2006. Innate Immunity Gone Awry: Linking Microbial Infections to Chronic Inflammation and Cancer. Cell 124(4), 823-835.

Kempadoo, K.A., Mosharov, E.V., Choi, S.J., Sulzer, D., Kandel, E.R., 2016. Dopamine release from the locus coeruleus to the dorsal hippocampus promotes spatial learning and memory. Proc Natl Acad Sci U S A 113(51), 14835-14840.

Kennedy, S.L., Nickerson, M., Campisi, J., Johnson, J.D., Smith, T.P., Sharkey, C., Fleshner, M., 2005. Splenic norepinephrine depletion following acute stress suppresses in vivo antibody response. J Neuroimmunol 165(1-2), 150-160.

Kobori, T., Hamasaki, S., Kitaura, A., Yamazaki, Y., Nishinaka, T., Niwa, A., Nakao, S., Wake, H., Mori, S., Yoshino, T., Nishibori, M., Takahashi, H., 2018. Interleukin-18 Amplifies Macrophage Polarization and Morphological Alteration, Leading to Excessive Angiogenesis. Front Immunol 9(334), 334.

Korte-Bouws, G.A.H., van Heesch, F., Westphal, K.G.C., Ankersmit, L.M.J., van Oosten, E.M., Gunturkun, O., Korte, S.M., 2018. Bacterial Lipopolysaccharide Increases Serotonin Metabolism in Both Medial Prefrontal Cortex and Nucleus Accumbens in Male Wild Type Rats, but Not in Serotonin Transporter Knockout Rats. Pharmaceuticals (Basel) 11(3), 66.

Krishna, S., Lin, Z., de La Serre, C.B., Wagner, J.J., Harn, D.H., Pepples, L.M., Djani, D.M., Weber, M.T., Srivastava, L., Filipov, N.M., 2016. Time-dependent behavioral, neurochemical, and metabolic dysregulation in female C57BL/6 mice caused by chronic high-fat diet intake. Physiol Behav 157, 196-208.

Lin, Z., Dodd, C.A., Filipov, N.M., 2013. Short-term atrazine exposure causes behavioral deficits and disrupts monoaminergic systems in male C57BL/6 mice. Neurotoxicol Teratol 39, 26-35.

Locker, A.R., Michalovicz, L.T., Kelly, K.A., Miller, J.V., Miller, D.B., O'Callaghan, J.P., 2017. Corticosterone primes the neuroinflammatory response to Gulf War Illness-relevant organophosphates independently of acetylcholinesterase inhibition. Journal of neurochemistry 142(3), 444-455.

Macht, V.A., Woodruff, J.L., Maissy, E.S., Grillo, C.A., Wilson, M.A., Fadel, J.R., Reagan, L.P., 2019. Pyridostigmine bromide and stress interact to impact immune function, cholinergic neurochemistry and behavior in a rat model of Gulf War Illness. Brain, Behavior, and Immunity.

Megahed, T., Hattiangady, B., Shuai, B., Shetty, A.K., 2014. Parvalbumin and neuropeptide Y expressing hippocampal GABA-ergic inhibitory interneuron numbers decline in a model of Gulf War illness. Front Cell Neurosci 8, 447.

Miller, J.V., LeBouf, R.F., Kelly, K.A., Michalovicz, L.T., Ranpara, A., Locker, A.R., Miller, D.B., O'Callaghan, J.P., 2018. The Neuroinflammatory Phenotype in a Mouse Model of Gulf War Illness is Unrelated to Brain Regional Levels of Acetylcholine as Measured by Quantitative HILIC-UPLC-MS/MS. Toxicological Sciences 165(2), 302-313.

O'Callaghan, J.P., Kelly, K.A., Locker, A.R., Miller, D.B., Lasley, S.M., 2015. Corticosterone primes the neuroinflammatory response to DFP in mice: potential animal model of Gulf War Illness. J Neurochem 133(5), 708-721.

Ojo, J.O., Abdullah, L., Evans, J., Reed, J.M., Montague, H., Mullan, M.J., Crawford, F.C., 2014. Exposure to an organophosphate pesticide, individually or in combination with other Gulf War agents, impairs synaptic integrity and neuronal differentiation, and is accompanied by subtle microvascular injury in a mouse model of Gulf War agent exposure. Neuropathology 34(2), 109-127.

Parihar, V.K., Hattiangady, B., Shuai, B., Shetty, A.K., 2013. Mood and memory deficits in a model of Gulf War illness are linked with reduced neurogenesis, partial neuron loss, and mild inflammation in the hippocampus. Neuropsychopharmacology 38(12), 2348-2362.

Parkitny, L., Middleton, S., Baker, K., Younger, J., 2015. Evidence for abnormal cytokine expression in Gulf War Illness: A preliminary analysis of daily immune monitoring data. BMC Immunol 16, 57.

Pavese, N., Metta, V., Bose, S.K., Chaudhuri, K.R., Brooks, D.J., 2010. Fatigue in Parkinson's disease is linked to striatal and limbic serotonergic dysfunction. Brain 133(11), 3434-3443.

Pott Godoy, M.C., Ferrari, C.C., Pitossi, F.J., 2010. Nigral neurodegeneration triggered by striatal AdIL-1 administration can be exacerbated by systemic IL-1 expression. J Neuroimmunol 222(1-2), 29-39.

Proctor, S.P., Heaton, K.J., Heeren, T., White, R.F., 2006. Effects of sarin and cyclosarin exposure during the 1991 Gulf War on neurobehavioral functioning in US army veterans. Neurotoxicology 27(6), 931-939.

Rath, M., Muller, I., Kropf, P., Closs, E.I., Munder, M., 2014. Metabolism via Arginase or Nitric Oxide Synthase: Two Competing Arginine Pathways in Macrophages. Front Immunol 5, 532.

Rayhan, R.U., Stevens, B.W., Timbol, C.R., Adewuyi, O., Walitt, B., VanMeter, J.W., Baraniuk, J.N., 2013. Increased brain white matter axial diffusivity associated with fatigue, pain and hyperalgesia in Gulf War illness. PLoS One 8(3), e58493.

Sahay, A., Scobie, K.N., Hill, A.S., O'Carroll, C.M., Kheirbek, M.A., Burghardt, N.S., Fenton, A.A., Dranovsky, A., Hen, R., 2011. Increasing adult hippocampal neurogenesis is sufficient to improve pattern separation. Nature 472(7344), 466-U539.

Srivastava, L., Tundup, S., Choi, B.S., Norberg, T., Harn, D., 2014. Immunomodulatory glycan lacto-N-fucopentaose III requires clathrin-mediated endocytosis to induce alternative activation of antigen-presenting cells. Infect Immun 82(5), 1891-1903.

Steele, L., Sastre, A., Gerkovich, M.M., Cook, M.R., 2012. Complex factors in the etiology of Gulf War illness: wartime exposures and risk factors in veteran subgroups. Environ Health Perspect 120(1), 112-118.

Sudha, S., Pradhan, N., 1995. Stress-induced changes in regional monoamine metabolism and behavior in rats. Physiol Behav 57(6), 1061-1066.

Toomey, R., Alpern, R., Vasterling, J.J., Baker, D.G., Reda, D.J., Lyons, M.J., Henderson, W.G., Kang, H.K., Eisen, S.A., Murphy, F.M., 2009. Neuropsychological functioning of U.S. Gulf War veterans 10 years after the war. J Int Neuropsychol Soc 15(5), 717-729.

Tundup, S., Srivastava, L., Norberg, T., Watford, W., Harn, D., 2015. A Neoglycoconjugate Containing the Human Milk Sugar LNFPIII Drives Anti-Inflammatory Activation of Antigen Presenting Cells in a CD14 Dependent Pathway. PLoS One 10(9), e0137495.

White, R.F., Steele, L., O'Callaghan, J.P., Sullivan, K., Binns, J.H., Golomb, B.A., Bloom, F.E., Bunker, J.A., Crawford, F., Graves, J.C., Hardie, A., Klimas, N., Knox, M., Meggs, W.J., Melling, J., Philbert, M.A., Grashow, R., 2016. Recent research on Gulf War illness and other health problems in veterans of the 1991 Gulf War: Effects of toxicant exposures during deployment. Cortex 74, 449-475.

Willard, A.M., Bouchard, R.S., Gittis, A.H., 2015. Differential degradation of motor deficits during gradual dopamine depletion with 6-hydroxydopamine in mice. Neuroscience 301, 254-267.

Wisniewski, T., Goni, F., 2015. Immunotherapeutic approaches for Alzheimer's disease. Neuron 85(6), 1162-1176.

Wohleb, E.S., McKim, D.B., Shea, D.T., Powell, N.D., Tarr, A.J., Sheridan, J.F., Godbout, J.P., 2014. Re-establishment of anxiety in stress-sensitized mice is caused by monocyte trafficking from the spleen to the brain. Biol Psychiatry 75(12), 970-981.

Wu, H., Denna, T.H., Storkersen, J.N., Gerriets, V.A., 2019. Beyond a neurotransmitter: The role of serotonin in inflammation and immunity. Pharmacol Res 140, 100-114.

You, Z., Luo, C., Zhang, W., Chen, Y., He, J., Zhao, Q., Zuo, R., Wu, Y., 2011. Pro- and anti-inflammatory cytokines expression in rat's brain and spleen exposed to chronic mild stress: involvement in depression. Behav Brain Res 225(1), 135-141.

Zakirova, Z., Tweed, M., Crynen, G., Reed, J., Abdullah, L., Nissanka, N., Mullan, M., Mullan, M.J., Mathura, V., Crawford, F., Ait-Ghezala, G., 2015. Gulf War agent exposure causes impairment of long-term memory formation and neuropathological changes in a mouse model of Gulf War Illness. PLoS One 10(3), e0119579.

Zella, S.M.A., Metzdorf, J., Ciftci, E., Ostendorf, F., Muhlack, S., Gold, R., Tonges, L., 2019. Emerging Immunotherapies for Parkinson Disease. Neurol Ther 8(1), 29-44.

Zhu, B., Trikudanathan, S., Zozulya, A.L., Sandoval-Garcia, C., Kennedy, J.K., Atochina, O., Norberg, T., Castagner, B., Seeberger, P., Fabry, Z., Harn, D., Khoury, S.J., Guleria, I., 2012. Immune modulation by Lacto-N-fucopentaose III in experimental autoimmune encephalomyelitis. Clin Immunol 142(3), 351-361.

Ziemssen, T., Derfuss, T., de Stefano, N., Giovannoni, G., Palavra, F., Tomic, D., Vollmer, T., Schippling, S., 2016. Optimizing treatment success in multiple sclerosis. J Neurol 263(6), 1053-1065.

Figures

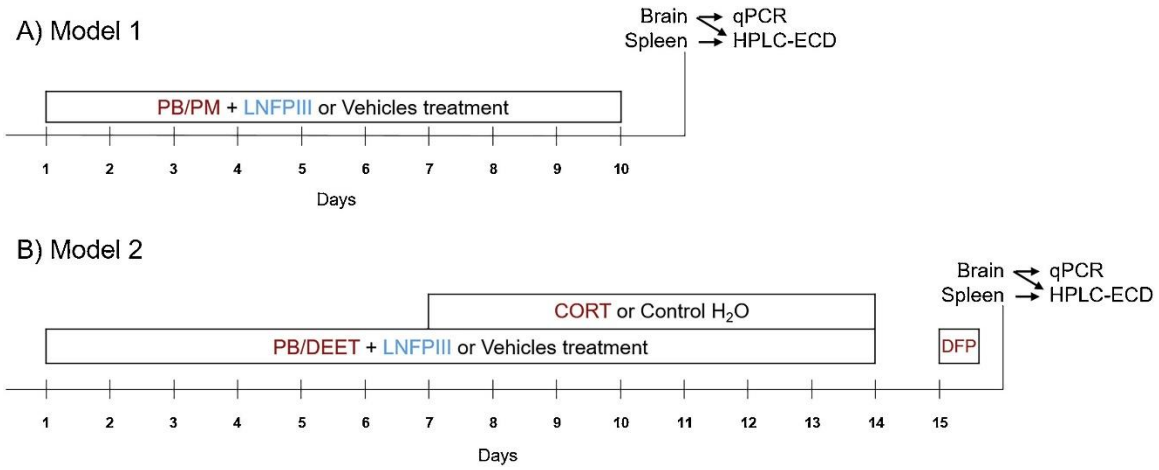

Fig. 2.1. Experimental design and description of the Gulf War Illness models. A) GWI Model 1 (Zakirova et al., 2015) followed a 10 day treatment protocol of pyridostigmine bromide (PB; 0.7 mg/kg, IP) and permethrin (PM; 200 mg/kg, IP) or DMSO vehicle followed by concurrent administration of LNFPIII (35 µg, SC) or dextran vehicle (35 µg, SC). B) GWI Model 2 (O'Callaghan et al., 2015) induced GWI over a 15 day protocol in which PB (2 mg/kg, SC) and N,N-Diethyl-methylbenzamide (DEET;30 mg/kg, SC) or saline vehicle followed by concurrent LNFPIII (35 µg) or dextran vehicle (35 µg) were administered for 14 days. Corticosterone (CORT; 200 mg/L in 1.5% EtOH water) or vehicle were administered on days 7-14. A single injection of DFP (3.75 mg/kg) or saline vehicle was given on day 15. In both models, mice were sacrificed 6 h post the last treatment, and neurochemistry (HPLC-ECD) and qPCR analysis were then conducted on frozen brain and spleen tissues.

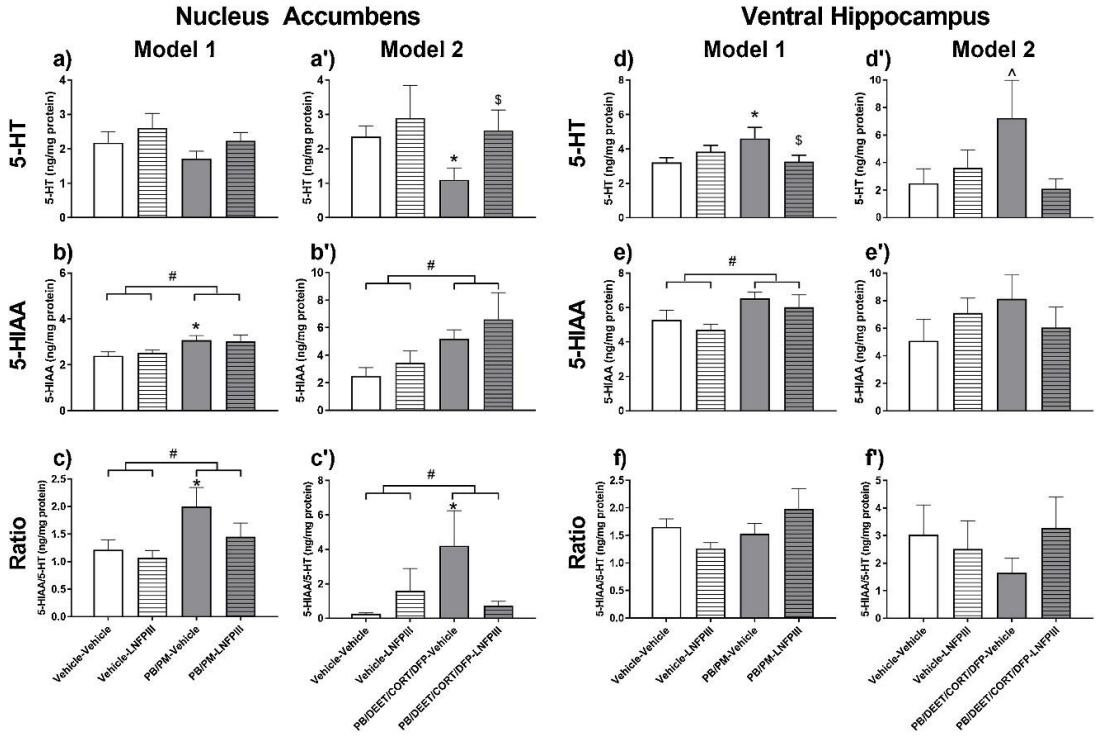

Fig. 2.2. Serotonergic alterations in the Nucleus Accumbens and Ventral Hippocampus in two models of Gulf War Illness. Data are presented as mean ± SEM; unit: ng/mg protein; n = 6 per group/treatment except PB/DEET/CORT/DFP-Vehicle group, which was n = 8. # indicates a significant main effect of GWI treatment (PB/PM (Model 1) or PB/DEET/CORT/DFP (Model 2)) after a two-way ANOVA ($p \leq 0.05$). * indicates a significant difference compared to Vehicle-Vehicle group ($p \leq 0.05$). ^ indicates trend compared to Vehicle-Vehicle group ($p < 0.10$). $ indicates significant difference compared to GWI-Vehicle group ($p \leq 0.05$). Abbreviations: 5-HT: serotonin; 5-HIAA: 5-hydroxyindoleacetic acid; acid; PB: pyridostigmine bromide; PM: permethrin; DEET: N,N-Diethyl-methylbenzamide; CORT: corticosterone; DFP: diisopropylfluorophosphate; LNFPIII: Lacto-N-fucopentaose III.

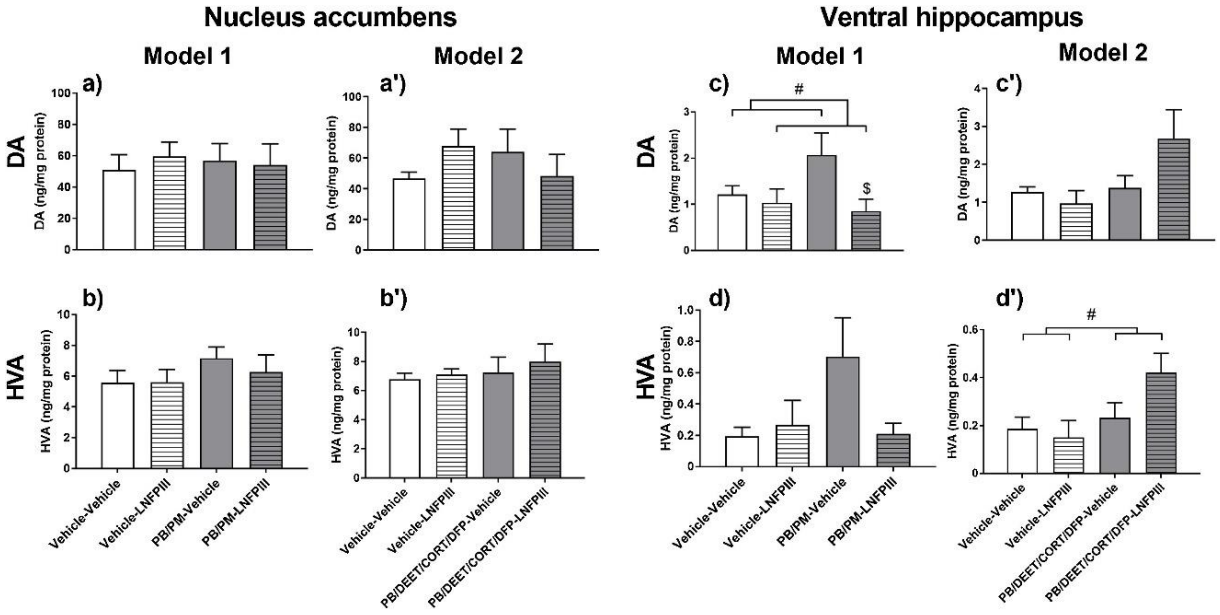

Fig. 2.3. Dopaminergic alterations in the Nucleus Accumbens and Ventral Hippocampus in two models of Gulf War Illness. Data are presented as mean ± SEM; unit: ng/mg protein; n = 6 per group/treatment except PB/DEET/CORT/DFP-Vehicle group, which was n = 8. # ($p \leq 0.05$) indicate a significant main effect of GWI treatment (PB/PM (Model 1) or PB/DEET/CORT/DFP (Model 2)) or LNFPIII treatment after a two-way ANOVA. $ indicates significant difference compared to GWI-vehicle group ($p \leq 0.05$). Abbreviations: DA: dopamine; HVA: homovanillic acid; PB: pyridostigmine bromide; PM: permethrin; DEET: N,N-Diethyl-methylbenzamide; CORT: corticosterone; DFP: diisopropylfluorophosphate; LNFPIII: Lacto-N-fucopentaose III.

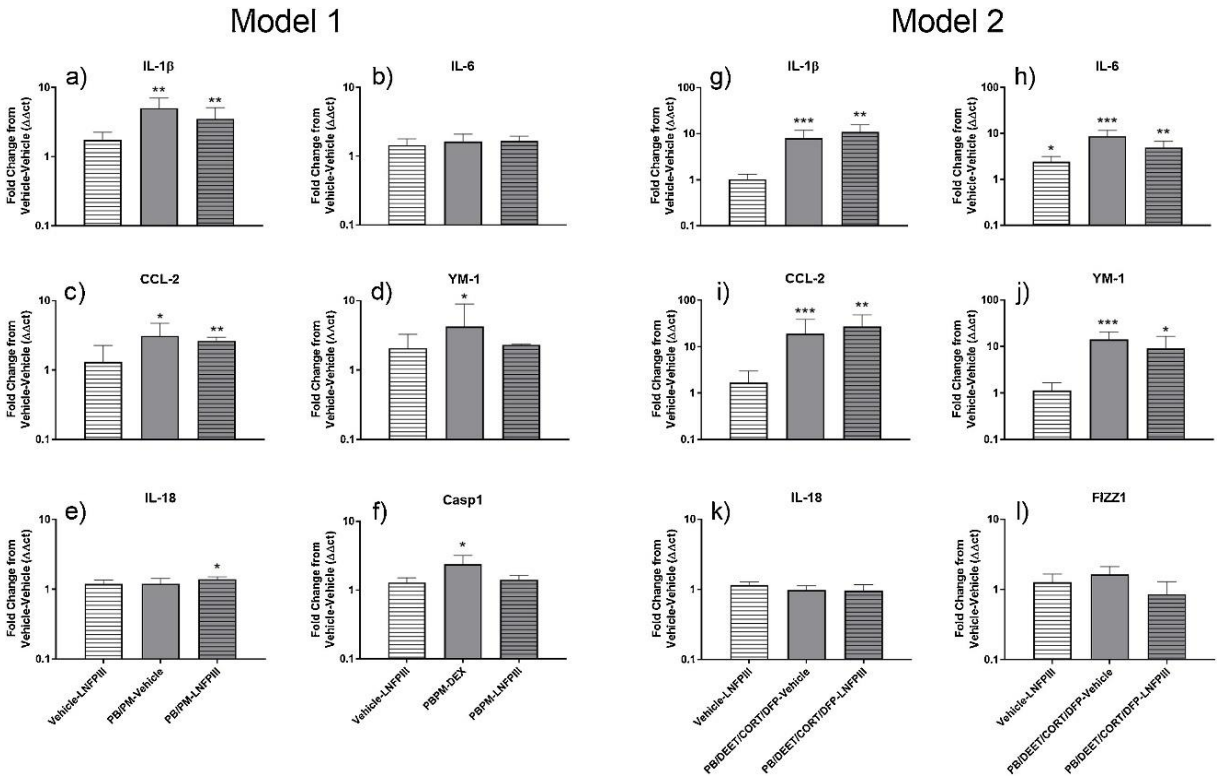

Fig. 2.4. Inflammatory markers in the ventral hippocampus in two models of Gulf War Illness. Data were analyzed by the $^{\Delta\Delta}$Ct method with 18S as the HKG and are presented as fold change from vehicle-vehicle control. *, **, *** indicate significant difference from control ($p \leq 0.05$, ≤ 0.01, and ≤ 0.001, respectively). n = 6/group for Model 1 and n = 5–7/group for Model 2. Abbreviations: PB: pyridostigmine bromide; PM: permethrin; DEET: N,N-Diethyl-methylbenzamide; DFP: diisopropylfluorophosphate; CORT: corticosterone; LNFPIII: Lacto-N-fucopentaose III.

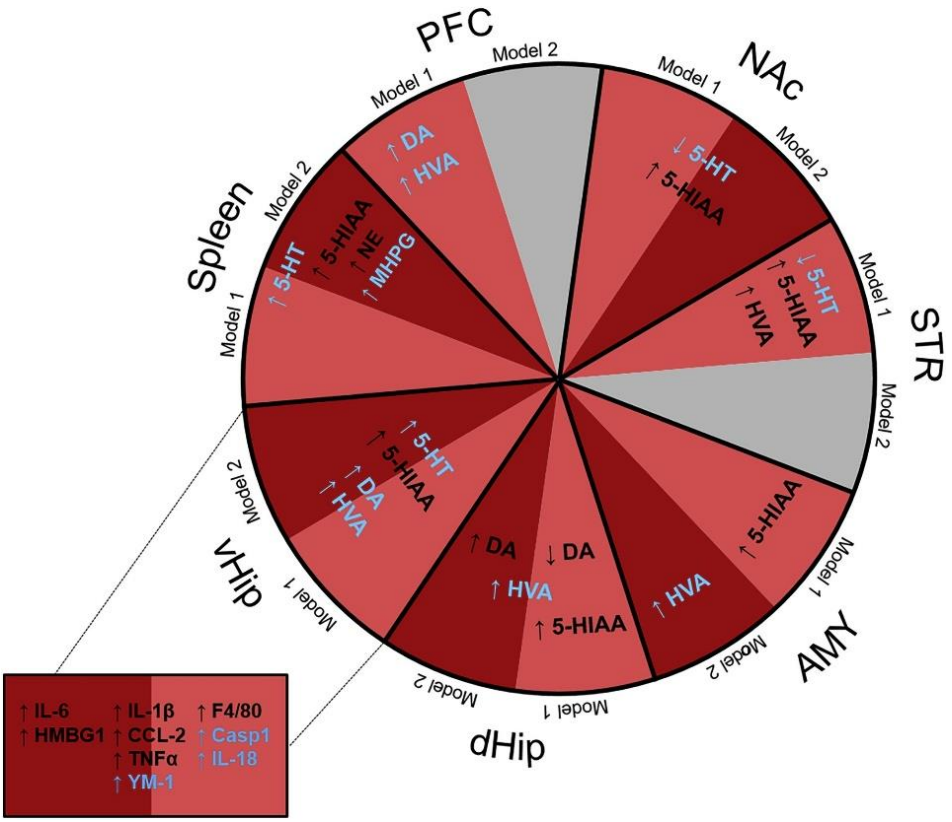

Fig. 2.5. Summary of the major neurochemical (monoamines) and neuroinflammatory (vHip) effects in the two GWI models and their modulation by LNFPIII. Effects of Model 1 (PB/PM; light red) and Model 2 (PB/DEET/CORT/DFP; dark red) on 5-HT, DA, NE and their metabolites in the spleen and brain regions (PFC, NAc, STR, AMY, dHip, vHip), as well as inflammatory gene expression in the vHip are indicated. Modulation of these effects by LNFPIII is represented in blue color. Abbreviations: PFC: prefrontal cortex; NAc: nucleus accumbens; STR: striatum; AMY: amygdala; dHip: dorsal hippocampus; vHip: ventral hippocampus; 5-HT: serotonin; 5-HIAA: 5-hydroxyindoleacetic acid; DA: dopamine; HVA: homovanillic acid; MHPG: 3-methoxy-4-hydroxyphenylglycol; NE: norepinephrine; PB: pyridostigmine bromide; PM: permethrin; DEET: N,N-Diethyl-methylbenzamide; DFP: diisopropylfluorophosphate; CORT: corticosterone LNFPIII: Lacto-N-fucopentaose III. (For interpretation of the references to color in this figure legend, the reader is referred to the web version of this article).

Table 1. Brain monoamines and their metabolites in male C57BL6/J mice 6 h post chemicals exposure in Model 1 of Gulf War Illness.

Brain Region	Monoamine or Metabolite	Treatment			
		Vehicle –Vehicle	Vehicle –LNFPIII	PB/PM –Vehicle	PB/PM –LNFPIII
PFC	5-HT	1.28 ± 0.30	2.23 ± 0.56	1.51 ± 0.28	1.37 ± 0.29
	5-HIAA	2.51 ± 0.12	2.46 ± 0.19	2.79 ± 0.31	2.64 ± 0.27
	DA	0.37 ± 0.07	0.26 ± 0.13	0.52 ± 0.21	0.24 ± 0.11
	HVA	0.70 ± 0.27	0.43 ± 0.16	1.40 ± 0.48	0.65 ± 0.21
STR	5-HT	2.50 ± 0.48	*3.02 ± 0.62*	1.72 ± 0.39	*3.05 ± 0.30*
	5-HIAA	3.15 ± 0.47	2.55 ± 0.16	**3.65 ± 0.46** [a]	**3.68 ± 0.32** [a]
	DA	97.62 ± 2.91	*106.60 ± 3.82*	*102.23 ± 6.36*	95.02 ± 3.95
	HVA	9.03 ± 0.46	9.25 ± 0.53	**11.63 ± 1.34** [a]	**10.24 ± 0.53** [a]
AMY	5-HT	3.80 ± 0.81	4.37 ± 0.37	4.30 ± 0.60	3.39 ± 0.75
	5-HIAA	3.65 ± 0.43	3.49 ± 0.34	**4.91 ± 0.42** [a]	**4.25 ± 0.44** [a]
	DA	17.15 ± 3.79	25.01 ± 5.28	16.08 ± 4.44	19.02 ± 6.23
	HVA	2.79 ± 0.71	2.87 ± 0.27	2.79 ± 0.44	2.84 ± 0.67
dHip	5-HT	1.25 ± 0.33	1.69 ± 0.23	1.41 ± 0.22	1.59 ± 0.17
	5-HIAA	2.96 ± 0.22	3.32 ± 0.60	**3.99 ± 0.44** [a]	**4.36 ± 0.59** [a]
	DA	0.24 ± 0.08	0.26 ± 0.05	*0.20 ± 0.06*	*0.14 ± 0.04*
	HVA	0.15 ± 0.02	0.20 ± 0.04	0.25 ± 0.06	0.25 ± 0.08

Table 2.1. Brain monoamines and their metabolites in male C57BL6/J mice 6 h post chemicals exposure in Model 1 of Gulf War Illness. Data are presented as mean ± SEM; unit: ng/mg protein; $n = 6$ per group. [a], [b] or [c] indicate significant main effect for GWI treatment (PB/PM), LNFPIII treatment or Treatment (GWI x LNFPIII) interaction, respectively, after a two-way ANOVA ($p \leq 0.05$) and are bolded. Italicized values indicate trend ($p < 0.10$) for main effect. *Abbreviations*: PFC: prefrontal cortex; NAc: nucleus accumbens; STR: striatum; AMY: amygdala; dHip: dorsal hippocampus; vHip: ventral hippocampus; 5-HT: serotonin; 5-HIAA: 5-hydroxyindoleacetic acid; DA: dopamine; HVA: homovanillic acid; PB: pyridostigmine bromide; PM: permethrin; LNFPIII: Lacto-N-fucopentaose III.

Table 2. Brain monoamines and their metabolites in male C57BL6/J mice 6 h post chemicals exposure in Model 2 of Gulf War Illness.

Brain Region	Monoamine or Metabolite	Treatment			
		Vehicle –Vehicle	Vehicle –LNFPIII	PB/DEET/CORT/DFP – Vehicle	PB/DEET/CORT/DFP- LNFPIII
PFC	5-HT	1.55 ± 0.38	4.91 ± 3.80	4.46 ± 3.10	1.47 ± 0.33
	5-HIAA	2.64 ± 0.32	*3.50 ± 0.62*	2.52 ± 0.45	*3.87 ± 0.95*
	DA	0.56 ± 0.22	0.45 ± 0.13	0.54 ± 0.14	0.58 ± 0.19
	HVA	0.46 ± 0.12	*1.35 ± 0.60*	0.55 ± 0.15	*1.50 ± 0.60*
STR	5-HT	2.47 ± 0.50	2.63 ± 0.48	1.64 ± 0.34	2.64 ± 0.59
	5-HIAA	2.64 ± 0.35	2.00 ± 0.58	2.81 ± 0.44	2.17 ± 0.75
	DA	112.54 ± 8.75	105.11 ± 13.92	122.32 ± 6.93	102.28 ± 6.08
	HVA	10.82 ± 1.40	9.26 ± 0.89	10.16 ± 1.16	11.73 ± 0.70
AMY	5-HT	3.84 ± 0.87	4.59 ± 0.71	4.72 ± 1.06	4.39 ± 1.46
	5-HIAA	2.72 ± 0.64	2.86 ± 0.26	9.14 ± 3.57	3.42 ± 0.46
	DA	12.87 ± 1.53	13.47 ± 3.54	13.63 ± 2.59	25.25 ± 6.76
	HVA	4.10 ± 1.19	*4.40 ± 2.06*	*3.27 ± 1.09*	7.92 ± 2.35
dHip	5-HT	1.17 ± 0.39	0.97 ± 0.19	0.74 ± 0.23	1.02 ± 0.32
	5-HIAA	3.41 ± 1.04	2.73 ± 0.49	5.66 ± 1.30	3.91 ± 1.04
	DA	0.36 ± 0.12	0.27 ± 0.06	**2.36 ± 1.84** [a]	**0.84 ± 0.27** [a]
	HVA	0.11 ± 0.02	**0.27 ± 0.07** [b]	**0.78 ± 0.15** [a]	**1.45 ± 0.53** [ab]

Table 2.2. Brain monoamines and their metabolites in male C57BL6/J mice 6 h post chemicals exposure in Model 2 of Gulf War Illness. Data are presented as mean ± SEM; unit: ng/mg protein; n = 6 per group, except the PB/DEET/CORT/DFP-Vehicle group, which was n = 8). [a] and [b] indicate significant main effect for GWI treatment (PB/DEET/CORT/DFP) or LNFPIII treatment, respectively, after a two-way ANOVA ($p \leq 0.05$) and are bolded. Italicized values indicate trend ($p < 0.10$) for main effect. *Abbreviations*: PFC: prefrontal cortex; NAc: nucleus accumbens; STR: striatum; AMY: amygdala; dHip: dorsal hippocampus; vHip: ventral hippocampus; 5-HT: serotonin; 5-HIAA: 5-hydroxyindoleacetic acid; DA: dopamine; HVA: homovanillic acid; PB: pyridostigmine bromide; DEET: N,N-Diethyl-methylbenzamide; DFP: diisopropylfluorophosphate; CORT: corticosterone; LNFPIII: Lacto-N-fucopentaose III.

Table 3. Splenic monoamines and their metabolites in male C57BL6/J mice 6 h post chemicals exposure in two models of Gulf War Illness.

Monoamine or metabolite	Model 1				Model 2			
	Vehicle – Vehicle	Vehicle – LNFPIII	PB/PM – Vehicle	PB/PM – LNFPIII	Vehicle – Vehicle	Vehicle – LNFPIII	PB/DEET/ CORT/ DFP – Vehicle	PB/DEET/ CORT/ DFP-LNFPIII
5-HT	80.29 ± 7.02	**94.69 ± 4.46** [b]	**96.99 ± 6.78** [b]	81.30 ± 6.60	80.29 ± 9.30	69.29 ± 5.78	**107.44 ± 9.30** [a]	**100.87 ± 14.27** [a]
5-HIAA	0.66 ± 0.04	0.71 ± 0.13	0.74 ± 0.09	0.66 ± 0.06	0.66 ± 0.12	0.71 ± 0.09	**1.02 ± 0.22** [a]	**1.42 ± 0.25** [a]
NE	66.83 ± 8.12	70.10 ± 12.17	59.16 ± 5.43	62.21 ± 8.90	95.83 ± 6.65	93.08 ± 9.90	90.84 ± 3.67	110.32 ± 11.65
MHPG	43.21 ± 1.98	48.77 ± 3.10	41.90 ± 1.80	47.55 ± 5.96	34.96 ± 2.58	*39.45 ± 4.81*	**43.15 ± 3.79** [a]	***51.82 ± 3.24*** [a]

Table 2.3. Splenic monoamines and their metabolites in male C57BL6/J mice 6 h post chemicals exposure in two models of Gulf War Illness. Data are presented as mean ± SEM; unit: ng/mg protein; n = 6 per group, except the PB/DEET/CORT/DFP-Vehicle group, which was n = 8). [a] and [b] indicate significant main effect for PB/DEET/CORT/DFP or Treatment (PB/PM x LNFPIII) interaction, respectively, after a two-way ANOVA ($p \leq 0.05$) and are bolded. Italicized values indicate trend ($p < 0.10$) for main effect of LNFPIII. *Abbreviations*: 5-HT: serotonin; 5-HIAA: 5-hydroxyindoleacetic acid; MHPG: 3-methoxy-4-hydroxyphenylglycol; NE: norepinephrine; PB: pyridostigmine bromide; PM: Permethrin; DEET: N,N-Diethyl-methylbenzamide; DFP: diisopropylfluoro-phosphate; CORT: corticosterone; LNFPIII: Lacto-N-fucopentaose III.

Table 4. Gene expression in the ventral hippocampus of male C57BL6/J mice 6 h post exposure termination in two models of Gulf War Illness.

	Model 1 Treatment			**Model 2 Treatment**		
	Vehicle – LNFPIII	PB/PM – Vehicle	PB/PM – LNFPIII	Vehicle – LNFPIII	PB/DEET/ CORT/DFP – Vehicle	PB/DEET/ CORT/DFP – LNFPIII
Gene	Fold ± SEM	Fold ± SEM	Fold ± SEM	Fold ± SEM	Fold ± SEM	Fold ± SEM
CD206	0.70 ± 0.39	0.91 ± 1.24	1.32 ± 0.56	1.28 ± 0.61	0.97 ± 0.37	0.75 ± 0.15
COX2	1.94 ± 0.58	1.60 ± 0.72	1.38 ± 0.40	1.44 ± 0.37	1.18 ± 0.49	*2.13 ± 0.42*
F4/80	1.20 ± 0.16	**1.42 ± 0.16***	**1.70 ± 0.35***	1.00 ± 0.19	1.47 ± 0.22	0.98 ± 0.16
FIZZ1	1.44 ± 1.05	2.10 ± 0.53	1.01 ± 0.14	1.27 ± 0.40	1.64 ± 0.49	0.85 ± 0.44
GFAP	0.60 ± 0.23	1.53 ± 0.85	0.79 ± 0.18	0.91 ± 0.28	1.01 ± 0.37	1.24 ± 0.40
HMGB1	1.15 ± 0.19	1.26 ± 0.15	0.99 ± 0.10	*1.53 ± 0.25*	*1.44 ± 0.25*	1.16 ± 0.18
LIF	1.11 ± 0.37	1.14 ± 0.37	0.98 ± 0.25	1.36 ± 0.12	0.81 ± 0.20	1.66 ± 1.56
NLRP3	1.04 ± 0.21	1.13 ± 0.23	0.90 ± 0.96	1.43 ± 0.31	1.37 ± 0.49	1.23 ± 0.31
TNF-α	1.25 ± 0.47	*1.87 ± 0.38*	1.78 ± 0.40	1.56 ± 0.43	*2.30 ± 0.67*	1.72 ± 0.54
Arg1	0.70 ± 0.14	1.96 ± 2.32	2.36 ± 2.42	1.77 ± 0.63	1.34 ± 2.16	1.28 ± .0.80
NOS2	1.02 ± 0.33	1.07 ± 0.20	1.20 ± 0.12	1.46 ± 0.23	1.04 ± 0.28	0.81 ± 0.20
Arg1:NOS2	1.05 ± 0.02	0.98 ± 0.03	0.98 ± 0.03	1.00 ± 0.02	1.00 ± 0.03	0.99 ± 0.03
BDNF	1.07 ± 0.31	0.94 ± 0.28	0.84 ± 0.32	1.31 ± 0.36	0.87 ± 0.59	1.14 ± 0.08
NGF	0.87 ± 0.11	0.81 ± 0.30	0.76 ± 0.14	1.42 ± 0.22	1.20 ± 0.28	1.44 ± 0.23

Table 2.4. Gene expression in the ventral hippocampus of male C57BL6/J mice 6 h post exposure termination in two models of Gulf War Illness. Data were analyzed by the $^{\Delta\Delta}$Ct method with 18S as the HKG and are presented as fold change from vehicle-vehicle control. The Arg1:NOS2 ratio was calculated based on the $^{\Delta}$Ct values. n = 6/group for Model 1 and n = 5–7/group for Model 2. * indicates significant difference from control and are bolded ($p \leq 0.05$). Italicized values indicate trend ($p \leq 0.10$) for treatment compared to control within both models. 18S was used as the housekeeping gene. *Abbreviations*: PB: pyridostigmine bromide; PM: Permethrin; DEET: N,N-Diethyl-methylbenzamide; DFP: diisopropylfluorophosphate; CORT: corticosterone; LNFPIII: Lacto-N-fucopentaose III.

Supporting Information

Target	Forward Primer 5'-> 3'	Reverse Primer 5' -> 3'
18S	GGGAGCCTGAGAAACGGC	GGGTCGGGAGTGGGTAATTT
Arg-1	CTCCAAGCCAAAGTCCTTAGAG	AGGAGCTGTCATTAGGGACATC
BDNF	TGCAGGGGCATAGACAAAAGG	CTTATGAATCGCCAGCCAATTCTC
Casp1	GAGATGGTGAAAGAGGTGAA	GTGTTGAAGAGCAGAAAGCA
CCL-2	AGGTCCCTGTCATGCTT	TCTGGACCCATTCCTTCTTG
CD206	CAGGTGTGGGCTCAGGTAGT	TGTGGTGAGCTGAAAGGTGA
COX-2	CCAGCACTTCACCCATCAGTT	ACCCAGGGTCCTCGCTTATGA
F4/80	TGCCTTACAACTATGAAGCTCCAC	ACACCACAAGAAAGTGCATAGGAA
Fizz1	CCCTCCACTGTAACGAAGACTC	CACACCCAGTAGCAGTCATCC
GFAP	AGGGGCAGATTTAGTCCAAC	AGGGAGTGGAGGAGTCATTC
HMGB1	CGTGGGACTATTAGGATCAAGC	TTTGGGGATACATTCTCAGGTC
IL-10	ATAACTGCACCCACTTCCCA	GGGCATCACTTCTACCAGGT
IL-18	TGGTTCCATGCTTTCTGGACTCCT	TTCCTGGGCCAAGAGGAAGTGATT
IL-1b	ATGGCAACTGTTCCTGAACTCAACT	CAGGACAGGTATAGATTCTTTCCTTT
IL-6	ATGGATGCTACCAAACTGGAT	TGAAGGACTCTGGCTTTGTCT
LIF	CAAGAATCAACTGGCACAGC	AGTGGGGTTCAGGACCTTCT
NGF	ACACTCTGATCACTGCGTTTTTG	CCTTCTGGGACATTGCTATCTGT
NLRP3	TGCTCTTCACTGCTATCAAGCCCT	ACAAGCCTTTGCTCCAGACCCTAT
NOS-2	ACCTTGTTCAGCTACGCCTT	CATTCCCAAATGTGCTTGTC
TNFα	GCAGGTCTACTTTGGAGTCATTGC	TCCCTTTGCAGAACTCAGGAATGG
YM-1	CTGGAATTGGTGCCCCTACA	CAAGCATGGTGGTTTTACAGGA

Supplemental Table 2.1. List of Targets and Primers for qPCR.

CHAPTER 3

DELAYED TREATMENT WITH THE IMMUNOTHERAPEUTIC LNFPIII AMELIORATES MULTIPLE NEUROLOGICAL DEFICITS IN A PESTICIDE-NERVE AGENT PROPHYLACTIC MOUSE MODEL OF GULF WAR ILLNESS

Jessica M. Carpenter, Kyle A. Brown, Alexa N. Diaz, Rachel L. Dockman, Robert A. Benbow, Donald A. Harn, Thomas Norberg, John J. Wagner, Nikolay M. Filipov
Published in Neurotoxicology and Teratology 2021.
Reprinted here with the permission of publisher.

Abstract

Residual effects of the 1990-1991 Gulf War (GW) still plague veterans 30 years later as Gulf War Illness (GWI). Thought to stem mostly from deployment-related chemical overexposures, GWI is a disease with multiple neurological symptoms with likely immunological underpinnings. Currently, GWI remains untreatable, and the long-term neurological disease manifestation is not characterized fully. The present study sought to expand and evaluate the long-term implications of prior GW chemicals exposure on neurological function 6-8 months post GWI-like symptomatology induction. Additionally, the beneficial effects of delayed treatment with the glycan immunotherapeutic Lacto-N-fucopentaose III (LNFPIII) were evaluated. Male C57BL/6J mice underwent a 10-day combinational exposure to GW chemicals, the nerve agent prophylactic pyridostigmine bromide (PB) and the insecticide permethrin (PM; 0.7 and 200 mg/kg, respectively). Beginning four months after PB/PM exposure, a subset of the mice were treated twice a week until study completion with LNFPIII. Evaluation of cognition/memory, motor function, and mood was performed beginning 1 month after LNFPIII treatment initiation. Prior exposure to PB/PM produced multiple locomotor, neuromuscular, and sensorimotor deficits across several motor tests. Subtle anxiety-like behavior was also present in PB/PM mice in mood tests. Further, PB/PM-exposed mice learned at a slower rate, mostly during early phases of the learning and memory tests employed. LNFPIII treatment restored or improved many of these behaviors, particularly in motor and cognition/memory domains. Electrophysiology data collected from hippocampal slices 8 months post PB/PM exposure revealed modest aberrations in basal synaptic transmission and long-term potentiation in the dorsal or ventral hippocampus that were improved by LNFPIII treatment.

Immunohistochemical analysis (tyrosine hydroxylase; TH) did not detect major PB/PM effects along the nigrostriatal pathway, but LNFPIII increased striatal TH. Additionally, neuroinflammatory cells were increased in PB/PM mice, an effect reduced by LNFPIII. Collectively, long-term neurobehavioral and neurobiological dysfunction associated with prior PB/PM exposure was characterized; delayed LNFPIII treatment provided multiple behavioral and biological protective effects in the context of GWI, highlighting its potential as a GWI therapeutic.

Abbreviations: BDNF, Brain-derived neurotrophic factor; BM, Barnes Maze; CV, cresyl violet; DAB, 3,3′ diaminobenzidine; dH, Dorsal hippocampus; ERK, Extracellular signal regulated kinase; EZM, Elevated Zero Maze; fEPSP, field excitatory postsynaptic potential; GFAP, glial fibrillary acidic protein; GS, Grip Strength; GW, Gulf War; GWI, Gulf War Illness; LNFPIII, Lacto-N-fucopentaose-III; LTP, Long-term potentiation; MB, Marble Burying; NOR, Novel Object Recognition; OF, Open Field; PB, Pyridostigmine bromide; PM, Permethrin; PT, Pole Test; PPF, Paired-pulse facilitation; RAM, Radial Arm Maze; SP, Sucrose Preference; SR, Sticker Removal; ST, Swim Test; STR, Striatum; TH, tyrosine hydroxylase; vH, Ventral hippocampus.

Keywords: Gulf War Illness, Permethrin, Pyridostigmine bromide, Behavior, Electrophysiology, LNFPIII

1. Introduction

Documented associations of wartime related chemical exposures and delayed adverse health outcomes in veterans exist for several conflicts. One notable example is the Vietnam War where increased incidence of certain cancers, reproductive abnormalities, and neurological problems in the years following the war have been attributed, in part, to extensive exposures to pesticides, such as Agent Orange (NASEM et al., 2018; Stellman and Stellman, 2018). More recent war-related exposures that have impacted veterans' health negatively occurred during the 1990-1991 Gulf War (GW). Approximately 30% of GW veterans suffer from Gulf War Illness (GWI), a complex, multi-symptomatic chronic disease with neurological, immunological, and gastrointestinal ailments that appeared shortly after veterans returned from deployment and have progressively worsened over the last 30 years (DDGWIRP, 2018; Porter et al., 2020; White et al., 2016; Zundel et al., 2019). Precise etiology and pathophysiology of this disease are still being investigated, but combinational and frequent exposures to pesticides (e.g. Permethrin: PM, chlorpyrifos), insect repellants (N-Diethyl-3-methylbenzamide [DEET]), a nerve agent prophylactic (pyridostigmine bromide: PB), and, in some cases, chemical nerve agents (sarin and cyclosarin) are implicated and have been investigated in laboratory models of GWI (Sullivan et al., 2003; White et al., 2016).

The symptomatology experienced by GWI veterans encapsulates a number of neurological complaints including cognitive and memory dysfunction, motor impairments, and affect alterations (Anger et al., 1999; Hubbard et al., 2014; Proctor et al., 2006; Sullivan et al., 2018; Toomey et al., 2009; White et al., 2016). Many of these behavioral deficits have been recapitulated in rodent GWI laboratory studies utilizing varying GW chemical

exposure combinations (Abdullah et al., 2011; Abdullah et al., 2013; Abou-Donia et al., 2004; Abou-Donia et al., 2002; Hattiangady et al., 2014; Joshi et al., 2018; Joshi et al., 2020; Macht et al., 2019; Ojo et al., 2014; Parihar et al., 2013; Torres-Altoro et al., 2011). Several pathogenic factors within GWI, including central nervous system structural changes (Chao et al., 2011; Chao et al., 2010; Chao et al., 2015; Heaton et al., 2007; Rayhan et al., 2013; White et al., 2016), neurotransmitter dyshomeostasis (Carpenter et al., 2020; Carreras et al., 2018; Megahed et al., 2014), and persistent immune system disruption (Alshelh et al., 2020; Broderick et al., 2013; Broderick et al., 2018; Parkitny et al., 2015), are associated with and/or could be responsible for these behavioral deficits. Further, inflammation, especially neuroinflammation, is consistent among several GWI laboratory studies; widespread brain increases in gliosis and inflammatory markers, particularly in the hippocampus, are common findings (Carpenter et al., 2020; Carreras et al., 2018; Macht et al., 2019; Madhu et al., 2019; Megahed et al., 2014; Miller et al., 2018; O'Callaghan et al., 2015; Parihar et al., 2013; Zakirova et al., 2016; Zakirova et al., 2015). In some GWI studies where neuroinflammation was demonstrated, cognitive and affect deficits were also reported (Carreras et al., 2018; Joshi et al., 2018; Parihar et al., 2013; Zakirova et al., 2016; Zakirova et al., 2015).

Because precise etiology of GWI is still unknown, laboratory models have utilized several combinations of GW-relevant chemicals due to reports GWI veterans were exposed to higher rates of the nerve agent prophylactic, PB, and pesticides (Steele et al., 2012; White et al., 2016). One established GWI model that includes short-term exposure to PB and the insecticide PM (Zakirova et al., 2015) has been used by our group to study the acute and chronic effects of these GWI chemicals (Carpenter et al., 2020; Mote et al.,

2020). This model produced behavioral changes consistent with GWI clinical symptomology including anxiety, psychomotor, and cognitive problems, months after exposure termination (Abdullah et al., 2011; Joshi et al., 2018; Joshi et al., 2020; Zakirova et al., 2016; Zakirova et al., 2015). Further, this GWI chemical exposure paradigm leads to increases in hippocampal neuroinflammation, manifested with increased inflammatory cytokines as well as glial activation in the hippocampus and the cortex (Carpenter et al., 2020; Zakirova et al., 2016; Zakirova et al., 2015). However, the magnitude of short-term neuroinflammation following PB/PM exposure is less than in a model that incorporates a nerve agent surrogate and corticosterone to emulate stress (O'Callaghan et al., 2015), suggesting the PB/PM model may exhibit effective construct and etiological validity for milder versions of GWI (Carpenter et al., 2020). Utilizing distinct animal models to recapitulate more or less severe forms of GWI may be particularly relevant to clinical GWI as this disease state presents in a heterogeneous manner depending on the duration, frequency, type, and intensity of chemical exposure (Steele et al., 2012). Moreover, multiple neurobehavioral and neuropathological alterations observed in the PB/PM model overlap with clinical presentation of GWI (Joshi et al., 2018; Joshi et al., 2020; Zakirova et al., 2016; Zakirova et al., 2015), making the model suitable for an in-depth investigation of GWI pathobiology and evaluating novel GWI treatments.

Efficacious treatment options for GWI are limited, in part due to the heterogeneous presentation of disease symptomology (DDGWIRP, 2018). Nevertheless, therapeutic interventions have been explored and have provided some symptom benefits (Baraniuk et al., 2013; DDGWIRP, 2018; Donta et al., 2004; Golier et al., 2016; Golomb et al., 2014; Helmer et al., 2020; Holton et al., 2020). Because of the underlying immune dysfunction

in GWI, immunomodulatory therapies may be an advantageous treatment option. Lacto-N-fucopentaose III (LNFPIII) is an immunomodulatory glycan found in human milk that, to date, has had no documented adverse effects (Atochina et al., 2008; Bhargava et al., 2012; Carpenter et al., 2020; Srivastava et al., 2014; Tundup et al., 2015; Zhu et al., 2012). When conjugated to a dextran carrier, LNFPIII activates CD14/TLR-4 signaling for extracellular signal-regulated kinase (ERK)-dependent production of anti-inflammatory mediators to skew the inflammatory balance of the innate immune system in an anti-inflammatory direction, including in pathological disease states such as experimental autoimmune encephalomyelitis and diet-induced obesity (Atochina et al., 2008; Bhargava et al., 2012; Srivastava et al., 2014; Tundup et al., 2015; Zhu et al., 2012). In fact, in an earlier GWI study, we found LNFPIII was beneficial in preventing acute monoaminergic disbalance, particularly the utilization of serotonin and dopamine, in multiple cognition- and motor-regulating brain regions and reducing inflammation within the hippocampus (Carpenter et al., 2020).

Our earlier study utilizing this established PB/PM exposure paradigm provided insight into the acute neuroinflammation and monoaminergic effects of GWI treatment in multiple cognition- and motor-regulating brain regions (Carpenter et al., 2020). However, while concurrent LNFPIII treatment induced acute beneficial effects with GWI chemical exposure (Carpenter et al., 2020), it is unknown whether it will be beneficial when given long after the termination of GWI exposure, i.e., restorative effects. Additionally, the long-term impact of PB/PM exposure on motor and sensorimotor function, as well as electrophysiological aberrations that may shape cognitive deficits associated with this model are yet to be characterized. Thus, the present study sought to expand and evaluate

the long-term implications of prior PB/PM exposure on neurobehavioral and neurobiological function 6-8 months post GWI symptomatology induction. Further, we characterized the neuroinflammatory profile of this model by evaluating glial markers. Finally, we examined whether delayed treatment with the immunotherapeutic LNFPIII was beneficial.

2. Materials and Methods

2.1 Materials

Pyridostigmine bromide (PB; ≥ 98% purity; Sigma Aldrich, St. Louis, MO) and permethrin (PM; 29.5% cis/69.5% trans isomer; 99% purity; Chem Service Inc., West Chester, PA) were used for GW animal treatments. Lacto-N-fucopentaose III (LNFPIII) dextran conjugate was produced as previously described (Tundup et al., 2015). Briefly, LNFPIII purified from human milk (> 95% purity; Dextra, United Kingdom), and 40 kDa Dextran (Sigma-Aldrich) were shipped to Dr. Thomas Norberg who prepared the LNFPIII-Dextran conjugate using proprietary linker-spacer and conjugation chemistry. All additional chemicals and reagents, unless otherwise noted, were of analytical or higher grade and were obtained from Sigma-Aldrich or Fisher Scientific (Hampton, NH).

2.2 Animals

Male C57BL/6J mice (8-9 weeks old; Jackson Laboratories, Bar Harbor, ME) were housed 4 per cage in an environmentally controlled room (22-24° C) and maintained on a 12 h light/dark cycle (0700-1900 lights on) for 1 week of acclimation and throughout the study. Mice were handled daily for 1 week prior to the start of the study to minimize experimenter-induced stress. Food and water were available *ad libitum*. All procedures

were approved in advance by the University of Georgia Institutional Animal Care and Use Committee and were in accordance with the latest National Institutes of Health guidelines.

2.3 GWI Model

Following (Zakirova et al., 2015), mice (N=61) weighing 24.4 ± 0.19 g (mean ± SEM) were randomly divided into GWI (PB/PM) and vehicle (DMSO) treatment groups and treated daily for 10 days with a combination of PB and PM (0.7 and 200 mg/kg, respectively) or DMSO vehicle (i.p.). Four months after the initial GWI-chemicals exposure, mice within each of the two original treatments were randomly subdivided into an LNFPIII or a vehicle group and were treated twice a week until study completion with LNFPIII or dextran vehicle (both 35 µg/mouse; s.c.) diluted in sterile saline as in (Carpenter et al., 2020). Thus, from this point onward there were 4 treatment groups: Vehicle-Vehicle (DMSO-Dextran, n=14), Vehicle-LNFPIII (DMSO-LNFPIII, n=15), PB/PM-Vehicle (PB/PM-Dextran, n=16), and PB/PM-LNFPIII (n=16). Body weights were measured daily during GWI chemicals exposure and biweekly after the last GWI exposure until study completion. During the radial arm maze (RAM), in which mice underwent food restriction, weight measurements were taken daily for monitoring as described under the RAM testing protocol. Refer to Figure 1A for a detailed experimental timeline.

2.4 Behavioral Tests

One month after LNFPIII treatment inception, a battery of behavioral tests for assessment of cognition/memory, mood, and motor function were performed as described below. All behavioral testing, scoring, and analysis were done in a treatment-blind manner. Refer to Figure 1B for a detailed behavioral timeline.

2.4.1 Nest Building

Nest building was assessed prior to the Sucrose Preference test on behavioral day 1 to measure cognitive and motor functions; it has been shown that severe hippocampal damage leads to deficits in nest building (Deacon, 2012). Marked striatal damage also leads to these deficits, likely through a substantial impairment in forelimb and orofacial dexterity (Hofele et al., 2001). Mice were individually housed with a fresh paper nestlet (Bed-r'Nest, The Anderson's Inc., Maumee, OH); pictures of the nests were taken from above at different time points (30 min, 60 min, 90 min, 120 min, 180 min, 240 min, 300 min, 360 min, and 24 h) after nestlet placement and scored based on a 4-point scale (1 = untouched, 4 = nest completed) as in (Deacon, 2012).

2.4.2 Sucrose Preference (SP)

The SP test (two-bottle choice paradigm) used to measure depressive like behavior, specifically anhedonia (Eagle et al., 2016), was performed during behavioral days 1-8. Briefly, individually housed mice were given access to two bottles filled with tap water for 4 days to establish a baseline and then given access to one bottle of tap water and one bottle of 1.5% sucrose water for 4 additional days. Solution intake was measured daily by weighing bottles, and bottle position was switched after each measurement to prevent side preference. Sucrose preference (%) was determined using the following equation [(total sucrose intake / (sucrose + water intake)) x 100].

2.4.3 Elevated Zero Maze (EZM)

The EZM is a test frequently used to assess anxiety-like behaviors in mice but can also be expanded to assess certain motor function-related parameters (Braun et al., 2011;

Conrad et al., 2011). On behavioral day 12, an EZM apparatus (Stoelting Co., Wood Dale, IL) was used under dim illumination (8 W red bulb). Lighting conditions, measured with an URCERI light meter, were 30-40 lx and 10-15 lx in the open and closed quadrants, respectively. Starting at a central, open quadrant position facing a closed quadrant, mice were allowed to freely explore the maze for 5 min. All behaviors were tracked and scored using ANY-Maze software (Stoelting). Mice were considered to be in a quadrant when 70% of their body was in the area. Scored parameters of interest included time spent in the open and closed areas, number of entries into the open and closed areas, and the latency to enter the closed area at the start of the test.

2.4.4 Marble Burying (MB)

Following a 3 h resting period post EZM, anxiety-like behaviors were assessed using the MB test as previously described (Krishna et al., 2016) with slight modifications. Briefly, clean testing cages were filled with 5 cm of corn cob bedding (Bed-o'Cobs ¼ inch, The Anderson's Inc., Maumee, OH), and mice were individually placed in these cages for 10 min (habituation phase). After a 1 h resting period, mice were returned to the leveled testing cages with 20 marbles (diameter 10 mm, Panacea Products Corp., Columbus, OH) aligned 4 x 5 in the cage for 20 min (testing phase). A baseline and post-test picture were captured, and the number of marbles buried (>70%) was counted for statistical analysis as in (Krishna et al., 2016).

2.4.5 Open field (OF)

Locomotor activity and anxiety-like behavior was assessed in an OF test as previously described (Krishna et al., 2016) on behavior day 14. Briefly, mice were individually placed into an open field arena (25 cm x 25 cm x 40 cm; Coulbourn

Instruments, Whitehall, PA) and allowed to freely explore for 30 min. Locomotor parameters (distance traveled and number of rearings) and anxiety-like behaviors (time spent in the center and periphery) were tracked and scored with the Limelight software (Actimetrics, Wilmette, IL) for both the total 30 min and per 5 min intervals.

2.4.6 Pole Test (PT)

Following a 5 min resting period after the OF, a PT for motor coordination was used as described (Krishna et al., 2016). Mice were placed upright on a vertical pole (55 cm h x 2 cm d) and the times to turn and complete the test by reaching the bottom (total time) of the pole were recorded. Each mouse underwent 4 trials (5 min inter-trial interval) with the last 3 used for statistical analysis.

2.4.7 Grip Strength (GS)

After a resting period following the PT, forelimb GS (in newtons, N) for assessment of neuromuscular function was measured using a gauge attached to a mouse-specific wire grid (Bioseb, France) as previously described (Krishna et al., 2016). Mice were gently placed on the grid and the grip strength was assessed over 4 trials (1-min inter-trial interval). Body-weight-normalized average and max grip strengths were used for statistical analysis.

2.4.8 Novel Object Recognition (NOR)

The NOR test was performed on day 15 as previously described (Krishna et al., 2016) to evaluate short-term recognition memory. Briefly, the OF on the previous day was used as a habituation phase for the NOR. During the identical phase of the NOR, mice were placed in the open field with two identical objects and allowed to freely explore them for 5 min. Mice were then returned to their home cage for 1 h. During the novel phase, one

identical object was replaced with a novel object. Mice were placed in the open field and allowed to explore the novel and identical objects. The number of approaches and time spent at the novel object were scored for the first 20 s of the novel phase as described in (Broadbent et al., 2009; Leger et al., 2013) with Limelight software (Actimetrics). The novel preference index (NPI) was calculated as described in (Lin et al., 2013).

2.4.9 Gait Test

Following a 3-h resting period after the NOR, motor function was evaluated using the gait test as described in (Mulherkar et al., 2013) and (Wang et al., 2017) with slight modifications. Briefly, a runway (82 cm long, 5.5 cm wide with 8 cm high walls) lined with paper was used; an empty cage with home cage bedding was placed at the end of the runway during testing for escape. Prior to testing, the front and hind paws of the mice were painted with non-toxic red and black ink, respectively (Office Depot, item: #839-994 and #839-967). Two trials were conducted (5 min apart), a pre-trial and the actual trial that was used for subsequent statistical analyses. Between each trial, the runway was cleaned with 70% EtOH and a new paper strip was placed in it. Gait stride length, base width, inter/intra-step distance, stride variability, total steps, and velocity were determined from (Mulherkar et al., 2013) and (Wang et al., 2017).

2.4.10 Sticker Removal (SR)

The SR test was used to determine sensorimotor function (Fleming et al., 2013) on behavioral day 17. Food was removed from the rodents' home cage and ¾ of the bedding was transferred to a clean holding cage where the mice acclimated for 1 h. During the testing phase, a small circular sticker (Avery ¼" round label 5793, Office Depot item: # 113019) was applied using forceps to the nose of the mouse, and the mouse was placed

into the home cage. This test was performed over three 90 s trials with a 5 min inter-trial rest. Parameters used for statistical analysis included the average and fastest times for contact and removal of the sticker (Fleming et al., 2013).

2.4.11 Swim Test (ST)

Following a 3 h rest after the SR, depressive-like behaviors (e.g. despair) were assessed using the ST as previously described (Krishna et al., 2016). Briefly, mice were placed in a large beaker filled with 3 L of water (29 ± 2 ºC) for 15 min. After each test, the beaker was sanitized thoroughly. Total climbing counts and time spent climbing, mobile, and immobile were scored using Limelight software (Actimetrics). Additionally, the time to the first immobile bout was measured using ANY-Maze (Stoelting).

2.4.12 Barnes Maze (BM)

The BM test was used to assess spatial learning and memory on behavioral testing days 19-24 (Sunyer et al., 2007). Using a 20-hole circular maze (Stoelting) in which one is equipped with an escape box (target hole; TH). The maze is brightly illuminated to promote anxiogenic escape motivation (~1000 lx measured by URCERI light meter). During the acquisition phase (days 1-4), mice were trained to learn and escape into the TH over four 3-min trials, and after trial completion, mice remained or were manually placed into the TH for 1 min. For the probe trial, the escape box was removed, and mice explored the maze for 90 s. Between mice, the maze was rotated and sanitized to remove any residual olfactory cues. The latency, distance, and number of errors to reach the TH were tracked and scored automatically using ANY-Maze software (Stoelting).

2.4.13 Radial Arm Maze (RAM)

An 8-arm RAM (Med Associates, St. Albans, VT) was used to assess learning and memory function (Babb and Crystal, 2006; Preston et al., 2019) in animals 7 months post-PB/PM exposure (refer to Figure 1B). The maze has a food trough at the end of each arm with a photosensor activated dispenser (20 mg sucrose pellet). External visual cues were located around the room to facilitate spatial navigation. MED-PC 4.0 (Med Associates) was used to control and record photosensor, food, and door signals from an adjacent room. Prior to RAM testing, mice were single-housed and underwent a 14-day food restriction protocol until they reached 85% of their free-fed body weight; this was used to motivate learning of the RAM apparatus. During the last 3 days of the food restriction period, mice were behaviorally acclimated to the RAM, and the apparatus was cleaned as in (Preston et al., 2019).

Spatial short-term working memory was assessed by an 8-arm RAM foraging task over 10 consecutive days. Following a 20 min room acclimation period, each mouse was placed in the central RAM hub for 1 min before all 8 doors to each arm opened and allowed free access to all arms. In the foraging task, each arm is “baited” so that one food reward was dispensed upon the first head poke into the food trough of each arm. An error in spatial short-term working memory was defined as an animal revisiting a trough after the initial visit, and the total number of errors for each animal was recorded. Animal performance was assessed by the average total number of errors of the first 3 days of testing, the last 3 days of testing, and comparing the two.

Spatial long-term working memory was evaluated over 10 consecutive days using a modified delayed spatial Win-Shift task after the last day of the foraging task (Clark et al., 2015; Furgerson et al., 2014). This test incorporates a 2-phase (the study phase and the

test phase) procedure with an interposed delay. During the study phase, 4 arms were randomly opened, allowing the animal to receive a reward from 4 baited arms. Following the completion of the study phase, the animal was returned to the home cage for a 4 min retention interval, and the maze was cleaned. Then, the animal was returned to the central hub for 1 min (total retention interval of 5 min) before the initiation of the test phase in which all 8 doors were opened, allowing free access to all arms. However, only the 4 arms that were unopened in the study phase dispensed food reward. An error in spatial long-term working memory was defined as a visit to an arm that was baited in the study phase and the total number of errors was recorded. Animal performance was determined by assessing the mean errors from the first 3 days of testing, the last 3 days of testing, and comparing the two as in (Clark et al., 2015).

2.5 Slice preparation and electrophysiology

Two weeks after completion of the RAM, brains from the mice slated for electrophysiological assessment were removed following deep anesthetization with halothane (Sigma) and were submerged in oxygenated (95% O_2 / 5% CO_2), ice-cold dissection artificial cerebrospinal fluid (dACSF; 120 mM NaCl, 3 mM KCl, 4 mM $MgCl_2$, 1 mM NaH_2PO_4, 2 6mM $NaHCO_3$, and 10 mM glucose). A mid-sagittal cut was made, and half of the brain was mounted on its dorsal pole and sectioned along the horizontal plane with a vibratome to obtain 400 µm sections containing the vH. The other half was mounted on its caudal pole and sectioned along the horizontal plane with a vibratome to obtain 400 µm sections containing the dH. The vH and dH were subdissected from the rest of the slice and the CA3 region was removed. Slices were then transferred to a submersion-type chamber and perfused with oxygenated (95% O_2 / 5% CO_2) ACSF (120 mM NaCl, 3 mM

KCl, 1.5 mM $MgCl_2$, 1 mM NaH_2PO_4, 2.5 mM $CaCl_2$, 26 mM $NaHCO_3$, and 10 mM glucose) and allowed to recover for 45 min at room temperature followed by 45 min at the recording temperature of 30 °C. Next, a bipolar stimulating electrode (Kopf Instruments, Tujunga, CA) and a 1.0 MΩ tungsten recording microelectrode (World Precision Instruments, Sarasota, FL) were placed in the stratum radiatum of CA1. A stimulus pulse was applied once every min consisting of a single square wave of 270 µs duration to elicit field excitatory postsynaptic potentials (fEPSPs) at Schaffer collateral-CA1 synapses.

A stimulus-response curve was acquired at the beginning of each experiment by incrementally delivering single 15 µA stimulus pulses ranging from 45 to 180 µA in intensity and measuring fEPSP slope (mV/ms) in a 1 ms interval immediately following the fiber volley. The stimulus intensity was adjusted to elicit stable baseline responses of approximately 35% of the maximal fEPSP slope. Paired-pulse responses were monitored each min for 5 min via paired-pulse stimulation with an interpulse interval of 50 ms. Baseline responses were recorded each min for 30 min prior to a high-frequency stimulation (HFS) protocol (3 x 100 Hz/1 s train at 20 s intervals) to induce long-term potentiation. fEPSP responses were monitored for the subsequent 60 min following HFS. fEPSP responses were normalized to baseline using the average value of the five responses immediately prior to HFS. LTP magnitude was determined via averaging the normalized fEPSP slope values at 56–60 min post-HFS. Electrophysiology data was digitized at 10 kHz, low-pass filtered at 1 kHz, and analyzed with pCLAMP 10.2 software (Axon Instruments, Sunnyvale, CA).

Average values for electrophysiology response variables were determined by calculating the average value for each response within a particular treatment group.

Reported n-values (x(y)) for the number of slices (x) and the number of mice (y) assessed were as follows: Vehicle-Vehicle (dH, n=14(6); vH, n=14(6)), Vehicle-LNFPIII (dH, n=9(6); vH, n=20(6)), PB/PM-Vehicle (dH, n=12(6); vH, n=21(6)), and PB/PM-LNFPIII (dH, n=13(6); vH, n=17(6)).

2.6 Tissue Collection

The remaining mice not used for electrophysiology were euthanized at month 9. Following euthanasia, brains were removed and a sagittal cut was made; one half was quickly frozen on dry while the other half was immersion fixed in 4% paraformaldehyde as in (Krishna et al., 2016). All tissues were stored at -80 °C until analysis.

2.7 Immunohistochemistry

Fixed brains were coronally sectioned into 40 μm thick sections that were placed in phosphate buffer at 4°C until staining. Free-floating sections containing the striatum (STR) were labeled with anti-tyrosine hydroxylase (TH) for assessment of dopamine neuron terminal health as done previously (Filipov et al., 2009; Krishna et al., 2014). Briefly, endogenous peroxidase activity was quenched with 0.3% hydrogen peroxide (30%) and 0.3% normal goat serum in 1x TBS for 5 min (bright field) and blocked in 3% normal goat serum for 30 min at room temperature (RT; bright field and immunofluorescence). Following blocking, sections for bright field were immunostained with anti-TH primary antibody (1:2000; Millipore AB152) for 48 h at 4°C. Following primary antibody incubation, sections were thoroughly washed and incubated with the appropriate biotinylated secondary antibody (1:200; Vector Laboratories) for 30 min at RT, followed by a 30 min incubation with a Vector ABC reagent standard detection kit (Vector Labs, Burlingame, CA). TH was visualized by development in 3,3′ diaminobenzidine

(DAB) for approximately 3 min, followed by incubation in cresyl violet (CV) for 3 min to stain all neurons. For immunofluorescent sections, sections were incubated with a primary antibody cocktail (1:1000 rabbit anti-IBA-1 microglia marker, Wako Chemicals, Richmond, VA; and 1:3000 chicken anti-glial fibrillary acidic protein (GFAP) astrocyte marker, Aves Labs, Davis, CA) diluted in 0.1% TritonX-100 in PBS for 48 h at 4°C. Following primary antibody incubation, sections were thoroughly washed and incubated with the appropriate secondary fluorescent antibodies (GFAP: 1:1000 goat anti-rabbit 594, Abcam; and IBA-1: 1:1000 goat anti-chicken 488, Abcam) for 2 h at RT in the dark, followed by incubation with a nuclear stain for 5 min (Hoechst 33258, Invitrogen). Following the final washes, sections were mounted to slides, fixed with an ethanol gradient followed by xylene clearing, and cover slipped with VectaMount (Vector Labs).

Images were taken on a Zeiss Axioscope A1 and analysis of TH intensity, GFAP+ or IBA-1+ cells and signal intensity was done using ImageJ software. Regions of interest (ROIs) in the STR included the dorsolateral and ventromedial STR and were captured at 5x (n = 15 images per treatment group/ROI). The hilus region of the hippocampus was captured at 40x (n =11-19 images per treatment group). At the higher magnification (40x) GFAP+/Hoescht+ and IBA-1+/Hoescht+ cells were counted using the Cell counter plugin of ImageJ. For statistical analysis, the images' signal intensity (STR) or cell counts (hippocampus) were averaged per animal and treatment group means were analyzed as in section 2.8.

2.8 Statistical analysis

A two-way analysis of variance (ANOVA) was used to determine main effects of treatments or treatment interactions. If an ANOVA was significant ($p \leq 0.05$), treatment

means were separated by Student-Newman-Keuls (SNK) post hoc test or planned pairwise comparisons (Student's t-test, as appropriate). All data, except electrophysiology and the RAM, were analyzed using SigmaPlot 12.5 (San Jose, CA), and all graphs were generated using GraphPad Prism 5 (San Diego, CA). Statistical analyses for electrophysiology and RAM data were analyzed using R version 3.3.2 (R Development Core Team, 2016, https://www.r-project.org/) and was completed via aov() function for analysis of variance (ANOVA) and the t.test function for the Student's t-test and paired t-test.

3. Results

3.1 Body weights

Body weights of the vehicle and PB/PM groups were not different at the start of the GWI treatment (24.45 ± 0.29 g vs. 24.33 ± 0.26 g, $p > 0.75$) or subsequent bi-weekly weigh-ins (p's ≥ 0.29) up to 4.5 months after the initial PB/PM exposure (Fig. 1C). At 5 months, the vehicle and PB/PM groups were randomly subdivided into a LNFPIII or a vehicle group for a total of 4 groups. There were no significant treatment differences for months 5-9 (Fig. 1C).

3.2 Motor effects after prior PB/PM exposure and delayed LNFPIII treatment

3.2.1 Pole Test (PT)

Motor coordination performance during the PT was unaffected by either PB/PM or LNFPIII. The means and fastest times to turn ($p \geq 0.18$) and complete the test ($p \geq 0.18$) were not different among treatments (data not shown).

3.2.2 Grip Strength (GS)

Weight-normalized GS, an indicator of neuromuscular function, tended to be decreased by prior PB/PM exposure (average GS $p = 0.08$; max GS $p = 0.09$; Fig. 2A).

LNFPIII treatment did not affect the performance of mice in this test significantly (Fig. 2A).

3.2.3 Sticker Removal (SR)

Sensorimotor function was affected by prior PB/PM treatment in which both the fastest removal ($p \leq 0.05$; Fig. 2B) times of the sticker were increased. Similar increases were observed for the fastest contact (Fig. 2B), average contact, and average removal, but were not significant. LNFPIII treatment reduced these increased latencies, and in the case of the fastest removal, where the PB/PM effect was significant, the beneficial effect of LNFPIII was also significant ($p \leq 0.01$; Fig. 2B).

3.2.4 Open Field (OF)

Locomotor activity was significantly affected by prior PB/PM exposure regardless of LNFPIII as evident by decreases in the distance traveled ($p \leq 0.01$; Fig. 2C), line crossings ($p \leq 0.01$; data not shown), and vertical activity (e.g., rears; $p \leq 0.05$; Fig. 2C) during the first 5 min in the exploratory phase of the test. These locomotor effects did not persist, although there was a similar non-significant decrease in the distance traveled for the overall 30 min (data not shown). As expected, all mice habituated to the arena as all groups traveled less distance (Fig. 2D) and made fewer line crossings over time (data not shown) (time effect p's ≤ 0.001).

3.2.5 Gait Test

Prior PB/PM exposure caused few specific alterations in gait parameters. PB/PM mice took significantly more steps ($p \leq 0.05$; Fig. 2E) and exhibited a numerical increase in hindlimb base width (data not shown). The step deficit caused by prior PB/PM treatment was not seen in mice treated with LNFPIII (Fig. 2E). Additionally, LNFPIII treatment had

beneficial effects on gait irrespective of PB/PM; it increased the stride length significantly ($p \leq 0.01$; Fig. 2F) and forepaw interstep distance numerically ($p = 0.08$; data not shown), while decreasing stride length variability ($p \leq 0.05$; Fig. 2G) and paw overlap (right paw, $p \leq 0.05$; data not shown). Average speed, cadence, or time to finish were unaffected (data not shown).

3.2.6 Elevated Zero Maze (EZM)

Motor function with the EZM was evaluated by timing the closed-arm entry. There were no significant differences of treatments, but PB/PM treated mice were numerically slower to enter the closed arm after initial placement on the maze ($p = 0.12$; Fig 2H).

3.3 Long term mood effects of prior PB/PM exposure and delayed LNFPIII treatment

3.3.1 Marble Burying (MB) Test

The average number of buried marbles (≥ 70%) during the test, irrespective of treatment, was 9 (45%). Mice's performance in this test was unaffected statistically by either treatment. However, there was a trend ($p = 0.09$; Fig. 3A) for prior PB/PM treatment to decrease the number of buried marbles, likely due to a neuromuscular deficit rather than an anxiolytic effect.

3.3.2 Elevated Zero Maze (EZM)

A trending treatment interaction (PB/PM x LNFPIII, $p = 0.055$; Fig. 3B) was present for open entries, in which PB/PM mice ($p = 0.07$; Fig. 3B), but not PB/PM-LNFPIII mice, made fewer entries into the open arm than control mice. A similar trend was observed when times in open vs closed arms were analyzed, i.e., PB/PM mice spent less and more time on the open and closed arms, respectively, and LNFPIII prevented this anxiety-like trend ($p = 0.10$; data not shown).

3.3.3 Open Field (OF)

PB/PM treated mice exhibited more anxiety-like behavior in the OF; they spent less and more time in the center and periphery of the OF arena, respectively (p's ≤ 0.05; Fig. 3C). These anxiety-like effects by PB/PM exposure were not seen in mice treated with LNFPIII (Fig. 3C).

3.3.4 Swim Test (ST)

Climbing attempts and times spent mobile vs. immobile were not affected by PB/PM and/or LNFPIII during the 1st 5 min of the test or for the total 15 min test duration (immobile time: $p \geq 0.12$; Fig. 3D), albeit the climbing was numerically decreased by PB/PM treatment (data not shown). When the latency to the first bout of immobility was analyzed, there was a trend ($p = 0.06$) for a potentially anxiety-driven increase in the latency in the PB/PM treated mice, a trend that was less in mice treated with LNFPIII (Fig. 3E).

3.3.5 Sucrose Preference (SP)

All groups exhibited strong sucrose preference ($p \leq 0.001$; data not shown) and there were no significant main treatment differences (%: $p \geq 0.16$; Fig 3F). Interestingly, there was a significant treatment interaction (PB/PM x LNFPIII, $p \leq 0.05$; data not shown) for total sucrose consumed in which LNFPIII increased sucrose consumption within PB/PM groups, suggesting LNFPIII may be beneficial in increasing sensitivity to rewarding stimuli in animals previously exposed to GWI chemicals.

3.4 Cognition and memory effects of prior PB/PM exposure and delayed LNFPIII treatment

3.4.1 Nest Building

Nest building was not affected by either treatment as all groups built full nests over the course of 24 h (time effect, $p \leq 0.001$; Fig. 4A). Moreover, at each time point, there were no differences between PB/PM or LNFPIII treatments, suggesting prior PB/PM exposure did not cause severe hippocampal and/or striatal deficits that are associated with decreased performance in this test.

3.4.2 Barnes Maze (BM) Test

Significant main effects of day for response variables such as path length, latency to the target hole, and errors demonstrated that all animals learned the target hole (TH) location as they took less time, made fewer errors, and traveled less distance over the 4 days of maze training (p's ≤ 0.001; errors, Fig. 4B). However, prior PB/PM treatment led to acquisition phase deficits. Specifically, PB/PM mice were slower to learn and remember the TH location as evident on the last day of training (day 4), where PB/PM treated groups, irrespective of LNFPIII treatment, exhibited significant increases in path length ($p \leq 0.01$; data not shown), latency to TH ($p \leq 0.01$; data not shown), and errors ($p \leq 0.001$; Fig. 4B). Mice's performance in the probe trial was unaffected across groups (e.g., probe trial errors; $p \geq 0.85$; data not shown).

3.4.3 Novel Object Recognition (NOR)

Short-term object recognition memory assessed with the NOR was impaired by PB/PM. Prior PB/PM exposure led to significant decreases in the novelty preference index (NPI)($p \leq 0.05$; Fig. 4C), as well as novel object approaches and time spent at the novel

object (p's ≤ 0.05; data not shown). LNFPIII treatment did not modulate these effects significantly.

3.4.4 Radial Arm Maze (RAM)

Following 10 consecutive days of training in a dH-dependent 8-arm radial arm maze (RAM) uninterrupted foraging task (Potvin et al., 2006), all mice significantly improved their performance over time ($p \leq 0.001$; Fig. 4D). These data suggest that PB/PM exposure did not significantly impair dH-dependent short-term spatial working memory. Interestingly, LNFPIII treated mice initially (days 1-3) made significantly fewer errors (LNFPIII main effect $p \leq 0.01$; Fig. 4D), suggesting that LNFPIII improves early performance in this task irrespective of PB/PM treatment.

Similar to the foraging task, following 10 consecutive days of training in a vH-dependent modified Win-shift task to assess long-term spatial working memory (Clark et al., 2015; Floresco et al., 1997; O'Neill et al., 2013; Tamura et al., 2017), a significant main effect of training (Days 1-3 vs Days 8-10; $p \leq 0.05$), but not treatment, on performance over time was present (Fig. 4E). This main training effect was not due to a group-specific error reduction. Rather, it was due to a significantly worse (more errors) performance of PB/PM mice compared to control mice on days 1-3 ($p \leq 0.05$; Fig. 4E), an effect not seen in PB/PM mice that were also treated with LNFPIII.

3.5 Dorsal and ventral hippocampal electrophysiology 8 months post PB/PM exposure and 4 months post-LNFPIII treatment initiation

At 8 months post-PB/PM exposure and roughly 4 months after LNFPIII treatment initiation, no significant main effect of PB/PM exposure on dH LTP magnitude was observed. However, a significant main effect of LNFPIII treatment resulted in increased

dH LTP magnitude ($p \leq 0.01$), leading to enhanced dH LTP magnitude in LNFPIII treated mice compared to their vehicle counterparts (p's ≤ 0.05; Fig. 5A). A significant treatment interaction effect (PB/PM x LNFPIII; $p \leq 0.05$) on basal synaptic transmission resulted in reduced dH basal synaptic activity at 90, 105, 135, 150, 165, and 180 μA stimulus intensities in PB/PM exposed animals (p's ≤ 0.05); this was not seen in animals also treated with LNFPIII (Fig. 5B). Further, dH paired-pulse facilitation (PPF) was not impacted by either treatment (Supplemental Fig. 1A).

In the vH, LTP magnitude was unaffected by PB/PM; however, LNFPIII enhanced vH LTP magnitude (PB/PM-LNFPIII vs PB/PM-vehicle mice; $p < 0.05$; Fig. 5C). A significant PB/PM treatment x stimulus intensity interaction effect resulted in a reduction of vH basal synaptic transmission in PB/PM exposed animals ($p \leq 0.001$). Specifically, there was a significant reduction in vH basal synaptic transmission at stimulus intensities of 90, 120, 135, and 150 μA (p's ≤ 0.05) and a trending reduction at 105 and 165 μA ($p = 0.053$ and $p = 0.054$, respectively) in PB/PM mice compared to control mice (Fig. 5D). Further, LNFPIII treatment significantly recovered vH basal synaptic transmission at 75, 90, and 105 μA (p's ≤ 0.05) and numerically at 120, 150, and 165 μA stimulus intensities (p's ≤ 0.10) in PB/PM exposed mice (Fig. 5D). No significant treatment effects were observed on vH PPF (Supplemental Fig. 1B).

3.6 Tyrosine hydroxylase (TH) immunoreactivity in the dorsolateral and ventromedial striatum 9 months post PB/PM exposure and delayed LNFPIII treatment

In the dorsolateral striatum (DL STR), there were no significant main treatment effects for TH immunoreactivity. However, LNFPIII increased TH optical density in the

Vehicle-LNFPIII mice ($p \leq 0.05$; Fig. 6A). A similar effect was also apparent in the ventromedial (VM) STR, in which there were no significant main effects of either treatment on TH levels, but there was a trend for TH increase in the Vehicle-LNFPIII group ($p = 0.06$; Fig. 6B). See Figure 6C for representative images.

3.7 GFAP and IBA-1 immunoreactivity in the hilus region of the hippocampus 9 months post PB/PM exposure and delayed LNFPIII treatment

Analysis of astrocytes (GFAP+/Hoescht+) in the hilus region of the hippocampus revealed a trending interaction (PB/PM x LNFPIII; $p = 0.06$); pairwise-comparisons between the Vehicle-Vehicle and PB/PM-Vehicle groups revealed increased GFAP by PB/PM ($p \leq 0.05$; Fig. 7A). This PB/PM increase in GFAP was eliminated by LNFPIII ($p \leq 0.05$; Fig. 7A). A similar analysis of microglia (IBA-1+/Hoescht+) in the hilus revealed a significant interaction (PB/PM x LNFPIII; $p \leq 0.05$) in which LNFPIII reduced the abundance of IBA-1 immunoreactivity within PB/PM-treated mice ($p \leq 0.05$; Fig. 7B). See Figure 7C for representative GFAP/IBA-1 immunohistochemistry.

4. Discussion

Multiple preclinical studies have characterized acute and persisting neurological aberrations in PB/PM-based GWI models (Abdullah et al., 2011; Abdullah et al., 2013; Joshi et al., 2018; Joshi et al., 2020; Joshi et al., 2019; Zakirova et al., 2016; Zakirova et al., 2017; Zakirova et al., 2015), but some knowledge gaps remain. The present study sought to extensively evaluate the long-term implications of prior GWI chemical (PB/PM) exposure on neurobehavioral and neurobiological function 6-8 months post GWI-related symptomology induction. Additionally, treatment with an immunomodulatory agent, LNFPIII, was initiated several months post PB/PM exposure to assess its beneficial effects

in the context of GWI. As expected, prior PB/PM-treatment led to multiple behavioral deficits in motor, mood, and cognitive/memory functions that, at this stage, were mild to moderate in nature. LNFPIII treatment, initiated months after PB/PM exposure, improved multiple outcomes. The PB/PM-related deficits and benefits of LNFPIII were further examined through ex-vivo electrophysiology recordings for hippocampal function and post-mortem immunohistochemical analysis of dopamine homeostasis and glial status in the brain.

To identify potential mechanisms influencing the observed motor and mood behavioral deficits, striatal tyrosine hydroxylase (TH), the rate-limiting enzyme for dopamine (DA) synthesis, was evaluated immunohistochemically. In an earlier study, we examined the effects of PB/PM on DA 6 h post-exposure and found that PB/PM increased DA turnover (utilization) in the striatum (STR) (Carpenter et al., 2020); however, whether these effects persist long-term remained undetermined. Historically, neuropathological alterations along the nigrostriatal pathway, comprised of DA projections from the substantia nigra pars compacta (SNpc) to the STR (medial, dorsolateral), are associated with motor impairments (dyskinesia, rigidity, and posture instability) seen in neurodegenerative disorders, such as Parkinson's Disease (PD) (Kalia and Lang, 2015). Additionally, disruption in the mesolimbic pathway, consisting of DA projections from the ventral tegmental area (VTA) to the ventromedial (VM) STR, which contains the nucleus accumbens, can lead to affect disorders such as anhedonia, anxiety, and depression, also observed in some patients with PD (Cooney and Stacy, 2016). Current data indicate that 9 months post PB/PM exposure, nigral and/or VTA DA neuron terminals are not affected significantly. Given that DA neurons, especially nigrostriatal ones, decline with age and

GWI veterans experience accelerated aging (Zundel et al., 2019), it will be prudent to evaluate this axis 10-14 months post-exposure with the GWI model used here. Interestingly, LNFPIII treatment, independent of PB/PM exposure, increased the levels of DA terminal field (TH) intensity in both the dorsolateral (DL) and VM STR, suggesting that LNFPIII may be beneficial outside of GWI. LNFPIII treatment may also be beneficial later in the progression of the disease, e.g., in the aged veterans with GWI, but this needs to be investigated.

In this study, several parameters of motor function were impacted by the PB/PM treatment. Neuromuscular function (grip strength) was modestly decreased by prior PB/PM exposure. These results are consistent with an earlier study demonstrating a short-term decrease in grip strength post-PB/PM exposure, where PM was applied topically and the PB/PM ratio/duration of exposure differed from the present study (Abou-Donia et al., 2004). Of note, sensorimotor function was impaired as PB/PM mice performed worse than controls in the sticker removal (SR) task, and this deficit was eliminated by LNFPIII. This new information is in line with reports of GWI veterans exhibiting sensorimotor problems (Axelrod and Milner, 1997; Proctor et al., 2006; Toomey et al., 2009), and suggests that LNFPIII might ameliorate this aberration. Additionally, PB/PM exposure decreased marble-burying activity, an effect normally interpreted as an inhibition of anxiety-like behavior. However, considering the neuromuscular and sensorimotor deficits observed, the decreased burying in mice exposed to PB/PM might be indicative of a motor impairment. Modest impaired locomotor performance was present in the EZM, as PB/PM mice entered the closed arms more slowly than controls post placement on the maze. Open field locomotor deficits by prior PB/PM treatment presented as decreases in distance traveled

and rearing during the exploratory phase of the test. These results align with a similar study in which 1 month post-PB/PM exposure, there was a decrease in total distance traveled (Abdullah et al., 2011). Together, the present study and Abdullah et al., (2011), suggest that motor deficits, especially in exploratory behavior, manifest early and likely persist post-PB/PM exposure. Further, these deficits in locomotor function may be propagated by PB/PM gait deficiencies as PB/PM mice took significantly more steps and exhibited increased hindlimb base width in the gait test. No fat distribution differences existed among groups (data not shown), suggesting that PB/PM mice exhibited a wider stance for postural stability. This interpretation is in line with a previous report demonstrating that PB/PM treatment-induced subtle, ataxic-like effects (Abdullah et al., 2011). Taken together with previous motor data, gait deficiencies observed in this study suggest that PB/PM mice have a compromised ability and/or compensate more to achieve normal locomotor function from controls. LNFPIII prevented the increased step number and stride length, and it also reduced stride length variability, suggesting this immunotherapeutic has gait and postural effects that may not only be beneficial in the context of GWI, but overall, as well.

Altered mood has been consistently reported in veterans with GWI (Janulewicz et al., 2017; Sullivan et al., 2003) and experimental GWI models (Abdullah et al., 2013; Carreras et al., 2018; Joshi et al., 2018; Parihar et al., 2013; Phillips et al., 2019; Zakirova et al., 2016). Here, months after PB/PM exposure, mood impairments were predominantly anxiety-like. In the EZM, subtle anxiety-like behaviors were identified by numerical decreases in open arm entries and time spent in open arms for PB/PM mice. PB/PM-associated anxiety-like behavior also manifested as significant decreases and increases in time spent in the center and periphery in the OF, respectively; these anxiety-like effects

were not seen in mice that were treated with LNFPIII. Differences in depressive-like behaviors were not observed among groups for behavioral despair (ST) or anhedonia (SP). Although climbing attempts, an escape behavior in the ST, were numerically decreased in PB/PM mice, this finding aligns more with the observed motor impairments than with mood dysfunction. Interestingly, PB/PM mice were mobile for a longer duration prior to the first bout of immobility, suggesting this effect may also be anxiety-related. It has been suggested that certain forms of anxiety (i.e. hyperactive and panic states) may precede depression; thus, this increased latency to behavioral despair may be due to the initial anxiogenic effect of the ST (Boyer, 2000; Merikangas et al., 2003; Paul, 1988; Polani, 2004). Of note, this PB/PM effect was lessened with LNFPIII, further suggesting that this novel treatment ameliorates GWI-related affect dysfunction. Mood alterations in experimental GWI models vary and depend on the animal's age and GW chemicals used to recapitulate the disease (Abdullah et al., 2011; Carreras et al., 2018; Joshi et al., 2018; Zakirova et al., 2016). For example, studies investigating behaviors at early time points post GW chemicals/manipulations (e.g. DEET, diisopropylfluorophosphate, and stress) indicated increases in both anxiety- and depressive-like behaviors (Carreras et al., 2018; Parihar et al., 2013; Phillips et al., 2019). However, studies utilizing the PB/PM paradigm only detected anxiety-like behaviors shortly after exposure (Abdullah et al., 2012). Interestingly, long-term studies did not observe persistent anxiety-like behavior in PB/PM treated mice on the Elevated Plus Maze and OF, but did observe depressive-like behavior in the ST 10 and 13 months post-exposure (Joshi et al., 2018; Zakirova et al., 2016). The present findings observed anxiety-like, but not depressive-like, behavior 6-7 months post PB/PM exposure, providing insight into the progression of mood alterations of animals

tested 6-7 months post-PB/PM exposure. Our findings shed additional light on a possible shift from anxiety to depression in the context of GWI and other conditions over time (Merikangas et al., 2003; Paul, 1988).

Consistent with clinical complaints of GWI veterans (White et al., 2016), previous animal studies have observed several learning and memory deficits months after PB/PM exposure that are generally attributed to pathological changes in the hippocampus (Abdullah et al., 2011; Joshi et al., 2018; Zakirova et al., 2016; Zakirova et al., 2015). The dorsal (dH) and the ventral (vH) hippocampus are increasingly appreciated as functionally distinct structures where the dH primarily serves as a center for higher order cognitive processing whereas the vH is fundamentally involved in regulating stress/emotional responses (Fanselow and Dong, 2010; Papatheodoropoulos, 2018). Here, profound PB/PM-induced impairments were not observed in dH- and vH- dependent learning and memory tasks such as the Radial Arm Maze (RAM), Barnes Maze (BM), and nesting behavior tests. However, short-term, dH- and perirhinal cortex-specific recognition memory was impaired in the Novel Object Recognition (NOR) task by prior PB/PM exposure. Further, although PB/PM exposed mice improved their performance in the BM, they did so at a significantly slower rate than controls in the acquisition; LNFPIII did not improve these measures. This finding is consistent with a previous study examining performance in the BM 15 months post PB/PM exposure (Zakirova et al., 2016). Similar studies assessing the impact of PB/PM exposure on BM performance did not observe this effect at 5- or 22-months post-exposure, highlighting a potential transient, adverse neurological effect on reference memory at 8-15 months after PB/PM exposure (Zakirova et al., 2016; Zakirova et al., 2015), but this needs further investigation. Likewise, all groups

improved their performance in the dH-dependent short-term spatial working memory RAM foraging task. Of note, LNFPIII groups performed significantly better early in this test. No observable deficits in the vH-dependent long-term spatial working memory RAM Win-shift task were noted by the end of training in the paradigm. However, similar to the training phase of the BM, PB/PM mice performed significantly worse early-on, an effect that was not observed in PB/PM mice that received LNFPIII treatment. Overall, these data suggest modest aberrant and ameliorative effects of, respectively, PB/PM exposure and LNFPIII treatment, on dH and vH-dependent behavioral function. Identifying hippocampal dorsoventral-specific effects of prior PB/PM exposure and delayed LNFPIII treatment on synaptic plasticity and transmission may be critical for interpreting the subtle hippocampal-dependent behavioral abnormalities/ameliorations presented here.

Previous studies indicate PB/PM exposure can lead to a neuroinflammatory phenotype that manifests with prolonged aberrations in glial function and sustained inflammation (Abdullah et al., 2011; Carpenter et al., 2020; Joshi et al., 2018; Joshi et al., 2019; Zakirova et al., 2016). Under conditions of neuroinflammation, enhanced inflammatory cytokine production leads to aberrant activation of glial cells and subsequent impairment of hippocampal synaptic plasticity and transmission, resulting in deficits in learning and memory (Habbas et al., 2015; Kelly et al., 2013; Maher et al., 2006; Prieto and Cotman, 2017). Furthermore, enhanced expression of pro-inflammatory cytokines reduces the secretion of hippocampal brain-derived neurotrophic factor (BDNF) (Barrientos et al., 2004; Littlefield et al., 2015; Yirmiya and Goshen, 2011), a critical trophic factor involved in synaptic transmission (Kang and Schuman, 1995). Studies utilizing the PB/PM GWI model have found varying results surrounding glial activation in

the hippocampus during the progression of GWI. In one study, at 5 months post PB/PM exposure, astrogliosis but not microgliosis was apparent (Abdullah et al., 2011), whereas both were observed at 15 months (Abdullah et al., 2016; Joshi et al., 2018), but, perhaps due to age-related neuroinflammation, not different from controls at 22 months (Zakirova et al., 2016). These results highlight the persistent neuroimmune activation within this GWI model, specifically modest astrocyte activation and are in line with the current study. Here, at 9 months post-prior PB/PM exposure, immunohistochemical analysis of GFAP (astrocytes) and IBA-1 (microglia) revealed a PB/PM-dependent GFAP increase and a less pronounced one of IBA-1 in the hippocampus. Importantly, LNFPIII treatment reduced both GFAP and IBA-1 within the GWI context, indicative of its anti-inflammatory properties. This sustained neuroinflammation post-GWI exposures may underlie the persisting impairments in hippocampal synaptic transmission as well as be the target for the beneficial effects of LNFPIII discussed herein.

Hippocampal electrophysiology data revealed reduced dH and vH basal synaptic transmission by PB/PM, an effect that is consistent with a GWI study employing a different exposure paradigm that observed prolonged deficits in excitatory and inhibitory hippocampal neurotransmission (Wang et al., 2020). A separate investigation also detected acute and persisting impairments in hippocampal synaptic transmission in a different GWI animal model (Gargas et al., 2021). These preclinical findings of persisting disruptions in neurotransmission that are, in part, mediated by excitatory neurotransmitters such as glutamate are in line with emerging clinical evidence indicating that glutamatergic dysfunction contributes to GWI pathophysiology (Baraniuk et al., 2021; Holton et al., 2020; Joyce and Holton, 2020). Interestingly, LNFPIII recovered vH, but not dH, basal

synaptic transmission, which may be attributed to LNFPIII-mediated normalization of glial function, namely of pro-inflammatory cytokine secretion and enhancement of anti-inflammatory cytokine production in this inflammation-sensitive hippocampal sector (Kyran et al., 2018; Onufriev et al., 2017; Pearson-Leary et al., 2019; Pearson-Leary et al., 2017; Pearson-Leary et al., 2020; Zheng et al., 2017).

Finally, hippocampal LTP, a well-established synaptic substrate for learning and memory (Bliss and Collingridge, 1993; Whitlock et al., 2006), was assessed to determine if PB/PM exposure adversely impacted hippocampal synaptic plasticity and if LNFPIII would be beneficial. While PB/PM exposure did not affect LTP, an enhancement of dH and vH LTP magnitude was detected in LNFPIII-treated mice, suggesting prolonged treatment likely increased ERK-1/2 phosphorylation (Tundup et al., 2015) and potentiated hippocampal synaptic efficacy. Additionally, a lack of a PB/PM-induced effect on a presynaptic-related mechanism of synaptic plasticity (i.e., paired-pulse facilitation) in addition to PB/PM-mediated impairments of dH and vH synaptic transmission is consistent with a decrease in the density of synapses in the CA1 subfield. This interpretation is in line with preclinical GWI studies that observed reductions in hippocampal CA1 apical dendritic spine density (Speed et al., 2011), CA1 principal cell postsynaptic density protein 95 expression (Wang et al., 2020), as well as decreased hippocampal neuronal cellular proliferation and neurogenesis months after GWI-related exposures (Kodali et al., 2018; Megahed et al., 2014; Parihar et al., 2013; Shetty et al., 2020; Wang et al., 2020). Although previous studies indicated synaptic density and hippocampal neurogenesis may be persistently impaired in animals exposed to GW chemicals, normalization of the fEPSP slope value in the LTP response provides the opportunity to detect the LNFPIII induced

enhancement of LTP magnitude. Accordingly, while delayed LNFPIII treatment enhanced dH and vH LTP magnitude irrespective of prior PB/PM exposure, given the progressive nature of the disease, LNFPIII may be an even more efficacious treatment for ameliorating synaptic anomalies that underlie GWI-related cognitive impairments later in the course of the disease.

5. Conclusion

The findings in this study indicate long-term neurobehavioral and neurobiological maladaptive alterations months after the initial exposure to a well-established GWI animal model (PB/PM; see summary Figure 8). Collectively, the neurobehavioral (i.e., motor, mood, and cognitive impairments) and neurobiological dysfunction (i.e., glial activation and reduced hippocampal synaptic transmission) associated with prior PB/PM exposure shown here further characterizes many of the nuances of this GWI model as well as the symptomology experienced by GWI veterans. Importantly, LNFPIII treatment demonstrated many protective effects within this study, highlighting its promising role as an efficacious GWI therapeutic. Further investigations into the long-term mechanisms and assessing the beneficial effects of LNFPIII within this model are ongoing.

Author Contributions

NMF conceived and designed the study. TN and DAH synthesized, characterized, and provided LNFPIII used in the study. NMF, JMC, RLD, AND, and KAB assisted in investigation and sample collection. JMC, KAB, AND, RLD, and RAB performed sample and data analysis. JMC, KAB, NMF, and JJW wrote the manuscript with input from DAH. All authors read/contributed editorially and approved the final manuscript version.

Declaration of Competing Interest

The authors declare no conflicts of interest.

Acknowledgements

This research was supported by Department of Defense grant number W81XWH-16-1-0586 to NMF. AND and RAB's participation in this research was made possible by National Institute of Health (NIH) grant T35OD010433.

References:

Abdullah, L., Crynen, G., Reed, J., Bishop, A., Phillips, J., Ferguson, S., Mouzon, B., Mullan, M., Mathura, V., Mullan, M., Ait-Ghezala, G., Crawford, F., 2011. Proteomic CNS profile of delayed cognitive impairment in mice exposed to Gulf War agents. NeuroMolecular Medicine 13, 275-288.

Abdullah, L., Evans, J.E., Bishop, A., Reed, J.M., Crynen, G., Phillips, J., Pelot, R., Mullan, M.A., Ferro, A., Mullan, C.M., Mullan, M.J., Ait-Ghezala, G., Crawford, F.C., 2012. Lipidomic profiling of phosphocholine-containing brain lipids in mice with sensorimotor deficits and anxiety-like features after exposure to Gulf War agents. NeuroMolecular Medicine 14, 349-361.

Abdullah, L., Evans, J.E., Joshi, U., Crynen, G., Reed, J., Mouzon, B., Baumann, S., Montague, H., Zakirova, Z., Emmerich, T., Bachmeier, C., Klimas, N., Sullivan, K., Mullan, M., Ait-Ghezala, G., Crawford, F., 2016. Translational potential of long-term decreases in mitochondrial lipids in a mouse model of Gulf War Illness. Toxicology 372, 22-33.

Abdullah, L., Evans, J.E., Montague, H., Reed, J.M., Moser, A., Crynen, G., Gonzalez, A., Zakirova, Z., Ross, I., Mullan, C., 2013. Chronic elevation of phosphocholine containing lipids in mice exposed to Gulf War agents pyridostigmine bromide and permethrin. Neurotoxicology and Teratology 40, 74-84.

Abou-Donia, M.B., Dechkovskaia, A.M., Goldstein, L.B., Abdel-Rahman, A., Bullman, S.L., Khan, W.A., 2004. Co-exposure to pyridostigmine bromide, DEET, and/or permethrin causes sensorimotor deficit and alterations in brain acetylcholinesterase activity. Pharmacology Biochemistry and Behavior 77(2), 253-262.

Abou-Donia, M.B., Dechkovskaia, A.M., Goldstein, L.B., Bullman, S.L., Khan, W.A., 2002. Sensorimotor Deficit and Cholinergic Changes following Coexposure with Pyridostigmine Bromide and Sarin in Rats. Toxicological Sciences 66(1), 148-158.

Alonso, M., Medina, J.H., Pozzo-Miller, L., 2004. ERK1/2 activation is necessary for BDNF to increase dendritic spine density in hippocampal CA1 pyramidal neurons. Learning & memory 11(2), 172-178.

Alshelh, Z., Albrecht, D.S., Bergan, C., Akeju, O., Clauw, D.J., Conboy, L., Edwards, R.R., Kim, M., Lee, Y.C., Protsenko, E., Napadow, V., Sullivan, K., Loggia, M.L., 2020.

In-vivo imaging of neuroinflammation in veterans with Gulf War illness. Brain, Behavior, and Immunity.

Anger, W.K., Storzbach, D., Binder, L.M., Campbell, K.A., Rohlman, D.S., McCauley, L., Kovera, C.A., Davis, K.L., 1999. Neurobehavioral deficits in Persian Gulf veterans: Evidence from a population-based study. Journal of the International Neuropsychological Society 5(3), 203-212.

Atochina, O., Da'dara, A.A., Walker, M., Harn, D.A., 2008. The immunomodulatory glycan LNFPIII initiates alternative activation of murine macrophages in vivo. Immunology 125(1), 111-121.

Axelrod, B.N., Milner, I.B., 1997. Neuropsychological findings in a sample of Operation Desert Storm veterans. The Journal of Neuropsychiatry and Clinical Neurosciences 9(1), 23-28.

Babb, S.J., Crystal, J.D., 2006. Discrimination of what, when, and where is not based on time of day. Learning & Behavior 34(2), 124-130.

Baraniuk, J.N., El-Amin, S., Corey, R., Rayhan, R., Timbol, C., 2013. Carnosine treatment for gulf war illness: a randomized controlled trial. Glob J Health Sci 5(3), 69-81.

Baraniuk, J.N., Kern, G., Narayan, V., Cheema, A., 2021. Exercise modifies glutamate and other metabolic biomarkers in cerebrospinal fluid from Gulf War Illness and Myalgic encephalomyelitis / Chronic Fatigue Syndrome. PLOS ONE 16(1), e0244116.

Barrientos, R.M., Sprunger, D.B., Campeau, S., Watkins, L.R., Rudy, J.W., Maier, S.F., 2004. BDNF mRNA expression in rat hippocampus following contextual learning is blocked by intrahippocampal IL-1β administration. Journal of Neuroimmunology 155(1-2), 119-126.

Bhargava, P., Li, C., Stanya, K.J., Jacobi, D., Dai, L., Liu, S., Gangl, M.R., Harn, D.A., Lee, C.H., 2012. Immunomodulatory glycan LNFPIII alleviates hepatosteatosis and insulin resistance through direct and indirect control of metabolic pathways. Nature Medicine 18(11), 1665-1672.

Bliss, T.V., Collingridge, G.L., 1993. A synaptic model of memory: long-term potentiation in the hippocampus. Nature 361(6407), 31.

Boyer, P., 2000. Do anxiety and depression have a common pathophysiological mechanism? Acta Psychiatrica Scandinavica 102, 24-29.

Braun, A.A., Skelton, M.R., Vorhees, C.V., Williams, M.T., 2011. Comparison of the elevated plus and elevated zero mazes in treated and untreated male Sprague–Dawley rats: Effects of anxiolytic and anxiogenic agents. Pharmacology Biochemistry and Behavior 97(3), 406-415.

Broadbent, N.J., Gaskin, S., Squire, L.R., Clark, R.E., 2009. Object recognition memory and the rodent hippocampus. Learn Mem 17(1), 5-11.

Broderick, G., Ben-Hamo, R., Vashishtha, S., Efroni, S., Nathanson, L., Barnes, Z., Fletcher, M.A., Klimas, N., 2013. Altered immune pathway activity under exercise challenge in Gulf War Illness: An exploratory analysis. Brain, Behavior, and Immunity 28, 159-169.

Broderick, G., Fletcher, M.A., Gallagher, M., Barnes, Z., Vernon, S.D., Klimas, N.G., 2018. Exploring the Diagnostic Potential of Immune Biomarker Co-expression in Gulf War Illness. Psychoneuroimmunology, 101-120.

Carpenter, J.M., Gordon, H.E., Ludwig, H.D., Wagner, J.J., Harn, D.A., Norberg, T., Filipov, N.M., 2020. Neurochemical and neuroinflammatory perturbations in two Gulf War Illness models: Modulation by the immunotherapeutic LNFPIII. NeuroToxicology 77, 40-50.

Carreras, I., Aytan, N., Mellott, T., Choi, J.-K., Lehar, M., Crabtree, L., Leite-Morris, K., Jenkins, B.G., Blusztajn, J.K., Dedeoglu, A., 2018. Anxiety, neuroinflammation, cholinergic and GABAergic abnormalities are early markers of Gulf War illness in a mouse model of the disease. Brain Res 1681, 34-43.

Chao, L.L., Abadjian, L., Hlavin, J., Meyerhoff, D.J., Weiner, M.W., 2011. Effects of low-level sarin and cyclosarin exposure and Gulf War Illness on Brain Structure and Function: A study at 4T. NeuroToxicology 32(6), 814-822.

Chao, L.L., Rothlind, J.C., Cardenas, V.A., Meyerhoff, D.J., Weiner, M.W., 2010. Effects of low-level exposure to sarin and cyclosarin during the 1991 Gulf War on brain function and brain structure in US veterans. NeuroToxicology 31(5), 493-501.

Chao, L.L., Zhang, Y., Buckley, S., 2015. Effects of low-level sarin and cyclosarin exposure on white matter integrity in Gulf War Veterans. NeuroToxicology 48, 239-248.

Clark, J.K., Furgerson, M., Crystal, J.D., Fechheimer, M., Furukawa, R., Wagner, J.J., 2015. Alterations in synaptic plasticity coincide with deficits in spatial working memory in presymptomatic 3xTg-AD mice. Neurobiology of Learning and Memory 125, 152-162.

Conrad, K.L., Louderback, K.M., Gessner, C.P., Winder, D.G., 2011. Stress-induced alterations in anxiety-like behavior and adaptations in plasticity in the bed nucleus of the stria terminalis. Physiology & Behavior 104(2), 248-256.

Cooney, J.W., Stacy, M., 2016. Neuropsychiatric Issues in Parkinson's Disease. Current Neurology and Neuroscience Reports 16(5), 49.

DDGWIRP, 2018. The Gulf War Illness Landscape in: Programs, D.o.D.C.D.M.R. (Ed.).

Deacon, R., 2012. Assessing burrowing, nest construction, and hoarding in mice. J Vis Exp(59), e2607.

Donta, S.T., Engel, C.C., Jr., Collins, J.F., Baseman, J.B., Dever, L.L., Taylor, T., Boardman, K.D., Kazis, L.E., Martin, S.E., Horney, R.A., Wiseman, A.L., Kernodle, D.S., Smith, R.P., Baltch, A.L., Handanos, C., Catto, B., Montalvo, L., Everson, M., Blackburn, W., Thakore, M., Brown, S.T., Lutwick, L., Norwood, D., Bernstein, J., Bacheller, C., Ribner, B., Church, L.W., Wilson, K.H., Guduru, P., Cooper, R., Lentino, J., Hamill, R.J., Gorin, A.B., Gordan, V., Wagner, D., Robinson, C., DeJace, P., Greenfield, R., Beck, L., Bittner, M., Schumacher, H.R., Silverblatt, F., Schmitt, J., Wong, E., Ryan, M.A., Figueroa, J., Nice, C., Feussner, J.R., Group, V.A.C., 2004. Benefits and harms of doxycycline treatment for Gulf War veterans' illnesses: a randomized, double-blind, placebo-controlled trial. Ann Intern Med 141(2), 85-94.

Eagle, A.L., Mazei-Robison, M., Robison, A.J., 2016. Sucrose Preference Test to Measure Stress-induced Anhedonia. Bio-protocol 6(11), e1822.

Fanselow, M.S., Dong, H.-W., 2010. Are the dorsal and ventral hippocampus functionally distinct structures? Neuron 65(1), 7-19.

Filipov, N.M., Norwood, A.B., Sistrunk, S.C., 2009. Strain-specific sensitivity to MPTP of C57BL/6 and BALB/c mice is age dependent. NeuroReport 20(7).

Fleming, S.M., Ekhator, O.R., Ghisays, V., 2013. Assessment of sensorimotor function in mouse models of Parkinson's disease. Journal of visualized experiments : JoVE(76), 50303.

Floresco, S.B., Seamans, J.K., Phillips, A.G., 1997. Selective roles for hippocampal, prefrontal cortical, and ventral striatal circuits in radial-arm maze tasks with or without a delay. Journal of Neuroscience 17(5), 1880-1890.

Furgerson, M., Clark, J.K., Crystal, J.D., Wagner, J.J., Fechheimer, M., Furukawa, R., 2014. Hirano body expression impairs spatial working memory in a novel mouse model. Acta Neuropathologica Communications 2(1), 131.

Gargas, N.M., Ethridge, V.T., Miklasevich, M.K., Rohan, J.G., 2021. Altered hippocampal function and cytokine levels in a rat model of Gulf War illness. Life Sciences 274, 119333.

Golier, J.A., Caramanica, K., Michaelides, A.C., Makotkine, I., Schmeidler, J., Harvey, P.D., Yehuda, R., 2016. A randomized, double-blind, placebo-controlled, crossover trial of mifepristone in Gulf War veterans with chronic multisymptom illness. Psychoneuroendocrinology 64, 22-30.

Golomb, B.A., Allison, M., Koperski, S., Koslik, H.J., Devaraj, S., Ritchie, J.B., 2014. Coenzyme Q10 benefits symptoms in Gulf War veterans: results of a randomized double-blind study. Neural Comput 26(11), 2594-2651.

Habbas, S., Santello, M., Becker, D., Stubbe, H., Zappia, G., Liaudet, N., Klaus, F.R., Kollias, G., Fontana, A., Pryce, C.R., 2015. Neuroinflammatory TNFα impairs memory via astrocyte signaling. Cell 163(7), 1730-1741.

Hattiangady, B., Mishra, V., Kodali, M., Shuai, B., Rao, X., Shetty, A.K., 2014. Object location and object recognition memory impairments, motivation deficits and depression in a model of Gulf War illness. Front Behav Neurosci 8, 78.

Heaton, K.J., Palumbo, C.L., Proctor, S.P., Killiany, R.J., Yurgelun-Todd, D.A., White, R.F., 2007. Quantitative magnetic resonance brain imaging in US army veterans of the 1991 Gulf War potentially exposed to sarin and cyclosarin. NeuroToxicology 28(4), 761-769.

Helmer, D.A., Van Doren, W.W., Litke, D.R., Tseng, C.L., Ho, L., Osinubi, O., Pasinetti, G.M., 2020. Safety, Tolerability and Efficacy of Dietary Supplementation with Concord Grape Juice in Gulf War Veterans with Gulf War Illness: A Phase I/IIA, Randomized, Double-Blind, Placebo-Controlled Trial. Int J Environ Res Public Health 17(10).

Hofele, K., Sedelis, M., Auburger, G.W., Morgan, S., Huston, J.P., Schwarting, R.K.W., 2001. Evidence for a Dissociation between MPTP Toxicity and Tyrosinase Activity Based on Congenic Mouse Strain Susceptibility. Experimental Neurology 168(1), 116-122.

Holton, K.F., Kirkland, A.E., Baron, M., Ramachandra, S.S., Langan, M.T., Brandley, E.T., Baraniuk, J.N., 2020. The Low Glutamate Diet Effectively Improves Pain and Other Symptoms of Gulf War Illness. Int J Environ Res Public Health 12(9), 2593.

Hubbard, N.A., Hutchison, J.L., Motes, M.A., Shokri-Kojori, E., Bennett, I.J., Brigante, R.M., Haley, R.W., Rypma, B., 2014. Central Executive Dysfunction and Deferred Prefrontal Processing in Veterans with Gulf War Illness. Clin Psychol Sci 2(3), 319-327.

Janulewicz, P.A., Krengel, M.H., Maule, A., White, R.F., Cirillo, J., Sisson, E., Heeren, T., Sullivan, K., 2017. Neuropsychological characteristics of Gulf War illness: A meta-analysis. PloS One 12(5), e0177121-e0177121.

Joshi, U., Evans, J.E., Joseph, R., Emmerich, T., Saltiel, N., Lungmus, C., Oberlin, S., Langlois, H., Ojo, J., Mouzon, B., 2018. Oleoylethanolamide treatment reduces neurobehavioral deficits and brain pathology in a mouse model of Gulf War Illness. Scientific reports 8(1), 12921.

Joshi, U., Evans, J.E., Pearson, A., Saltiel, N., Cseresznye, A., Darcey, T., Ojo, J., Keegan, A.P., Oberlin, S., Mouzon, B., 2020. Targeting sirtuin activity with nicotinamide riboside reduces neuroinflammation in a GWI mouse model. NeuroToxicology 79, 84-94.

Joshi, U., Pearson, A., Evans, J.E., Langlois, H., Saltiel, N., Ojo, J., Klimas, N., Sullivan, K., Keegan, A.P., Oberlin, S., 2019. A permethrin metabolite is associated with adaptive immune responses in Gulf War Illness. Brain, Behavior, and Immunity(81), 545-559.

Joyce, M.R., Holton, K.F., 2020. Neurotoxicity in Gulf War Illness and the potential role of glutamate. Neurotoxicology 80, 60-70.

Kalia, L.V., Lang, A.E., 2015. Parkinson's disease. The Lancet 386(9996), 896-912.

Kang, H., Schuman, E.M., 1995. Long-lasting neurotrophin-induced enhancement of synaptic transmission in the adult hippocampus. Science 267(5204), 1658-1662.

Kelly, R.J., Minogue, A.M., Lyons, A., Jones, R.S., Browne, T.C., Costello, D.A., Denieffe, S., O'Sullivan, C., Connor, T.J., Lynch, M.A., 2013. Glial activation in AβPP/PS1 mice is associated with infiltration of IFNγ-producing cells. Journal of Alzheimer's Disease 37(1), 63-75.

Kimono, D., Bose, D., Seth, R.K., Mondal, A., Saha, P., Janulewicz, P., Sullivan, K., Lasley, S., Horner, R., Klimas, N., Chatterjee, S., 2020. Host Akkermansia muciniphila Abundance Correlates With Gulf War Illness Symptom Persistence via NLRP3-Mediated Neuroinflammation and Decreased Brain-Derived Neurotrophic Factor. Neuroscience Insights 15, 2633105520942480.

Kodali, M., Hattiangady, B., Shetty, G., Bates, A., Shuai, B., Shetty, A., 2018. Curcumin treatment leads to better cognitive and mood function in a model of Gulf War Illness with enhanced neurogenesis, and alleviation of inflammation and mitochondrial dysfunction in the hippocampus. Brain, Behavior, and Immunity 69, 499-514.

Krishna, S., Dodd, C.A., Hekmatyar, S.K., Filipov, N.M., 2014. Brain deposition and neurotoxicity of manganese in adult mice exposed via the drinking water. Arch Toxicol 88(1), 47-64.

Krishna, S., Lin, Z., de La Serre, C.B., Wagner, J.J., Harn, D.H., Pepples, L.M., Djani, D.M., Weber, M.T., Srivastava, L., Filipov, N.M., 2016. Time-dependent behavioral, neurochemical, and metabolic dysregulation in female C57BL/6 mice caused by chronic high-fat diet intake. Physiology & Behavior 157, 196-208.

Kyran, E.L., Robinson, C., Kocovski, P., Li, Z., Dang, P.T., Hale, M.W., Orian, J.M., 2018. Multiple pathological mechanisms contribute to hippocampal damage in the experimental autoimmune encephalomyelitis model of multiple sclerosis. NeuroReport 29(1), 19-24.

Leger, M., Quiedeville, A., Bouet, V., Haelewyn, B., Boulouard, M., Schumann-Bard, P., Freret, T., 2013. Object recognition test in mice. Nature Protocols 8(12), 2531-2537.

Lin, Z., Dodd, C.A., Filipov, N.M., 2013. Short-term atrazine exposure causes behavioral deficits and disrupts monoaminergic systems in male C57BL/6 mice. Neurotoxicology and Teratology 39, 26-35.

Littlefield, A.M., Setti, S.E., Priester, C., Kohman, R.A., 2015. Voluntary exercise attenuates LPS-induced reductions in neurogenesis and increases microglia expression of a proneurogenic phenotype in aged mice. Journal of Neuroinflammation 12(1), 138.

Macht, V.A., Woodruff, J.L., Maissy, E.S., Grillo, C.A., Wilson, M.A., Fadel, J.R., Reagan, L.P., 2019. Pyridostigmine bromide and stress interact to impact immune function, cholinergic neurochemistry and behavior in a rat model of Gulf War Illness. Brain, Behavior, and Immunity.

Madhu, L.N., Attaluri, S., Kodali, M., Shuai, B., Upadhya, R., Gitai, D., Shetty, A.K., 2019. Neuroinflammation in Gulf War Illness is linked with HMGB1 and complement activation, which can be discerned from brain-derived extracellular vesicles in the blood. Brain, Behavior, and Immunity 81, 430-443.

Maher, F.O., Clarke, R.M., Kelly, A., Nally, R.E., Lynch, M.A., 2006. Interaction between interferon γ and insulin-like growth factor-1 in hippocampus impacts on the ability of rats to sustain long-term potentiation. Journal of Neurochemistry 96(6), 1560-1571.

Megahed, T., Hattiangady, B., Shuai, B., Shetty, A.K., 2014. Parvalbumin and neuropeptide Y expressing hippocampal GABA-ergic inhibitory interneuron numbers decline in a model of Gulf War illness. Front Cell Neurosci 8, 447.

Merikangas, K.R., Zhang, H., Avenevoli, S., Acharyya, S., Neuenschwander, M., Angst, J., 2003. Longitudinal Trajectories of Depression and Anxiety in a Prospective Community Study: The Zurich Cohort Study. Archives of General Psychiatry 60(10), 993-1000.

Michalovicz, L.T., Kelly, K.A., Sullivan, K., O'Callaghan, J.P., 2020. Acetylcholinesterase inhibitor exposures as an initiating factor in the development of Gulf War Illness,

a chronic neuroimmune disorder in deployed veterans. Neuropharmacology 171, 108073.

Miller, J.V., LeBouf, R.F., Kelly, K.A., Michalovicz, L.T., Ranpara, A., Locker, A.R., Miller, D.B., O'Callaghan, J.P., 2018. The Neuroinflammatory Phenotype in a Mouse Model of Gulf War Illness is Unrelated to Brain Regional Levels of Acetylcholine as Measured by Quantitative HILIC-UPLC-MS/MS. Toxicological Sciences 165(2), 302-313.

Minichiello, L., 2009. TrkB signalling pathways in LTP and learning. Nature Reviews Neuroscience 10(12), 850.

Mote, R.S., Carpenter, J.M., Dockman, R.L., Steinberger, A.J., Suen, G., Norberg, T., Harn, D.A., Wagner, J.J., Filipov, N.M., 2020. Assessing the Beneficial Effects of the Immunomodulatory Glycan LNFPIII on Gut Microbiota and Health in a Mouse Model of Gulf War Illness. Int J Environ Res Public Health 17(19), 7081.

Mulherkar, S., Liu, F., Chen, Q., Narayanan, A., Couvillon, A.D., Shine, H.D., Tolias, K.F., 2013. The small GTPase RhoA is required for proper locomotor circuit assembly. PLoS One 8(6), e67015.

NASEM, National Academies of Sciences, E., Medicine, 2018. Veterans and Agent Orange: Update 11 (2018). The National Academies Press, Washington, DC.

O'Callaghan, J.P., Kelly, K.A., Locker, A.R., Miller, D.B., Lasley, S.M., 2015. Corticosterone primes the neuroinflammatory response to DFP in mice: potential animal model of Gulf War Illness. Journal of Neurochemistry 133(5), 708-721.

O'Neill, P.-K., Gordon, J.A., Sigurdsson, T., 2013. Theta oscillations in the medial prefrontal cortex are modulated by spatial working memory and synchronize with the hippocampus through its ventral subregion. Journal of Neuroscience 33(35), 14211-14224.

Ojo, J.O., Abdullah, L., Evans, J., Reed, J.M., Montague, H., Mullan, M.J., Crawford, F.C., 2014. Exposure to an organophosphate pesticide, individually or in combination with other Gulf War agents, impairs synaptic integrity and neuronal differentiation, and is accompanied by subtle microvascular injury in a mouse model of Gulf War agent exposure. Neuropathology 34(2), 109-127.

Onufriev, M., Freiman, S., Moiseeva, Y.V., Stepanichev, M.Y., Lazareva, N., Gulyaeva, N., 2017. Accumulation of corticosterone and interleukin-1β in the hippocampus after focal ischemic damage of the neocortex: Selective vulnerability of the ventral hippocampus. Neurochemical Journal 11(3), 236-241.

Papatheodoropoulos, C., 2018. Electrophysiological evidence for long-axis intrinsic diversification of the hippocampus. Frontiers in Bioscience (Landmark Ed) 23, 109-145.

Parihar, V.K., Hattiangady, B., Shuai, B., Shetty, A.K., 2013. Mood and memory deficits in a model of Gulf War illness are linked with reduced neurogenesis, partial neuron loss, and mild inflammation in the hippocampus. Neuropsychopharmacology 38(12), 2348-2362.

Parkitny, L., Middleton, S., Baker, K., Younger, J., 2015. Evidence for abnormal cytokine expression in Gulf War Illness: A preliminary analysis of daily immune monitoring data. BMC Immunol 16, 57-57.

Paul, S.M., 1988. Anxiety and depression: a common neurobiological substrate? The Journal of clinical psychiatry 49 Suppl, 13-16.

Pearson-Leary, J., Eacret, D., Bhatnagar, S., 2019. Interleukin-1α in the ventral hippocampus increases stress vulnerability and inflammation-related processes. Stress, 1-10.

Pearson-Leary, J., Eacret, D., Chen, R., Takano, H., Nicholas, B., Bhatnagar, S., 2017. Inflammation and vascular remodeling in the ventral hippocampus contributes to vulnerability to stress. Translational Psychiatry 7(6), e1160-e1160.

Pearson-Leary, J., Zhao, C., Bittinger, K., Eacret, D., Luz, S., Vigderman, A.S., Dayanim, G., Bhatnagar, S., 2020. The gut microbiome regulates the increases in depressive-type behaviors and in inflammatory processes in the ventral hippocampus of stress vulnerable rats. Molecular Psychiatry 25(5), 1068-1079.

Phillips, K.F., Santos, E., Blair, R.E., Deshpande, L.S., 2019. Targeting Intracellular Calcium Stores Alleviates Neurological Morbidities in a DFP-Based Rat Model of Gulf War Illness. Toxicological Sciences 169(2), 567-578.

Polani, P.E., 2004. Attacks of anxiety, panic and frenzy, and their related depression: a hypothesis. Medical Hypotheses 63(1), 124-127.

Porter, B., Long, K., Rull, R.P., Dursa, E.K., 2020. Prevalence of Chronic Multisymptom Illness/Gulf War Illness Over Time Among Millennium Cohort Participants, 2001 to 2016. Journal of occupational and environmental medicine 62(1), 4-10.

Potvin, O., Allen, K., Thibaudeau, G., Doré, F.Y., Goulet, S., 2006. Performance on spatial working memory tasks after dorsal or ventral hippocampal lesions and adjacent damage to the subiculum. Behavioral Neuroscience 120(2), 413.

Preston, C.J., Brown, K.A., Wagner, J.J., 2019. Cocaine conditioning induces persisting changes in ventral hippocampus synaptic transmission, long-term potentiation, and radial arm maze performance in the mouse. Neuropharmacology 150, 27-37.

Prieto, G.A., Cotman, C.W., 2017. Cytokines and cytokine networks target neurons to modulate long-term potentiation. Cytokine & Growth Factor Reviews 34, 27-33.

Proctor, S.P., Heaton, K.J., Heeren, T., White, R.F., 2006. Effects of sarin and cyclosarin exposure during the 1991 Gulf War on neurobehavioral functioning in US army veterans. NeuroToxicology 27(6), 931-939.

R Development Core Team, 2016, https://www.r-project.org/. R: A language and environment for statistical computing. R Foundation for Statistical Computing, Vienna, Austria.

Rayhan, R.U., Stevens, B.W., Timbol, C.R., Adewuyi, O., Walitt, B., VanMeter, J.W., Baraniuk, J.N., 2013. Increased brain white matter axial diffusivity associated with fatigue, pain and hyperalgesia in Gulf War illness. PLoS One 8(3), e58493.

Ribeiro, A.C., Zhu, J., Kronfol, M.M., Jahr, F.M., Younis, R.M., Hawkins, E., McClay, J.L., Deshpande, L.S., 2020. Molecular mechanisms for the antidepressant-like effects of a low-dose ketamine treatment in a DFP-based rat model for Gulf War Illness. NeuroToxicology.

Shetty, A.K., Attaluri, S., Kodali, M., Shuai, B., Shetty, G.A., Upadhya, D., Hattiangady, B., Madhu, L.N., Upadhya, R., Bates, A., 2020. Monosodium luminol reinstates redox homeostasis, improves cognition, mood and neurogenesis, and alleviates neuro-and systemic inflammation in a model of Gulf War Illness. Redox Biology 28, 101389.

Speed, H.E., Blaiss, C.A., Kim, A., Haws, M.E., Melvin, N.R., Jennings, M., Eisch, A.J., Powell, C.M., 2011. Delayed reduction of hippocampal synaptic transmission and

spines following exposure to repeated subclinical doses of organophosphorus pesticide in adult mice. Toxicological Sciences 125(1), 196-208.

Srivastava, L., Tundup, S., Choi, B.S., Norberg, T., Harn, D., 2014. Immunomodulatory glycan lacto-N-fucopentaose III requires clathrin-mediated endocytosis to induce alternative activation of antigen-presenting cells. Infect Immun 82(5), 1891-1903.

Steele, L., Sastre, A., Gerkovich, M.M., Cook, M.R., 2012. Complex factors in the etiology of Gulf War illness: wartime exposures and risk factors in veteran subgroups. Environ Health Perspect 120(1), 112-118.

Stellman, J.M., Stellman, S.D., 2018. Agent Orange During the Vietnam War: The Lingering Issue of Its Civilian and Military Health Impact. Am J Public Health 108(6), 726-728.

Sullivan, K., Krengel, M., Bradford, W., Stone, C., Thompson, T.A., Heeren, T., White, R.F., 2018. Neuropsychological functioning in military pesticide applicators from the Gulf War: Effects on information processing speed, attention and visual memory. Neurotoxicology and Teratology 65, 1-13.

Sullivan, K., Krengel, M., Proctor, S.P., Devine, S., Heeren, T., White, R.F., 2003. Cognitive Functioning in Treatment-Seeking Gulf War Veterans: Pyridostigmine Bromide Use and PTSD. Journal of Psychopathology and Behavioral Assessment 25(2), 95-103.

Sunyer, B., Patil, S., Höger, H., Lubec, G., 2007. Barnes maze, a useful task to assess spatial reference memory in the mice. Protocol Exchange.

Tamura, M., Spellman, T.J., Rosen, A.M., Gogos, J.A., Gordon, J.A., 2017. Hippocampal-prefrontal theta-gamma coupling during performance of a spatial working memory task. Nature Communications 8(1), 2182.

Toomey, R., Alpern, R., Vasterling, J.J., Baker, D.G., Reda, D.J., Lyons, M.J., Henderson, W.G., Kang, H.K., Eisen, S.A., Murphy, F.M., 2009. Neuropsychological functioning of U.S. Gulf War veterans 10 years after the war. J Int Neuropsychol Soc 15(5), 717-729.

Torres-Altoro, M.I., Mathur, B.N., Drerup, J.M., Thomas, R., Lovinger, D.M., O'Callaghan, J.P., Bibb, J.A., 2011. Organophosphates dysregulate dopamine

signaling, glutamatergic neurotransmission, and induce neuronal injury markers in striatum. Journal of Neurochemistry 119(2), 303-313.

Tundup, S., Srivastava, L., Norberg, T., Watford, W., Harn, D., 2015. A Neoglycoconjugate Containing the Human Milk Sugar LNFPIII Drives Anti-Inflammatory Activation of Antigen Presenting Cells in a CD14 Dependent Pathway. PLoS One 10(9), e0137495.

Wang, X., Wang, Q.M., Meng, Z., Yin, Z., Luo, X., Yu, D., 2017. Gait disorder as a predictor of spatial learning and memory impairment in aged mice. PeerJ 5, e2854.

Wang, X., Xu, Z., Zhao, F., Lin, K.J., Foster, J.B., Xiao, T., Kung, N., Askwith, C.C., Bruno, J.P., Valentini, V., 2020. Restoring tripartite glutamatergic synapses: A potential therapy for mood and cognitive deficits in Gulf War illness. Neurobiology of Stress, 100240.

White, R.F., Steele, L., O'Callaghan, J.P., Sullivan, K., Binns, J.H., Golomb, B.A., Bloom, F.E., Bunker, J.A., Crawford, F., Graves, J.C., Hardie, A., Klimas, N., Knox, M., Meggs, W.J., Melling, J., Philbert, M.A., Grashow, R., 2016. Recent research on Gulf War illness and other health problems in veterans of the 1991 Gulf War: Effects of toxicant exposures during deployment. Cortex 74, 449-475.

Whitlock, J.R., Heynen, A.J., Shuler, M.G., Bear, M.F., 2006. Learning induces long-term potentiation in the hippocampus. Science 313(5790), 1093-1097.

Yirmiya, R., Goshen, I., 2011. Immune modulation of learning, memory, neural plasticity and neurogenesis. Brain, Behavior, and Immunity 25(2), 181-213.

Zakirova, Z., Crynen, G., Hassan, S., Abdullah, L., Horne, L., Mathura, V., Crawford, F., Ait-Ghezala, G., 2016. A Chronic Longitudinal Characterization of Neurobehavioral and Neuropathological Cognitive Impairment in a Mouse Model of Gulf War Agent Exposure. Front Integr Neurosci 9, 71-71.

Zakirova, Z., Reed, J., Crynen, G., Horne, L., Hassan, S., Mathura, V., Mullan, M., Crawford, F., Ait-Ghezala, G., 2017. Complementary proteomic approaches reveal mitochondrial dysfunction, immune and inflammatory dysregulation in a mouse model of Gulf War Illness. PROTEOMICS–Clinical Applications 11(9-10), 1600190.

Zakirova, Z., Tweed, M., Crynen, G., Reed, J., Abdullah, L., Nissanka, N., Mullan, M., Mullan, M.J., Mathura, V., Crawford, F., Ait-Ghezala, G., 2015. Gulf War agent exposure causes impairment of long-term memory formation and neuropathological changes in a mouse model of Gulf War Illness. PloS One 10(3), e0119579-e0119579.

Zheng, J., Jiang, Y.-Y., Xu, L.-C., Ma, L.-Y., Liu, F.-Y., Cui, S., Cai, J., Liao, F.-F., Wan, Y., Yi, M., 2017. Adult hippocampal neurogenesis along the dorsoventral axis contributes differentially to environmental enrichment combined with voluntary exercise in alleviating chronic inflammatory pain in mice. Journal of Neuroscience 37(15), 4145-4157.

Zhu, B., Trikudanathan, S., Zozulya, A.L., Sandoval-Garcia, C., Kennedy, J.K., Atochina, O., Norberg, T., Castagner, B., Seeberger, P., Fabry, Z., Harn, D., Khoury, S.J., Guleria, I., 2012. Immune modulation by Lacto-N-fucopentaose III in experimental autoimmune encephalomyelitis. Clin Immunol 142(3), 351-361.

Zundel, C.G., Krengel, M.H., Heeren, T., Yee, M.K., Grasso, C.M., Janulewicz Lloyd, P.A., Coughlin, S.S., Sullivan, K., 2019. Rates of Chronic Medical Conditions in 1991 Gulf War Veterans Compared to the General Population. Int J Environ Res Public Health 16(6).

Figures

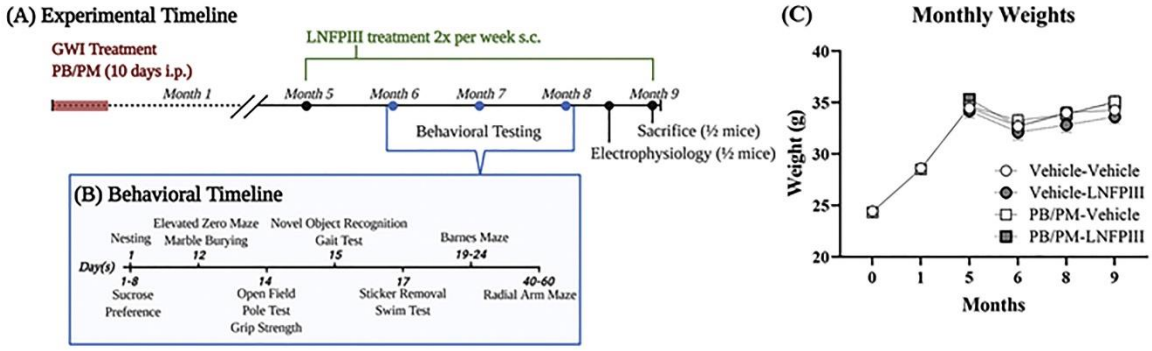

Fig. 3.1. Experimental and behavioral timelines. (A) depicts the experimental timeline for both the short- and long-term studies in which mice received pyridostigmine bromide (PB) and permethrin (PM) daily for 10 days. Lacto-N-fucopentaose III (LNFPIII) treatment began 4 months after PB/PM exposure. Electrophysiology was performed during month 8. (B) is a detailed timeline of behavioral tests that were performed during months 6–8. (C) Monthly weights were monitored and are presented for the start of study (0), post PB/PM treatment (1), start of LNFPIII treatment (5), prior to RAM FR (6), post RAM FR (8), and sacrifice (9). *Abbreviations:* FR: food restriction; GWI: Gulf War Illness; i.p.: intraperitoneally; LNFPIII: Lacto-N-fucopentaose III; PB: pyridostigmine bromide; PM: permethrin; RAM: radial arm maze; s.c.: subcutaneously.

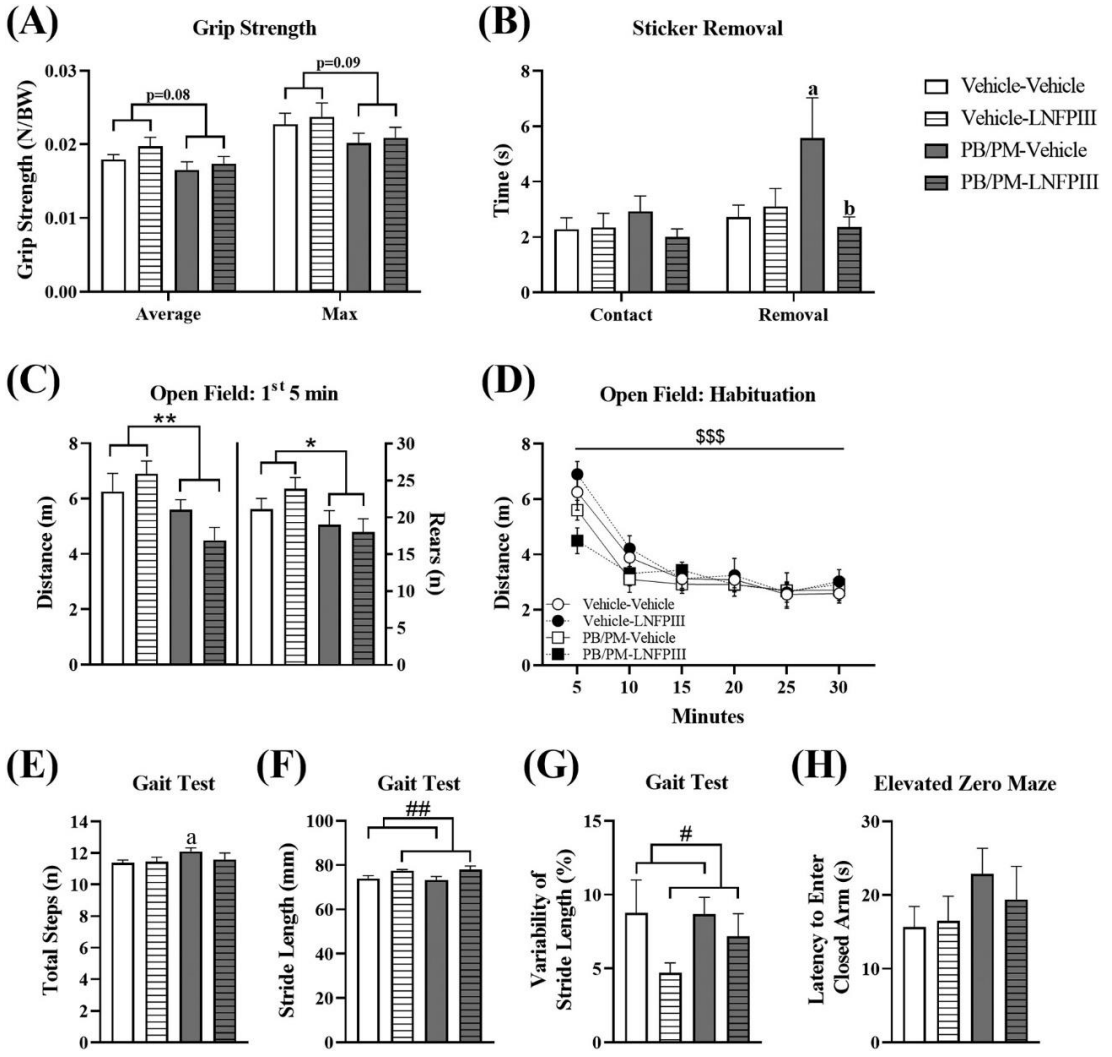

Fig. 3.2. Effects of prior PB/PM exposure and delayed LNFPIII treatment on motor function. Several motor effects of prior PB/PM exposure and LNFPIII treatment were evaluated by grip strength (N/body weight) (A); sticker removal time (B); 5 min distance and rears (C) and habituation over time (D) in the open field; total steps (E), stride length (F), and stride length variability (G) in the gait test; entry time into the closed arm (H) of the elevated zero maze. Data are presented as mean ± SEM (n = 8–10 for grip strength, OF, and gait test; n = 14–16 for sticker removal and elevated zero maze). * and ** indicate $p < 0.05$ and 0.01, respectively for PB/PM main effects. # and ## indicates $p < 0.05$ and 0.01, respectively for main effect of LNFPIII treatment. $$$ indicates $p < 0.001$ of time in the OF. a and b indicate $p < 0.05$ for Vehicle-Vehicle vs. PB/PM-Vehicle and PB/PM-Vehicle vs. PB/PM-LNFPIII, respectively.

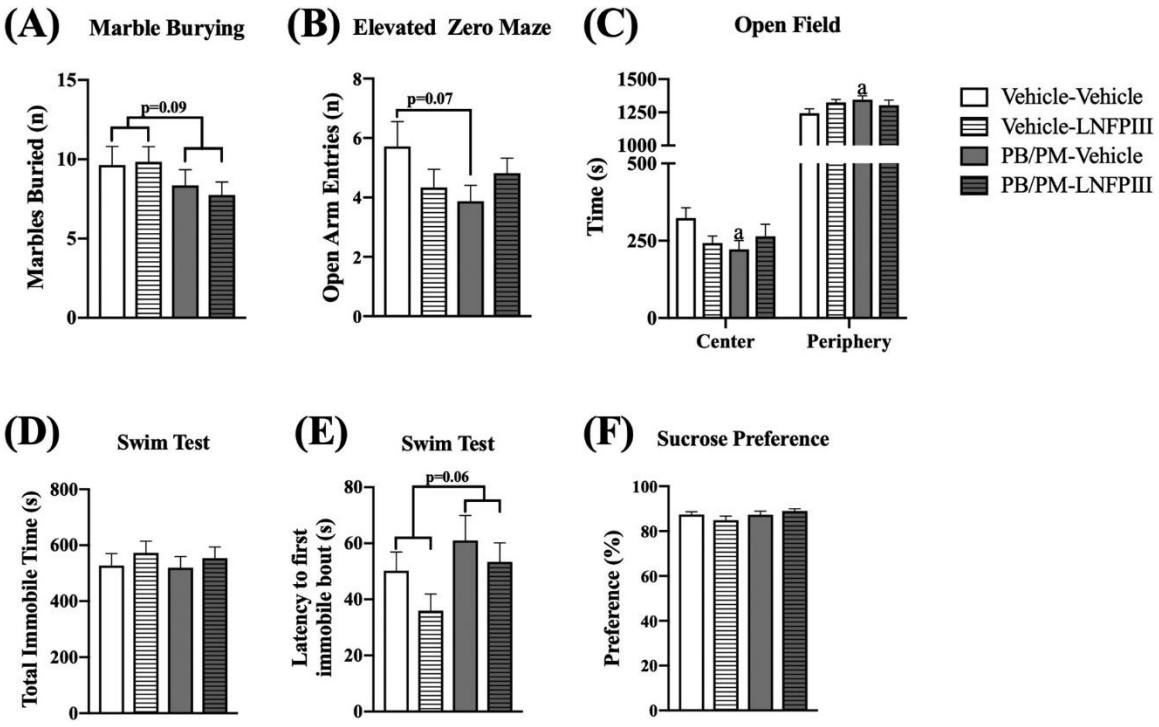

Fig. 3.3. Long term mood effects of prior PB/PM exposure and delayed LNFPIII treatment. Mood disturbances of prior PB/PM exposure and LNFPIII treatment were evaluated by several tests for anxiety-like and depressive-like behaviors: number of marbles buried (A) in the marble burying test; open arm entries (B) in the elevated zero maze; center and periphery time (C) in the open field; immobile time (D) and latency to first immobile bout (E) in the swim test; sucrose preference (F) in the sucrose preference test. Data are presented as mean ± SEM (n = 8–10 for open field; n = 14–16 for marble burying, elevated zero maze, swim, and sucrose preference test). [a] indicates $p < 0.05$ for Vehicle-Vehicle vs PB/PM-Vehicle.

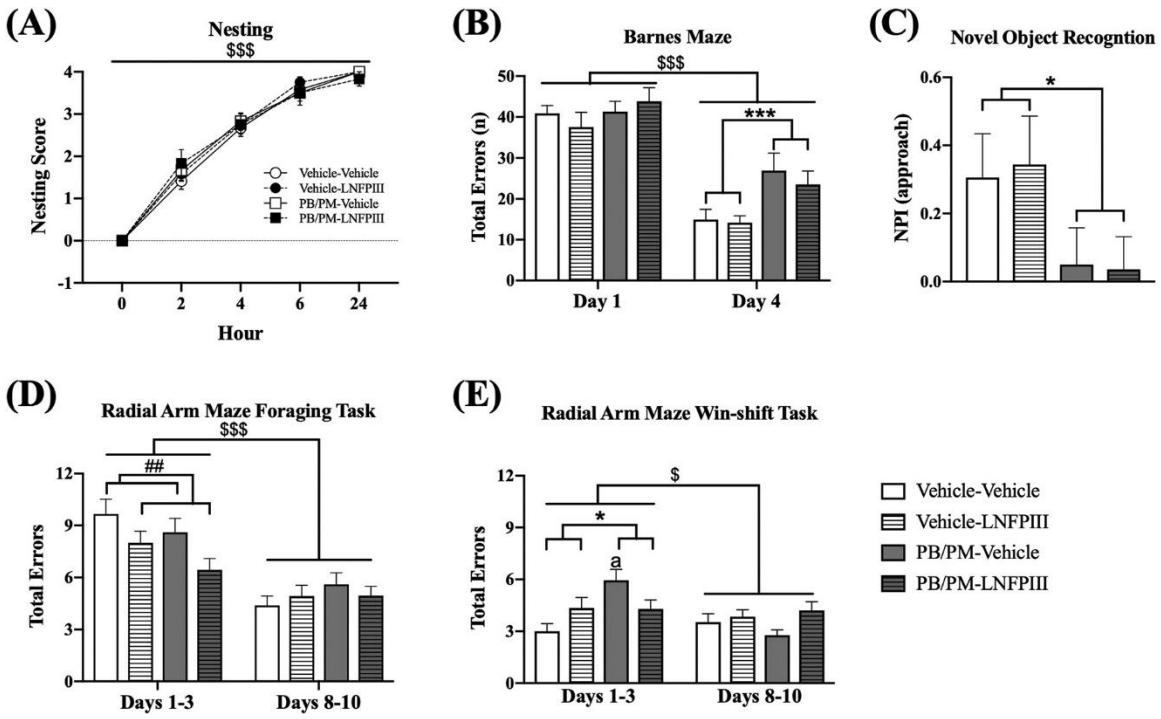

Fig. 3.4. Cognition and memory effects of prior PB/PM exposure and delayed LNFPIII treatment. Cognitive/memory effects of prior PB/PM exposure and LNFPIII treatment were evaluated by several tests: nest-building ability (A) in the nesting test; total errors (B) during the training phase of the Barnes maze; approach novelty preference index (NPI) (C) in the novel object recognition test; total errors in the radial arm maze foraging (D) and Win-shift tasks (E). Data are presented as mean ± SEM (n = 14–16 for nesting, Barnes maze, and novel object recognition; n = 13–15 for radial arm maze). $^{\$}$ and $^{\$\$\$}$ indicate $p < 0.05$ and 0.001 for time. * and *** indicate $p < 0.05$ and 0.001, respectively, for PB/PM main effects. $^{\#\#}$ indicates $p < 0.01$ for main effect of LNFPIII treatment. ^{a} indicates $p < 0.05$ for Vehicle-Vehicle vs. PB/PM-Vehicle.

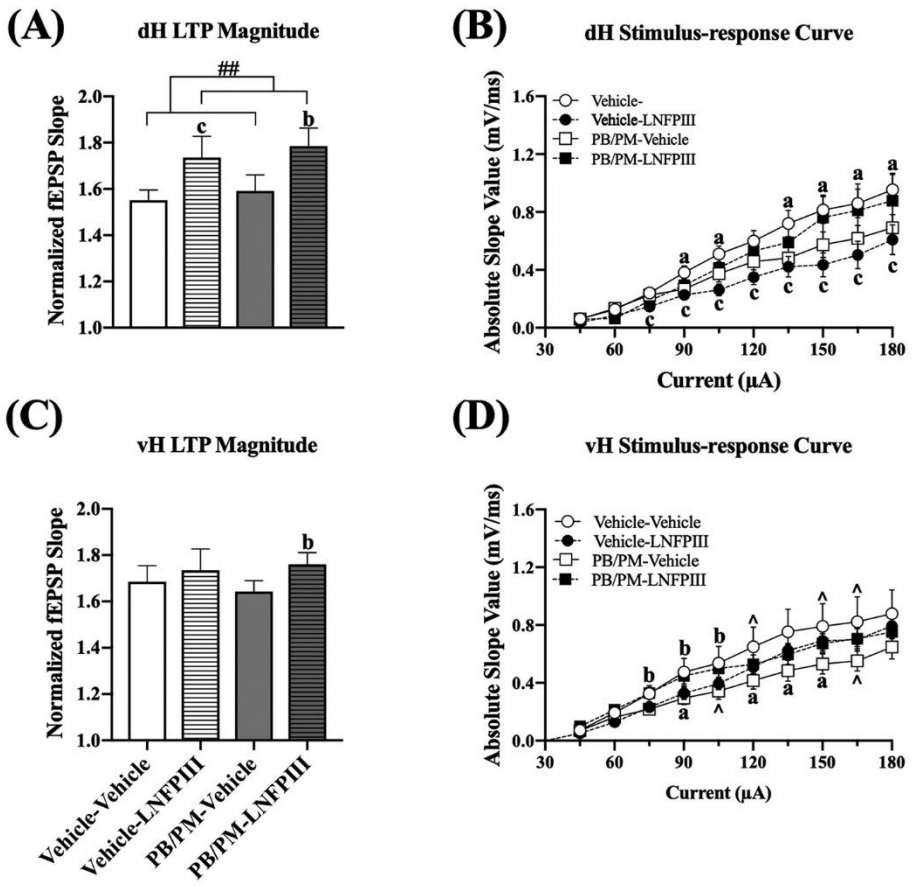

Fig. 3.5. Hippocampal measurements of synaptic plasticity and transmission after prior PB/PM exposure and delayed LNFPIII treatment. A) and C) show summary quantification of dorsal hippocampus (dH) and ventral hippocampus (vH), respectively, LTP magnitude recorded 8 months after PB/PM exposure. B) and D) show the stimulus-response relationship of the average fEPSP slopes elicited by increasing stimulus intensities from the dH and vH, respectively. Data are presented as mean ± SEM. Reported *n*-values (x(y)) indicate the number of slices (x) and the number of mice (y) assessed: Vehicle-Vehicle (dH, $n = 14(6)$; vH, $n = 14(6)$), Vehicle-LNFPIII (dH, $n = 9(6)$; vH, $n = 20(6)$), PB/PM-Vehicle (dH, $n = 12(6)$; vH, $n = 21(6)$), and PB/PM-LNFPIII (dH, $n = 13(6)$; vH, $n = 17(6)$). ## indicates main effect of LNFPIII treatment. a, b, and c indicate $p < 0.05$ for Vehicle-Vehicle vs PB/PM-Vehicle, PB/PM-Vehicle vs PB/PM-LNFPIII, and Vehicle-Vehicle vs Vehicle-LNFPIII groups, respectively. ^ indicates trend $p < 0.10$ for either Vehicle-Vehicle vs PB/PM-Vehicle or PB/PM-Vehicle vs PB/PM-LNFPIII.

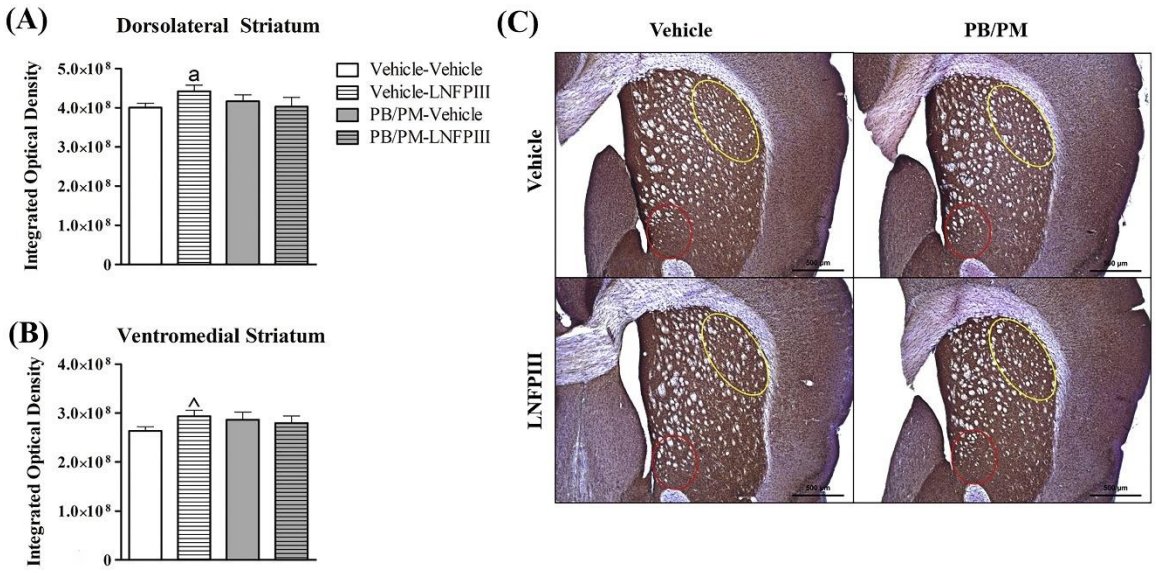

Fig. 3.6. Tyrosine hydroxylase (TH) immunoreactivity in the dorsolateral and ventromedial striatum 9 months post PB/PM exposure and delayed LNFPIII treatment. Semi-quantitative analysis (integrated optical density) of TH+ CV+ cells in the (A) dorsolateral and (B) ventromedial striatum was conducted using ImageJ. Representative images shown in (C) depict the dorsolateral (yellow oval) and ventromedial (red oval) striatum at 5×. Data are presented as mean ± SEM. $n = 5$ animals per group/3 sections per animal. [a] and ^ indicate $p \leq 0.05$ or $p \leq 0.10$ for Vehicle-Vehicle vs. Vehicle-LNFPIII, respectively. (For interpretation of the references to color in this figure legend, the reader is referred to the web version of this article.)

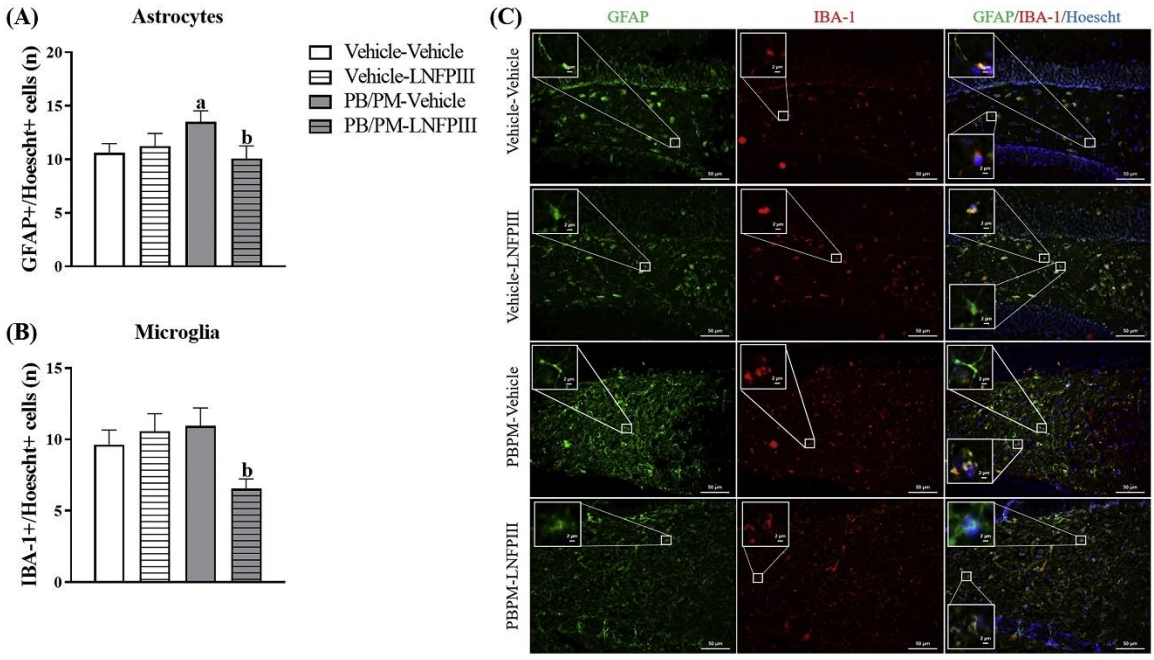

Fig. 3.7. GFAP and IBA-1 immunoreactivity in the hilus region of the hippocampus 9 months post-PB/PM exposure and delayed LNFPIII treatment. Double-stained (A) astrocytes (GFAP/Hoescht) or (B) microglia (IBA-1/Hoescht) were analyzed using the cell counter plugin in ImageJ. Representative images in (C) depict astrocytes (GFAP; column 1), microglia (IBA-1; column 2), and GFAP and IBA-1 overlay with nuclear staining (Hoescht; column 3) in the hilus region of the hippocampus at 40× magnification. Data are presented as mean ± SEM. n = 11–19 images per group. [a] and [b] indicate $p \leq 0.05$ for Vehicle-Vehicle vs. PB/PM-Vehicle and PB/PM-Vehicle vs. PB/PM-LNFPIII comparisons, respectively.

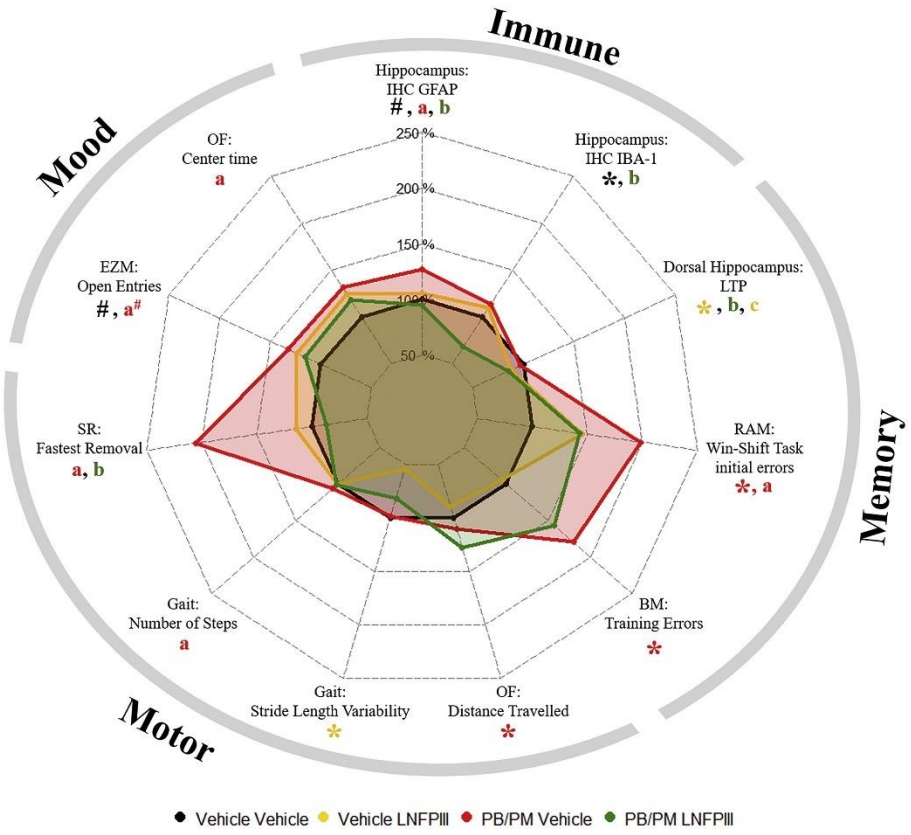

Fig. 3.8. Summary of key findings. The radar plot highlights the neurobehavioral and neurobiological effects of prior PB/PM exposure and delayed LNFPIII treatment at study completion. Higher and lower percentage values from the Vehicle-Vehicle group indicate aberrations and improvements, respectively, for study parameters. * denotes main/interaction effect ($p < 0.05$) whereas # denotes trending main/interaction effect ($p < 0.10$). Yellow indicates an LNFPIII effect, red denotes a PB/PM effect, and green denotes a beneficial effect of LNFPIII in the presence of PB/PM. a, b, and c indicate a significant ($p < 0.05$) pairwise effect for Vehicle-Vehicle vs PB/PM-Vehicle (red), PB/PM-Vehicle vs PB/PM-LNFPIII (green), and Vehicle-Vehicle vs Vehicle-LNFPIII (yellow), respectively. a# indicates a trending ($p < 0.10$) pairwise effect for Vehicle-Vehicle vs PB/PM-Vehicle (red). (For interpretation of the references to color in this figure legend, the reader is referred to the web version of this article.)

Supplementary Data

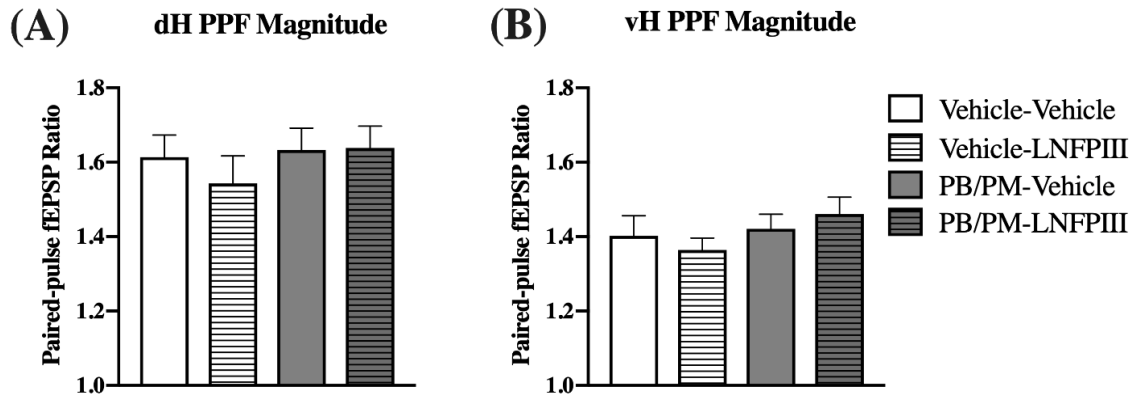

Supplemental Figure 3.1. Paired-pulse facilitation magnitude post PB/PM exposure and delayed LNFPIII treatment. The PPF magnitude for dH **(A)** and vH **(B)** recorded after PB/PM chemicals exposure (interpulse interval = 50 ms). Data are expressed as mean ± SEM. Reported n-values (x(y)) indicate the number of slices (x) and the number of mice (y) assessed: Vehicle-Vehicle (dH, n=14(6); vH, n=14(6)), Vehicle-LNFPIII (dH, n=9(6); vH, n=20(6)), PB/PM-Vehicle (dH, n=12(6); vH, n=21(6)), and PB/PM-LNFPIII (dH, n=13(6); vH, n=17(6)).

CHAPTER 4

ASSESSING THE BENEFICIAL EFFECTS OF THE IMMUNOMODULATORY GLYCAN LNFPIII ON GUT MICROBIOTA AND HEALTH IN A MOUSE MODEL OF GULF WAR ILLNESS

Jessica M. Carpenter, Ryan S. Mote, Rachel L. Dockman, Andrew J. Steinberger, Garret Suen, Thomas Norberg, Donald A. Harn, John J. Wagner, Nikolay M. Filipov
Published in *International Journal of Environmental Research and Public Health* 2020.
Reprinted here with the permission of publisher.

Abstract

The microbiota's influence on host (patho) physiology has gained interest in the context of Gulf War Illness (GWI), a chronic disorder featuring dysregulation of the gut–brain–immune axis. This study examined short- and long-term effects of GWI-related chemicals on gut health and fecal microbiota and the potential benefits of Lacto-N-fucopentaose-III (LNFPIII) treatment in a GWI model. Male C57BL/6J mice were administered pyridostigmine bromide (PB; 0.7 mg/kg) and permethrin (PM; 200 mg/kg) for 10 days with concurrent LNFPIII treatment (35 μg/mouse) in a short-term study (12 days total) and delayed LNFPIII treatment (2×/week) beginning 4 months after 10 days of PB/PM exposure in a long-term study (9 months total). Fecal 16S rRNA sequencing was performed on all samples post-LNFPIII treatment to assess microbiota effects of GWI chemicals and acute/delayed LNFPIII administration. Although PB/PM did not affect species composition on a global scale, it affected specific taxa in both short- and long-term settings. PB/PM elicited more prominent long-term effects, notably, on the abundances of bacteria belonging to *Lachnospiraceae* and *Ruminococcaceae* families and the genus *Allobaculum*. LNFPIII improved a marker of gut health (i.e., decreased lipocalin-2) independent of GWI and, importantly, increased butyrate producers (e.g., *Butyricoccus*, *Ruminococcous*) in PB/PM-treated mice, indicating a positive selection pressure for these bacteria. Multiple operational taxonomic units correlated with aberrant behavior and lipocalin-2 in PB/PM samples; LNFPIII was modulatory. Overall, significant and lasting GWI effects occurred on specific microbiota and LNFPIII treatment was beneficial.

Keywords: Gulf War Illness; gut inflammation and health; gut microbiome; Lacto-N-fucopentaose-III (LNFPIII); permethrin; pyridostigmine bromide

1. Introduction

Gulf War Illness (GWI), which afflicts one-third of the veterans from the 1990–1991 Gulf War (GW), is a chronic disorder presenting with a myriad of debilitating symptoms, including neurological, musculoskeletal, immunological and gastrointestinal disturbances that appeared shortly after veterans returned from deployment and have persisted or worsened throughout the last 30 years (White et al., 2016). Epidemiological evidence suggests that co-exposure to numerous toxicants, including neuro-prophylactics (pyridostigmine bromide: PB), pesticides (permethrin: PM and N,N-Diethyl-methylbenzamide: DEET), and chemical nerve agents (sarin) during the GW may be linked to GWI etiopathogenesis (White et al., 2016). Previous work suggests GW-related exposures accelerate age-related chronic conditions, such as high blood pressure, increased heart attack and stroke risk, diabetes, and arthritis (Zundel et al., 2019); many of the persisting symptoms GWI veterans experience (i.e., cognitive, memory and motor impairments) could be exacerbated by accelerated aging (White et al., 2016; Zundel et al., 2019). Veterans with GWI report more symptoms akin to Parkinson's Disease (PD) than GW controls (Chao, 2019). GWI and PD share gastrointestinal (GI) ailments and motor dysfunction in their symptomatology (Dunphy et al., 2003; Klingelhoefer and Reichmann, 2017; Toomey et al., 2009; White et al., 2016). Moreover, GI disturbances precede PD motor dysfunction, and a recent study suggests that aberrant gut–brain–immune axis plays a role in the neurobehavioral deficits in this disease.

Although veterans with GWI experience GI symptoms, such as nausea, diarrhea and abdominal pain/cramps, and GI dysfunction is a prominent GWI diagnostic characteristic (Dunphy et al., 2003; Koch and Emory, 2005; Maule et al., 2018; White et

al., 2016), studies investigating GI disturbances remain limited. Recent work found that enteric dysbiosis occurs within GWI context (Alhasson et al., 2017; Janulewicz et al., 2019). It was also suggested that alterations in the gut–brain–immune axis may be involved in GWI, as veterans with GWI and GI ailments have higher levels of circulating tumor necrosis factor receptor 1 (TNF-RI) (Janulewicz et al., 2019). Exposing laboratory models to GW chemicals (i.e., PB alone or PB and PM) resulted in alterations in the murine microbiota, gut motility, and inflammatory signaling (e.g., toll-like receptor 4; TLR-4) in both the gut and brain (Alhasson et al., 2017; Hernandez et al., 2019; Seth et al., 2018). While clinical reports of peripheral and central inflammation are, respectively, variable and sparse, a consensus for immune disruption has emerged in GWI etiology, as GWI veterans exhibit increases in circulating cytokines and glial (TSPO) activation compared to controls (Alshelh et al., 2020; Broderick et al., 2013; Broderick et al., 2018; Parkitny et al., 2015). Immune alterations are further driven by (neuro) inflammatory increases in multiple laboratory models of GWI; this showcases how interplay between the nervous and immune systems impacts GWI development, specifically regarding the effects of inflammation on neurological and neurobehavioral function (Carpenter et al., 2020; Macht et al., 2019; Megahed et al., 2014; O'Callaghan et al., 2016; Parihar et al., 2013; Zakirova et al., 2015a; Zakirova et al., 2015b). However, the relationship between GWI GI symptomology, immune alterations, and behavioral outcomes have not been investigated.

Interestingly, one clinical study found the only circulating molecule (cytokine-related) significantly affected in GWI veterans was the soluble TNF-RI and that GI symptoms did not influence bacteria found to be significantly different between veterans with GWI and controls (Janulewicz et al., 2019). Another recent study found administration

of sodium butyrate through oral gavage in a mouse model of GWI restored enteric niacin receptor, tight junction protein, and TLR-4 expression levels to control levels (Seth et al., 2018). Additionally, butyrate administration increased levels of bacteria that produce butyrate and have been the focus of intense investigation due to their use in potential probiotics (e.g., *Roseburia* sp., *Bifidobacterium;* (Seth et al., 2018)). While these bacteria increased in GWI animals treated with butyrate, it is unclear whether these increases are a result of direct butyrate administration, as these bacteria do not utilize butyrate for sustenance or growth. Finally, evidence for the beneficial effects of *Bifidobacterium*, another genus commonly studied as a probiotic, is equivocal as only some strains within this genus may be beneficial for patients with GI disorders (Jeon et al., 2012; Medina et al., 2007; Moran et al., 2009; Mylonaki et al., 2005; Scanlan et al., 2006; Wang et al., 2014). This suggests that genus, and perhaps, strain specific maladaptation of the GWI microbiota ought to be tested. Overall, the interactions along the gut–brain–immune axis are incredibly complex (Belkaid and Hand, 2014; Rea et al., 2016), but are worthy of further investigation in the context of GWI pathophysiology and potential treatments.

Cure-all treatments for GWI do not currently exist due, in part, to GWI's complexity; however, experimental therapeutic interventions have provided benefits to some GWI symptoms (Baraniuk et al., 2013; DDGWIRP, 2018; Donta et al., 2004; Golomb et al., 2014). Current treatments for GI disorders in general, include altering diet and/or lifestyle, probiotic supplementation, and fecal microbiota transplants; some have been beneficial to patients with neurological disorders including PD, Multiple Sclerosis, and Alzheimer's Disease (Vendrik et al., 2020; Westfall et al., 2017). However, explored

treatment interventions for gut health in veterans with GWI remain limited (Seth et al., 2018).

Immunotherapies may be an advantageous treatment option considering the pathogenic role inflammation and immune dysregulation play in GWI symptomology. Lacto-N-fucopentaose III (LNFPIII), a glycan found in human milk that, to date, has had no documented adverse outcomes and has shown promising immunomodulatory effects by reducing peripheral and central inflammation (Atochina et al., 2008; Bhargava et al., 2012; Carpenter et al., 2020; Srivastava et al., 2014; Tundup et al., 2015; Zhu et al., 2012). When conjugated to a dextran carrier, LNFPIII skews the inflammatory balance of the innate immune system in an anti-inflammatory direction by activating CD14/TLR-4 signaling for extracellular signal-regulated kinase (ERK) dependent production of anti-inflammatory mediators (Atochina et al., 2008; Bhargava et al., 2012; Srivastava et al., 2014; Tundup et al., 2015; Zhu et al., 2012). Thus, within the context of GWI, LNFPIII may be beneficial in absolving GWI-induced gut inflammation and subsequent neuroinflammation through its modified anti-inflammatory TLR-4 signaling (Alhasson et al., 2017). In fact, our earlier studies demonstrated LNFPIII's beneficial effects in preventing and reducing brain wide monoaminergic disbalance and inflammation in the hippocampus after acute experimental GWI exposure (Carpenter et al., 2020), as well as restoring long-term behavioral deficits caused by PB/PM exposure, particularly in motor function. Whether LNFPIII modulates gut microbiota and gut health is currently unknown.

This study examines the effects of exposure to GW-related chemicals on GI microbial ecology in an established model of GWI (PB/PM). Our earlier studies using this established exposure paradigm indicated acute neurological (Carpenter et al., 2020) and

long-term neurobehavioral deficits that were largely restored by the immunotherapeutic, LNFPIII. However, while some data exist on the human and animal GI effects of GWI after exposure, the short- and long-term GI effects of this GWI treatment paradigm have not been investigated. Moreover, while LNFPIII had beneficial effects on neuroinflammation and altering behavioral deficits, there is no published evidence that it is beneficial for targeting GWI GI-related symptoms. Thus, the objectives of the present study were to (i) characterize the short- and long-term implications of PB/PM exposure on gut microbiota, gut motility, and intestinal inflammation, and (ii) correlate gut health to GWI-related neurological aberrations (i.e., motor deficits). Finally, LNFPIII treatment, including when treatment was initiated months after PB/PM exposure ended, was evaluated for its beneficial effects in modulating the aforementioned parameters.

2. Materials and Methods

2.1. Materials

Pyridostigmine bromide (PB; ≥98% purity; Sigma Aldrich, St. Louis, MO, USA) and permethrin (PM; 29.5% cis/69.5% trans isomer; 99% purity; Chem Service Inc., West Chester, PA, USA) were used for animal treatments in this study. Lacto-N-fucopentaose III (LNFPIII) dextran conjugate was produced as previously described (Tundup et al., 2015). Carmine red powder (Sigma) and methylcellulose (Sigma) were used for the gut motility test. All additional chemicals and reagents used in this study, unless otherwise noted, were of analytical or higher grade and were obtained from Sigma or Fisher Scientific (Hampton, NH, USA).

2.2. Animals

Male C57BL/6J mice (8–9 weeks old; Jackson Laboratories, Bar Harbor, ME, USA) were housed 4 per cage in an environmentally controlled room (22–24 °C) and maintained on a 12 h light/dark cycle (0700–1900 lights on) for one week of acclimation and throughout the study. Mice were handled daily for one week prior to the start of the study to minimize experimenter-induced stress. Food and water were available ad libitum. All procedures were approved in advance by the University of Georgia Institutional Animal Care and Use Committee (initial approval date: 14 April 2016) and were in accordance with the latest National Institutes of Health guidelines.

2.3. GWI Model

The experimental design for this study is shown in Figure 1. Following the Zakirova (Zakirova et al., 2015a) model in both the short- (12 days; $N = 24$ mice) and long-term (9 months; $N = 59$) studies, mice were randomly divided into treatment groups and treated daily for 10 days with a combination of PB and PM (0.7 and 200 mg/kg, respectively) or DMSO vehicle (i.p.). In the short-term study, the immunomodulatory treatment, LNFPIII, or dextran vehicle (both 35 µg/mouse; s.c.) were administered concurrently with PB/PM as in (Carpenter et al., 2020). The treatment groups in the short-term study were as follows: DMSO-Dextran ($n = 6$), DMSO-LNFPIII ($n = 6$), PB/PM-Dextran ($n = 6$), and PB/PM-LNFPIII ($n = 6$). In the long-term study, four months after the initial PB/PM exposure, mice were randomly subdivided into LNFPIII or vehicle groups and were treated twice a week until study completion with LNFPIII or dextran vehicle (both 35 µg/mouse; s.c.). Thus, from this point onward there were 4 treatment groups:

DMSO-Dextran (n = 13), DMSO-LNFPIII (n = 14), PB/PM-Dextran (n = 14), and PB/PM-LNFPIII (n = 14).

2.4. Gut Motility

The carmine red gut transit test (Nagakura et al., 1996) was used to determine gut motility deficits with the modifications described in (Asuzu et al., 2011). This test was performed monthly by administering the dye via oral gavage (6% carmine red in 0.5% methylcellulose; 0.3 mL/mouse) and monitoring the mouse for the first appearance of colored fecal pellet over a 6 h period. For the test, each mouse was single housed and food restricted for 1 h prior to carmine red administration. Once the latency was recorded, each mouse was returned to its home cage.

2.5. Lipocalin-2 ELISA

Intestinal inflammation was determined by measuring fecal and plasma levels of Lipocalin-2 (Lcn-2), a protein upregulated in multiple inflammatory diseases including inflammatory bowel disease (IBD), by utilizing methods described in (Chassaing et al., 2012). Briefly, a small sample from previously frozen fecal content was weighed and transferred to a new, sterile polypropylene tube. Samples were reconstituted in 0.1% Tween 20 PBS (100 mg/mL) and vortexed for 25 min until fully homogenized. Samples were then centrifuged for 10 min at 13,200 rcf and 4 °C, supernatants were collected, and Lcn-2 levels were measured. For this test, a Duoset murine Lcn-2 ELISA kit (R&D Systems, Minneapolis, MN, USA) was used per manufacturer's instructions. Fecal supernatants were run neat and plasma was diluted 1:500 in ELISA reagent diluent prior to analysis. All samples were run in duplicate.

2.6. Sample Collection

Following euthanasia, blood (approximately 1 mL) was collected in tubes (Na citrate 0.109 M, 3.2% BD Vacutainer, Becton, Dickinson and Company, San Jose, CA, USA) for plasma harvesting. Immediately afterwards, organs (brain, inguinal lymph nodes, spleen, thymus, liver and kidney) were weighed and frozen on dry ice. Fecal contents were collected from the cecum and weighed under sterile conditions prior to storage placement in a sterile polypropylene tube. All samples were stored at −80 °C until analysis.

2.7. Plasma Cytokine Analysis

A Milliplex Cytokine Panel (EMD Millipore Corporation; Billerica, MA, USA) was used to assess plasma concentrations of the following cytokines/chemokines: interferon gamma (IFNγ), macrophage inflammatory protein 3 alpha (MIP-3α/CCL20), interleukin (IL)-1β, IL-22, IL-23, IL-27p70, IL-27, IL-15, IL-17A, Il-17/IL-25, IL-17F, IL-33, IL-31, tumor necrosis factor alpha (TNFα) and beta (TNFβ), IL-4, IL-5, IL-28B, IL-10, IL-13, granulocyte-macrophage colony-stimulating factor (GM-CSF), CD40 ligand (CD40L), and IL-2. Briefly, plasma samples were added to a 96-well plate followed by the addition of premixed, antibody-immobilized beads and incubated with agitation on a shaker at 4 °C overnight. Following washes (3×), detection antibodies were added and incubated for 1 h followed by addition of Streptavdidin-Phycoerythrin for 30 min with agitation on a shaker at room temperature. After final washes (3×), sheath fluid was added, and the data from the plate was collected on a MagPix instrument using xPONENT v.4.2 (Luminex Corp., Austin, TX, USA). Data were analyzed with Milliplex Analyst software, v.5.1 (EMD Millipore, Burlington, MA, USA). Data were extracted based on either a 4- or 5-parameter log curve.

2.8. DNA Extraction

Fecal genomic DNA was extracted using commercially available Qiagen (Qiagen; Hilden, Germany) DNeasy PowerSoil Kit (100; Cat. No.: 12888-100) following the manufacturer's protocols. All extracted DNA samples were resuspended in Tris-EDTA (TE) buffer and quantified using a Qubit® Fluorometer (Invitrogen, San Diego, CA, USA). Extracted DNA samples and TE buffer negative control were then taken through the amplification protocol below.

2.9. DNA Amplification and Sequencing

Samples were diluted to 1 ng/µL for amplification, and universal bacterial primers for the 16S rRNA variable region V4, as previously described in detail (Kozich et al., 2013), were used in the amplification reactions. Water was used for PCR negative control. The sequenced controls and samples were taken through quality filtering and normalization procedures described next.

2.10. 16S rRNA Fecal Sequence Processing and Bioinformatics Analysis

Raw sequence files were obtained in fastq format and processed using mothur v.1.38.1 (Schloss et al., 2009) as in (de Oliveira et al., 2013) and modified in (Mote et al., 2020). Alpha diversity metrics were tested for effects by exposure to GWI chemicals and LNFPIII by using the non-parametric Kruskal–Wallis test by ranks. A non-parametric permutational analysis of variance (PERMANOVA) was used to test for effects on the entire microbiota community with a 2 × 2 factorial design using GWI treatment (±) and LNFPIII (±) exposure as the two factors. Linear discriminant analysis effect size (LefSe) was performed using the Huttenhower lab's galaxy instance with the relative abundance table as input (https://huttenhower.sph.harvard.edu/galaxy/; (Segata et al., 2011));

Kruskall–Wallis ($p < 0.05$); Pairwise Wilcoxon ($p < 0.05$); logarithmic Linear discriminant analysis (LDA) score (>2.0). All other statistical microbiota analyses were performed using R (R Development Core Team, 2016). Correlational analyses were performed using the Hmisc R package (https://cran.r-project.org/web/packages/Hmisc/index.html) with Spearman correlation coefficient and significance set to $p < 0.05$. Heatmaps were generated using gplots library (Warnes et al., 2009) and final iterations were edited in Microsoft PowerPoint (Redmond, WA, USA).

2.11. Accession Number(s) of DNA Sequences

All DNA sequences are publicly available in the NCBI Sequence Read Archive and are accessible under BioProject accession No. PRJNA665703.

2.12. Statistical Analysis for Gut Motility, Lcn-2, and Plasma Cytokines

A two-way analysis of variance (ANOVA) was used to determine main treatment effects or interactions. If an ANOVA was significant ($p \leq 0.05$), treatment means were separated by Student–Newman–Keuls (SNK) post-hoc test or planned pairwise comparisons (Student's t-test, as appropriate). All data were analyzed using SigmaPlot 12.5 (San Jose, CA, USA), and all graphs were generated using GraphPad Prism 5 (San Diego, CA, USA). A heat map of the plasma cytokines post-statistical analysis was generated using gplots library in R 3.4.2 software (Warnes et al., 2009).

3. Results

3.1. Alpha/Beta Diversity Metrics and Global Fecal Microbiota Effects

All samples had an average Good's coverage of 99.85 ± 0.01% ($\bar{x}$ ± SD; range: 99.59–99.94%), indicating that the sequencing depth captured most of the species diversity. Exposures to PB/PM or LNFPIII had no significant effect ($p \geq 0.12$) on the global

microbiota composition at either the acute or chronic time points when using the Bray–Curtis (abundance) or Jaccard (presence/absence) dissimilarity matrices. In addition, there were no significant main effect ($p > 0.05$) on either Shannon's diversity or Chao1 richness (Figure S1) profiles of PB/PM or LNFPIII at any time point. However, the fecal microbiota's Shannon's diversity 9 months after PB/PM exposure exhibited the following trend ($p = 0.074$): PB/PM-Dextran resulted in an increase, while LNFPIII lowered the diversity index to control levels (Figure S1).

3.2. Linear Discriminant Analysis of Effect Size (LEfSe)

LEfSe is a method for determining organisms that are most likely to explain biological differences by applying non-parametric statistical tests taking into account effect size (Segata et al., 2011). While PERMANOVA revealed no statistically significant effects of GWI chemical exposure or LNFPIII based on global microbiota composition, LEfSe uncovered specific taxa, most prominent in the chronic study samples, that are significantly affected. When all treatment groups from the 6 h samples were compared, only one bacterial family/genus was found to be affected by any treatment: a significant increase in the genus *Lactobacillus* within the PB/PM-Dextran group (Figure 2A). LEfSe did not identify any significantly affected bacteria at the 48 h time point. However, multiple taxa were significantly affected in the fecal samples 9 months post PB/PM treatment (Figure 2B). Numerous taxa were significantly increased in the DMSO-Dextran group, but the *Verrucomicrobiaceae* genus *Akkermansia* was the only one found to be increased in the DMSO-LNFPIII group (Figure 2B). Interestingly, the genus *Allobaculum,* within the family *Erysipelotrichaceae,* was significantly increased in the PB/PM-Dextran group, but the relative abundance of this genus in the PB/PM-LNFPIII group was similar to control

levels (Figure 2B). Similar results were observed for the *Turicibacter* and *Adlercreutzia* genera, which are part of the families *Erysipelotrichaceae* and *Coriobacteriaceae*, respectively (Figure 2B). Of note, in PB/PM-LNFPIII mice, the genera *Ruminococcus* and *Butyricoccus* were significantly increased (Figure 2B). Figure 3 highlights the significant increase in the relative abundance of the genus *Allobaculum* in PB/PM-Dextran mice and the significant increase in the relative abundance of the genera *Ruminococcus* and *Butyricoccus* in mice exposed to PB/PM-LNFPIII when compared to all other treatments.

After comparing taxa between mice exposed to DMSO-Dextran and PB/PM-Dextran to assess effects of GWI-related chemicals in the absence of LNFPIII, no significant effects were found in the 6 h samples (Figure S2). At 48 h, PB/PM-Dextran exposure significantly increased the abundance of the family *Alcaligenaceae* and genus *Sutterella,* while it significantly decreased the genera *Brevibacterium* and *Ruminococcus* (Figure 4A). Most differences were observed in the samples from the chronic study. Thus, the *Adlercreutzia, Bifidobacterium, Ruminococcus, Allobaculum, Sutterella, Turicibacter,* and *Lactobacillus* genera were all significantly increased in GWI mice when compared to controls DMSO-Dextran), whereas the genera *Citricoccus*, *Prevotella*, *Alistipes, Enterococcus, Blautia, Clostridium, Paucibacter,* and *Pseudomonas* were decreased by PB/PM-Dextran (Figure 4B). Multiple other classes, orders, and families were influenced by GWI-related chemicals exposure (Figure 4B).

Interestingly, when LNFPIII effects were evaluated within PB/PM context in the chronic samples, LNFPIII administration led to a significant increase in the abundance *Butyricoccus* genus, which was decreased by PB/PM, and it prevented increases in the abundances of *Akkermansia*, *Christensenellaceae* and *Erysipelotrichaceae* (Figure 5).

3.3. Gut Motility

There were no significant differences in carmine red gut transit time between DMSO and PB/PM groups 4 months post GW chemical exposure (Figure 6). One month later (month 5), after 1 month of LNFPIII treatment, there was a significant decrease in gut transit time (e.g., shorter transit time) for PB/PM groups (Figure 6; $p \leq 0.01$), suggesting GI disruption. However, this was a transient effect, as no significant differences between treatments for transit time were present at 7 months (Figure 6) or for the overall average of the 3 months (months 5–7; data not shown) post LNFPIII treatment initiation.

3.4. Lipocalin-2 ELISA

Fecal Lcn-2 levels at the end of the chronic study were numerically elevated by prior PB/PM exposure. LNFPIII treatment significantly decreased the levels of fecal Lcn-2 (Figure 7a; $p \leq 0.05$) in both DMSO and PB/PM groups, suggesting an overall reduction in intestinal inflammation with this treatment. Similar trends, although not significant, were present in plasma Lcn-2 levels (Figure 7b).

3.5. Plasma Cytokines

There were no statistically significant differences among the plasma cytokines/chemokines examined. However, there were numerical increases in the PB/PM-Dextran group that were not observed in samples from mice treated with LNFPIII for IL-6, IL-15, IL-17A, IL-17F, and IL-22 (Figure S3). Further, there was a numeric decrease in IL-28b levels in the PB/PM treated groups compared to the DMSO groups (Figure S3). Several cytokines (i.e., IL-10, TNFα and TNFβ) were at or below the limit of detection.

3.6. Correlational Analysis between Bacterial OTUs and Behavioral Task/Lcn-2

A concurrent study focused on long-term neurological effects of PB/PM found that PB/PM treatment increased sticker removal time (a sensorimotor coordination test), and LNFPIII eliminated this effect. Using these data revealed eight OTUs (relative bacterial abundance) that significantly ($p < 0.05$) correlated, in both groups, with fastest sticker removal time (Figure 8). Of those OTUs with relative abundance higher in the PB/PM-Dextran mice, two, belonging to *Ruminococcaceae Oscillospira,* were positively correlated with fastest removal time in PB/PM-Dextran and negatively correlated in PB/PM-LNFPIII mice. In contrast, two *Lachnospiraceae,* one *Rikenellaceae,* and one candidate family S24-7 OTUs were significantly negatively correlated in PB/PM-Dextran mice, but significantly positively correlated in PB/PM-LNFPIII mice (Figure 8). Of those OTUs with relative abundance higher in PB/PM-LNFPIII mice, two belonging to the *Lachnospiraceae* were significantly negatively correlated in PB/PM-Dextran and positively correlated in PB/PM-LNFPIII mice (Figure 8).

Next, significant correlations ($p < 0.05$) were investigated between bacterial OTUs and fecal Lcn-2 levels. Unlike the correlations with sticker removal performance, there were no OTUs that significantly correlated with fecal Lcn-2 in both PB/PM-dextran and PB/PM-LNFPIII treatment groups. However, numerous OTUs correlated to Lcn-2 within groups (Figure 9). For example, within the PB/PM-Dextran group, OTUs belonging to *Anaeroplasma*, *Clostridium,* and *Bacteroides*, along with OTUs within the families *Lachnospiraceae/Mogibacteriaceae* were significantly positively correlated with fecal Lcn-2. In contrast, one *Lachnospiraceae,* one *Oscillospira* (family *Ruminococcaceae*) and one unclassified *Clostridiales* OTU were all negatively correlated (Figure 9). In the

PB/PM-LNFPIII group, three *Lachnospiraceae*, one *Clostridium (Ruminococcaceae)*, and one unclassified OTUs were all significantly positively correlated, whereas one candidate family S24-7 OTU was significantly negatively correlated with fecal Lcn-2 (Figure 9). Correlations between OTUs and Lcn-2 in all animals that received LNFPIII (i.e., both DMSO-LNFPIII and PB/PM-LNFPIII) were also assessed; ten and one OTUs were significantly positively and negatively correlated, respectively (Figure 9). Similar to the PB/PM-LNFPIII analysis, only one candidate family S24-7 OTU was negatively correlated with Lcn-2. Seven *Lachnospiraceae*, one *Alcaligenaceae*, one *Ruminococcaceae*, and one candidate family S24-7 OTUs were significantly positively correlated with Lcn-2 in all LNFPIII mice (Figure 9). Of note, four identical OTUs, belonging to the *Lachnospiraceae* (2), *Clostridium* (1), and S24-7 (1), correlated with fecal Lcn-2 within the PB/PM-LNFPIII and across both LNFPIII-treated groups (Figure 9).

4. Discussion

Recent evidence suggests that the enteric microbiome, in conjunction with widespread immunological perturbations, may play a significant role in GWI symptomology, as well as provide novel therapeutic targets for veterans with this chronic illness. This study sought to evaluate microbiota perturbations in mice exposed to two chemicals that are epidemiologically associated with GWI development and used in an established model of GWI (Zakirova et al., 2015b). The second goal of this study was to assess whether an immunomodulatory glycan, LNFPIII, could potentially provide therapeutic benefit through the complex interaction between the microbiota, immune system, and physiological homeostasis. While exposure to PB/PM and/or LNFPIII did not significantly impact the species composition of the microbiota on a global scale, this study

found that both PB/PM and LNFPIII resulted in the enrichment/depletion of specific bacterial taxa, and that some bacterial OTUs were significantly correlated with GWI (patho)physiological endpoints of interest.

There were no significant effects of exposure to GWI-related chemicals or LNFPIII on either alpha diversity metric considered (i.e., Chao1 richness or Shannon's diversity index), with the exception of the chronic study where Shannon's diversity was increased slightly by PB/PM. Notably, LNFPIII treatment skewed diversity towards control levels. A recent study in a GWI mouse model, that is based on the same GWI chemicals used in the current study, but also includes stress, reported significant increases in both richness and diversity (Alhasson et al., 2017). Veterans with GWI, regardless of GI symptom presence, had significantly higher sample richness and numerically lower Shannon's diversity in a small preliminary study (Janulewicz et al., 2019). Other studies focused on the effects of GWI on the enteric microbiota and/or putative therapeutic interventions did not report diversity analysis. Overall, the data herein aligns with previous studies in mouse models of GWI. The data on alpha diversity in GWI veterans might need to be stratified by exposure severity and/or type to have better concordance between rodent models and GWI veterans.

Importantly, this study found significant perturbations of specific bacterial taxa. Notably, *Allobaculum* was increased in the PB/PM-Dextran group, with LNFPIII administration returning *Allobaculum* abundance to near control levels. This genus was previously found to be significantly increased in another mouse model of GWI (Alhasson et al., 2017) and has been shown to have increased abundance in rats on a high-cholesterol diet alongside a negative correlation with colonic IL-10 and Foxp3 mRNA expression (Lee

et al., 2015). Interestingly, only Foxp3 was significantly decreased in the high-cholesterol group and the negative correlation coefficient between *Allobaculum* and Foxp3 was stronger than with IL-10. Considering that LNFPIII attenuated *Allobaculum* increases in mice exposed to GWI chemicals, the relationship between *Allobaculum* spp., GWI-related exposures, and enteric Foxp3, or other anti-inflammatory genes, is worthy of investigation. How *Allobaculum* affects volatile fatty acids (VFA) status, a key indicator of gut health, is up for debate and subject to investigation. While one study investigating a novel bacterium, *Allobaculum stercoricanis*, in canine feces found that butyrate is one by-product of glucose metabolism (Greetham et al., 2004), another study of *Allobaculum* spp. in the murine microbiota found that lactate, acetate, and propionate are prominent glucose metabolites (Herrmann et al., 2017). Overall, while consistent increases in the *Allobaculum* genus have been identified by us and (Alhasson et al., 2017), further interrogation of the *Allobaculum* species/strains may provide greater insights into the role *Allobaculum* changes may play in promotion/attenuation of GWI-related symptoms, including by promoting favorable VFA profile, i.e., increased butyrate.

One recent study investigating the interaction between the microbiota, enteric/systemic inflammation, and GWI found that butyrate priming might be therapeutically valuable after finding GWI models exhibited statistically significant decreases in *Bifidobacterium* and *Lactobacillus* (Seth et al., 2018). While this previous study did not provide pertinent details about how GWI treatment effected the microbiota prior to butyrate administration, they found that butyrate priming in a GWI mouse model resulted in a slight increase in the abundance of bacteria with the genera *Bifidobacterium, Lactobacillus, and Roseburia,* as well as recovery from leaky gut syndrome and other

metabolic indicators (Seth et al., 2018). While these results may have beneficial implications for future GWI therapeutics, the bacteria identified do not utilize butyrate as a metabolic substrate and the main VFA produced by *Lactobacillus* is lactate. Thus, the connection between butyrate priming and recovery of pathophysiological signs is likely a result of increased butyrate bioavailability along the enteric tract from exogenous administration. Moreover, while identifying bacterial taxa at the genus level can be a beneficial step towards developing beneficial probiotics, blanket generalization of certain genera may have mixed effects, as is the case for bacteria in the genera *Bifidobacterium* (Jeon et al., 2012; Medina et al., 2007; Moran et al., 2009; Mylonaki et al., 2005; Scanlan et al., 2006; Wang et al., 2014) and *Roseburia* (Hillman et al., 2020). However, it is plausible that increasing the abundance of butyrate producing bacteria is one potential therapeutic route to alleviate GI and, perhaps other, symptoms in veterans with GWI (Sun et al., 2017). In this light, data provided herein is noteworthy as LNFPIII treatment increased the *Ruminococcus* and *Butyricoccus* genera, indicating this immunomodulatory glycan may influence the microbiota in a manner that enables increased butyrate production. Although we did not measure this critical, or other, VFAs, it would be important that future work evaluates the abundance of VFAs within the enteric tract, while, concomitantly, performs deep sequencing of these two genera; this will delineate specific species and/or strain-specific effects that might be beneficial for alleviating GWI symptomology.

This study was unable to identify persisting, significant effects of either GWI or LNFPIII on gut motility after 4 months of exposure to GWI chemicals. A significant decrease in gut transit time, suggestive of GI disruption, was present in PB/PM groups at

month 5. However, this effect was transient, as it was not observed at any other timepoints. While effects of GWI on enteric inflammation and physiology have been previously identified (Alhasson et al., 2017; Seth et al., 2018), only one other study assessed gut motility and found that exposure to PB caused acute and chronic alterations in gut motility (Hernandez et al., 2019). On the other hand, previous studies have consistently found exposures associated with GWI result in impairments in gut wall integrity and alterations of the enteric inflammatory profile (Alhasson et al., 2017; Hernandez et al., 2019; Janulewicz et al., 2019; Seth et al., 2018). Herein, fecal and plasma Lcn-2 (NGAL), a protein that has been shown to elicit intestinal inflammation and is a good biomarker of intestinal inflammation (Toyonaga et al., 2016), was numerically increased in mice exposed to PB/PM, when compared to controls. Further, LNFPIII decreased both fecal (significantly) and plasma (trend) Lcn-2 levels when compared to either set of controls, indicating a potential beneficial role for LNFPIII in reducing intestinal inflammation not only in GWI, but also in normal aging. The mice in the chronic study were almost a year old at the time of fecal sample collection for Lcn-2. Aging is consistently associated with increases in GI inflammation (Nagpal et al., 2018; Thevaranjan et al., 2018). The fact that LNFPIII also decreased fecal Lcn-2 in control mice suggests an added benefit of this molecule in preventing age-related gut inflammation. Although the levels of circulating plasma cytokines were mostly unaffected by either treatment, numerical increases in inflammatory cytokines such as IL-6, IL-15, and IL-17 F by PB/PM were observed. These peripheral inflammatory increases were not apparent in LNFPIII groups, and this treatment had a further modulating impact on inflammatory IL-17A and IL-22 levels. While it is unclear whether exposure to the PB/PM mixture can negate the effects of PB alone on gut

motility (Hernandez et al., 2019), the influence of GWI-related chemicals on intestinal inflammation in this study is consistent to a previous report (Seth et al., 2018), but perhaps less pronounced due to the nature of the model and/or timing of assessment.

Another point of recent interest in the larger microbiome community has been the interaction between the gut microbiota, neuroinflammation, and alterations in motor behavior, namely motor deficits. This interest is derived from the suggested use of primary GI symptoms as early biomarkers of potential neurodegenerative diseases, such as PD (Sampson et al., 2016). In fact, in addition to the beneficial effects of butyrate in the gut, studies have indicated that increases in butyrate improve neurobehavioral function including cognitive, mood, and motor functions in numerous settings (Dash et al., 2009; Liu et al., 2017; Yamawaki et al., 2012; Yamawaki et al., 2018). Considering the relationship between GWI, motor deficits and PD, this study sought to identify preliminary associations between the hindgut microbiota and a sensorimotor task (sticker removal). This sensorimotor task requires a mouse to detect and have the ability to remove a sticker placed on its snout, with increased latency to contact and removal of the sticker indicating a motor deficit (Fleming et al., 2013). Behavioral data in mice treated with PB/PM indicated a deficiency in this task, which LNFPIII treatment prevented (unpublished). Eight OTUs (two *Ruminococcaceae*, four *Lachnospiraceae*, one *Rikenellaceae*, and one candidate *S24-7*) were identified that significantly correlated with the fastest sticker removal time in both PB/PM-Dextran and PB/PM-LNFPIII. Of note, the correlation coefficients of these OTUs were opposite between the two experimental treatment groups for all OTUs, indicating some interplay may exist between these bacteria, GWI-related exposures, LNFPIII modulation, and fine motor tasks. Although this will require further

investigation, this is an important starting point moving forward for understanding the interplay of these factors and the complexity of GWI, with the ultimate goal of providing relief to veterans experiencing GWI from GI, neurological, and perhaps other symptoms.

Finally, this study identified numerous OTUs that were significantly correlated with fecal Lcn-2 and these OTUs were different across treatments. While most OTUs identified were from the predominant families (i.e., *Lachnospiraceae* and *Ruminococcaceae)* and have been previously reported in GWI context (Janulewicz et al., 2019), it is worth noting that some have previously been correlated with symptoms of IBS as well (Rinninella et al., 2019). Notably, there were a number of OTUs from mice treated with LNFPIII which correlated with fecal Lcn-2; several of them were correlated with Lcn-2 regardless of PB/PM treatment. Given that LNFPIII decreased fecal Lcn-2 irrespective of GWI treatment, future studies further investigating the modulatory role that these bacteria play in intestinal inflammation are warranted.

5. Conclusions

This study provides additional evidence to support previous work showing that GWI-related chemical exposure induces significant perturbations of select bacterial taxa of the mouse GI microbiota. Additionally, LNFPIII treatment mitigated increases in certain bacteria (e.g., *Allobaculum*) thought to be associated with pathophysiological outcomes of interest in GWI mouse models. Administration of LNFPIII concomitantly resulted in an increase in specific genera that include species known to produce butyrate, a beneficial VFA, thought to have potential multi-factorial benefits in a GWI context. These benefits extend to altering gut health by reducing gut inflammation produced by prior GWI exposure and aging. Overall, this work provides additional support for moving forward and

investigating the complex interactions between the microbiome/GI health, immune and nervous systems, under the umbrella of GWI, while providing additional information about how immunomodulatory compounds (e.g., LNFPIII) could provide multi-level benefits for GWI symptom management. In addition to more mechanistic studies, it will be important to integrate these findings in clinical studies where LNFPIII's benefits are evaluated in veterans with GWI.

Supplementary Materials

The following are available online at https://www.mdpi.com/1660-4601/17/19/7081/s1, Figure S1: Chao1 richness and inverse of Simpson's diversity index in the long-term GWI study, Figure S2: LEfSe 6 h post GWI exposures, Figure S3: Heat map of selected plasma cytokines at the end of the long-term GWI study.

Author Contributions

N.M.F. conceived and designed the study with input from J.J.W. and D.A.H. T.N. and D.A.H. synthesized, characterized, activity-tested, and provided LNFPIII for the study. J.M.C., R.L.D., and N.M.F. conducted the study and collected samples. R.S.M., J.M.C., A.J.S., G.S., and N.M.F., performed the sample processing and data analyses. R.S.M., J.M.C., and N.M.F. wrote the manuscript with editorial input from G.S., D.A.H., and J.J.W. All authors have read and agreed to the published version of the manuscript.

Funding

Department of Defense grant number W81XWH-16-1-0586 to N.M.F. supported this research. We also acknowledge support by the Sharma Distinguished Professorship in Toxicology endowment to N.M.F.

Acknowledgments

We would like to thank James Barber in the College of Veterinary Medicine Cytometry Core Facility at the University of Georgia for his assistance with the multiplex cytokine analysis. We also thank the Interdisciplinary Toxicology Program, the Department of Physiology and Pharmacology, and the Graduate School of the University of Georgia for partial support to R.S.M.

Conflicts of Interest

The authors declare no conflict of interest.

References

Alhasson, F., Das, S., Seth, R., Dattaroy, D., Chandrashekaran, V., Ryan, C.N., Chan, L.S., Testerman, T., Burch, J., Hofseth, L.J., Horner, R., Nagarkatti, M., Nagarkatti, P., Lasley, S.M., Chatterjee, S., 2017. Altered gut microbiome in a mouse model of Gulf War Illness causes neuroinflammation and intestinal injury via leaky gut and TLR4 activation. PLoS One 12(3), e0172914.

Alshelh, Z., Albrecht, D.S., Bergan, C., Akeju, O., Clauw, D.J., Conboy, L., Edwards, R.R., Kim, M., Lee, Y.C., Protsenko, E., Napadow, V., Sullivan, K., Loggia, M.L., 2020. In-vivo imaging of neuroinflammation in veterans with Gulf War illness. Brain Behav Immun 87, 498-507.

Asuzu, D.T., Hayashi, Y., Izbeki, F., Popko, L.N., Young, D.L., Bardsley, M.R., Lorincz, A., Kuro, O.M., Linden, D.R., Farrugia, G., Ordog, T., 2011. Generalized neuromuscular hypoplasia, reduced smooth muscle myosin and altered gut motility in the klotho model of premature aging. Neurogastroenterol Motil 23(7), e309-323.

Atochina, O., Da'dara, A.A., Walker, M., Harn, D.A., 2008. The immunomodulatory glycan LNFPIII initiates alternative activation of murine macrophages in vivo. Immunology 125(1), 111-121.

Baraniuk, J.N., El-Amin, S., Corey, R., Rayhan, R., Timbol, C., 2013. Carnosine treatment for gulf war illness: a randomized controlled trial. Glob J Health Sci 5(3), 69-81.

Belkaid, Y., Hand, T.W., 2014. Role of the microbiota in immunity and inflammation. Cell 157(1), 121-141.

Bhargava, P., Li, C., Stanya, K.J., Jacobi, D., Dai, L., Liu, S., Gangl, M.R., Harn, D.A., Lee, C.H., 2012. Immunomodulatory glycan LNFPIII alleviates hepatosteatosis and insulin resistance through direct and indirect control of metabolic pathways. Nat Med 18(11), 1665-1672.

Broderick, G., Ben-Hamo, R., Vashishtha, S., Efroni, S., Nathanson, L., Barnes, Z., Fletcher, M.A., Klimas, N., 2013. Altered immune pathway activity under exercise challenge in Gulf War Illness: an exploratory analysis. Brain Behav Immun 28, 159-169.

Broderick, G., Fletcher, M.A., Gallagher, M., Barnes, Z., Vernon, S.D., Klimas, N.G., 2018. Exploring the Diagnostic Potential of Immune Biomarker Co-expression in Gulf War Illness. Methods Mol Biol 1781, 101-120.

Carpenter, J.M., Gordon, H.E., Ludwig, H.D., Wagner, J.J., Harn, D.A., Norberg, T., Filipov, N.M., 2020. Neurochemical and neuroinflammatory perturbations in two Gulf War Illness models: Modulation by the immunotherapeutic LNFPIII. Neurotoxicology 77, 40-50.

Chao, L., 2019. Do Gulf War veterans with high levels of deployment-related exposures display symptoms suggestive of Parkinson's disease? Int J Occup Med Environ Health 32(4), 503-526.

Chassaing, B., Srinivasan, G., Delgado, M.A., Young, A.N., Gewirtz, A.T., Vijay-Kumar, M., 2012. Fecal lipocalin 2, a sensitive and broadly dynamic non-invasive biomarker for intestinal inflammation. PLoS One 7(9), e44328.

Dash, P.K., Orsi, S.A., Moore, A.N., 2009. Histone deactylase inhibition combined with behavioral therapy enhances learning and memory following traumatic brain injury. Neuroscience 163(1), 1-8.

DDGWIRP, 2018. The Gulf War Illness Landscape in: Programs, D.o.D.C.D.M.R. (Ed.).

de Oliveira, M.N., Jewell, K.A., Freitas, F.S., Benjamin, L.A., Totola, M.R., Borges, A.C., Moraes, C.A., Suen, G., 2013. Characterizing the microbiota across the gastrointestinal tract of a Brazilian Nelore steer. Vet Microbiol 164(3-4), 307-314.

Donta, S.T., Engel, C.C., Jr., Collins, J.F., Baseman, J.B., Dever, L.L., Taylor, T., Boardman, K.D., Kazis, L.E., Martin, S.E., Horney, R.A., Wiseman, A.L.,

Kernodle, D.S., Smith, R.P., Baltch, A.L., Handanos, C., Catto, B., Montalvo, L., Everson, M., Blackburn, W., Thakore, M., Brown, S.T., Lutwick, L., Norwood, D., Bernstein, J., Bacheller, C., Ribner, B., Church, L.W., Wilson, K.H., Guduru, P., Cooper, R., Lentino, J., Hamill, R.J., Gorin, A.B., Gordan, V., Wagner, D., Robinson, C., DeJace, P., Greenfield, R., Beck, L., Bittner, M., Schumacher, H.R., Silverblatt, F., Schmitt, J., Wong, E., Ryan, M.A., Figueroa, J., Nice, C., Feussner, J.R., Group, V.A.C., 2004. Benefits and harms of doxycycline treatment for Gulf War veterans' illnesses: a randomized, double-blind, placebo-controlled trial. Ann Intern Med 141(2), 85-94.

Dunphy, R.C., Bridgewater, L., Price, D.D., Robinson, M.E., Zeilman, C.J., 3rd, Verne, G.N., 2003. Visceral and cutaneous hypersensitivity in Persian Gulf war veterans with chronic gastrointestinal symptoms. Pain 102(1-2), 79-85.

Fleming, S.M., Ekhator, O.R., Ghisays, V., 2013. Assessment of sensorimotor function in mouse models of Parkinson's disease. JoVE (Journal of Visualized Experiments)(76), e50303.

Golomb, B.A., Allison, M., Koperski, S., Koslik, H.J., Devaraj, S., Ritchie, J.B., 2014. Coenzyme Q10 benefits symptoms in Gulf War veterans: results of a randomized double-blind study. Neural Comput 26(11), 2594-2651.

Greetham, H.L., Gibson, G.R., Giffard, C., Hippe, H., Merkhoffer, B., Steiner, U., Falsen, E., Collins, M.D., 2004. Allobaculum stercoricanis gen. nov., sp. nov., isolated from canine feces. Anaerobe 10(5), 301-307.

Hernandez, S., Fried, D.E., Grubisic, V., McClain, J.L., Gulbransen, B.D., 2019. Gastrointestinal neuroimmune disruption in a mouse model of Gulf War illness. FASEB J 33(5), 6168-6184.

Herrmann, E., Young, W., Rosendale, D., Reichert-Grimm, V., Riedel, C.U., Conrad, R., Egert, M., 2017. RNA-Based Stable Isotope Probing Suggests Allobaculum spp. as

Particularly Active Glucose Assimilators in a Complex Murine Microbiota Cultured In Vitro. Biomed Res Int 2017, 1829685.

Hillman, E.T., Kozik, A.J., Hooker, C.A., Burnett, J.L., Heo, Y., Kiesel, V.A., Nevins, C.J., Oshiro, J., Robins, M.M., Thakkar, R.D., Wu, S.T., Lindemann, S.R., 2020. Comparative genomics of the genus Roseburia reveals divergent biosynthetic pathways that may influence colonic competition among species. Microb Genom.

Janulewicz, P.A., Seth, R.K., Carlson, J.M., Ajama, J., Quinn, E., Heeren, T., Klimas, N., Lasley, S.M., Horner, R.D., Sullivan, K., Chatterjee, S., 2019. The Gut-Microbiome in Gulf War Veterans: A Preliminary Report. Int J Environ Res Public Health 16(19), 3751.

Jeon, S.G., Kayama, H., Ueda, Y., Takahashi, T., Asahara, T., Tsuji, H., Tsuji, N.M., Kiyono, H., Ma, J.S., Kusu, T., Okumura, R., Hara, H., Yoshida, H., Yamamoto, M., Nomoto, K., Takeda, K., 2012. Probiotic Bifidobacterium breve induces IL-10-producing Tr1 cells in the colon. PLoS Pathog 8(5), e1002714.

Klingelhoefer, L., Reichmann, H., 2017. Chapter Twenty-Six - The Gut and Nonmotor Symptoms in Parkinson's Disease, in: Chaudhuri, K.R., Titova, N. (Eds.), International Review of Neurobiology. Academic Press, pp. 787-809.

Koch, T.R., Emory, T.S., 2005. Evaluation of chronic gastrointestinal symptoms following Persian Gulf War exposure. Mil Med 170(8), 696-700.

Kozich, J.J., Westcott, S.L., Baxter, N.T., Highlander, S.K., Schloss, P.D., 2013. Development of a dual-index sequencing strategy and curation pipeline for analyzing amplicon sequence data on the MiSeq Illumina sequencing platform. Appl Environ Microbiol 79(17), 5112-5120.

Lee, S.M., Han, H.W., Yim, S.Y., 2015. Beneficial effects of soy milk and fiber on high cholesterol diet-induced alteration of gut microbiota and inflammatory gene expression in rats. Food Funct 6(2), 492-500.

Liu, J., Wang, F., Liu, S., Du, J., Hu, X., Xiong, J., Fang, R., Chen, W., Sun, J., 2017. Sodium butyrate exerts protective effect against Parkinson's disease in mice via stimulation of glucagon like peptide-1. Journal of the Neurological Sciences 381, 176-181.

Macht, V.A., Woodruff, J.L., Maissy, E.S., Grillo, C.A., Wilson, M.A., Fadel, J.R., Reagan, L.P., 2019. Pyridostigmine bromide and stress interact to impact immune function, cholinergic neurochemistry and behavior in a rat model of Gulf War Illness. Brain Behav Immun 80, 384-393.

Maule, A.L., Janulewicz, P.A., Sullivan, K.A., Krengel, M.H., Yee, M.K., McClean, M., White, R.F., 2018. Meta-analysis of self-reported health symptoms in 1990-1991 Gulf War and Gulf War-era veterans. BMJ Open 8(2), e016086.

Medina, M., Izquierdo, E., Ennahar, S., Sanz, Y., 2007. Differential immunomodulatory properties of Bifidobacterium logum strains: relevance to probiotic selection and clinical applications. Clin Exp Immunol 150(3), 531-538.

Megahed, T., Hattiangady, B., Shuai, B., Shetty, A.K., 2014. Parvalbumin and neuropeptide Y expressing hippocampal GABA-ergic inhibitory interneuron numbers decline in a model of Gulf War illness. Front Cell Neurosci 8, 447.

Moran, J.P., Walter, J., Tannock, G.W., Tonkonogy, S.L., Sartor, R.B., 2009. Bifidobacterium animalis causes extensive duodenitis and mild colonic inflammation in monoassociated interleukin-10-deficient mice. Inflamm Bowel Dis 15(7), 1022-1031.

Mote, R.S., Hill, N.S., Skarlupka, J.H., Tran, V.T., Walker, D.I., Turner, Z.B., Sanders, Z.P., Jones, D.P., Suen, G., Filipov, N.M., 2020. Toxic tall fescue grazing increases susceptibility of the Angus steer fecal microbiota and plasma/urine metabolome to environmental effects. Sci Rep 10(1), 2497.

Mylonaki, M., Rayment, N.B., Rampton, D.S., Hudspith, B.N., Brostoff, J., 2005. Molecular characterization of rectal mucosa-associated bacterial flora in inflammatory bowel disease. Inflamm Bowel Dis 11(5), 481-487.

Nagakura, Y., Naitoh, Y., Kamato, T., Yamano, M., Miyata, K., 1996. Compounds possessing 5-HT3 receptor antagonistic activity inhibit intestinal propulsion in mice. Eur J Pharmacol 311(1), 67-72.

Nagpal, R., Mainali, R., Ahmadi, S., Wang, S., Singh, R., Kavanagh, K., Kitzman, D.W., Kushugulova, A., Marotta, F., Yadav, H., 2018. Gut microbiome and aging: Physiological and mechanistic insights. Nutrition and healthy aging 4(4), 267-285.

O'Callaghan, J.P., Michalovicz, L.T., Kelly, K.A., 2016. Supporting a Neuroimmune Basis of Gulf War Illness. EBioMedicine 13, 5-6.

Parihar, V.K., Hattiangady, B., Shuai, B., Shetty, A.K., 2013. Mood and memory deficits in a model of Gulf War illness are linked with reduced neurogenesis, partial neuron loss, and mild inflammation in the hippocampus. Neuropsychopharmacology 38(12), 2348-2362.

Parkitny, L., Middleton, S., Baker, K., Younger, J., 2015. Evidence for abnormal cytokine expression in Gulf War Illness: A preliminary analysis of daily immune monitoring data. BMC Immunol 16, 57.

R Development Core Team, 2016. R: A language and environment for statistical computing. R Foundation for Statistical Computing, Vienna, Austria.

Rea, K., Dinan, T.G., Cryan, J.F., 2016. The microbiome: A key regulator of stress and neuroinflammation. Neurobiol Stress 4, 23-33.

Rinninella, E., Raoul, P., Cintoni, M., Franceschi, F., Miggiano, G.A.D., Gasbarrini, A., Mele, M.C., 2019. What is the healthy gut microbiota composition? A changing ecosystem across age, environment, diet, and diseases. Microorganisms 7(1), 14.

Sampson, T.R., Debelius, J.W., Thron, T., Janssen, S., Shastri, G.G., Ilhan, Z.E., Challis, C., Schretter, C.E., Rocha, S., Gradinaru, V., 2016. Gut microbiota regulate motor deficits and neuroinflammation in a model of Parkinson's disease. Cell 167(6), 1469-1480. e1412.

Scanlan, P.D., Shanahan, F., O'Mahony, C., Marchesi, J.R., 2006. Culture-independent analyses of temporal variation of the dominant fecal microbiota and targeted bacterial subgroups in Crohn's disease. J Clin Microbiol 44(11), 3980-3988.

Schloss, P.D., Westcott, S.L., Ryabin, T., Hall, J.R., Hartmann, M., Hollister, E.B., Lesniewski, R.A., Oakley, B.B., Parks, D.H., Robinson, C.J., Sahl, J.W., Stres, B., Thallinger, G.G., Van Horn, D.J., Weber, C.F., 2009. Introducing mothur: open-source, platform-independent, community-supported software for describing and comparing microbial communities. Appl Environ Microbiol 75(23), 7537-7541.

Segata, N., Izard, J., Waldron, L., Gevers, D., Miropolsky, L., Garrett, W.S., Huttenhower, C., 2011. Metagenomic biomarker discovery and explanation. Genome Biol 12(6), R60.

Seth, R.K., Kimono, D., Alhasson, F., Sarkar, S., Albadrani, M., Lasley, S.K., Horner, R., Janulewicz, P., Nagarkatti, M., Nagarkatti, P., Sullivan, K., Chatterjee, S., 2018. Increased butyrate priming in the gut stalls microbiome associated-gastrointestinal inflammation and hepatic metabolic reprogramming in a mouse model of Gulf War Illness. Toxicol Appl Pharmacol 350, 64-77.

Srivastava, L., Tundup, S., Choi, B.S., Norberg, T., Harn, D., 2014. Immunomodulatory glycan lacto-N-fucopentaose III requires clathrin-mediated endocytosis to induce alternative activation of antigen-presenting cells. Infect Immun 82(5), 1891-1903.

Sun, M., Wu, W., Liu, Z., Cong, Y., 2017. Microbiota metabolite short chain fatty acids, GPCR, and inflammatory bowel diseases. J Gastroenterol 52(1), 1-8.

Thevaranjan, N., Puchta, A., Schulz, C., Naidoo, A., Szamosi, J.C., Verschoor, C.P., Loukov, D., Schenck, L.P., Jury, J., Foley, K.P., Schertzer, J.D., Larché, M.J.,

Davidson, D.J., Verdú, E.F., Surette, M.G., Bowdish, D.M.E., 2018. Age-Associated Microbial Dysbiosis Promotes Intestinal Permeability, Systemic Inflammation, and Macrophage Dysfunction. Cell Host Microbe 23(4), 570.

Toomey, R., Alpern, R., Vasterling, J.J., Baker, D.G., Reda, D.J., Lyons, M.J., Henderson, W.G., Kang, H.K., Eisen, S.A., Murphy, F.M., 2009. Neuropsychological functioning of U.S. Gulf War veterans 10 years after the war. J Int Neuropsychol Soc 15(5), 717-729.

Toyonaga, T., Matsuura, M., Mori, K., Honzawa, Y., Minami, N., Yamada, S., Kobayashi, T., Hibi, T., Nakase, H., 2016. Lipocalin 2 prevents intestinal inflammation by enhancing phagocytic bacterial clearance in macrophages. Sci Rep 6(1), 35014.

Tundup, S., Srivastava, L., Norberg, T., Watford, W., Harn, D., 2015. A Neoglycoconjugate Containing the Human Milk Sugar LNFPIII Drives Anti-Inflammatory Activation of Antigen Presenting Cells in a CD14 Dependent Pathway. PLoS One 10(9), e0137495.

Vendrik, K.E.W., Ooijevaar, R.E., de Jong, P.R.C., Laman, J.D., van Oosten, B.W., van Hilten, J.J., Ducarmon, Q.R., Keller, J.J., Kuijper, E.J., Contarino, M.F., 2020. Fecal Microbiota Transplantation in Neurological Disorders. Front Cell Infect Microbiol 10, 98.

Wang, W., Chen, L., Zhou, R., Wang, X., Song, L., Huang, S., Wang, G., Xia, B., 2014. Increased proportions of Bifidobacterium and the Lactobacillus group and loss of butyrate-producing bacteria in inflammatory bowel disease. J Clin Microbiol 52(2), 398-406.

Warnes, G.R., Bolker, B., Bonebakker, L., Gentleman, R., Huber, W., Liaw, A., Lumley, T., Maechler, M., Magnusson, A., Moeller, S., 2009. gplots: Various R programming tools for plotting data, R package version. p. 1.

Westfall, S., Lomis, N., Kahouli, I., Dia, S.Y., Singh, S.P., Prakash, S., 2017. Microbiome, probiotics and neurodegenerative diseases: deciphering the gut brain axis. Cellular and molecular life sciences : CMLS 74(20), 3769-3787.

White, R.F., Steele, L., O'Callaghan, J.P., Sullivan, K., Binns, J.H., Golomb, B.A., Bloom, F.E., Bunker, J.A., Crawford, F., Graves, J.C., Hardie, A., Klimas, N., Knox, M., Meggs, W.J., Melling, J., Philbert, M.A., Grashow, R., 2016. Recent research on Gulf War illness and other health problems in veterans of the 1991 Gulf War: Effects of toxicant exposures during deployment. Cortex 74, 449-475.

Yamawaki, Y., Fuchikami, M., Morinobu, S., Segawa, M., Matsumoto, T., Yamawaki, S., 2012. Antidepressant-like effect of sodium butyrate (HDAC inhibitor) and its molecular mechanism of action in the rat hippocampus. The World Journal of Biological Psychiatry 13(6), 458-467.

Yamawaki, Y., Yoshioka, N., Nozaki, K., Ito, H., Oda, K., Harada, K., Shirawachi, S., Asano, S., Aizawa, H., Yamawaki, S., 2018. Sodium butyrate abolishes lipopolysaccharide-induced depression-like behaviors and hippocampal microglial activation in mice. Brain research 1680, 13-38.

Zakirova, Z., Crynen, G., Hassan, S., Abdullah, L., Horne, L., Mathura, V., Crawford, F., Ait-Ghezala, G., 2015a. A Chronic Longitudinal Characterization of Neurobehavioral and Neuropathological Cognitive Impairment in a Mouse Model of Gulf War Agent Exposure. Front Integr Neurosci 9, 71.

Zakirova, Z., Tweed, M., Crynen, G., Reed, J., Abdullah, L., Nissanka, N., Mullan, M., Mullan, M.J., Mathura, V., Crawford, F., Ait-Ghezala, G., 2015b. Gulf War agent exposure causes impairment of long-term memory formation and neuropathological changes in a mouse model of Gulf War Illness. PLoS One 10(3), e0119579.

Zhu, B., Trikudanathan, S., Zozulya, A.L., Sandoval-Garcia, C., Kennedy, J.K., Atochina, O., Norberg, T., Castagner, B., Seeberger, P., Fabry, Z., Harn, D., Khoury, S.J.,

Guleria, I., 2012. Immune modulation by Lacto-N-fucopentaose III in experimental autoimmune encephalomyelitis. Clin Immunol 142(3), 351-361.

Zundel, C.G., Krengel, M.H., Heeren, T., Yee, M.K., Grasso, C.M., Janulewicz Lloyd, P.A., Coughlin, S.S., Sullivan, K., 2019. Rates of Chronic Medical Conditions in 1991 Gulf War Veterans Compared to the General Population. Int J Environ Res Public Health 16(6), 949.

Figures

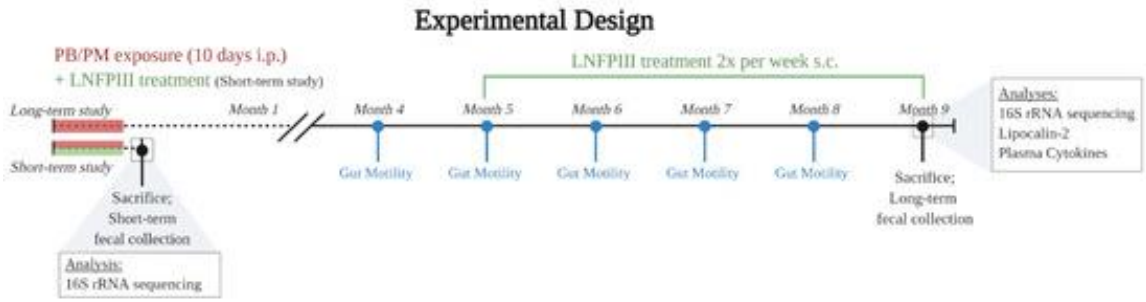

Figure 4.1. Experimental design. In both the short- and long-term studies, mice were exposed to pyridostigmine bromide (PB) and permethrin (PM) for 10 days for Gulf War Illness (GWI) induction. Lacto-N-fucopentaose-III (LNFPIII) treatment was given concurrently during the short-term study and beginning 4 months post PB/PM exposure in the long-term study. Gut motility was examined monthly from month 4 to 8. Microbiota sequencing of the 16S rRNA gene was performed in both the short- and long-term studies. Additionally, in the long-term study, lipocalin-2 (fecal, plasma) and cytokines (plasma) levels were examined.

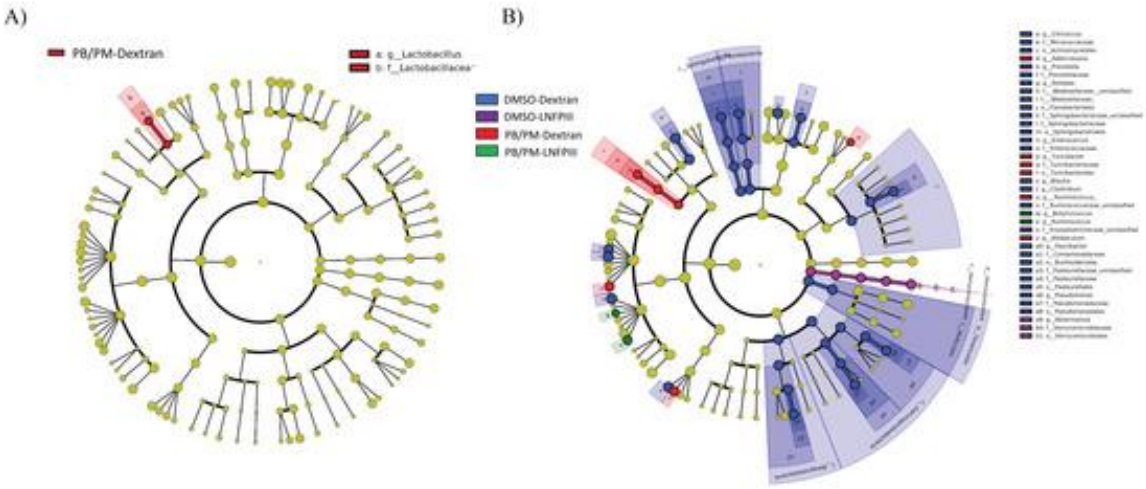

Figure 4.2. Linear discriminant analysis (LDA) effect size (LEfSe; Kruskall–Wallis ($p < 0.05$); Pairwise Wilcoxon ($p < 0.05$); logarithmic LDA score > 2.0) of the fecal microbiota of mice exposed to either DMSO-Dextran, DMSO-LNFPIII, PB/PM-Dextran, or PB/PM-LNFPIII. Greater sequence abundance for specific taxa at (**A**) 6 h, where red indicates increased abundance in PB/PM-Dextran samples or (**B**) 9 months, where blue, purple, red, and green shading indicates greater abundance in DMSO-Dextran, DMSO-LNFPIII, PB/PM-Dextran, or PB/PM-LNFPIII mice, respectively. Taxonomic rank labels are provided before bacterial names: "p_; c_; o_; f_; g_" indicate phylum, class, order, family, and genus, respectively. Letters and numbers within the cladograms refer to bacterial names located in the key to the right of each cladogram.

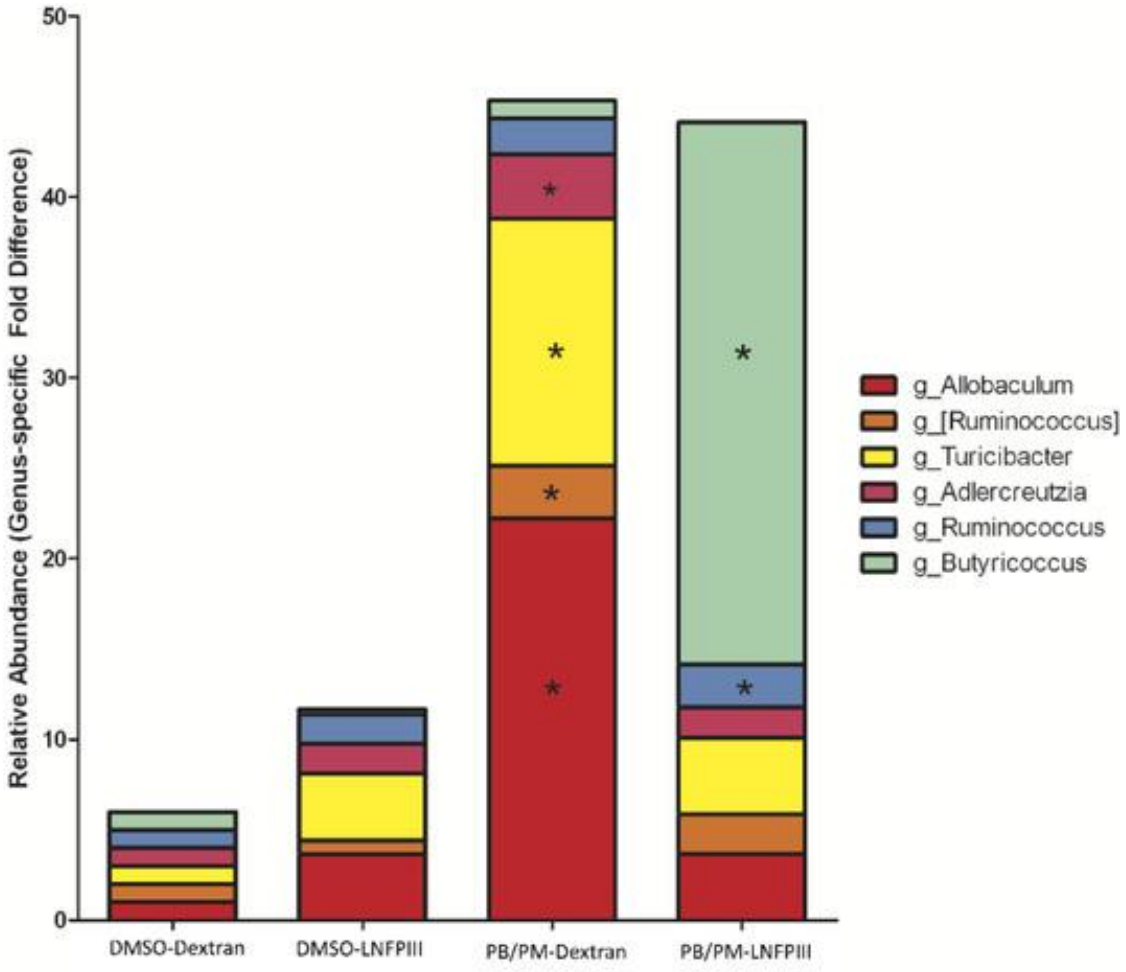

Figure 4.3. Genus-specific fold differences in relative sequence abundance for mice exposed either DMSO-LNFPIII, PB/PM-Dextran, or PB/PM-LNFPIII 9 months prior to sample collection relative to DMSO-Dextran control. (*) indicates statistical significance with respect to sequence abundance relative to all other treatment groups as determined using the Kruskall–Wallis one-way ANOVA on ranks ($p < 0.05$). Brackets indicate proposed relative bacterial abundance (OTUs) within the *Ruminococcus* genus (*Lachnospiraceae* family).

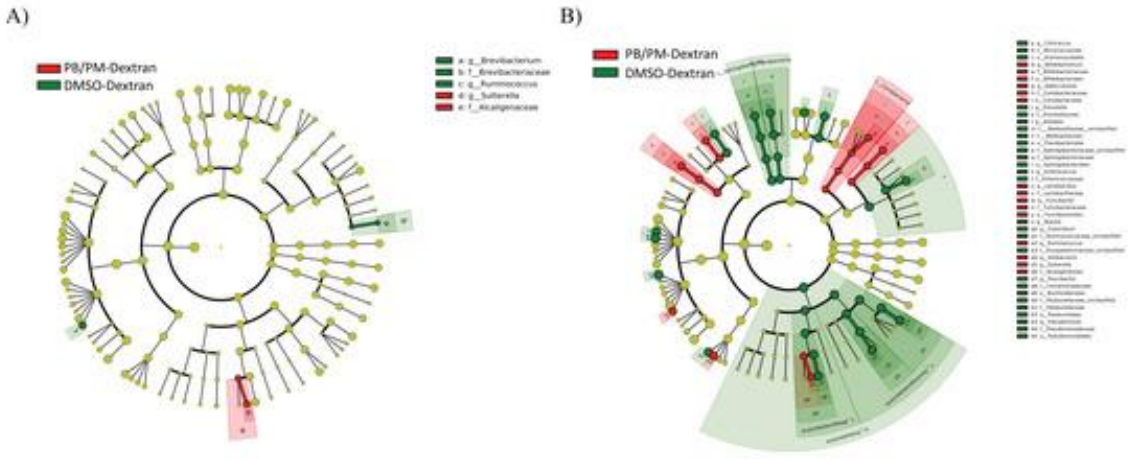

Figure 4.4. Linear discriminant analysis (LDA) effect size (LEfSe; Kruskall–Wallis ($p < 0.05$); Pairwise Wilcoxon ($p < 0.05$); logarithmic LDA score > 2.0) of the fecal microbiota of mice exposed to either DMSO-Dextran or PB/PM-Dextran. Taxa with increased sequence abundance after (**A**) 48 h or (**B**) 9 months post GWI exposures are indicated for PB/PM-Dextran (Red), DMSO-Dextran (Green) groups. Taxonomic rank labels are provided before bacterial names: "p_; c_; o_; f_; g_" indicate phylum, class, order, family, and genus, respectively. Letters and numbers within the cladograms refer to bacterial names located in the key to the right of each cladogram.

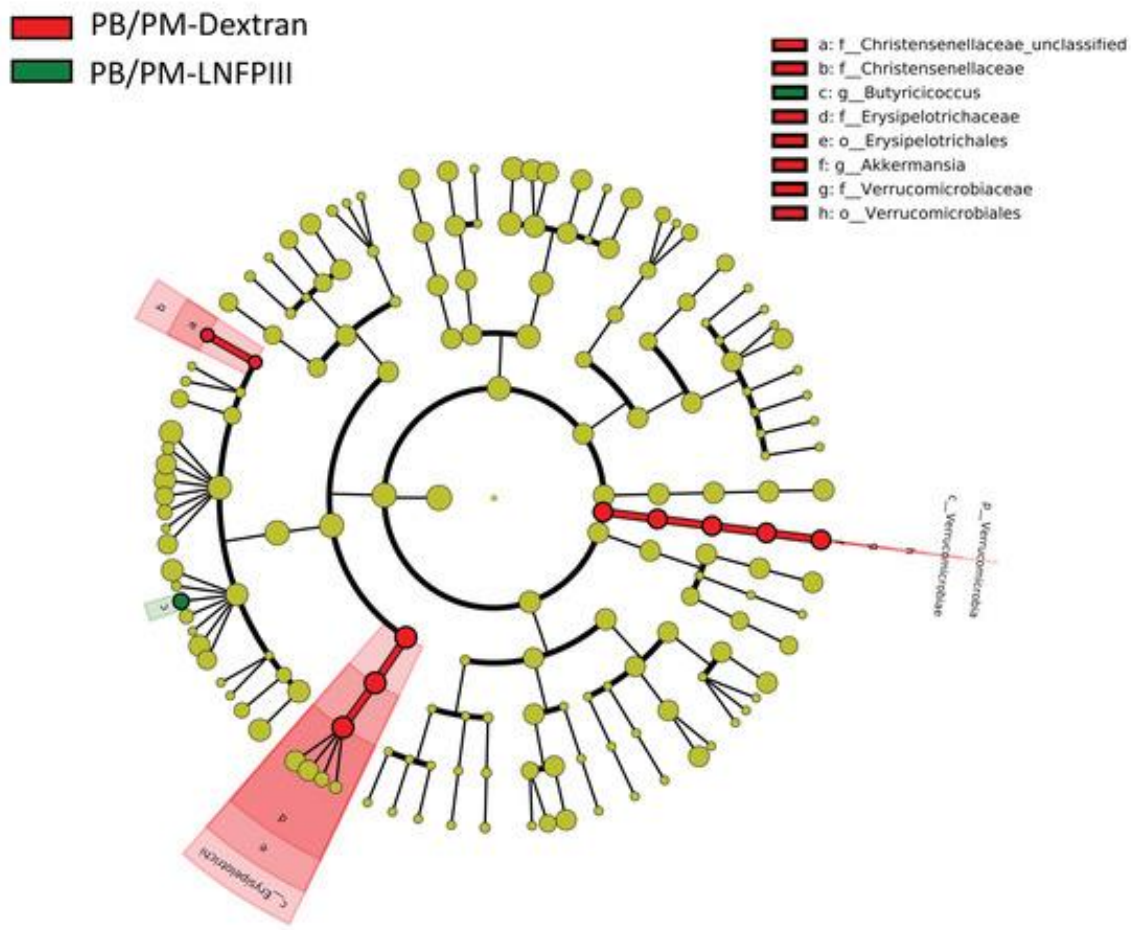

Figure 4.5. Linear discriminant analysis (LDA) effect size (LEfSe; Kruskall–Wallis ($p < 0.05$); Pairwise Wilcoxon ($p < 0.05$); logarithmic LDA score > 2.0) of the fecal microbiota of PB/PM-Dextran or PB/PM-LNFPIII mice collected 9 months after GWI exposures. Taxa with increased sequence abundances in either PB/PM-Dextran (Red) or PB/PM-LNFPIII (Green) are marked. Taxonomic rank labels are provided before bacterial names: "p_; c_; o_; f_; g_" indicate phylum, class, order, family, and genus, respectively. Letters within the cladogram refer to bacterial names located in the key to the right.

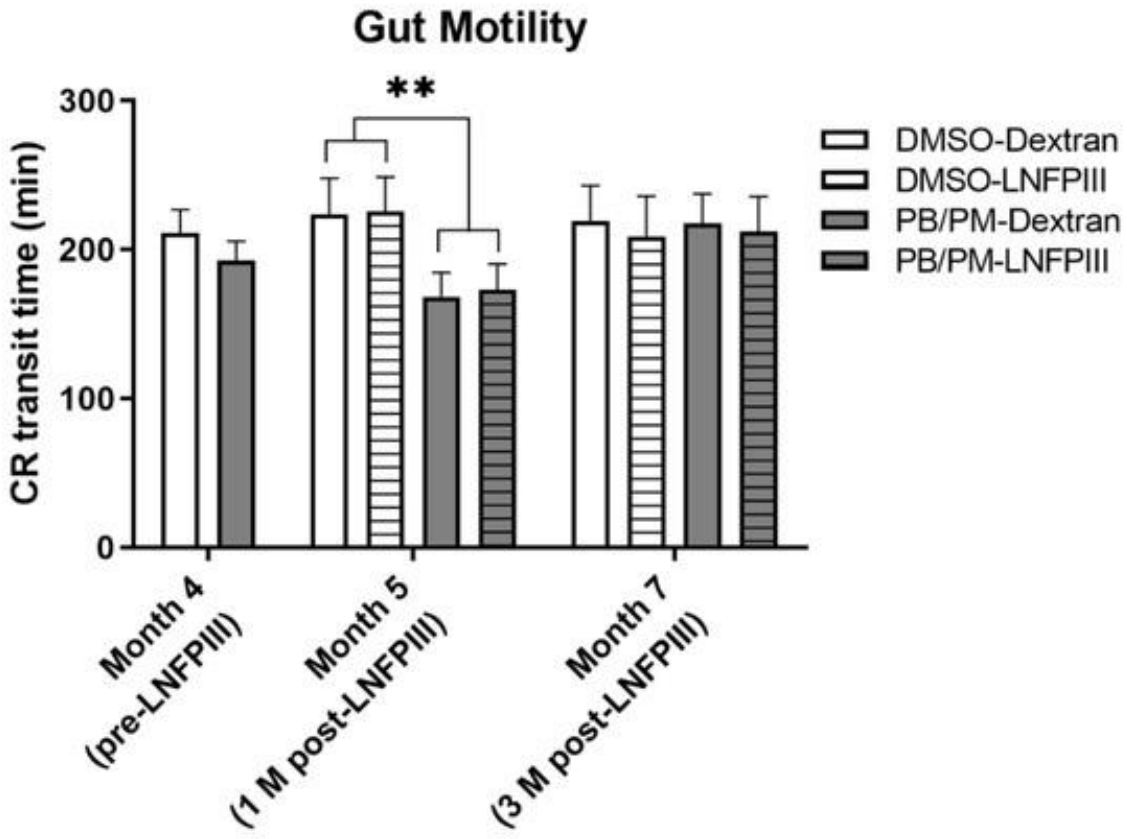

Figure 4.6. Bar plot showing gut transit time of carmine red (CR), 4, 5 or 7 months after mice were exposed to DMSO vehicle or PB/PM. Dextran vehicle or LNFPIII treatments started after CR testing at 4 months. Data are presented as mean ± SEM and sample sizes were n = 27–29/group at 4 months and n = 13–16 at months 5–7. (** $p <$ 0.01).

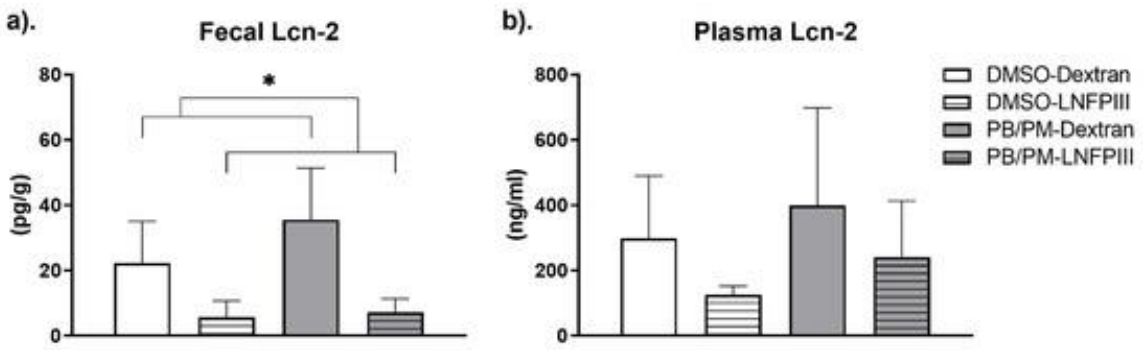

Figure 4.7. Bar plot showing levels of Lipocalin-2 (Lcn-2), as detected by ELISA, in mouse (a) fecal (pg/mL) and (b) plasma (ng/mL) samples from mice that were exposed to either DMSO-Dextran, DMSO-LNFPIII, PB/PM-Dextran, or PB/PM-LNFPIII and sacrificed 9 months later. Data are presented as mean ± SEM (n = 6/group). (* p < 0.05 post PB/PM treatment).

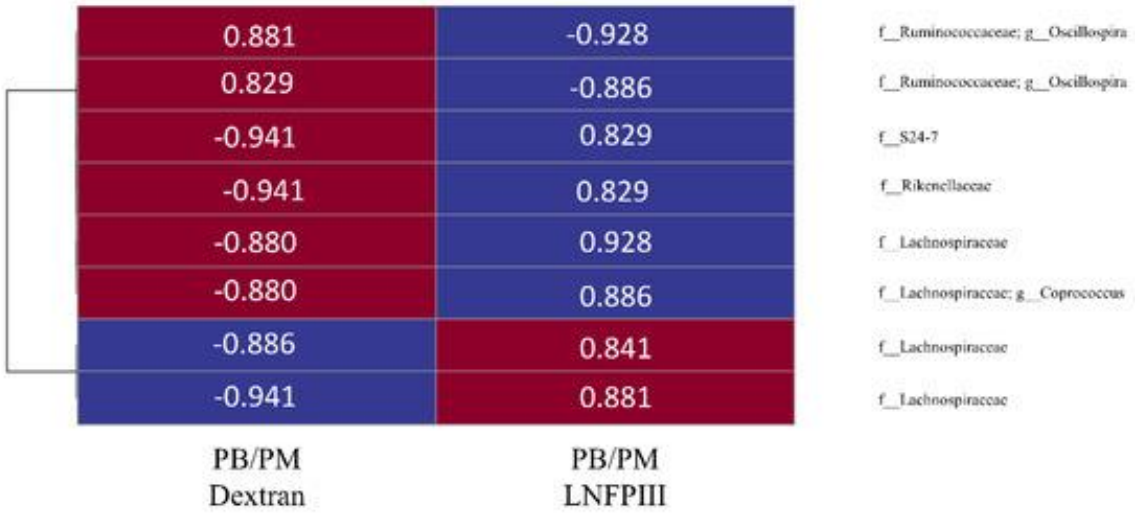

Figure 4.8. Heat map representing the relative bacterial abundance (OTUs) belonging to families specified to the right of the figure that were significantly ($p < 0.05$) correlated with the fastest sticker removal time (sec) in mice exposed to PB/PM-Dextran (left column) or PB/PM-LNFPIII (right column). White numerals indicate the correlation coefficient between relative abundance and fastest removal time for each respective OTU. The "f_" indicates family level and "g_" indicates genus level of taxonomic ranks. If no genus is provided, the OTU was unclassified at the genus level. Red boxes indicate increased and blue color indicate decreased relative abundance of each family/genus OTU in that respective treatment group (column). No sign in front of the number indicates it is a positive correlation coefficient, whereas a negative sign indicates a negative correlation coefficient.

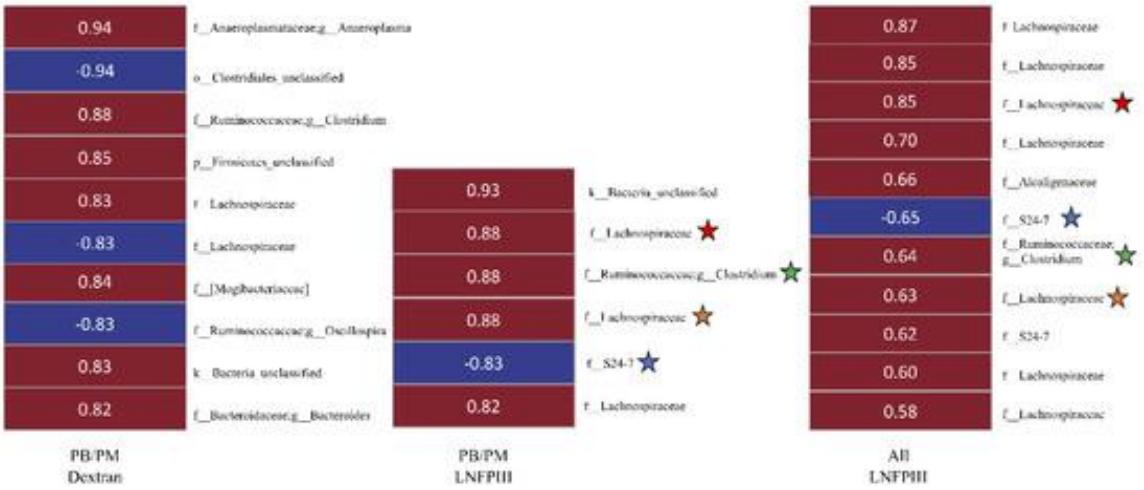

Figure 4.9. Heat map representing the relative abundance of OTUs that were significantly ($p < 0.05$) correlated with the fecal lipocalin-2 (Lcn-2) levels in mice exposed to PB/PM-Dextran (left column), PB/PM-LNFPIII (middle column), or collapsed LNFPIII groups (right column). White numerals display the correlation coefficient between relative abundance and fecal Lcn-2. Each OTU phylogenetic identification is provided to the right of each column. Stars (color-matched) designate OTUs that overlap between PB/PM-LNFPIII and collapsed LNFPIII treatment groups. Taxonomic rank labels are provided with "k_; p_; o_; f_; g_" indicating kingdom, phylum, order, family, and genus, respectively. If no genus is provided, the OTU was unclassified at the genus level. Here, red and blue boxes indicated positive or negative correlation coefficients, respectively, with the exact correlation coefficient within each treatment being listed within the respective box.

Supplementary Materials

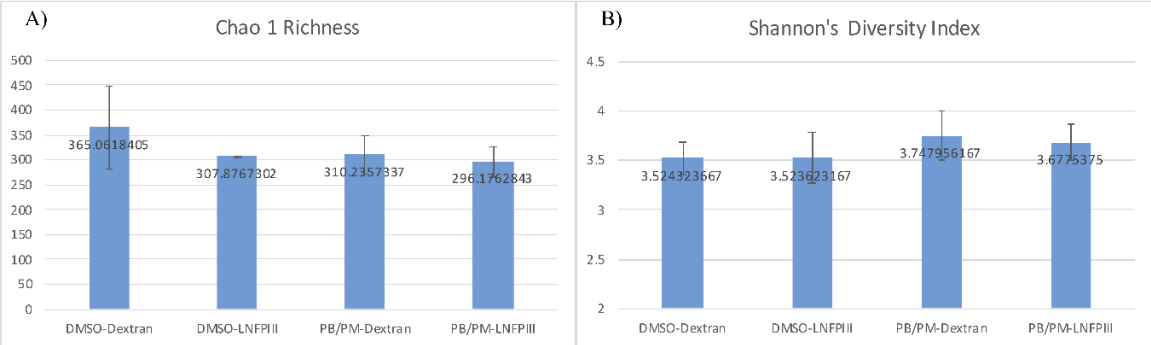

Figure 4.S1: Changes in (A) richness (Chao1 richness) and (B) diversity (inverse of Simpson's diversity index) in the mice exposed to either DMSO-Dextran, DMSO-LNFPIII, PB/PM-Dextran, and PB/PM-LNFPIII in the long-term (chronic) study.

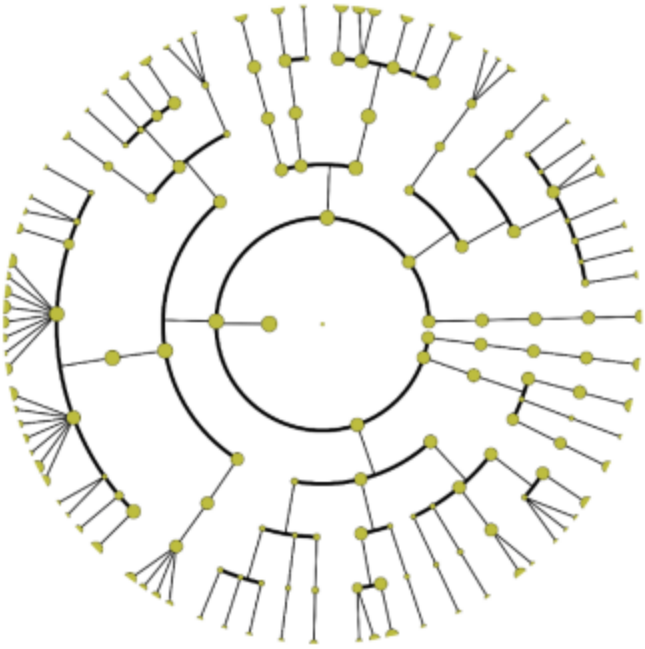

Figure 4.S2. Linear discriminant analysis (LDA) effect size (LEfSe; Kruskall-Wallis [$P < 0.05$]; Pairwise Wilcoxon [$P < 0.05$]; logarithmic LDA score > 2.0) of the fecal microbiota of mice exposed to either DMSO-Dextran or PB/PM-Dextran after 6 h post GWI exposures. As no taxa were altered, no groups are highlighted and no labels are provided.

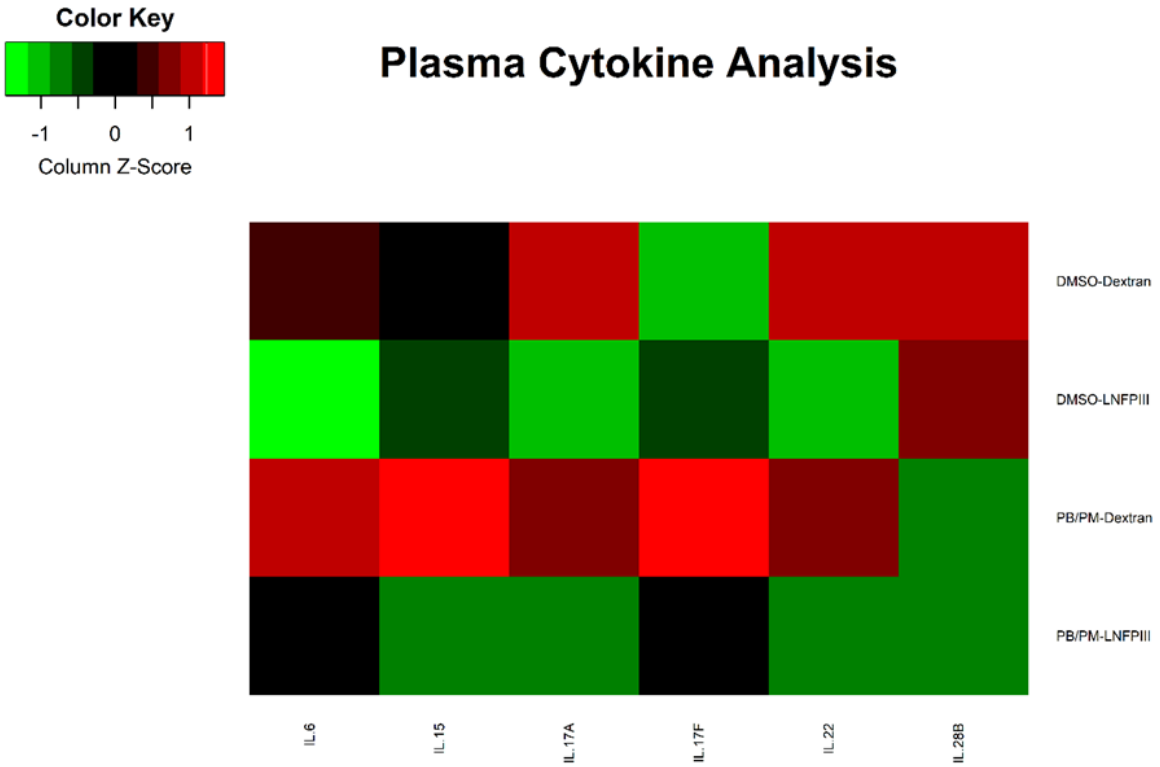

Figure 4.S3. Heat map of selected plasma cytokines. Heat map representing selected cytokines in mice exposed to DMSO-Dextran (n=6), DMSO-LNFPIII (n=6), PB/PM-Dextran (n=7), and PB/PM-LNFPIII (n=7). Red and green color indicates increases and decreases, respectively, of plasma cytokine levels. Color key with Z-scores is located on the upper left.

CHAPTER 5

EVALUATION OF DELAYED LNFPIII TREATMENT INITIATION PROTOCOL ON IMPROVING LONG-TERM BEHAVIORAL AND NEUROINFLAMMATORY PATHOLOGY IN A MOUSE MODEL OF GULF WAR ILLNESS

Jessica M. Carpenter, Kyle A. Brown, Lukas Veltmaat, Helaina D. Ludwig, Kendall B. Clay, Thomas Norberg, Donald A. Harn, John J. Wagner, Nikolay M. Filipov
To be submitted to Neurobiology of Disease

Abstract

Chemical overexposures and war-related stress during the 1990-91 Gulf War (GW) are implicated in the persisting pathological symptoms that GW veterans continue to endure. These symptoms culminate into a disease known as Gulf War Illness (GWI) and affect about a third of the GW veteran population. Currently, there are no effective treatment options available. Here, an established GWI mouse model was utilized to explore the (1) long-term behavioral and neuroinflammatory effects of deployment-related GW chemicals exposure and (2) ability of the immunotherapeutic LNFPIII to restore GWI-related deficits when given months after the end of GW chemicals exposure. Male C57BL6/J mice (8-9 weeks) were administered pyridostigmine bromide (PB) and DEET for 14 days and concurrent corticosterone (CORT) water exposure (latter 7 days) to emulate wartime stress. On day 15, a single injection of the nerve agent surrogate diisopropylfluorophosphate (DFP) was given. LNFPIII treatment began 7 months post GW chemicals and continued until study completion. A battery of behavioral tests for assessment of cognition/memory, mood and motor function in rodents was performed beginning 8 months post GW chemicals exposure followed by immunohistochemical evaluation of neuroinflammation. Within tests of motor function, prior GW chemical exposure led to locomotor hyperactivity and impaired sensorimotor function. LNFPIII attenuated these motor-related deficits and improved overall grip strength. GWI treated mice also exhibited more anxiety-like behavior that was reduced by LNFPIII, and this was test specific. Short-term, but not long-term memory, was impaired by prior GWI exposure; LNFPIII improved this measure. In the brain of GWI mice, glial activation was increased, and LNFPIII reduced this effect. Overall, it appears that months after exposure to GW-related chemicals, behavioral deficits

and neuroinflammation are still present. Many of these deficits were attenuated by LNFPIII when treatment began months post GW chemical exposure, highlighting its therapeutic potential for veterans with GWI.

1. Introduction

Thirty years after the 1990-1991 Gulf War (GW), approximately 30% of the United States personnel that served in it continue to suffer from Gulf War Illness (GWI) (White et al., 2016). GWI is characterized by a multitude of symptoms, including neurological and immunological aberrations. While multiple etiological factors have been investigated, wartime chemical exposures are heavily implicated in GWI pathogenesis (White et al., 2016). These deployment-related overexposures include a chemical nerve agent prophylactic, pesticides, and nerve agents, with war related psychological and environmental stressors superimposed with the overexposures. Combinational chemical overexposures are thought to culminate in the symptom presentation of GWI, and associations between GW deployment-related exposures and GWI symptomology are well-documented (Janulewicz et al., 2017; Proctor et al., 2006; Proctor et al., 1998; Toomey et al., 2009; Zundel et al., 2019).

GWI veterans undergoing neuropsychological evaluations report deficits in motor (Anger et al., 1999; Hom et al., 1997; Proctor et al., 2006; Toomey et al., 2009) and cognitive (Anger et al., 1999; Goldstein et al., 1996; Hom et al., 1997; Janulewicz et al., 2017; Toomey et al., 2009) tasks. GWI veterans also present with higher rates of mood dysfunction (Binder et al., 1999; Hom et al., 1997; Lindem et al., 2003; Sillanpaa et al., 1997) that might impact other reported symptoms (i.e., cognitive and memory complaints) and performance in neuropsychological tests of sustained attention, motor coordination, and executive functioning (Binder et al., 1999; Lindem et al., 2003; Sillanpaa et al., 1997). These behavioral deficits may be linked to altered brain architecture, as numerous clinical MRI studies have revealed abnormalities in brain areas, such as the hippocampus and

cerebellum, that govern these behaviors (Calley et al., 2010; Chao, 2020; Chao et al., 2011; Chao et al., 2016; Chao et al., 2010; Chao et al., 2015; Christova et al., 2017; Gopinath et al., 2012; Hubbard et al., 2014; James et al., 2017; Van Riper et al., 2017; Washington et al., 2020; Wylie et al., 2019; Zhang et al., 2020; Zhang et al., 2021).

Accumulating clinical evidence highlights immune system dysregulation and in particular, inflammation, at the core of GWI (Alshelh et al., 2020; Broderick et al., 2013; Broderick et al., 2011; Khaiboullina et al., 2015; Parkitny et al., 2015). Due to the innate difficulties in assessing the neuroimmune state in the brains of living GWI veterans, the majority of these data relied on peripheral measures of inflammation. However, a recent MRI study observed widespread cortical neuroinflammation in the brains of GWI veterans; primary motor and somatosensory areas were among the affected parts of the cortex (Alshelh et al., 2020).

Current GWI preclinical research focuses on utilizing various paradigms of GW relevant chemical overexposures to elucidate the mechanisms underlying GWI. Relevant GW chemicals include insecticides/repellants (i.e., permethrin, DEET, chlorpyrifos), a nerve agent prophylactic (pyridostigmine bromide, PB), and an organophosphate nerve agent exposure mimic (diisopropylfluorophosphate, DFP) (Ribeiro and Deshpande, 2021). As key features of GWI pathophysiology have been recapitulated in these animal models evidenced by aberrations in behavioral performance (i.e., cognitive, motor, mood dysfunction, and pain) and numerous biological parameters (i.e., gut dysbiosis, elevated oxidative stress, glial activation, neurochemical alterations, chronic neuroinflammation, and leaky blood-brain barrier), the translational value of these models has been established (for review, (Dickey et al., 2021; Ribeiro and Deshpande, 2021; White et al., 2016).

One established GWI model utilizes exposure to the GW relevant chemicals PB, the insect repellent DEET, corticosterone (CORT) to emulate war-related stress and diisopropylfluorophosphate (DFP), a sarin surrogate (O'Callaghan et al., 2015). Acutely, the PB/DEET/CORT/DFP model produced widespread neuroinflammation in multiple areas of the brain including the prefrontal cortex, hippocampus, and striatum (O'Callaghan et al., 2015). In our studies, we found similar acute neuroinflammatory (i.e., increases in TNF-α, IL-1β, IL-6, CCL-2, YM-1 and HMGB1) effects within the hippocampus (Carpenter et al., 2020). Additionally, widespread monoaminergic disbalance was evident by increases in the utilization of serotonin (nucleus accumbens and ventral hippocampus) and dopamine (nucleus accumbens, dorsal hippocampus, and ventral hippocampus) (Carpenter et al., 2020). Further, detailed time-course characterization of this model at 48 h, 7-, and 11-months post GWI chemicals exposure termination provided insights into the progression of hippocampal impairments, particularly in regard to synaptic plasticity and transmission (Brown et al., 2021a). In this study (Brown et al., 2021a), we found that basal synaptic transmission was increased at 48 h, had no change at 7 months, and decreased at 11 months post-PB/DEET/CORT/DFP exposure. Similar results were seen at 11 months when long-term potentiation was evaluated, and these delayed reductions were consistent with a delayed onset of hippocampal neuroinflammation (IL-6) at this time point (Brown et al., 2021a). However, the long-term behavioral consequences in this GWI model remain unknown.

Curative treatment modalities for GWI do not exist. Nevertheless, several disease-modifying therapeutic interventions have been explored including cognitive behavioral therapy (Chao et al., 2021; Donta et al., 2003; Mathersul et al., 2020), mindfulness-based

stress reduction (Kearney et al., 2016), dietary changes (Holton et al., 2020; Holton et al., 2021), and various pharmacological treatments and supplements (Baraniuk et al., 2013; Donovan et al., 2021; Donta et al., 2004; Golier et al., 2016; Golomb et al., 2014; Helmer et al., 2020; Holodniy and Kaiser, 2019). Although these therapies have provided some symptomatic relief, they have limited efficacy in resolving the underlying causes of GWI (Dickey et al., 2021). Thus, one aim of preclinical GWI research is focused on broader therapeutic target identification and testing. Considering the immune dysfunction in GWI, recent preclinical studies have explored the efficacy of several immune-targeted compounds that have shown some promising results (Joshi et al., 2018; Kodali et al., 2018; Ribeiro et al., 2020; Shetty et al., 2020). Our studies have focused on one potent immunomodulatory and anti-inflammatory treatment, Lacto-N-fucopentaose III (LNFPIII), that may be an advantageous treatment option for GWI as we have shown in two GWI models (Brown et al., 2021a; Brown et al., 2021b; Carpenter et al., 2021; Carpenter et al., 2020; Mote et al., 2020). LNFPIII is a Lewis(X)-containing immunomodulatory glycan found in human breast milk and on parasitic helminths that, to date, has had no documented adverse effects (Atochina et al., 2008; Bhargava et al., 2012; Srivastava et al., 2014; Tundup et al., 2015; Zhu et al., 2012). When conjugated to a dextran carrier, LNFPIII activates CD14/TLR-4 signaling for extracellular signal-regulated kinase (ERK)-dependent production of anti-inflammatory mediators to skew the inflammatory balance of the innate immune system in an anti-inflammatory direction (Atochina et al., 2008; Bhargava et al., 2012; Srivastava et al., 2014; Tundup et al., 2015; Zhu et al., 2012) (Carpenter et al., 2021; Carpenter et al., 2020). Within our GWI studies, utilizing the PB/DEET/CORT/DFP and PB/PM models, LNFPIII was beneficial in

restoring acute monoaminergic disbalance and neuroinflammation (both models) as well as long-term behavioral deficits (PB/PM), neuroinflammation, and hippocampal synaptic plasticity impairments (Brown et al., 2021a; Brown et al., 2021b; Carpenter et al., 2021; Carpenter et al., 2020).

Our earlier studies utilizing the PB/DEET/CORT/DFP GWI exposure paradigm determined the acute neuroinflammatory and monoaminergic effects (Carpenter et al., 2020), as well as neuroinflammatory effects and hippocampal functional alterations months post GWI treatment termination (Brown et al., 2021a), with neuroinflammation evaluation being limited to inflammatory cytokine mRNA in the hippocampus. However, the long-term impact of this GWI treatment on behavioral measures or central glial activation has not been characterized within this model. Moreover, whether LNFPIII treatment will be beneficial is unknown. Thus, the present study sought to evaluate the long-term implications of prior GWI exposure on neurobehavioral function and brain inflammatory status post GWI symptomatology induction. Additionally, we examined whether delayed treatment with the immunotherapeutic LNFPIII will be beneficial.

2. Materials and Methods

2.1 Materials

The following chemicals were used for animal treatments: pyridostigmine bromide (PB; Sigma Aldrich, St. Louis, MO), N-Diethyl-3-methylbenzamide (DEET; Sigma Aldrich), corticosterone (CORT; Steraloids, Newport, RI), and diisopropylfluorophosphate (DFP; Sigma Aldrich). Lacto-N-fucopentaose III (LNFPIII) dextran conjugate was produced as in (Carpenter et al., 2021). All additional chemicals and reagents, unless

otherwise noted, were of analytical or higher grade and were obtained from Sigma Aldrich or Fisher Scientific (Hampton, NH).

2.2 Animals

Male C57BL/6J mice (8-9 weeks old; N=54, Jackson Laboratories, Bar Harbor, ME) were housed 4 per cage in an environmentally controlled room (22-24° C) and maintained on a 12 h light/dark cycle (0700-1900 lights on) for one week of acclimation and throughout the study. Mice were handled daily for one week prior to the start of the study to minimize experimenter-induced stress. Food and water were available *ad libitum*. All procedures were approved in advance by the University of Georgia Institutional Animal Care and Use Committee and were in accordance with the latest National Institutes of Health guidelines. Body weights were measured daily during GW chemicals exposure and biweekly after the last GWI exposure until study completion. During the radial arm maze (RAM), in which mice underwent food restriction, weight measurements were taken daily for monitoring as described under the RAM testing protocol. Refer to Figure 1A for a detailed experimental timeline.

2.3 GWI Model and LNFPIII Treatment

Following O'Callaghan et al. (2015) and our earlier work (Brown et al., 2021a; Carpenter et al., 2020), mice were treated for 14 days with a combination of PB and DEET (2 and 30 mg/kg, respectively; SC), or saline vehicle after randomization. On days 8-14, these mice were also administered CORT via drinking water (200 mg/L in 1.5% EtOH tap water) *ad libitum*; control mice were given the 1.5% EtOH vehicle water during this period. On day 15, mice received a single IP injection of DFP (3.75 mg/kg) or saline vehicle.

At 7 months post exposure, mice within each of the two original treatments were randomly subdivided into a LNFPIII or dextran vehicle group. Mice were treated with LNFPIII or dextran vehicle (both 35 μg/mouse diluted in sterile saline; SC) twice a week until study completion as in (Carpenter et al., 2021). At this stage of the study, treatment groups were as follows: Vehicle-Vehicle (Saline/water/saline-Dextran, n=16), Vehicle-LNFPIII (Saline /water/saline-LNFPIII, n=12), GWI-Vehicle (PB/DEET/CORT/DFP-Dextran, n=13), and GWI-LNFPIII (PB/DEET/CORT/DFP-LNFPIII, n=13).

2.4 Behavioral Tests

One month after LNFPIII treatment initiation, a battery of behavioral tests for assessment of cognition/memory, mood, and motor function were performed as done previously (Carpenter et al., 2021). All behavioral testing, scoring, and analysis were done in a randomized, treatment-blind manner. Refer to Figure 1B for a detailed behavioral testing timeline.

2.4.1 Nest Building

Nest building was used to measure cognitive and motor functions as severe hippocampal (Deacon, 2012) and/or striatal (Hofele et al., 2001) damage leads to deficits in nest building independent of sex. Briefly, mice were individually housed with a fresh paper nestlet (Bed-r'Nest, The Anderson's Inc., Maumee, OH); nests pictures were taken from above at different time points (30 min, 60 min, 90 min, 120 min, 180 min, 240 min, 300 min, 360 min, and 24 h) after nestlet placement were scored based on a modified 4-point scale (1 = untouched, 4 = nest completed) as in (Carpenter et al., 2021; Deacon, 2012).

2.4.2 Sucrose Preference (SP)

The SP test, used to measure anhedonia in mice (two-bottle choice paradigm) (Eagle et al., 2016), was performed during behavioral days 1-8. Individually housed mice were given access to two bottles filled with tap water for 4 days to establish a baseline and then given access to one bottle of tap water and one bottle of 1.5% sucrose water for 4 additional days. Solution intake was measured daily by weighing bottles, and bottle position was switched after each measurement to prevent side preference. Sucrose preference (%) was determined using the following equation [(total sucrose intake / (sucrose + water intake)) x 100].

2.4.3 Elevated Zero Maze (EZM)

The EZM is a test frequently used to assess anxiety-like behaviors in mice but can also be expanded to assess certain motor function-related parameters (Braun et al., 2011; Conrad et al., 2011), including in a GWI context (Carpenter et al., 2021). On behavioral day 12, an EZM apparatus (Stoelting Co., Wood Dale, IL) was used under dim illumination (8W red bulb). Lighting conditions, measured with an URCERI light meter, were 30-40 lux and 10-15 lux in the open and closed quadrants, respectively. Starting at a central, open quadrant position facing a closed quadrant, mice were allowed to freely explore the maze for 5 min. All behaviors were tracked and scored using ANY-Maze software (Stoelting). Mice were in a quadrant when 70% of their body was in the area. Scored parameters of interest included time spent in the open and closed areas, number of entries into the open and closed areas, and the latency to enter the closed area at the start of the test as in (Carpenter et al., 2021).

2.4.4 Marble Burying (MB)

Anxiety-like behaviors were also assessed using the MB test as previously described 3 h after the EZM (Carpenter et al., 2021). Briefly, clean testing cages were filled with 5 cm of corn cob bedding (Bed-o'Cobs ¼ inch, The Anderson's Inc., Maumee, OH), and mice were individually placed in these cages for 10 min (habituation phase). After a 1 h resting period, mice were returned to the leveled testing cages with 20 marbles (diameter 10 mm, Panacea Products Corp., Columbus, OH) aligned 4 x 5 in the cage for 20 min (testing phase). A baseline and post-test picture were captured, and the number of marbles buried (>70%) was counted for statistical analysis as in (Carpenter et al., 2021).

2.4.5 Open field (OF)

Locomotor activity was assessed in an OF test as previously described (Carpenter et al., 2021) on behavior day 14. Briefly, mice were individually placed into an open field arena (25 cm x 25 cm x 40 cm; Coulbourn Instruments, Whitehall, PA) and allowed to freely explore for 30 min. The distance traveled, time spent in the center and periphery, and the number of rearings was tracked and scored with the Limelight software (Actimetrics, Wilmette, IL) for both the total 30 min and per 5 min intervals.

2.4.6 Pole Test (PT)

Following a 5-min resting period after the OF, a PT for motor coordination was used as in (Carpenter et al., 2021). Mice were placed upright on a vertical pole (1 x 55 cm; d x h) and the times to turn and complete the test by reaching the bottom (total time) of the pole were recorded. Each mouse underwent 4 trials (5 min inter-trial interval) with the last 3 used for statistical analysis.

2.4.7 Grip Strength (GS)

After a resting period following the PT, forelimb GS (in newtons, N) was measured over 4 trials (1-min inter-trial interval) using a gauge attached to a mouse-specific wire grid (Bioseb, France) as detailed in (Carpenter et al., 2021). Average and max grip strengths were used for statistical analysis.

2.4.8 Novel Object Recognition (NOR)

The NOR test (Carpenter et al., 2021) was performed on day 15. Briefly, the OF on the previous day was used as a habituation phase for the NOR. During the identical phase of the NOR, mice were placed in the open field with two identical objects and allowed to freely explore them for 5 min. Mice were then returned to their home cage for 1 h. During the novel phase, one identical object was replaced with a novel object. Mice were placed in the open field and allowed to explore both objects. The number of novel object approaches and time spent were scored for the first 20 s of the novel phase and the total 5 min with Limelight software (Actimetrics) as in (Carpenter et al., 2021). The novel preference index (NPI) was calculated as described in (Lin et al., 2013).

2.4.9 Gait Test

Following a 3-h home cage resting period after the NOR, gait was evaluated using the gait test (Carpenter et al., 2021). Briefly, a runway (82 cm long, 5.5 cm wide with 8 cm high walls) lined with paper was used; an empty cage with home cage bedding was placed at the end of the runway during testing for escape. Prior to testing, the front and hind paws of the mice were painted with non-toxic red and black ink, respectively (Office Depot, item: #839-994 and #839-967). Two trials were conducted (5 min apart), a pre-trial and the actual trial that was used for subsequent statistical analyses. Between each trial, the runway

was cleaned with 70% EtOH and a new paper strip was placed in it. Gait stride length, base width, inter/intra-step distance, stride variability, total steps, and velocity were analyzed (Carpenter et al., 2021).

2.4.10 Sticker Removal (SR)

The SR test was used to determine sensorimotor function on behavioral day 17 as in (Carpenter et al., 2021; Fleming et al., 2013). Food was removed from the rodents' home cage and ¾ of the bedding was transferred to a clean holding cage where the mice acclimated for 1 h. During the testing phase, a small circular sticker (Avery ¼" round label 5793, Office Depot item: # 113019) was applied using forceps to the nose of the mouse, and the mouse was placed into the home cage. This test was performed over three 90 s trials with a 5 min inter-trial rest. Parameters used for statistical analysis included the average and fastest times for contact and removal of the sticker (Carpenter et al., 2021)

2.4.11 Swim Test (ST)

Following a 3 h rest after the SR, depressive-like behaviors were assessed using the ST as previously described (Carpenter et al., 2021). Briefly, mice were placed in a large beaker filled with 3 L of water (29 ± 2 °C) for 15 min. After each test, the beaker was sanitized thoroughly. Total climbing counts and time spent climbing, mobile, and immobile were scored using Limelight software (Actimetrics). Additionally, the time to the first immobile bout was measured using ANY-Maze (Stoelting).

2.4.12 Barnes Maze (BM)

The BM test was used to assess spatial learning and memory on behavioral testing days 19-24 (Carpenter et al., 2021). Using a 20-hole circular maze (Stoelting) in which one hole is equipped with an escape box (target hole; TH). The maze is brightly illuminated to

promote anxiogenic escape motivation (~1000 lux measured by URCERI light meter). During the acquisition phase (days 1-4), mice were trained to learn and escape into the TH over four 3-min trials, and after trial completion, mice remained or were manually placed into the TH for 1 min. For the probe trial, the escape box was removed, and mice explored the maze for 90 s. Between mice, the maze was rotated and sanitized to remove any residual olfactory cues. The latency, distance, and number of errors to reach the TH were tracked and scored with the ANY-Maze software (Stoelting).

2.4.13 Radial Arm Maze (RAM)

An 8-arm RAM (Med Associates, St. Albans, VT) was used to assess learning and memory function 9 months post-GWI exposure as in (Carpenter et al., 2021) (refer to Figure 1B). Prior to RAM testing, mice were single-housed and underwent a 14-day food restriction protocol until they reached 85% of their free-fed body weight; this was used to motivate learning of the RAM apparatus. During the last 3 days of the food restriction period, mice were behaviorally acclimated to the RAM as in (Carpenter et al., 2021; Preston et al., 2019).

Spatial short-term working memory was assessed by an 8-arm RAM foraging task over 10 consecutive days. Following a 20 min room acclimation period, each mouse was placed in the central RAM hub for 1 min before all 8 doors to each arm opened and allowed free access to all arms. In the foraging task, each arm is “baited” so that one food reward was dispensed upon the first head poke into the food trough of each arm. An error in spatial short-term working memory was defined as an animal revisiting a trough after the initial visit, and the total number of errors for each animal was recorded. Animal performance

was assessed by the average total number of errors of the first three days of testing, the last three days of testing, and comparing the two (Carpenter et al., 2021).

Spatial long-term working memory was evaluated over 10 consecutive days using a modified spatial Win-Shift task after the last day of the foraging task (Carpenter et al., 2021; Clark et al., 2015; Furgerson et al., 2014). This test incorporates a 2-phase (a study phase and a test phase) procedure with an interposed delay. During the study phase, 4 arms were randomly opened, allowing the animal to receive a reward from 4 baited arms. Following the completion of the study phase, the animal was returned to the home cage for a 4 min retention interval, and the maze was cleaned. Then, the animal was returned to the central hub for 1 min (total retention interval of 5 min) before the initiation of the test phase in which all 8 doors were opened, allowing free access to all arms. However, only the 4 arms that were unopened in the study phase dispensed food reward. An error in spatial long-term working memory was defined as a visit to an arm that was baited in the study phase and the total number of errors was recorded. Animal performance was determined by assessing the mean errors from the first three days of testing, the last three days of testing, and comparing the two as in (Carpenter et al., 2021).

2.5. Tissue Processing and Immunohistochemistry

Eleven months post GW chemicals exposure, mice were euthanized, brains were removed, and split into two halves by a sagittal cut. One half was fresh frozen on dry ice and the other half was immersion fixed in 4% paraformaldehyde and transferred to 30% sucrose before flash freezing in isopentane as in Coban et al, 2007. All tissues were stored at -80 °C until analysis.

Fixed half-brains were coronally sectioned into 40 μm thick sections that were placed in phosphate buffer at 4° C until staining. To determine inflammation, free-floating sections containing the hippocampus were stained for microglia (IBA-1), astrocytes (GFAP) and an inflammasome marker, ASC. Sections were incubated, as appropriate, with the following primary antibodies: 1) 1:1000 chicken anti-IBA-1 microglia marker, Aves Lab, Davis, CA and 1:1000 rabbit anti-ASC, AdipoGen, San Diego, CA and 2) 1:2000 chicken anti-glial fibrillary acidic protein (GFAP) astrocyte marker, Aves Labs and 1:1000 rabbit anti-ASC, AdipoGen, all diluted in 0.1% TritonX-100 in PBS for 48 h at 4° C. Following primary antibody incubation, sections were thoroughly washed and incubated with the appropriate secondary fluorescent antibodies (GFAP: 1:1000 goat anti-chicken 488, Abcam; IBA-1: 1:1000 goat anti-chicken 488, Abcam; ASC: 1:1000 goat anti-rabbit 594, Abcam) for 2 h at RT in the dark, followed by incubation with a nuclear stain for 5 min (Hoechst 33258, Invitrogen). Following the final washes, sections were mounted to slides and coverslipped with VectaMount (Vector Labs).

Images were taken on a Zeiss Axioscope A1 microscope, and analysis of cell counts and signal intensity was conducted using ImageJ software. The dentate gyrus of the hippocampus was captured at 5x-40x. Signal intensity (IBA-1 and GFAP staining) and cell counts (all staining) were analyzed using ImageJ. For statistical analysis, the images' signal intensity and/or cell counts were averaged per animal and treatment group means were analyzed as in (Carpenter et al., 2021).

2.6. qPCR for IL-10 and HKG

In addition to analyses already completed on tissues from those animals described in (Brown et al., 2021a). mRNA levels of the anti-inflammatory cytokine IL-10 in the

dorsal and ventral hippocampus were analyzed in this study. Briefly, total RNA from a single hippocampal brain punch (1.5 mm diameter, 500 μm thick section) was isolated by an E.Z.N.A total RNA isolation kit (Omega Bio-Tek, Norcross, GA) according to the manufacturer's directions. RNA was quantified with a Take3 micro-volume plate and Epoch microplate spectrophotometer (BioTek, Winooski, VT). Seventy-five ng RNA/sample was used to synthesize cDNA with a Maxima first-strand cDNA synthesis kit for RT-qPCR (Thermo Fisher Scientific, Waltham, MA) and a PTC-200 Peltier thermal cycler (Bio-Rad, Hercules, CA; 10 min at 25 °C, 15 min at 50 °C, 5 min at 85 °C). Using one or two ng of cDNA per sample, expression of various inflammatory genes was determined by a qPCR with mouse-specific primers (IL-10 and 18S; RealTimePrimers, Elkins Park, PA; Supplemental Table 1) and Maxima SYBR Green/lowRox qPCR Master Mix (2x) (Thermo Fisher Scientific, Waltham, MA). Amplifications were performed on Mx3005 P qPCR machine (Stratagene, San Diego, CA) programed for initial warming cycle (95°C, 10 min) followed by 45 cycles (95°C, 15 s, 60°C, 1 min) with each sample run in duplicate.

2.7 Statistical Analyses

A two-way analysis of variance (ANOVA) or two-way repeated analysis of variance (RM-ANOVA), as appropriate, were used to determine main effects of treatments or treatment interactions. If an ANOVA was significant ($p \leq 0.05$), treatment means were separated by Student-Newman-Keuls (SNK) *post hoc* test or by pre-planned pairwise comparisons (Student's *t*-test, as appropriate). All data, except the RAM, were analyzed using SigmaPlot 12.5 (San Jose, CA), and all graphs were generated using GraphPad Prism (San Diego, CA). Statistical analyses for RAM data were analyzed using R version 3.3.2

(R Development Core Team, 2016, https://www.r-project.org/) and was completed via aov() function for analysis of variance (ANOVA) and the t.test function for the Student's *t*-test and paired *t*-test.

3. Results

3.1 Body Weights

Body weights of the vehicle and GWI groups were not different at the start of treatment (21.8 ± 0.21 g vs. 22.0 ± 0.24 g, $p > 0.65$), but significantly decreased in the GWI group after treatment (0.5 months, $p \leq 0.05$), an acute effect due to DFP treatment. Both groups gained weight over time ($F(13,688) = 903.42$, $p \leq 0.001$) and were not different (p's > 0.23) up to 6.5 months post exposure (Figure 2). At 7 months, these groups were randomly subdivided into a LNFPIII or vehicle group for a total of 4 groups. There were no significant group differences in weight for months 7–11 (Figure 2). Due to RAM food restriction during months 8 and 9, weights were significantly affected ($F(8,361) = 214.51$, $p \leq 0.001$; Figure 2), but recovered by the end of the study (9 vs. 11 months, $p \leq 0.001$; Figure 2) and treatment was not a significant factor ($p > 0.76$).

3.2 Motor alterations after prior GWI exposure and delayed LNFPIII treatment

3.2.1 Nest Building

Overall, nest building was not affected by any treatments as all groups built full nests over the course of 24 h ($F(7,350) = 334.25$, $p \leq 0.001$; Figure 3A). *Post hoc* analysis revealed a significant difference in nesting scores between the Vehicle-Vehicle and GWI-Vehicle groups ($p \leq 0.05$) at 4 hours, but this effect was transient, as there were no group differences at subsequent timepoints. This suggests that prior GWI exposure did not cause marked hippocampal or striatal deficits associated with decreased performance in this test.

3.2.2 Grip Strength (GS)

Grip strength (GS), a measure of neuromuscular function, was unaffected by prior GWI exposure (p's > 0.15) for average and max GS. However, LNFPIII increased both the average ($F(1,50) = 3.65$, $p = 0.06$; data not shown) and max ($F(1,50) = 4.13$, $p \leq 0.05$; Figure 3B) GS suggesting this treatment might improve neuromuscular function irrespective of GWI treatment.

3.2.3 Sticker Removal (SR)

Sensorimotor function, measured by SR, was affected by prior GW chemical exposure as a significant treatment interaction was present for fastest contact ($F(1,48) = 5.51$, $p \leq 0.05$; Figure 3C), with GWI-Vehicle mice taking significantly longer to contact the sticker than controls ($p \leq 0.05$). LNFPIII treatment prevented this GWI increase in sticker contact time ($p \leq 0.05$; Figure 3C). Similar numerical increases were observed in the GWI group for the average contact, average removal, and fastest removal, but were not significant (p's > 0.41). Additionally, LNFPIII treatment tended to reduce the latency for sticker removal ($F(1,48) = 3.71$, $p = 0.06$; data not shown).

3.2.4 Open Field (OF)

As expected, all mice habituated to the OF arena as evident by decreases in distance travelled ($F(5,250) = 175.86$, $p \leq 0.001$; data not shown) and line crossings ($F(5,250) = 139.94$, $p \leq 0.001$, data not shown) over time. All mice, compared to the Vehicle-Vehicle group (p's ≤ 0.01; Figure 3D), exhibited hyperactivity during the first 5 min of exploration, i.e., the distance travelled ($F(1,50) = 7.50$, $p \leq 0.01$, Figure 3D) and the line crossings ($F(1,50) = 5.89$, $p \leq 0.05$, data not shown) were increased. Notably, only GWI mice remained hyperactive for the duration of the test (total distance: GWI-Vehicle vs Vehicle-

Vehicle, $t(27) = 2.21$, $p \leq 0.05$, Figure 3D); this was not observed in mice treated with LNFPIII.

3.2.5 Pole Test (PT)

Motor coordination during the PT was largely unaffected by GWI or LNFPIII treatments as the average time to turn (p's > 0.87) and total time (p's > 0.15) were not significantly different. However, GWI mice descended the pole significantly faster ($F(1,50) = 4.86$, $p \leq 0.05$, Figure 3E), perhaps a reflection of their hyperactivity, while LNFPIII treated mice were slower to do so ($F(1,50) = 4.05$, $p \leq 0.05$, Figure 3E).

3.2.6 Gait Test

Prior GWI exposure led to specific gait alterations. GWI mice exhibited an increase in hindlimb base width ($F(1,50) = 6.59$, $p \leq 0.05$, Figure 3F), stride length ($F(1,50) = 7.47$, $p \leq 0.01$, Figure 3G), and interstep distance ($F(1,50) = 4.46$, $p \leq 0.05$, Figure 3H), which, together, are indicative of hyperactivity. LNFPIII prevented the increase in stride length ($p \leq 0.05$) and this preventative effect was numerical for interstep distance. Additionally, cadence was decreased by the LNFPIII treatment, an effect that approached significance ($F(1,50) = 3.78$, $p = 0.06$, data not shown).

3.3 Mood effects after prior GWI exposure and delayed LNFPIII treatment

3.3.1 Open Field (Mood parameters)

Prior GWI exposure led to more anxiety-like behavior in the OF. During the 1st 5 min of the OF test, GWI treated mice made significantly more entries into the corner ($F(1,50) = 15.29$, $p \leq 0.001$; Figure 4A) and this was not influenced by LNFPIII treatment. This effect persisted for the GWI-Vehicle group as they entered ($t(27) = 2.79$, $p \leq 0.01$; Figure 4A) and spent more time ($t(27) = 2.39$, $p \leq 0.05$; data not shown) in the corners than

Vehicle-Vehicle mice for the 30 min test duration; this was not seen with LNFPIII treatment. Additionally, overall, GWI-Vehicle mice spent less time in the center and more time in the periphery compared to Vehicle-Vehicle mice, but this was not significant (p's = 0.17, data not shown).

3.3.2 Marble Burying (MB)

The average number of marbles buried (≥ 50%) during the test, irrespective of treatment, was 15 (75%), and there were no significant main effects of GWI ($p = 0.10$) or LNFPIII ($p \geq 0.24$) on marbles buried. The GWI-LNFPIII mice buried numerically less than all other groups, with the difference between GWI-Vehicle being greatest ($t(24) = -1.70$, $p = 0.10$, Figure 4B), suggesting a trend for possible LNFPIII anxiolytic benefit in the presence of GWI.

3.3.3 Elevated Zero Maze (EZM)

No significant differences were observed when time spent in the open and closed arms of the EZM were analyzed (p's > 0.17), but there was a numerical decrease in open arm time for the GWI group that was not present with LNFPIII treatment ($t(24) = -1.34$, $p = 0.19$; Figure 4C). LNFPIII treated mice tended to spend longer periods of time in the open arms prior to their first entry into the closed arms ($F(1,50) = 3.66$, $p = 0.06$; Figure 4D), suggesting LNFPIII may have mild initial anxiolytic effects. Additionally, no significance differences were observed when the number of entries into either EZM segments were analyzed (data not shown).

3.3.4 Swim Test (ST)

Times spent immobile or mobile were not significantly affected by GWI or LNFPIII during the 1st 5 min of the test (p's > 0.29; Figure 4E), although a numerical

increase and decrease were present for immobile and mobile times, respectively, in the GWI-Vehicle group. In line with this observation, there was a trend for less climbing attempts in GWI-Vehicle mice that was not seen when LNFPIII was also on board ($t(24) = -1.71$, $p = 0.09$; Figure 4F).

3.3.5 Sucrose Preference

All mice displayed a strong sucrose preference ($F(4,98) = 349.38$, $p \leq 0.001$; Figure 4G), but there were no significant differences among treatment groups for sucrose consumption. However, for average water intake, GWI mice receiving LNFPIII treatment consumed significantly more water ($p \leq 0.001$; Figure 4G).

3.4 Cognition and memory effects after prior GWI and delayed LNFPIII treatment

3.4.1 Novel Object Recognition (NOR)

Prior GWI chemical exposure led to impairments in short-term object recognition memory in the NOR test. A significant GWI effect was present for the approach novelty preference index (NPI) for the first 20 s ($F(1,50) = 6.25$, $p \leq 0.05$; data not shown) and total test time ($F(1,50) = 6.95$, $p \leq 0.01$; Figure 5A) of the test. *Post hoc* test revealed that GWI-Vehicle mice had a lower NPI than Vehicle-Vehicle ($p \leq 0.05$; Figure 5A) overall. Further analysis revealed that Vehicle-Vehicle and Vehicle-LNFPIII mice approached the novel object more than the familiar one (p's ≤ 0.05; Figure 5B), while the GWI-Vehicle tended to approach the novel object less ($p = 0.09$; Figure 5B). LNFPIII treatment did not modulate these GWI effects.

3.4.2 Barnes Maze (BM)

During the acquisition phase of the Barnes Maze (BM), all mice learned the target hole (TH) location as they made fewer errors ($F(1,50) = 174.79$, $p \leq 0.001$), entered the TH

faster ($F(1,50) = 241.94$, $p \leq 0.001$, Figure 5C), and travelled less distance ($F(1,50) = 183.70$, $p \leq 0.001$) over the 4 training days. *Post hoc* analysis revealed that, within day 4, the Vehicle-Vehicle and GWI-LNFPIII groups tended to take longer to enter the TH (p's ≤ 0.05 and 0.07, respectively; Figure 5C), make more errors (p's > 0.06; data not shown), and travel more distance (p's > 0.05; data not shown) than Vehicle-LNFPIII and GWI-Vehicle groups, respectively. The average improvement from day 1 was 60% for time to TH, errors, and distance; in the parameter of time, the Vehicle-Vehicle and GWI-LNFPIII improvement was numerically less so than the Vehicle-LNFPIII and GWI-Vehicle groups (p's ≤ 0.10 Figure 5D). In the BM probe trial, there were no significant differences among groups for the number of errors before reaching the TH, latency to TH, or distance to TH (p's > 0.15; data not shown). However, mice treated with LNFPIII, irrespective of GWI, travelled less distance ($F(1,50) = 3.58$, $p = 0.07$; Figure 5F) and made significantly fewer entries into the TH ($F(1, 50) = 7.42$, $p \leq 0.01$, Figure 5E).

3.4.3 Radial Arm Maze (RAM)

Following 10 consecutive days of training in a dorsal hippocampus (dH)-dependent 8-arm radial arm maze foraging task, there was a significant main effect of training ($F(1,49) = 23.9$, $p \leq 0.001$; Figure 5G), a significant LNFPIII treatment x training interaction effect ($F(1,49) = 7.54$, $p \leq 0.01$), and a GWI x training interaction effect that approached significance ($F(1,49) = 3.29$, $p = 0.08$) on performance in the foraging task. *Post hoc* analyses revealed that initially, during days 1-3, GWI-LNFPIII mice made significantly more errors than GWI-Vehicle mice ($p \leq 0.05$, Figure 5G). However, GWI-LNFPIII treated mice significantly reduced their average total errors on days 8-10 compared to days 1-3 (p's < 0.01, Figure 5G). Improved performance in saline-LNFPIII treated mice also

approached significance ($p = 0.06$). These data suggest that GWI chemical exposure induced a persisting impairment in dH-dependent short-term spatial working memory and that delayed LNFPIII treatment ameliorated this deficit.

Animals then underwent training in a ventral hippocampus (vH)-dependent modified Win-shift task, a task that assesses long-term spatial working memory. There were no significant effects of training, GWI chemical exposure, or LNFPIII treatment on performance in the Win-shift task (p's > 0.13; Figure 5H). No significant treatment x training interaction effects were observed; however, a significant three-way interaction between GWI chemical exposure x LNFPIII treatment x training was detected ($F(1,49) = 4.09$, $p \leq 0.05$; Figure 5H). Notably, the performance of GWI-LNFPIII mice was significantly better than the GWI-Vehicle mice on days 1-3 ($p \leq 0.05$; Figure 5H), indicating that delayed LNFPIII treatment improved performance in the acquisition component of the Win-shift task months after exposure to GWI chemicals.

3.5 Evaluation of hippocampal inflammation post GWI exposure and delayed LNFPIII treatment

3.3.1 GFAP, IBA-1, and ASC Immunoreactivity

Prior exposure to GW chemicals led to hippocampal increases in glial activation that were attenuated by delayed LNFPIII treatment. Intensity analysis for astrocytes (GFAP+) revealed a significant GWI x LNFPIII interaction ($F(1,18) = 7.50$, $p \leq 0.05$, Figure 6A) in which prior exposure to GWI increased GFAP staining compared to Vehicle-Vehicle ($p \leq 0.05$). LNFPIII reduced this effect within GWI ($p \leq 0.01$, Figure 6A). Similar results were found for microglia (IBA-1+), in which there was a LNFPIII treatment effect ($F(1,18) = 3.79$, $p = 0.07$; Figure 6C) and a GWI x LNFPIII interaction ($F(1,18) = 4.21$, p

= 0.06; Figure 6C) that approached significance. These effects were driven primarily by a reduction in the microglia intensity staining by LNFPIII in the GWI group ($t(10) = -4.20$, $p \leq 0.01$, Figure 6C), suggesting that LNFPIII is beneficial in reducing glial activation.

Further, to identify possible neuroinflammatory mechanisms, the inflammasome marker ASC was examined in astrocytes and microglia. No significant differences among treatments were found for the number of GFAP/ASC+ or IBA-1/ASC+ cells (p's > 0.52). However, intensity analysis indicated that LNFPIII treatment reduced staining in GWI ASC+ microglia ($t(10) = -1.88$, $p = 0.09$; Figure 6D), suggesting that LNFPIII subtly attenuates inflammasome activation. A similar numerical reduction with LNFPIII was observed for ASC+ astrocytes but was not significant (Figure 6B).

3.3.2 qPCR

The expression of the anti-inflammatory mediator IL-10 was assessed in the dorsal and ventral hippocampus 11 months post GW chemical exposures and 4 months post LNFPIII treatment initiation. There were no significant differences within the dorsal hippocampus, but analysis within the ventral hippocampus revealed increased IL-10 expression in the GWI-LNFPIII group compared to Vehicle-Vehicle ($p \leq 0.05$) and GWI-Vehicle ($p = 0.08$) groups.

4. Discussion

Epidemiological evidence suggests that exposures to multiple toxicants during the Gulf War (GW) contributed to the development of GWI (White et al., 2016) and that these overexposures have accelerated age-related chronic conditions (Zundel et al., 2019). Because of the persistent and progressive nature of GWI, investigations into therapeutic interventions are imperative. The present GWI model (PB/DEET/CORT/DFP) has been

primarily characterized at acute timepoints post exposure (Carpenter et al., 2020; O'Callaghan et al., 2015), with limited studies examining the model's chronic effects on hippocampal electrophysiology (Brown et al., 2021a). As the GW occurred more than 30 years ago, it is crucial that GWI preclinical investigations align with the aging GWI veteran population. Thus, the current study aimed to further characterize the long-term behavioral and neuroinflammatory effects of PB/DEET/CORT/DFP exposure. Additionally, we examined whether delayed treatment with LNFPIII was beneficial in these measures.

Sensorimotor function was impacted by prior GWI exposure, as GWI mice exhibited higher latencies to contact the sticker in the sticker removal task; this sensorimotor deficit was eliminated by LNFPIII. These results align with the sensorimotor deficits observed previously in GWI veterans (Axelrod and Milner, 1997; Proctor et al., 2006; Toomey et al., 2009) and animal models (Abou-Donia et al., 2002; Carpenter et al., 2021) and suggest that LNFPIII may be beneficial in alleviating this deficit as it did in another GWI model (Carpenter et al., 2021). Neuromuscular function remained unaltered by prior GWI exposure as measured by grip strength, but LNFPIII treatment improved overall strength within this test. Further, all mice were able to build nests indicating that there were not any marked striatal or hippocampal deficits that are normally associated with this test. Interestingly, in this study, prior exposure to GWI related chemicals led to hyperactivity in several tests. This was notable in the open field (OF), as GWI treated mice traveled further distances and made more line crossings within the first 5 min of the test; however, this hyperactivity did not persist in GWI receiving LNFPIII treatment at 30 min suggesting LNFPIII may reduce the persistence of this deficit. This increased activity was in line with the observed GWI gait alterations in this study, as GWI mice exhibited

increased hindlimb base widths, stride lengths, and interstep distance; the latter two were prevented by LNFPIII treatment. Hyperactivity was also evident in the pole test, as GWI mice descended the pole faster. These increases in motor activity might be due to persisting effects of the AChE inhibitors PB (reversible) and DFP (irreversible) that were component of the GWI chemical exposure mixture. In fact, it has been shown that following sarin vapor exposure, sustained increases in locomotor activity were apparent 1 and 6 months post exposure in rats (Allon et al., 2011). Further investigation into the mechanisms underlying this increase in activity are warranted, but LNFPIII treatment was beneficial in this GWI model as it was in the PB/PM GWI model (Carpenter et al. 2021).

Affect symptoms have been widely self-reported by GWI veterans and present as increases in depressive and anxiety behaviors (Binder et al., 1999; Sullivan et al., 2018); these effects have been recapitulated in multiple GWI exposure paradigms (Carreras et al., 2018; Phillips and Deshpande, 2016; Zhu et al., 2020), especially those including a stress component (Abdullah et al., 2012; Parihar et al., 2013). Here, GWI mice exhibited subtle mood impairments, driven mostly by anxiety-like behaviors. Subtle, anxiety-like behavior was observed in the EZM as GWI-Vehicle mice spent less time in the open areas. In line with these EZM results, GWI treated mice also spent numerically less time in the anxiogenic center of the OF arena. Moreover, in the OF, GWI mice entered and spent more time in the arena's corners, suggestive of anxiety-like behavior. Notably, LNFPIII treatment increased the time spent exploring the open area of the EZM before entering the closed areas, reduced the number of marbles buried in the marble burying test, and decreased the overall amount of corner entries and time in the OF. These effects suggest that LNFPIII has some anxiolytic properties on multiple anxiety-like parameters.

Anhedonia, a behavior associated with depression, was not present in the sucrose preference test, as all tested mice preferred the sucrose solution to normal tap water. Depressive-like behavior was also evaluated using the swim test, and GWI mice tended to exhibit more depressive-like behavior within this test; they spent numerically more time immobile (e.g., behavior despair) and had fewer climbing attempts (e.g., escape behavior). These effects were not seen with control or LNFPIII treated groups. Clinical studies have shown that mood deficits experienced by GWI veterans can impact the reporting of other GWI symptoms and impact the results of neuropsychological evaluations like motor coordination and executive function (Binder et al., 1999; Lindem et al., 2003; Sillanpaa et al., 1997). Thus, the affect results observed here, albeit subtle, might impact other behavioral domains examined in this study.

Cognitive and memory aberrations remain a consistent feature among veterans with GWI, and numerous studies have shown poorer performance in cognitive/memory tasks (Goldstein et al., 1996; Hom et al., 1997; Janulewicz et al., 2017; Toomey et al., 2009). Further, GWI preclinical investigations also report deficits in tests of learning and memory (Carpenter et al., 2021; Hattiangady et al., 2014; Madhu et al., 2019; Parihar et al., 2013; Phillips and Deshpande, 2016). Here, no profound GWI-induced cognitive and memory impairments were observed in hippocampal dependent tasks such as nesting, the Barnes Maze (BM) and Radial Arm Maze; all animal performed at similar rates in these tasks. However, GWI treatment impaired short-term recognition memory in the Novel Object Recognition task. These results align with GWI veterans performing worse in visual memory tasks (both immediate and delayed recall, (Sullivan et al., 2018)), and NOR performance in another GWI model we reported on (Carpenter et al., 2021). In the BM, all

mice significantly improved their performance (~60%) over the course of the 4 day acquisition period indicative of learning. There were no significant GWI induced deficiencies within the BM probe trial, but LNFPIII treatment decreased the number of TH entries and distance travelled within the trial; this suggests that LNFPIII improved memory performance, as these mice travelled less after approaching the target hole. Similarly, in the RAM Foraging task, which measures dorsal hippocampal (dH) dependent short-term working spatial memory, all mice improved their performance in this task over time. While early on in this task, the GWI-LNFPIII group made more errors, this group improved the most overall with a 55% decrease in errors and this was significant compared to GWI-Vehicle, indicating LNFPIII treatment improved performance rate. There were no observable long-term memory deficits in the vH spatial working memory RAM Win Shift task by the end of training, but it is notable that GWI-LNFPIII mice performed better early on in the acquisition component of this task. These results align with a separate study on these mice investigating hippocampal synaptic plasticity and transmission at 11 months (Brown et al., 2021a) where prior PB/DEET/CORT/DFP exposure produced decreases in hippocampal basal synaptic plasticity and long-term potentiation (LTP) that were recovered by LNFPIII treatment. Taken together, these data suggest that LNFPIII may benefit some domains of cognition and memory in this model as it did in another one (Carpenter et al., 2021).

Prior investigations utilizing this GWI treatment paradigm revealed widespread acute neuroinflammation in multiple areas of the brain including the prefrontal cortex, hippocampus, and striatum (O'Callaghan et al., 2015). In our studies, we found similar acute neuroinflammatory (i.e., increases in TNF-α, IL-1β, IL-6, CCL-2, YM-1 and

HMGB1) effects within the hippocampus (Carpenter et al., 2020), with some also apparent at 11 months post exposure in some inflammatory measures (IL-6; (Brown et al., 2021a). Notably, at 11 months post GWI exposure, the increase in hippocampal IL-6 mRNA levels were less with LNFPIII treatment (Brown et al., 2021a). To determine if the LNFPIII-induced dampening of IL-6 was due to an increase in anti-inflammatory signaling, here, we measured IL-10, a cytokine already known to be affected by LNFPIII in a different setting (Tundep et al., 2015). Indeed, in the present study, hippocampal levels IL-10 were increased in mice exposed to GWI-LNFPIII treatment. Further, because enhanced inflammatory cytokine production can lead to glial activation and resulting behavioral deficits (Habbas et al., 2015; Miller, 2009; Minogue et al., 2012), immunohistochemical analysis of GFAP (astrocytes) and IBA-1 (microglia) was done in the hippocampus. Prior GWI treatment led to increases GFAP and IBA-1 immunoreactivity that were more pronounced for GFAP. Notably, LNFPIII significantly reduced these effects within GFAP+ and IBA-1+ cells indicative of its ability to counteract neuroinflammation. Additionally, inflammasome activation by ASC (apoptosis-associated spec-like protein) co-localization with GFAP+ and IBA-1+ cells was evaluated. Briefly, upon activation, ASC functions to form the NLRP3 inflammasome which in turn mediates caspase-1 activation of inflammatory IL-1β and IL-18 release (Yang et al., 2019). There were no differences in the number of ASC positive GFAP or IBA-1 cells. However, LNFPIII significantly reduced the intensity of ASC+/IBA-1+ cells within GWI mice, suggesting that inflammasome activation occurs more so in microglia and LNFPIII can modulate this activity.

Overall, this study provides valuable insights into the long-term neurological alterations of prior GWI relevant chemical exposures along a translationally relevant time course for current GWI veterans. Evaluating the neurological adaptions in this model have shown that prior exposure leads to deficits in behavioral domains (e.g., motor, mood, and cognitive function) and neuroinflammation (glial activation), all of which are prominent symptoms in the GWI veteran population. Moreover, the translational relevance of this model allows for the evaluation of therapeutic interventions such as LNFPIII. Importantly, the data in this study indicate that LNFPIII, when initiated months after GWI exposure, restored many of the observed deficits. Such include restoring locomotor and sensorimotor dysfunction, improving cognitive function, alleviating affect changes, and reducing hippocampal neuroinflammation. These data highlight that LNFPIII has widespread beneficial properties and suggests that it might be an efficacious therapy for the myriad of symptoms in GWI veterans.

Author contributions

NMF conceived and designed the study. TN and DAH synthesized, characterized, and provided LNFPIII used in the study. NMF, JMC, KAB, HDL, and KBC assisted in investigation and sample collection. JMC, LV, and KAB performed sample and data analysis. JMC and NMF wrote the manuscript with input from KAB, JJW, and DAH. All authors read/contributed editorially and approved the final manuscript version.

Declaration of competing interests

The authors declare no conflicts of interest.

Acknowledgements

This research was supported by Department of Defense grant numbers W81XWH1610586 and W81XWH2110661 to NMF.

References

Abdullah, L., Evans, J.E., Bishop, A., Reed, J.M., Crynen, G., Phillips, J., Pelot, R., Mullan, M.A., Ferro, A., Mullan, C.M., Mullan, M.J., Ait-Ghezala, G., Crawford, F.C., 2012. Lipidomic profiling of phosphocholine-containing brain lipids in mice with sensorimotor deficits and anxiety-like features after exposure to Gulf War agents. NeuroMolecular Medicine 14, 349-361.

Abou-Donia, M.B., Dechkovskaia, A.M., Goldstein, L.B., Bullman, S.L., Khan, W.A., 2002. Sensorimotor Deficit and Cholinergic Changes following Coexposure with Pyridostigmine Bromide and Sarin in Rats. Toxicological Sciences 66(1), 148-158.

Allon, N., Chapman, S., Egoz, I., Rabinovitz, I., Kapon, J., Weissman, B.A., Yacov, G., Bloch-Shilderman, E., Grauer, E., 2011. Deterioration in brain and heart functions following a single sub-lethal (0.8 LCt50) inhalation exposure of rats to sarin vapor:: A putative mechanism of the long term toxicity. Toxicology and Applied Pharmacology 253(1), 31-37.

Alshelh, Z., Albrecht, D.S., Bergan, C., Akeju, O., Clauw, D.J., Conboy, L., Edwards, R.R., Kim, M., Lee, Y.C., Protsenko, E., Napadow, V., Sullivan, K., Loggia, M.L., 2020. In-vivo imaging of neuroinflammation in veterans with Gulf War illness. Brain, Behavior, and Immunity 87, 498-507.

Anger, W., Storzbach, D., Binder, L., Campbell, K., Rohlman, D., McCauley, L., 1999. Evidence of cognitive deficits in Persian Gulf War veterans: interim report from a population-based study. J Int Neuropsychol Soc 5, 203-212.

Anger, W.K., Storzbach, D., Binder, L.M., Campbell, K.A., Rohlman, D.S., McCauley, L., Kovera, C.A., Davis, K.L., 1999. Neurobehavioral deficits in Persian Gulf veterans: Evidence from a population-based study. Journal of the International Neuropsychological Society 5(3), 203-212.

Atochina, O., Da'dara, A.A., Walker, M., Harn, D.A., 2008. The immunomodulatory glycan LNFPIII initiates alternative activation of murine macrophages in vivo. Immunology 125(1), 111-121.

Axelrod, B.N., Milner, I.B., 1997. Neuropsychological findings in a sample of Operation Desert Storm veterans. The Journal of Neuropsychiatry and Clinical Neurosciences 9(1), 23-28.

Baraniuk, J.N., El-Amin, S., Corey, R., Rayhan, R., Timbol, C., 2013. Carnosine treatment for gulf war illness: a randomized controlled trial. Glob J Health Sci 5(3), 69-81.

Bhargava, P., Li, C., Stanya, K.J., Jacobi, D., Dai, L., Liu, S., Gangl, M.R., Harn, D.A., Lee, C.H., 2012. Immunomodulatory glycan LNFPIII alleviates hepatosteatosis and insulin resistance through direct and indirect control of metabolic pathways. Nat Med 18(11), 1665-1672.

Binder, L.M., Storzbach, D., Anger, W.K., Campbell, K.A., Rohlman, D.S., of the Portland Environmental, O.M., Center, H.R., 1999. Subjective Cognitive Complaints, Affective Distress, and Objective Cognitive Performance in Persian Gulf War Veterans. Archives of Clinical Neuropsychology 14(6), 531-536.

Braun, A.A., Skelton, M.R., Vorhees, C.V., Williams, M.T., 2011. Comparison of the elevated plus and elevated zero mazes in treated and untreated male Sprague–Dawley rats: Effects of anxiolytic and anxiogenic agents. Pharmacology Biochemistry and Behavior 97(3), 406-415.

Broderick, G., Ben-Hamo, R., Vashishtha, S., Efroni, S., Nathanson, L., Barnes, Z., Fletcher, M.A., Klimas, N., 2013. Altered immune pathway activity under exercise challenge in Gulf War Illness: An exploratory analysis. Brain, Behavior, and Immunity 28, 159-169.

Broderick, G., Kreitz, A., Fuite, J., Fletcher, M.A., Vernon, S.D., Klimas, N., 2011. A pilot study of immune network remodeling under challenge in Gulf War Illness. Brain, Behavior, and Immunity 25(2), 302-313.

Brown, K.A., Carpenter, J.M., Preston, C.J., Ludwig, H.D., Clay, K.B., Harn, D.A., Norberg, T., Wagner, J.J., Filipov, N.M., 2021a. Lacto-N-fucopentaose-III ameliorates acute and persisting hippocampal synaptic plasticity and transmission deficits in a Gulf War Illness mouse model. Life Sci 279, 119707.

Brown, K.A., Preston, C.J., Carpenter, J.M., Ludwig, H.D., Norberg, T., Harn, D.A., Filipov, N.M., Wagner, J.J., 2021b. Lacto-N-fucopentaose-III (LNFPIII) ameliorates acute aberrations in hippocampal synaptic transmission in a Gulf War Illness animal model. Brain Res 1766, 147513.

Calley, C.S., Kraut, M.A., Spence, J.S., Briggs, R.W., Haley, R.W., Hart, J., 2010. The neuroanatomic correlates of semantic memory deficits in patients with Gulf War illnesses: a pilot study. Brain Imaging and Behavior 4(3), 248-255.

Carpenter, J.M., Brown, K.A., Diaz, A.N., Dockman, R.L., Benbow, R.A., Harn, D.A., Norberg, T., Wagner, J.J., Filipov, N.M., 2021. Delayed treatment with the immunotherapeutic LNFPIII ameliorates multiple neurological deficits in a pesticide-nerve agent prophylactic mouse model of Gulf War Illness. Neurotoxicol Teratol 87, 107012.

Carpenter, J.M., Gordon, H.E., Ludwig, H.D., Wagner, J.J., Harn, D.A., Norberg, T., Filipov, N.M., 2020. Neurochemical and neuroinflammatory perturbations in two Gulf War Illness models: Modulation by the immunotherapeutic LNFPIII. NeuroToxicology 77, 40-50.

Carreras, I., Aytan, N., Mellott, T., Choi, J.K., Lehar, M., Crabtree, L., Leite-Morris, K., Jenkins, B.G., Blusztajn, J.K., Dedeoglu, A., 2018. Anxiety, neuroinflammation, cholinergic and GABAergic abnormalities are early markers of Gulf War illness in a mouse model of the disease. Brain Res 1681, 34-43.

Chao, L.L., 2020. The Prevalence of Mild Cognitive Impairment in a Convenience Sample of 202 Gulf War Veterans. International Journal of Environmental Research and Public Health 17(19), 7158.

Chao, L.L., Abadjian, L., Hlavin, J., Meyerhoff, D.J., Weiner, M.W., 2011. Effects of low-level sarin and cyclosarin exposure and Gulf War Illness on Brain Structure and Function: A study at 4T. NeuroToxicology 32(6), 814-822.

Chao, L.L., Kanady, J.C., Crocker, N., Straus, L.D., Hlavin, J., Metzler, T.J., Maguen, S., Neylan, T.C., 2021. Cognitive behavioral therapy for insomnia in veterans with gulf war illness: Results from a randomized controlled trial. Life Sciences 279, 119147.

Chao, L.L., Reeb, R., Esparza, I.L., Abadjian, L.R., 2016. Associations between the self-reported frequency of hearing chemical alarms in theater and regional brain volume in Gulf War Veterans. Neurotoxicology 53, 246-256.

Chao, L.L., Rothlind, J.C., Cardenas, V.A., Meyerhoff, D.J., Weiner, M.W., 2010. Effects of low-level exposure to sarin and cyclosarin during the 1991 Gulf War on brain function and brain structure in US veterans. Neurotoxicology 31(5), 493-501.

Chao, L.L., Zhang, Y., Buckley, S., 2015. Effects of low-level sarin and cyclosarin exposure on white matter integrity in Gulf War Veterans. NeuroToxicology 48, 239-248.

Christova, P., James, L.M., Engdahl, B.E., Lewis, S.M., Carpenter, A.F., Georgopoulos, A.P., 2017. Subcortical brain atrophy in Gulf War Illness. Exp Brain Res 235(9), 2777-2786.

Clark, J.K., Furgerson, M., Crystal, J.D., Fechheimer, M., Furukawa, R., Wagner, J.J., 2015. Alterations in synaptic plasticity coincide with deficits in spatial working memory in presymptomatic 3xTg-AD mice. Neurobiology of Learning and Memory 125, 152-162.

Conrad, K.L., Louderback, K.M., Gessner, C.P., Winder, D.G., 2011. Stress-induced alterations in anxiety-like behavior and adaptations in plasticity in the bed nucleus of the stria terminalis. Physiology & Behavior 104(2), 248-256.

Deacon, R., 2012. Assessing burrowing, nest construction, and hoarding in mice. J Vis Exp(59), e2607.

Dickey, B., Madhu, L.N., Shetty, A.K., 2021. Gulf War Illness: Mechanisms Underlying Brain Dysfunction and Promising Therapeutic Strategies. Pharmacology & Therapeutics 220, 107716.

Donovan, E.K., Kekes-Szabo, S., Lin, J.C., Massey, R.L., Cobb, J.D., Hodgin, K.S., Ness, T.J., Hangee-Bauer, C., Younger, J.W., 2021. A Placebo-Controlled, Pseudo-Randomized, Crossover Trial of Botanical Agents for Gulf War Illness: Curcumin (Curcuma longa), Boswellia (Boswellia serrata), and French Maritime Pine Bark (Pinus pinaster). International Journal of Environmental Research and Public Health 18(5), 2468.

Donta, S.T., Clauw, D.J., Engel, J., Charles C., Guarino, P., Peduzzi, P., Williams, D.A., Skinner, J.S., Barkhuizen, A., Taylor, T., Kazis, L.E., Sogg, S., Hunt, S.C., Dougherty, C.M., Richardson, R.D., Kunkel, C., Rodriguez, W., Alicea, E., Chiliade, P., Ryan, M., Gray, G.C., Lutwick, L., Norwood, D., Smith, S., Everson, M., Blackburn, W., Martin, W., Griffiss, J.M., Cooper, R., Renner, E., Schmitt, J., McMurtry, C., Thakore, M., Mori, D., Kerns, R., Park, M., Pullman-Mooar, S., Bernstein, J., Hershberger, P., Salisbury, D.C., Feussner, J.R., Group, f.t.V.C.S.S., 2003. Cognitive Behavioral Therapy and Aerobic Exercise for Gulf War Veterans' IllnessesA Randomized Controlled Trial. JAMA 289(11), 1396-1404.

Donta, S.T., Engel, C.C., Jr., Collins, J.F., Baseman, J.B., Dever, L.L., Taylor, T., Boardman, K.D., Kazis, L.E., Martin, S.E., Horney, R.A., Wiseman, A.L., Kernodle, D.S., Smith, R.P., Baltch, A.L., Handanos, C., Catto, B., Montalvo, L., Everson, M., Blackburn, W., Thakore, M., Brown, S.T., Lutwick, L., Norwood, D., Bernstein, J., Bacheller, C., Ribner, B., Church, L.W., Wilson, K.H., Guduru, P., Cooper, R., Lentino, J., Hamill, R.J., Gorin, A.B., Gordan, V., Wagner, D., Robinson, C., DeJace, P., Greenfield, R., Beck, L., Bittner, M., Schumacher, H.R., Silverblatt, F., Schmitt, J., Wong, E., Ryan, M.A., Figueroa, J., Nice, C., Feussner, J.R., Group, V.A.C., 2004. Benefits and harms of doxycycline treatment for Gulf

War veterans' illnesses: a randomized, double-blind, placebo-controlled trial. Ann Intern Med 141(2), 85-94.

Eagle, A.L., Mazei-Robison, M., Robison, A.J., 2016. Sucrose Preference Test to Measure Stress-induced Anhedonia. Bio-protocol 6(11), e1822.

Fleming, S.M., Ekhator, O.R., Ghisays, V., 2013. Assessment of sensorimotor function in mouse models of Parkinson's disease. Journal of visualized experiments : JoVE(76), 50303.

Furgerson, M., Clark, J.K., Crystal, J.D., Wagner, J.J., Fechheimer, M., Furukawa, R., 2014. Hirano body expression impairs spatial working memory in a novel mouse model. Acta Neuropathologica Communications 2(1), 131.

Goldstein, G., Beers, S.R., Morrow, L.A., Shemansky, W.J., Steinhauer, S.R., 1996. A preliminary neuropsychological study of Persian Gulf veterans. Journal of the International Neuropsychological Society 2(4), 368-371.

Golier, J.A., Caramanica, K., Michaelides, A.C., Makotkine, I., Schmeidler, J., Harvey, P.D., Yehuda, R., 2016. A randomized, double-blind, placebo-controlled, crossover trial of mifepristone in Gulf War veterans with chronic multisymptom illness. Psychoneuroendocrinology 64, 22-30.

Golomb, B.A., Allison, M., Koperski, S., Koslik, H.J., Devaraj, S., Ritchie, J.B., 2014. Coenzyme Q10 benefits symptoms in Gulf War veterans: results of a randomized double-blind study. Neural Comput 26(11), 2594-2651.

Gopinath, K., Gandhi, P., Goyal, A., Jiang, L., Fang, Y., Ouyang, L., Ganji, S., Buhner, D., Ringe, W., Spence, J., Biggs, M., Briggs, R., Haley, R., 2012. FMRI reveals abnormal central processing of sensory and pain stimuli in ill Gulf War veterans. Neurotoxicology 33(3), 261-271.

Habbas, S., Santello, M., Becker, D., Stubbe, H., Zappia, G., Liaudet, N., Klaus, F.R., Kollias, G., Fontana, A., Pryce, C.R., 2015. Neuroinflammatory TNFα impairs memory via astrocyte signaling. Cell 163(7), 1730-1741.

Hattiangady, B., Mishra, V., Kodali, M., Shuai, B., Rao, X., Shetty, A.K., 2014. Object location and object recognition memory impairments, motivation deficits and depression in a model of Gulf War illness. Front Behav Neurosci 8, 78.

Helmer, D.A., Van Doren, W.W., Litke, D.R., Tseng, C.L., Ho, L., Osinubi, O., Pasinetti, G.M., 2020. Safety, Tolerability and Efficacy of Dietary Supplementation with Concord Grape Juice in Gulf War Veterans with Gulf War Illness: A Phase I/IIA, Randomized, Double-Blind, Placebo-Controlled Trial. Int J Environ Res Public Health 17(10).

Hofele, K., Sedelis, M., Auburger, G.W., Morgan, S., Huston, J.P., Schwarting, R.K.W., 2001. Evidence for a Dissociation between MPTP Toxicity and Tyrosinase Activity Based on Congenic Mouse Strain Susceptibility. Experimental Neurology 168(1), 116-122.

Holodniy, M., Kaiser, J.D., 2019. Treatment for Gulf War Illness (GWI) with KPAX002 (methylphenidate hydrochloride + GWI nutrient formula) in subjects meeting the Kansas case definition: A prospective, open-label trial. Journal of Psychiatric Research 118, 14-20.

Holton, K.F., Kirkland, A.E., Baron, M., Ramachandra, S.S., Langan, M.T., Brandley, E.T., Baraniuk, J.N., 2020. The Low Glutamate Diet Effectively Improves Pain and Other Symptoms of Gulf War Illness. Int J Environ Res Public Health 12(9), 2593.

Holton, K.F., Ramachandra, S.S., Murray, S.L., Baron, M., Baraniuk, J.N., 2021. Effect of the low glutamate diet on inflammatory cytokines in veterans with Gulf War Illness (GWI): A pilot study. Life Sciences 280, 119637.

Hom, J., Haley, R.W., Kurt, T.L., 1997. Neuropsychological correlates of Gulf War syndrome. Archives of Clinical Neuropsychology 12(6), 531-544.

Hubbard, N.A., Hutchison, J.L., Motes, M.A., Shokri-Kojori, E., Bennett, I.J., Brigante, R.M., Haley, R.W., Rypma, B., 2014. Central Executive Dysfunction and Deferred Prefrontal Processing in Veterans with Gulf War Illness. Clin Psychol Sci 2(3), 319-327.

James, L.M., Christova, P., Engdahl, B.E., Lewis, S.M., Carpenter, A.F., Georgopoulos, A.P., 2017. Human Leukocyte Antigen (HLA) and Gulf War Illness (GWI): HLA-DRB1*13:02 Spares Subcortical Atrophy in Gulf War Veterans. EBioMedicine 26, 126-131.

Janulewicz, P.A., Krengel, M.H., Maule, A., White, R.F., Cirillo, J., Sisson, E., Heeren, T., Sullivan, K., 2017. Neuropsychological characteristics of Gulf War illness: A meta-analysis. PloS One 12(5), e0177121-e0177121.

Joshi, U., Evans, J.E., Joseph, R., Emmerich, T., Saltiel, N., Lungmus, C., Oberlin, S., Langlois, H., Ojo, J., Mouzon, B., 2018. Oleoylethanolamide treatment reduces neurobehavioral deficits and brain pathology in a mouse model of Gulf War Illness. Scientific reports 8(1), 12921.

Kearney, D.J., Simpson, T.L., Malte, C.A., Felleman, B., Martinez, M.E., Hunt, S.C., 2016. Mindfulness-based Stress Reduction in Addition to Usual Care Is Associated with Improvements in Pain, Fatigue, and Cognitive Failures Among Veterans with Gulf War Illness. Am J Med 129(2), 204-214.

Khaiboullina, S.F., DeMeirleir, K.L., Rawat, S., Berk, G.S., Gaynor-Berk, R.S., Mijatovic, T., Blatt, N., Rizvanov, A.A., Young, S.G., Lombardi, V.C., 2015. Cytokine expression provides clues to the pathophysiology of Gulf War illness and myalgic encephalomyelitis. Cytokine 72(1), 1-8.

Kodali, M., Hattiangady, B., Shetty, G., Bates, A., Shuai, B., Shetty, A., 2018. Curcumin treatment leads to better cognitive and mood function in a model of Gulf War Illness with enhanced neurogenesis, and alleviation of inflammation and

mitochondrial dysfunction in the hippocampus. Brain, Behavior, and Immunity 69, 499-514.

Lin, Z., Dodd, C.A., Filipov, N.M., 2013. Short-term atrazine exposure causes behavioral deficits and disrupts monoaminergic systems in male C57BL/6 mice. Neurotoxicol Teratol 39, 26-35.

Lindem, K., Proctor, S.P., Heeren, T., Krengel, M., Vasterling, J., Sutker, P.B., Wolfe, J., Keane, T.M., White, R.F., 2003. Neuropsychological Performance in Gulf War Era Veterans: Neuropsychological Symptom Reporting. Journal of Psychopathology & Behavioral Assessment 25(2), 121-127.

Madhu, L.N., Attaluri, S., Kodali, M., Shuai, B., Upadhya, R., Gitai, D., Shetty, A.K., 2019. Neuroinflammation in Gulf War Illness is linked with HMGB1 and complement activation, which can be discerned from brain-derived extracellular vesicles in the blood. Brain, Behavior, and Immunity 81, 430-443.

Mathersul, D.C., Eising, C.M., DeSouza, D.D., Spiegel, D., Bayley, P.J., 2020. Brain and Physiological Markers of Autonomic Function Are Associated With Treatment-Related Improvements in Self-Reported Autonomic Dysfunction in Veterans With Gulf War Illness: An Exploratory Pilot Study. Glob Adv Health Med 9, 2164956120922812.

Miller, A.H., 2009. Norman Cousins Lecture. Mechanisms of cytokine-induced behavioral changes: psychoneuroimmunology at the translational interface. Brain, behavior, and immunity 23(2), 149-158.

Minogue, A.M., Barrett, J.P., Lynch, M.A., 2012. LPS-induced release of IL-6 from glia modulates production of IL-1β in a JAK2-dependent manner. Journal of Neuroinflammation 9(1), 126.

Mote, R.S., Carpenter, J.M., Dockman, R.L., Steinberger, A.J., Suen, G., Norberg, T., Harn, D.A., Wagner, J.J., Filipov, N.M., 2020. Assessing the Beneficial Effects of

the Immunomodulatory Glycan LNFPIII on Gut Microbiota and Health in a Mouse Model of Gulf War Illness. Int J Environ Res Public Health 17(19), 7081.

O'Callaghan, J.P., Kelly, K.A., Locker, A.R., Miller, D.B., Lasley, S.M., 2015. Corticosterone primes the neuroinflammatory response to DFP in mice: potential animal model of Gulf War Illness. Journal of Neurochemistry 133(5), 708-721.

Parihar, V.K., Hattiangady, B., Shuai, B., Shetty, A.K., 2013. Mood and memory deficits in a model of Gulf War illness are linked with reduced neurogenesis, partial neuron loss, and mild inflammation in the hippocampus. Neuropsychopharmacology 38(12), 2348-2362.

Parkitny, L., Middleton, S., Baker, K., Younger, J., 2015. Evidence for abnormal cytokine expression in Gulf War Illness: A preliminary analysis of daily immune monitoring data. BMC Immunol 16, 57.

Phillips, K.F., Deshpande, L.S., 2016. Repeated low-dose organophosphate DFP exposure leads to the development of depression and cognitive impairment in a rat model of Gulf War Illness. NeuroToxicology 52, 127-133.

Preston, C.J., Brown, K.A., Wagner, J.J., 2019. Cocaine conditioning induces persisting changes in ventral hippocampus synaptic transmission, long-term potentiation, and radial arm maze performance in the mouse. Neuropharmacology 150, 27-37.

Proctor, S.P., Heaton, K.J., Heeren, T., White, R.F., 2006. Effects of sarin and cyclosarin exposure during the 1991 Gulf War on neurobehavioral functioning in US army veterans. NeuroToxicology 27(6), 931-939.

Proctor, S.P., Heeren, T., White, R.F., Wolfe, J., Borgos, M.S., Davis, J.D., Pepper, L., Clapp, R., Sutker, P.B., Vasterling, J.J., Oznoff, D., 1998. Health status of Persian Gulf War veterans: self-reported symptoms, environmental exposures and the effect of stress. International Journal of Epidemiology 27(6), 1000-1010.

Ribeiro, A.C., Zhu, J., Kronfol, M.M., Jahr, F.M., Younis, R.M., Hawkins, E., McClay, J.L., Deshpande, L.S., 2020. Molecular mechanisms for the antidepressant-like effects of a low-dose ketamine treatment in a DFP-based rat model for Gulf War Illness. NeuroToxicology.

Ribeiro, A.C.R., Deshpande, L.S., 2021. A review of pre-clinical models for Gulf War Illness. Pharmacology & Therapeutics 228, 107936.

Shetty, A.K., Attaluri, S., Kodali, M., Shuai, B., Shetty, G.A., Upadhya, D., Hattiangady, B., Madhu, L.N., Upadhya, R., Bates, A., 2020. Monosodium luminol reinstates redox homeostasis, improves cognition, mood and neurogenesis, and alleviates neuro-and systemic inflammation in a model of Gulf War Illness. Redox Biology 28, 101389.

Sillanpaa, M.C., Agar, L.M., Milner, I.B., Podany, E.C., Axelrod, B.N., Brown, G.G., 1997. Gulf War veterans: a neuropsychological examination. J Clin Exp Neuropsychol 19(2), 211-219.

Srivastava, L., Tundup, S., Choi, B.S., Norberg, T., Harn, D., 2014. Immunomodulatory glycan lacto-N-fucopentaose III requires clathrin-mediated endocytosis to induce alternative activation of antigen-presenting cells. Infect Immun 82(5), 1891-1903.

Sullivan, K., Krengel, M., Bradford, W., Stone, C., Thompson, T.A., Heeren, T., White, R.F., 2018. Neuropsychological functioning in military pesticide applicators from the Gulf War: Effects on information processing speed, attention and visual memory. Neurotoxicology and Teratology 65, 1-13.

Toomey, R., Alpern, R., Vasterling, J.J., Baker, D.G., Reda, D.J., Lyons, M.J., Henderson, W.G., Kang, H.K., Eisen, S.A., Murphy, F.M., 2009. Neuropsychological functioning of U.S. Gulf War veterans 10 years after the war. J Int Neuropsychol Soc 15(5), 717-729.

Tundup, S., Srivastava, L., Norberg, T., Watford, W., Harn, D., 2015. A Neoglycoconjugate Containing the Human Milk Sugar LNFPIII Drives Anti-

Inflammatory Activation of Antigen Presenting Cells in a CD14 Dependent Pathway. PLoS One 10(9), e0137495.

Van Riper, S.M., Alexander, A.L., Koltyn, K.F., Stegner, A.J., Ellingson, L.D., Destiche, D.J., Dougherty, R.J., Lindheimer, J.B., Cook, D.B., 2017. Cerebral white matter structure is disrupted in Gulf War Veterans with chronic musculoskeletal pain. PAIN 158(12).

Washington, S.D., Rayhan, R.U., Garner, R., Provenzano, D., Zajur, K., Addiego, F.M., VanMeter, J.W., Baraniuk, J.N., 2020. Exercise alters cerebellar and cortical activity related to working memory in phenotypes of Gulf War Illness. Brain Communications 2(1).

White, R.F., Steele, L., O'Callaghan, J.P., Sullivan, K., Binns, J.H., Golomb, B.A., Bloom, F.E., Bunker, J.A., Crawford, F., Graves, J.C., Hardie, A., Klimas, N., Knox, M., Meggs, W.J., Melling, J., Philbert, M.A., Grashow, R., 2016. Recent research on Gulf War illness and other health problems in veterans of the 1991 Gulf War: Effects of toxicant exposures during deployment. Cortex 74, 449-475.

Wylie, G.R., Genova, H., Dobryakova, E., DeLuca, J., Chiaravalloti, N., Falvo, M., Cook, D., 2019. Fatigue in Gulf War Illness is associated with tonically high activation in the executive control network. Neuroimage Clin 21, 101641-101641.

Yang, Y., Wang, H., Kouadir, M., Song, H., Shi, F., 2019. Recent advances in the mechanisms of NLRP3 inflammasome activation and its inhibitors. Cell Death & Disease 10(2), 128.

Zhang, Y., Avery, T., Vakhtin, A.A., Mathersul, D.C., Tranvinh, E., Wintermark, M., Massaband, P., Ashford, J.W., Bayley, P.J., Furst, A.J., 2020. Brainstem atrophy in Gulf War Illness. NeuroToxicology 78, 71-79.

Zhang, Y., Vakhtin, A.A., Dietch, J., Jennings, J.S., Yesavage, J.A., Clark, J.D., Bayley, P.J., Ashford, J.W., Furst, A.J., 2021. Brainstem damage is associated with poorer

sleep quality and increased pain in gulf war illness veterans. Life Sciences 280, 119724.

Zhu, B., Trikudanathan, S., Zozulya, A.L., Sandoval-Garcia, C., Kennedy, J.K., Atochina, O., Norberg, T., Castagner, B., Seeberger, P., Fabry, Z., Harn, D., Khoury, S.J., Guleria, I., 2012. Immune modulation by Lacto-N-fucopentaose III in experimental autoimmune encephalomyelitis. Clin Immunol 142(3), 351-361.

Zhu, J., Hawkins, E., Phillips, K., Deshpande, L.S., 2020. Assessment of Ketamine and its Enantiomers in an Organophosphate-Based Rat Model for Features of Gulf War Illness. International Journal of Environmental Research and Public Health 17(13), 4710.

Zundel, C.G., Krengel, M.H., Heeren, T., Yee, M.K., Grasso, C.M., Janulewicz Lloyd, P.A., Coughlin, S.S., Sullivan, K., 2019. Rates of Chronic Medical Conditions in 1991 Gulf War Veterans Compared to the General Population. Int J Environ Res Public Health 16(6).

Figures

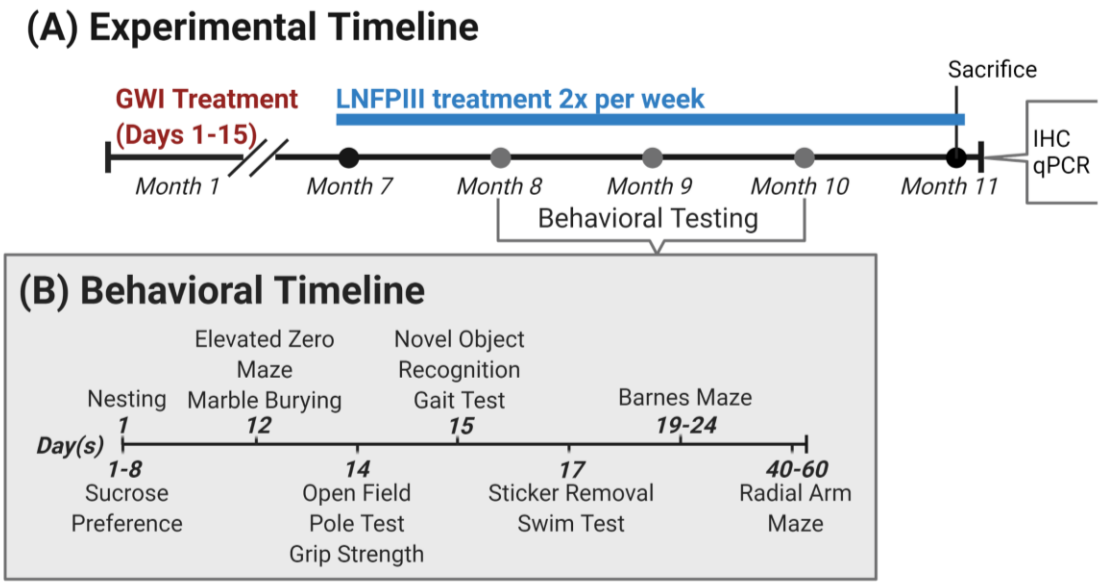

Figure 5.1. Experimental and behavioral timelines. (A) depicts the experimental timeline in which mice received GWI related chemicals: pyridostigmine bromide (PB) and DEET (days 1-14 s.c.), corticosterone (days 8-14), and diisopropylfluorophosphate (DFP, day 15). Lacto-N-fucopentaose III (LNFPIII) treatment began 7 months after GWI exposure. (B) is a detailed timeline of behavioral tests that were performed during months 8-10.

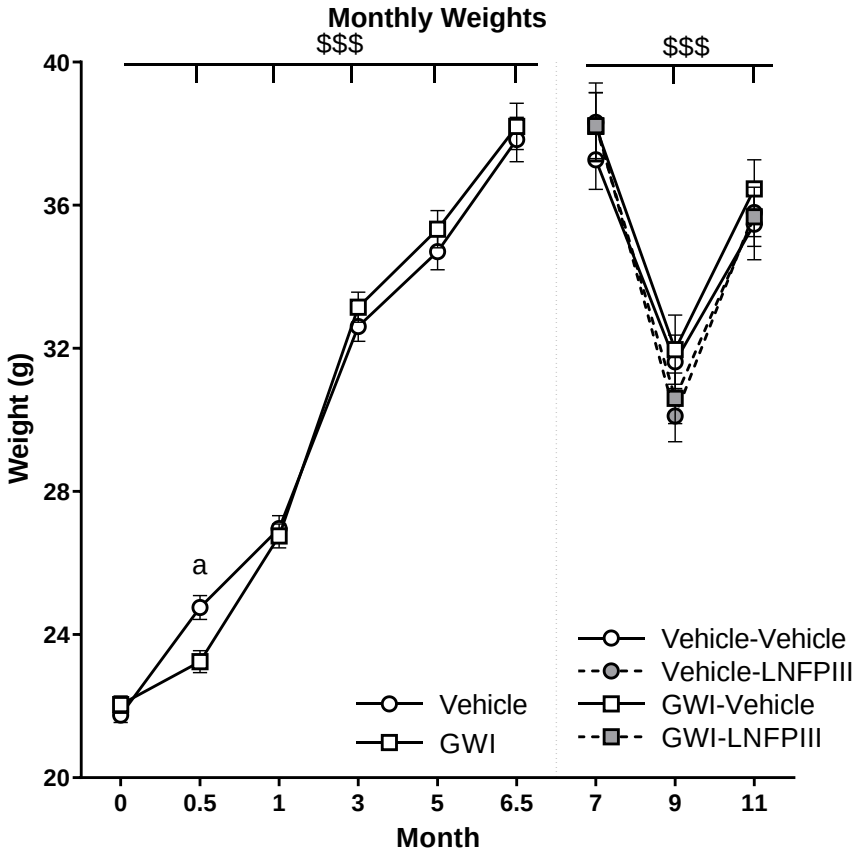

Figure 5.2. Monthly Weights. Monthly weights were monitored and are presented for the start of study (0), post PB/PM treatment (0.5), start of LNFPIII treatment (6.5), prior to Radial Arm Maze (RAM) food restriction (7), during RAM food restriction (9), and sacrifice (11).

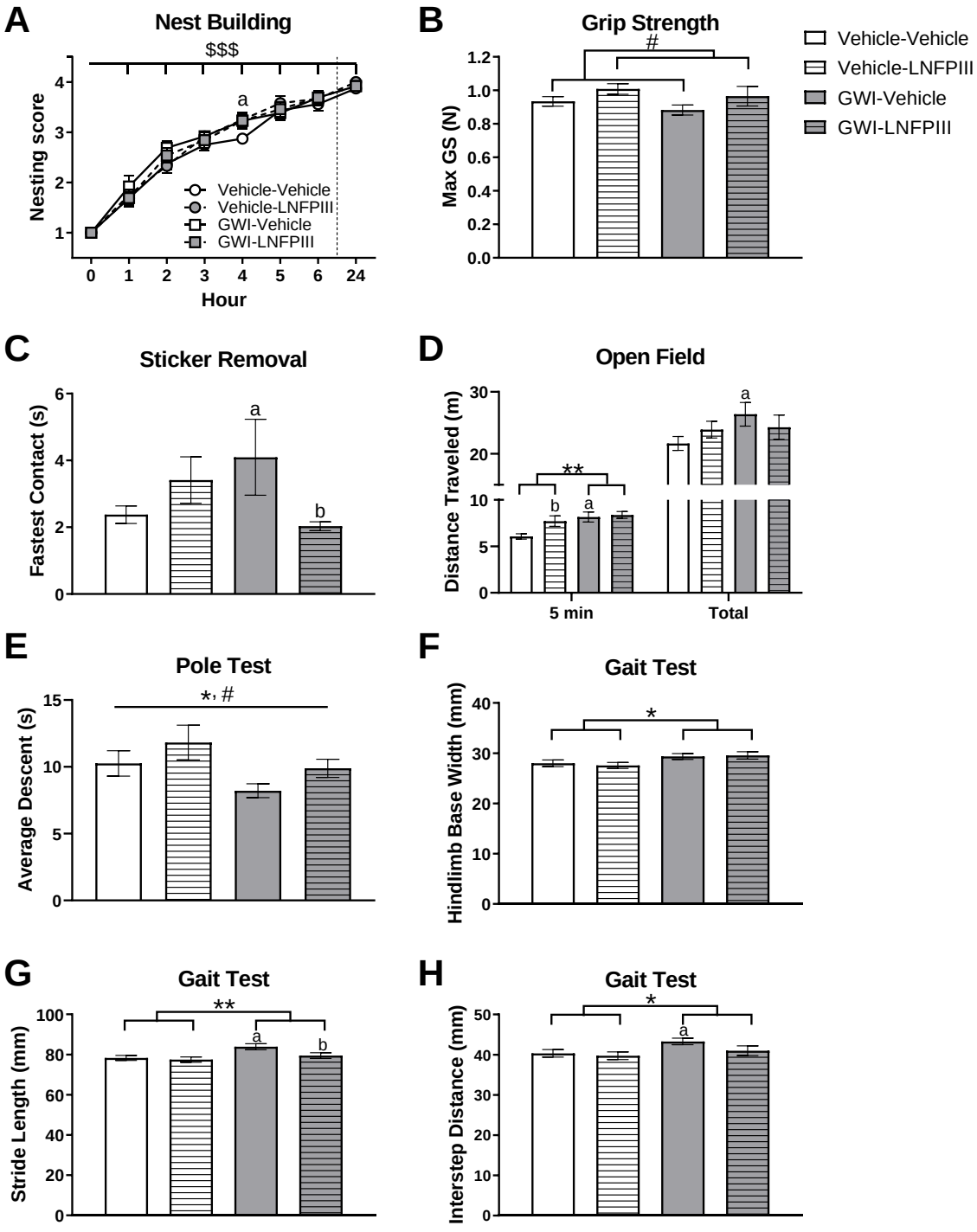
A
Nest Building
$$$
a
Nesting score
Hour
Vehicle-Vehicle
Vehicle-LNFPIII
GWI-Vehicle
GWI-LNFPIII
B
Grip Strength
#
Max GS (N)
C
Sticker Removal
Fastest Contact (s)
D
Open Field
**
Distance Traveled (m)
5 min
Total
E
Pole Test
*, #
Average Descent (s)
F
Gait Test
*
Hindlimb Base Width (mm)
G
Gait Test
**
Stride Length (mm)
H
Gait Test
*
Interstep Distance (mm)

Figure 5.3. Long term motor effects of prior GWI exposure and delayed LNFPIII treatment. Several motor effect of prior GWI exposure and LNFPIII treatment were evaluated by nest building (A); grip strength (B); sticker contact (C) in the sticker removal test; distance travelled (D) in the open field; descent time € in the pole test; and hindlimb base width (F), stride length (G), and interstep distance (H) in the gait test. Data are presented as mean ± SEM (n = 12-16/group).* and ** indicate significant main effect of GWI treatment, $p < 0.05$ and 0.01, respectively. $^{\$\$\$}$ indicates significant main effect of time, $p < 0.001$. $^{\#}$ indicates significant main effect of LNFPIII treatment, $p < 0.05$. ^{a} and ^{b} indicate $p < 0.05$ from Vehicle-Vehicle and GWI-Vehicle, respectively.

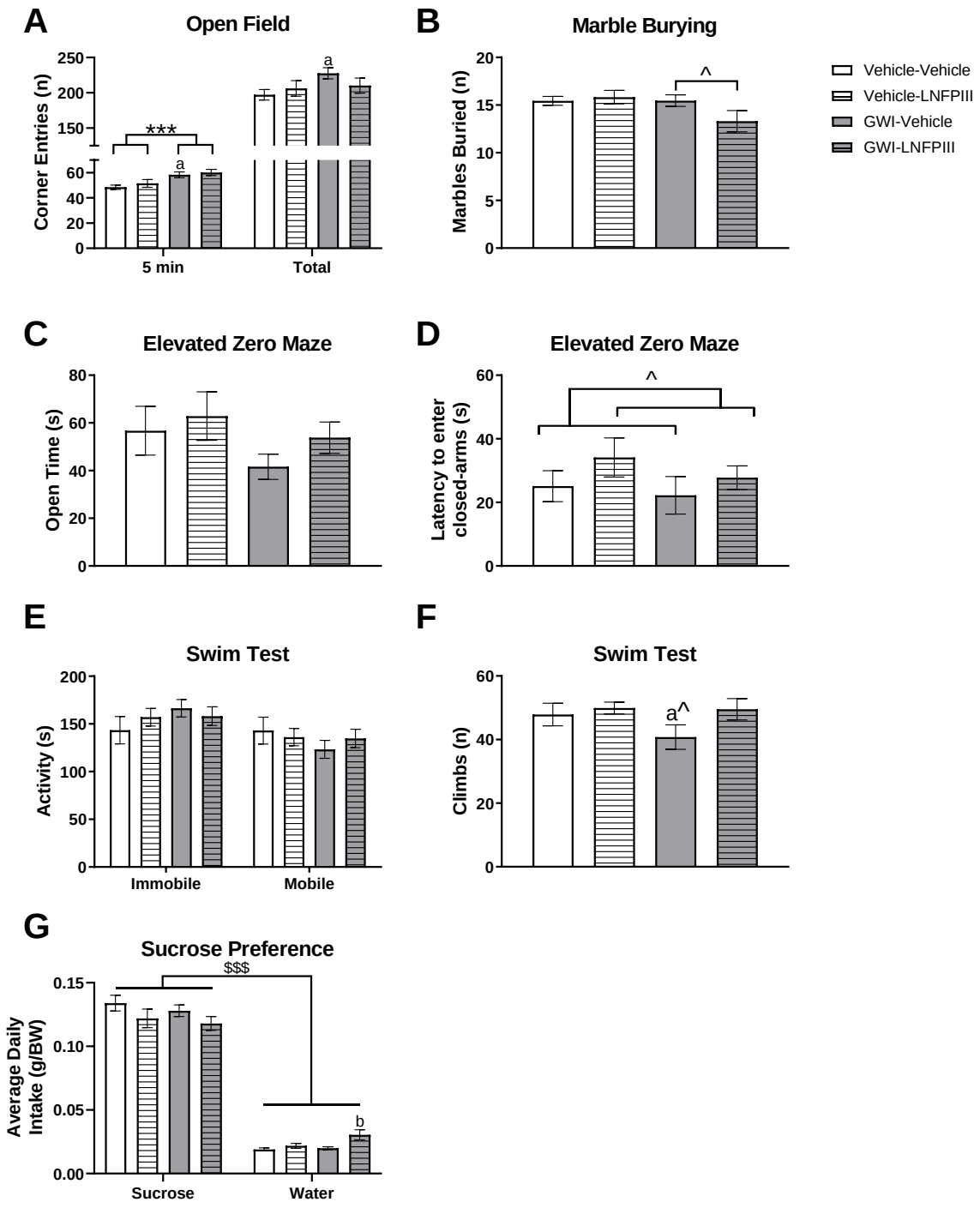
A
Open Field
Corner Entries (n)
250
200
150
60
40
20
0
***
a
a
5 min
Total
B
Marble Burying
Marbles Buried (n)
20
15
10
5
0
^
Vehicle-Vehicle
Vehicle-LNFPIII
GWI-Vehicle
GWI-LNFPIII
C
Elevated Zero Maze
Open Time (s)
80
60
40
20
0
D
Elevated Zero Maze
Latency to enter closed-arms (s)
60
40
20
0
^
E
Swim Test
Activity (s)
200
150
100
50
0
Immobile
Mobile
F
Swim Test
Climbs (n)
60
40
20
0
a^
G
Sucrose Preference
Average Daily Intake (g/BW)
0.15
0.10
0.05
0.00
$$$
b
Sucrose
Water

Figure 5.4. Long term mood effects of prior GWI exposure and delayed LNFPIII treatment. Mood disturbances of prior GWI exposure and LNFPIII treatment were evaluated by several tests for anxiety-like and depressive-like behaviors: corner entries (A) in the open field; number of marbles buried (B) in the marble burying test; open arm time (C) and latency to enter closed-arm (D) in the elevated zero maze; immobile and mobile time (E) and climbing attempts (F) in the swim test; average daily intake (G) in the sucrose preference test. Data are presented as mean ± SEM (n = 12-16/group).*** indicates significant main effect of treatment, $p < 0.001$. $^{\$\$\$}$ indicates significant main effect of drink in the SP test, $p < 0.001$. $^{\wedge}$ indicates $p < 0.10$. ^{a} and $^{a\wedge}$ indicate $p < 0.05$ or 0.10, respectively, from Vehicle-Vehicle. ^{b} indicates $p < 0.05$ from GWI-Vehicle.

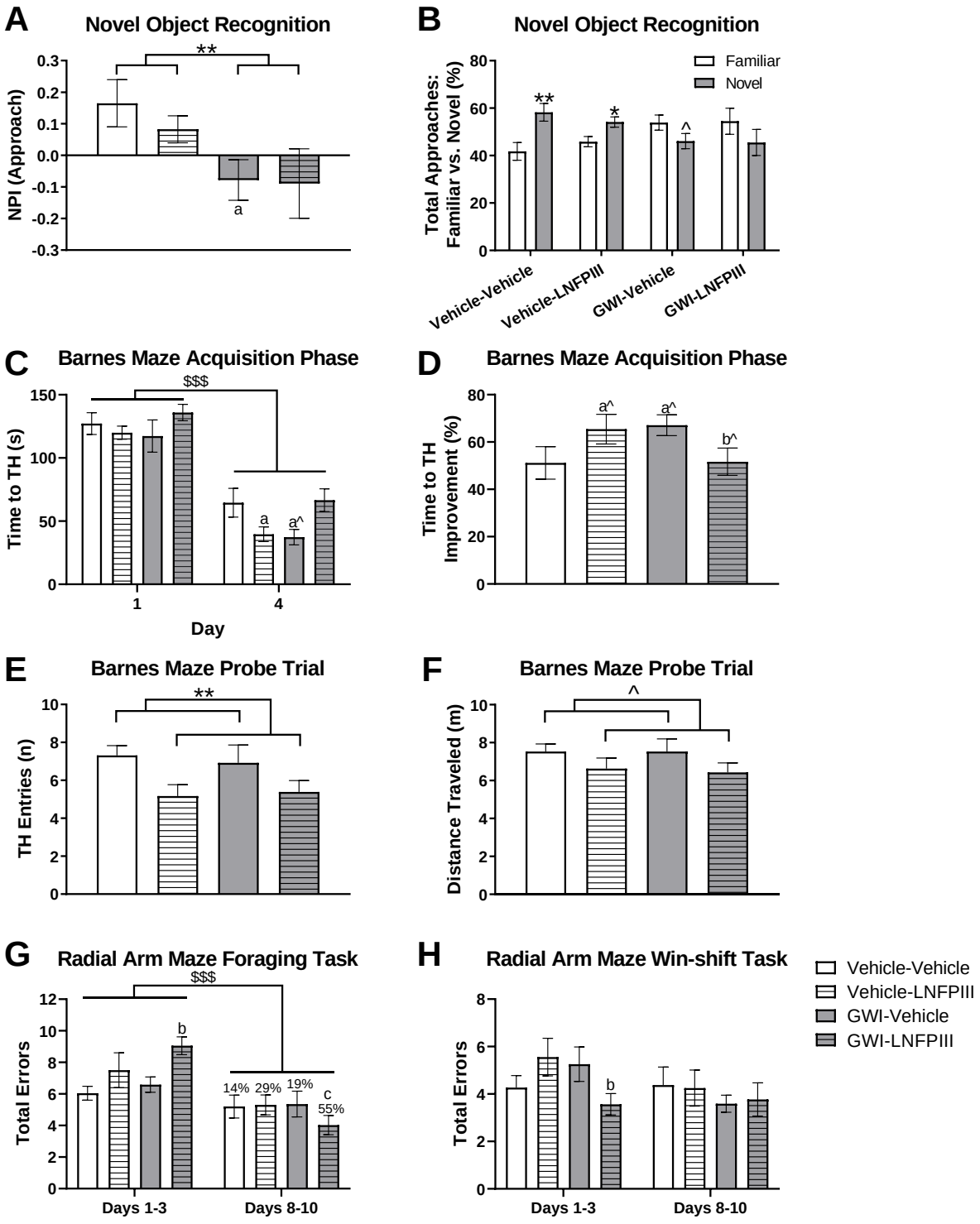
A
Novel Object Recognition
NPI (Approach)
**
a
B
Novel Object Recognition
Familiar
Novel
Total Approaches: Familiar vs. Novel (%)
**
*
^
Vehicle-Vehicle
Vehicle-LNFPIII
GWI-Vehicle
GWI-LNFPIII
C
Barnes Maze Acquisition Phase
Time to TH (s)
$$$
a
a^
Day
D
Barnes Maze Acquisition Phase
Time to TH Improvement (%)
a^
a^
b^
E
Barnes Maze Probe Trial
TH Entries (n)
**
F
Barnes Maze Probe Trial
Distance Traveled (m)
^
G
Radial Arm Maze Foraging Task
Total Errors
$$$
b
14%
29%
19%
c
55%
Days 1-3
Days 8-10
H
Radial Arm Maze Win-shift Task
Total Errors
b
Days 1-3
Days 8-10
Vehicle-Vehicle
Vehicle-LNFPIII
GWI-Vehicle
GWI-LNFPIII

Figure 5.5. Long term cognition and memory effects of prior GWI exposure and delayed LNFPIII treatment. Cognition and memory were evaluated by several tests: novel preference index (NPI) (A) and total approaches % (B) in the novel object recognition test; time to target hole (TH) (C) and time to TH improvement from days 1 to 4 (D) in the Barnes Maze; probe trial TH entries (E) and distance traveled (F) in the Barnes Mazes; and total errors in the Radial Arm Maze foraging task (G) and Win-shift task (H). Data are presented as mean ± SEM (n = 12-16/group).* and ** indicates significance, $p < 0.05$ and 0.01, respectively. $^{\$\$\$}$ indicates significant main effect of drink in the SP test, $p < 0.001$. $^{\wedge}$ indicates $p < 0.10$. ^{a} and $^{a\wedge}$ indicate $p < 0.05$ or 0.10, respectively, from Vehicle-Vehicle. ^{b} and $^{b\wedge}$ indicate $p < 0.05$ and 0.10, respectively, from GWI-Vehicle. ^{c} indicates $p < 0.05$ from days 1-3 in the radial arm maze.

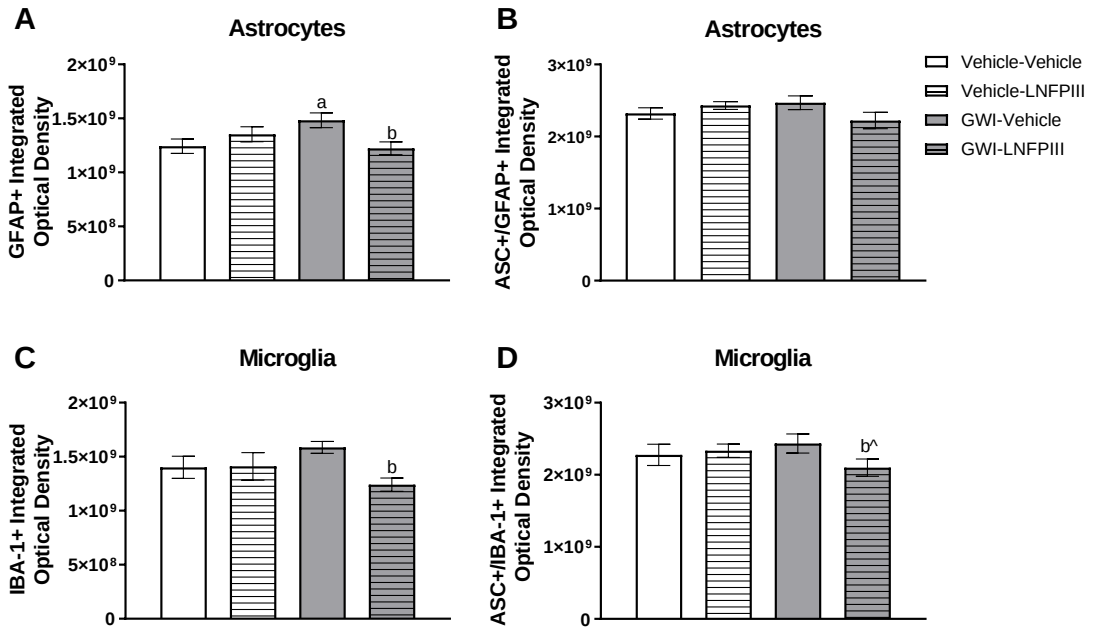

Figure 5.6. GFAP and IBA-1 immunoreactivity in the hilus region of the hippocampus 11 months post-GWI exposure and delayed LNFPIII treatment. Immunoreactivity of (A) GFAP+ and (B) GFAP+/ASC+ astrocytes and (C) IBA-1+ and (D) ASC+/IBA-1+ microglia were analyzed in ImageJ. Data are presented as mean ± SEM. [a] and [b] indicate $p \leq 0.05$ from Vehicle-Vehicle vs GWI-Vehicle and GWI-Vehicle vs GWI-LNFPIII, respectively. [b^] indicates $p \leq 0.10$ from GWI-Vehicle vs GWI-LNFPIII.

Table 1. Hippocampal IL-10										
	Vehicle-LNFPIII			GWI-Vehicle			GWI-LNFPIII			GWI-Vehicle vs GWI-LNFPIII
Region	fold change	se	p value	fold change	se	p value	fold change	se	p value	p value
Dorsal	0.95	0.43	0.89	1.15	0.73	0.74	1.04	0.26	0.90	0.83
Ventral	1.41	0.38	0.48	1.11	0.34	0.84	**3.41**	**4.15**	**0.03***	0.08 ^

Table 5.1. Hippocampal mRNA levels of IL-10 11 months post-GWI exposure and delayed LNFPIII treatment. The effect of GWI exposure and delayed LNFPIII treatment on the expression of anti-inflammatory IL-10 in the dorsal and ventral hippocampus measured by qPCR. Hippocampal samples from mice (n=4-6/treatment) were used for RNA isolation and subsequent qPCR analyses. Data were analyzed by the $2^{-\Delta\Delta Ct}$ method with 18S as the housekeeping gene and are expressed as a mean fold change from the Vehicle-Vehicle group ± SE. * indicates significant fold change from Vehicle-Vehicle, $p < 0.05$, and values are bolded. ^ indicates $p < 0.10$.

Supplemental Files

Supplemental Table 5.1. qPCR Primers

Gene		**Sequence 5' -> 3'**
18S	**Forward**	GGGAGCCTGAGAAACGGC
	Reverse	GGGTCGGGAGTGGGTAATTT
IL-10	**Forward**	ATAACTGCACCCACTTCCCA
	Reverse	GGGCATCACTTCTACCAGGT

CHAPTER 6

LONGITUDINAL ASSESSMENT OF STRUCTURAL BRAIN ALTERATIONS POST-GULF WAR RELATED CHEMICAL EXPOSURES IN TWO MOUSE MODELS OF GULF WAR ILLNESS

Jessica M. Carpenter, Sarah Nguyen, Ellie B. Decker Ramirez, Nikolay M. Filipov
To be submitted to Neurotoxicology

Abstract

Gulf War Illness (GWI) affects nearly 30% of the 1990-1991 Gulf War (GW) veterans and is a multi-symptom illness, with many of the symptoms of neurological nature attributed to in-theatre wartime chemical overexposures. Imaging studies have revealed structural and functional neurological alterations in veterans with GWI, including reduced volumes of multiple brain areas, connectivity, and signaling that correlate to poor performance in cognitive and motor tasks. GWI symptomology has been recapitulated in rodent models as behavioral, neurochemical, and neuroinflammatory aberrations; however, structural imaging studies remain limited. Thus, this study aimed to characterize the progression of brain structural alterations over the course of 12 months following two distinct, GWI chemical exposure paradigms. In the PB/PM model, male C57BL/6J mice (8-9 weeks) received daily exposure to the nerve agent prophylactic pyridostigmine bromide (PB) and pyrethroid insecticide permethrin (PM) for 10 days. In the PB/DEET/CORT/DFP model, mice received daily exposure to PB and the insect repellent DEET (days 1-14) and corticosterone (CORT; days 7-14). On day 15, mice received a single injection of the sarin surrogate diisopropylfluorophosphate (DFP). Using a Varian 7T Bore MRI System, structural (sagittal T2-weighted) scans were performed at 3, 6, 9, and 12 months post GWI exposures. Regions of interest (ROIs) including total brain, ventricles, cortex, hippocampus, cerebellum, and brainstem were delineated in the open source Aedes Toolbox in MATLAB, followed by volumetric analysis in ImageJ. The results of this study provide comparative similarities and distinctions between these two GWI exposure paradigms and aid in the understanding of GWI pathogenesis. Major similarities among the models include ventricular enlargement, alterations in cerebellar volumes, and

reductions in global brain and hippocampal volumes over time. Key differences were model specific, in which the PB/DEET/CORT/DFP model led to earlier reductions of total brain volume and to reduced brainstem volumes, while the PB/PM model produced cortical decreases over time. These effects align with previously observed behavioral deficits in these models such as reduced cognitive and motor performance. Overall, the effects seen here add translational validity to these two GWI models and their utility for evaluation of future GWI therapeutic interventions in a heterogeneous GWI chemical exposure context..

Keywords: Gulf War Illness, Magnetic Resonance Imaging (MRI), Pyridostigmine Bromide, Permethrin, DEET, Diisopropylfluorophosphate, corticosterone, longitudinal

1. Introduction

Gulf War Illness (GWI), a persisting multi-symptom illness predominantly affecting the nervous and immune systems, presents in about a third of the veterans from the 1990-1991 Gulf War (White et al., 2016). Major symptoms include fatigue, aberrations in cognition/memory, reduced motor function, and mood disturbances. Precise etiology of GWI is still unknown but is largely attributed to war-time chemical overexposures including to insecticides/repellents (permethrin [PM], chlorpyrifos, DEET), nerve agents (sarin/cyclosarin), and a nerve agent prophylactic (pyridostigmine bromide; PB). Further, due to the developing understanding and heterogenous nature of GWI, cure-all treatments do not exist; however, therapeutic interventions are being explored (White et al., 2016).

In a number of clinical imaging studies, the neuroanatomical correlates to the progressive, long-term aberrations in GWI symptomology have been evaluated. These structural magnetic resonance imaging (MRI) studies found GWI specific reductions in white and gray matter volume in multiple cortical and subcortical areas (hippocampus, hypothalamus, brainstem, cerebellum) in veterans (Chao, 2020; Chao et al., 2011; Chao et al., 2015; Christova et al., 2017; James et al., 2017; Rayhan et al., 2013; Van Riper et al., 2017; Zhang et al., 2020; Zhang et al., 2021). Functional MRI (fMRI) studies corroborated these structural abnormalities by detecting significant signal changes (activity) in regions governing cognitive, memory, motor and mood function such as the prefrontal, somatosensory, and motor cortices (Gopinath et al., 2012; Wylie et al., 2019), as well as the thalamus, caudate, and hippocampus (Calley et al., 2010; Cooper et al., 2016; Li et al., 2011). Additionally, an earlier clinical study detected neuronal loss in the basal ganglia with corresponding dopamine dysfunction (Haley et al., 2000). These structural and

functional abnormalities observed in these areas are consistent with reported symptomology by veterans and correlate strongly with performance deficits in working memory, attention, and motor tasks, as well as with mood impairments, pain, and sleep quality (Calley et al., 2010; Chao, 2020; Clarke et al., 2019; Hubbard et al., 2014; Washington et al., 2020; Zhang et al., 2021).

Many of the symptoms exhibited by GWI veterans have been recapitulated in GWI rodent models. Studies utilizing these models have demonstrated multiple aberrations in behavioral performance (i.e., cognition/memory, motor, and mood) and biological parameters (i.e., neuroinflammation) consistent with GWI veteran symptomology (Dickey et al., 2021; Macht et al., 2019; Megahed et al., 2014; Miller et al., 2018; O'Callaghan et al., 2015; Parihar et al., 2013; Ribeiro and Deshpande, 2021; Zakirova et al., 2016; Zakirova et al., 2015). To date, our group has explored the acute and long-term neurobiological and behavioral alterations (Brown et al., 2021a; Brown et al., 2021b; Carpenter et al., 2021; Carpenter et al., 2020) within two GWI models, one utilizing short-term PB and PM exposure (Zakirova et al., 2016; Zakirova et al., 2015) and another one employing PB, DEET, corticosterone (CORT), and diisopropylfluorophosphate (DFP) exposure (O'Callaghan et al., 2015). In these studies, we found acute monoaminergic disbalance in multiple brain regions associated with motor, memory, and mood function, as well as hippocampal neuroinflammation (Carpenter et al., 2020) and changes in hippocampal synaptic plasticity and transmission (Brown et al., 2021a; Brown et al., 2021b). Further, our long-term studies (6-10 months post GWI exposures) revealed multiple GWI-related behavioral deficits in motor function, cognition, and mood

(Carpenter et al., 2021) and alterations in hippocampal plasticity (Brown et al., 2021a; Carpenter et al., 2021).

While rodent GWI models produce GWI-like behavioral and pathological phenotypes, functional and structural imaging studies investigating the neuroanatomical changes in a GWI model context remain limited (Koo et al., 2018; Wu et al., 2021). This may be due to the complexity of conducting rodent imaging studies, especially studies involving repeated, within-subject imaging. Nevertheless, results from the few GWI available preclinical imaging studies provide highly translational and valuable insights into this chronic illness (Koo et al., 2018; Wu et al., 2021). In particular, high order diffusion MRI revealed distinct cortical and subcortical (hippocampus and hypothalamus) alterations that corresponded to neuroinflammation following exposure to the GWI relevant chemicals, DFP and CORT (Koo et al., 2018). Additionally, structurally significant increases in lateral ventricle volume and decreases in hippocampal and thalamic volumes were observed in another model (PB, PM, DEET, and restraint stress) 10 months post exposure that aligned with neurobehavioral impairments in cognition and mood function (Wu et al., 2021).

Due to the paucity of information surrounding GWI preclinical neuroanatomical changes and possible GWI exposure specific differences, the present study aimed to characterize the progression of brain structural alterations over the course of 12 months following two, distinct GWI chemical exposure paradigms. Here, we utilized the PB/PM (Zakirova et al., 2015) and PB/DEET/CORT/DFP (O'Callaghan et al., 2015) models to evaluate GWI neuroanatomical volume changes at 3, 6, 9 and 12 months post exposure in

multiple brain regions including the total brain, ventricles, cortex, hippocampus, cerebellum, and brainstem.

2. Methods

2.1 Materials

The following chemicals were used for animal treatments: pyridostigmine bromide (PB; Sigma Aldrich, St. Louis, MO), permethrin (PM; 29.5% cis/69.5% trans isomer; Chem Service Inc., West Chester, PA), diisopropylfluorophosphate (DFP; Sigma Aldrich), N-Diethyl-3-methylbenzamide (DEET; Sigma Aldrich), and corticosterone (CORT; Steraloids, Newport, RI). All additional chemicals and reagents used in this study, unless otherwise noted, were of analytical or higher grade and were obtained from Sigma Aldrich or Fisher Scientific (Hampton, NH).

2.2 Animals

Male C57BL/6J mice (8-9 weeks old; Jackson Laboratories, Bar Harbor, ME) were housed 4 per cage in an environmentally controlled room (22-24° C) and maintained on a 12 h light/dark cycle (0700-1900 lights on) throughout the study. Mice were handled daily for one week prior to the start of the study to minimize experimenter-induced stress. Food and water were available *ad libitum*. All procedures were approved in advance by the University of Georgia Institutional Animal Care and Use Committee and were in accordance with the latest National Institutes of Health guidelines.

Body weights were measured daily during GWI chemicals exposure and biweekly after the last GWI exposure until study completion. Study was terminated and mice were euthanized at 13.5 months post GWI chemicals exposure. At the time of euthanasia, body weight and length were measured to determine morphometric parameters including the

Body mass index (BMI; [Body weight (g)/length^2 (cm^2]) and the Lee index [body weight (g)/length(cm)] as in (Novelli et al., 2007). Brains were extracted, weighed, and split sagittally before one half was quickly frozen on dry ice and the other half was immersion fixed in 4% paraformaldehyde as in (Carpenter et al., 2021) for future analyses.

2.3 GWI Models

Two established, chemically different GWI treatment paradigms were utilized for this study. Following the Zakirova *et al.* 2015 model, mice were co-administering the nerve agent prophylactic pyridostigmine bromide (PB; 0.7 mg/kg body weight (BW); i.p.) and the pyrethroid insecticide permethrin (PM; 200 mg/kg BW; i.p.) or DMSO vehicle over 10 days. Following the O'Callaghan *et al.* 2015 model, mice received daily administration of PB (2 mg/kg BW; s.c.) and the insect repellent DEET (30 mg/kg BW; s.c.) or saline control for 14 days with concurrent stress (corticosterone (CORT): 200 mg/kg in 1.2% EtOH drinking water) exposure on days 8-14. On day 15, mice received a single dose of the nerve agent surrogate diisopropylfluorophosphate (DFP; 3.75 mg/kg BW; i.p.) or saline control. This resulted in 4 treatment groups (N=24, n=6/group/per model).

2.4 Structural Magnetic Resonance Imaging (MRI)

Structural brain images were acquired using a 7 Tesla magnet (Agilent, Santa Clara, CA), and MRI sequences were conducted on mice at 3 (PB/PM model only), 6, 9, and 12 months post GWI chemicals exposures (See experimental design, Figure 1). Prior to imaging, mice were anesthetized with isoflurane (3% for induction, 1.0-1.5% for maintenance) in a 30%:70% O_2:N_2 gas mixture with a flow rate 0.8–1.0 L/min. Respiratory rate was monitored using a small animal monitoring system (Small Animal Instruments, Inc., Stony Brook, NY) throughout the imaging period. Axial, two dimensional (2D) T1

weighted images were obtained using a spin echo sequence with the following acquisition parameters: TR 500 ms, TE 17 ms, 8 averages, data matrix 256 × 256, 17 slices, thickness 1.00 mm with no gap. Sagittal, 3D T2 weighted images were obtained using a fast spin echo sequence with the following parameters: TR 4000 ms, TE 33.38 ms, 2 averages, data matrix 256 x 256, 15 slices, thickness 1.00 mm with no gap.

2.5 Volume Measurements

Images were displayed and masked with the open source MATLAB toolbox AEDES using methods outlined in (Grant et al., 2020; Minkeviciene et al., 2019). Regions of interest (ROIs) including total brain, cortex, hippocampus, cerebellum, brainstem (medulla and pons), and ventricles (lateral, third, and fourth) were manually drawn according to the Allen Brain Atlas (https://mouse.brain-map.org/static/atlas). ROIs were saved individually as masks, and volumetric analysis was conducted on the masks by using the "Huang Dark Thresholding" method followed by the "Analyze Particles" method within ImageJ (Grant et al., 2020). Volume (mm^3) was calculated by multiplying the measured output with the calculated voxel volume. Refer to Figure 2 for representative masks.

2.6 Statistical Analysis

A two-way repeated analysis of variance (RM-ANOVA) was used to determine main effects of GWI treatment or treatment interactions within each model. If an ANOVA was significant ($p \leq 0.05$), treatment means were separated by Student-Newman-Keuls (SNK) *post hoc* test or pre-planned pairwise comparisons (Student's *t*-test, as appropriate). All data were analyzed using SigmaPlot 12.5 (San Jose, CA), and all graphs were generated using GraphPad Prism (San Diego, CA).

3. Results

3.1 Body Weights

Body weights were not different in either model at the beginning of the study (PB/PM model: control, 25.7 ± 0.76 vs PB/PM, 25.9 ± 0.62, $p > 0.89$; PB/DEET/CORT/DFP model: control 26.1 ± 0.77 vs PB/PM, 25.1 ± 0.70 $p > 0.38$). In both models, animal weights increased significantly over time (PB/PM model: $F(14,140) = 162.24$, $p \leq 0.001$, Figure 3A; PB/DEET/CORT/DFP model: $F(14,137) = 76.20$, $p \leq 0.001$, Figure 3C). In the PB/PM model, body weights were not significantly different between treatments throughout the study except for a numerical trend for greater weight in the control mice in this model at 12 months ($p = 0.10$, Figure 3A). A similar numerical trend for an increase was observed in the PB/DEET/CORT/DFP treated mice in the other GWI model ($p = 0.13$, Figure 3C). Further, there were no treatment differences for the calculated BMI or Lee index in the PB/PM model (p's > 0.33; Figure 3B). The Lee index was also unaffected by treatment ($p > 0.29$) in the PB/DEET/CORT/DFP GWI model. However, there was a trend for an increased BMI in the PB/DEET/CORT/DFP treated mice ($t(9) = 2.06$, $p = 0.07$, Figure 3D). Additionally, post-mortem brain weights did not differ in either model (p's > 0.43, data not shown).

3.2 Prior PB/DEET/CORT/DFP exposure, but not PB/PM exposure leads to global brain volume reduction

In the PB/PM model, there was a significant main effect of time ($F(3,30) = 3.25 \leq 0.05$, Figure 4A), in which both groups had decreased total brain volumes from 3 to 9 months ($p \leq 0.05$, Figure 4A), suggestive of age-related effects. In the PB/DEET/CORT/DFP model, there were significant changes in global brain volume for

treatment ($F(1,19) = 8.55$, $p \leq 0.05$, Figure 4B) and time ($F(2,19) = 7.22$, $p \leq 0.01$, Figure 4B). *Post hoc* analysis revealed that there were significant reductions in total brain volume for the PB/DEET/CORT/DFP group compared to control at the 6, 9, and 12-month time points (p's ≤ 0.05). Further within treatment, total brain volume was reduced significantly from 9 to 12 months in the PB/DEET/CORT/DFP ($p \leq 0.05$, Figure 4B) group; in the control mice, there was a trend for the age-related brain volume decrease ($p = 0.07$, Figure 4B). This suggests GWI-related early loss of brain volume that is accelerated by age.

3.3 Ventricular enlargement is present in the PB/PM model over time

Ventricular size (lateral and 3rd ventricles) was increased in the PB/PM ($F(3,30) = 9.82$, $p \leq 0.001$, Figure 5A) model over time. In the PB/PM model, this increase in ventricular size was present in both groups at 12 months compared to all other time points (p's ≤ 0.05, Figure 5A) and did not differ between treatments. There were no significant time or treatment differences in the PB/DEET/CORT/DFP model, except for a trend ($p = 0.052$, Figure 5B) at 6 months, in which the GWI group had smaller volumes; this effect was likely due to the treatment differences in overall brain volume.

Individual ventricles were delineated to further determine where the total ventricular volume increases originated. There was a significant increase in lateral ventricle size over time in the PB/PM model ($F(3,30) = 6.38$, $p \leq 0.01$, Table 1); here, the increase was significant at 12 months from all other time points for both groups (p's ≤ 0.05). This effect on lateral ventricle size was not observed in the PB/DEET/CORT/DFP model, however, there was a significant main effect of treatment ($F(1,19) = 5.61$, $p \leq 0.05$, Table 2) in which GWI mice had smaller lateral ventricles. Similar to the lateral ventricle results, there were significant increases in the 3rd ventricle over time in the PB/PM model (F(3,30)

= 3.57, $p \leq 0.05$, Table 1). In the PB/DEET/CORT/DFP model, there were no effects on 3rd ventricle volume (Table 2).

3.4 Cortical volume is decreased with time in the PB/PM model

Cortical volumes decreased over time in the PB/PM model ($F(3,30) = 4.35$, $p \leq 0.05$, Figure 6A) and this effect was independent of GWI and present at 6 and 12 months compared to 3 months ($p \leq 0.05$). In the PB/DEET/CORT/DFP model, cortical volumes were unaffected by age ($p > 0.64$). However, within 9 months, cortical volumes for the PB/DEET/CORT/DFP mice were significantly decreased compared to control ($t(10) = -2.20$, $p = 0.05$, Figure 6B); a similar, nonsignificant trend was observed at 12 months (Figure 6B).

3.5 Reductions in hippocampal volumes are present in both models over time

Reduced hippocampal volume was present over time in the PB/PM ($F(3,20) = 5.78$, $p \leq 0.01$, Figure 6C) and PB/DEET/CORT/DFP ($F(2,19) = 5.24$, $p \leq 0.05$, Figure 6D) models. *Post hoc* analysis revealed that hippocampal volume in the PB/PM model began to decline in the PB/PM group from month 6 to 9 ($p \leq 0.05$, Figure 6C) and continued to month 12 ($p \leq 0.01$, Figure 6C). In the control group, this effect was only observed at 12 months (9 vs 12 months, $p \leq 0.05$, Figure 6C). In the PB/DEET/CORT/DFP model, both groups had reduced hippocampal volumes at 12 months (9 vs 12 months, $p \leq 0.05$, Figure 6D).

3.6 Cerebellar volumes increase with time in both models

Interestingly, cerebellar volumes increased slightly in both models over time (PB/PM: $F(3,30) = 12.39$, $p \leq 0.001$, Figure 6E; PB/DEET/CORT/DFP: $F(2,19) = 6.59$, $p \leq 0.01$, Figure 6F). This main effect was driven by the control mice, especially in the

PB/DEET/CORT/DFP model. In the PB/PM model, there was a decrease in cerebellar volume observed in both groups at month 9 (p's ≤ 0.07, Figure 6E), that was not apparent at month 12 (p's ≤ 0.01, Figure 6E). In the PB/DEET/CORT/DFP model, the increase in cerebellar volume was observed earlier for control (6 vs 9 months, p ≤ 0.05, Figure 6F) than the PB/DEET/CORT/DFP group (6 vs 12 months, p ≤ 0.05, Figure 6F). Notably, in addition to the significant effect of time, there was also a significant treatment effect in the PB/DEET/CORT/DFP model ($F(1,19) = 7.54$, p ≤ 0.05, Figure 6F). Here, a significant treatment difference was observed within month 9, in which the GWI group had decreased cerebellar volume (p ≤ 0.05); at the 6 and 12 month time points, the decrease was only numeric.

3.7 Brainstem volume alterations in both models

There was a significant effect of treatment ($F(1,19) = 8.10$, p ≤ 0.05, Figure 6H) in the PB/DEET/CORT/DFP model for the brainstem (medulla and pons), where there was a reduction in brainstem volume for the PB/DEET/CORT/DFP group within months 9 and 12 (p's = 0.07 and 0.08, respectively, Figure 6H). There was a trending effect of time within the PB/PM model ($F(3,30) = 2.88$, $p = 0.052$, Figure 6G), in which the control group exhibited a transient decrease in brainstem volume at 6 months (3 vs 6 months, p ≤ 0.05, Figure 6G) that rebounded by 12 months (6 vs 12 months, p ≤ 0.001, Figure 6G).

Similar to the ventricular volumetric analysis, the medulla and pons were also individually analyzed to gather more specific information on the effects observed in the brainstem. The volume of the medulla decreased with time in both the PB/PM ($F(3,30) = 4.25$, p ≤ 0.05, Table 1) and PB/DEET/CORT/DFP ($F(2,19) = 10.87$, p ≤ 0.001, Table 2) models. *Post hoc* analysis revealed that medulla size was reduced earlier in

PB/DEET/CORT/DFP mice (6 vs 9 months, $p \leq 0.05$, Table 2) compared to control (6 vs 12 months, $p \leq 0.05$, Table 2). Interestingly in the PB/PM model, medulla volumes were smaller in the control mice early on (3 vs 6 months, $p \leq 0.01$, Table 1) and this was significantly different from the PB/PM group (6 months, $p \leq 0.05$, Table 1). This effect was transient as it was not seen at 9 or 12 months.

Pontine volume increased over time for both models (PB/PM: $F(3,30) = 17.00$, $p \leq 0.001$, Table 1, and PB/DEET/CORT/DFP: $F(2,19) = 9.44$, $p \leq 0.001$, Table 2). Additionally, treatment differences were observed in both models (PB/PM: $F(1,30) = 3.79$, $p = 0.08$, Table 1) and PB/DEET/CORT/DFP: $F(1,30) = 10.62$, $p \leq 0.01$, Table 2). In the PB/PM model, there was a decrease in pons volume in both groups at 9 months (p's ≤ 0.05, Table 1) that was not seen at 12 months as both groups had significantly larger pons volumes (3 vs 12 months, $p \leq 0.05$, Table 1). Similarly, both groups in the PB/DEET/CORT/DFP model exhibited increased pons volumes at a similar rate (6 vs 12 months, p's ≤ 0.05, Table 2). Further, overall, the volume of the pons was smaller in the PB/DEET/CORT/DFP group compared to the control ($p \leq 0.01$, Table 2).

4. Discussion

This study sought to evaluate the progression of structural brain alterations in two GWI preclinical models over the course of 12 months. The results of this study provide comparative similarities and distinctions between these two GWI exposure paradigms and aid in the understanding of GWI pathogenesis and endophenotypes. Major similarities among the models include ventricular enlargement, alterations in cerebellar volumes, and reductions in global brain and hippocampal volumes over time. Key differences were model specific, in which the PB/DEET/CORT/DFP model led to reduced brainstem

volumes and an early and persistent loss of total brain volume, while the PB/PM model produced cortical decreases over time.

Weights were measured for overall health monitoring throughout this study. There were no significant treatment differences over the course of the study (13.5 months). However, PB/PM treated mice weighed numerically less than controls, while PB/DEET/CORT/DFP mice gained more weight over time and trended higher in BMI than controls at the end of the study. These results align with the higher rates of overweight and obesity observed in GWI veterans (Breland et al., 2017; Coughlin et al., 2011), and suggest that prior exposure to this model's specific chemicals (PB/DEET/DFP) and stress may impact weight (e.g., metabolic function) later in life. Studies show that higher BMI's and obesity is associated with brain structural changes (e.g. reduced volumes (Ward et al., 2005)), neuroinflammation, changes in cognitive function, and increased risk of neurological diseases, such as dementias or Alzheimer's Disease (O'Brien et al., 2017; Whitmer et al., 2008). Further investigations into fat distribution and metabolic dysregulation in a model-specific context is warranted.

Many of the effects observed in this study occurred over time, indicating that normal aging is an important factor to consider. In fact, numerous clinical studies have shown that with age, particularly beginning around middle-age, global and regional brain volumes decrease in size (Gur et al., 1991; Murphy et al., 1992; Scahill et al., 2003). At the time of study completion (13.5 months post exposures), mice were approximately 15 months old, an age that corresponds to late middle-age in humans and current status of many GWI veterans. Of note, at the end of the study, there were no differences in either model for gross wet brain weight, however, MRI analysis did reveal longitudinal

alterations in global brain volume over time that were most pronounced at the latest scanning (12 month). It has been shown that with age and age-related diseases, such as Alzheimer's and Parkinson's, increases in brain water are associated with gray matter atrophy and the breakdown of white matter (Chad et al., 2018; Gullett et al., 2020; Maier-Hein et al., 2015; Ofori et al., 2015). Thus, the lack of changes in brain weight at the end of this study might be an indicator of increased extracellular water compensating for decreases in gray matter. Indeed, significant treatment differences were observed for global brain volume in the PB/DEET/CORT/DFP model, in which GWI mice exhibited smaller brain volumes compared to control at each timepoint; however, reductions in brain volume did not appear until the 12 month time point in the control mice. Gradual reductions in global brain volume occurred over time in the PB/PM model that were most prominent in both groups at 9 months post exposure. Interestingly, this effect was not seen at 12 months, and may be due to ventricular enlargement. Further, it appears that these global changes begin earlier in the PB/PM model and are discernible at 9 months followed by PB/DEET/CORT/DFP treatment at 12 months. It is notable that both control (DMSO) and GWI groups decreased within the PB/PM model and only the GWI group in the PB/DEET/CORT/DFP model, suggesting that these effects may be driven predominantly by treatment. Nevertheless, both models have similar decreases in brain volume, albeit at differing time points, which suggests that this effect may be dependent on treatment-age interactions. Follow-up imaging at an event later point of life would be needed to affirm this notion.

It has been shown that ventricular size increases with age (Preul et al., 2006; Scahill et al., 2003) and is associated with declines in brain structure (e.g., cortical thinning) and

consequently, neurobehavioral function like cognitive performance (Carmichael et al., 2007a; Carmichael et al., 2007b; Preul et al., 2006). Here, total ventricular volume was increased at 12 months post exposures in both groups of the PB/PM model. Enlargement of ventricular volume within the PB/PM model at this time point may explain the increase in total brain volume at 12 months. To further characterize where the increase in ventricular volume occurred, ventricles were delineated by the lateral and 3rd ventricles and examined; these measures revealed distinction across the models evaluated. Lateral ventricle size significantly increased in the PB/PM model at 12 months and these results correspond to another GWI study investigating volumetric changes within this region at 10 months (Wu et al., 2021). While there were numerical treatment differences within the PB/DEET/CORT/DFP model for total and lateral ventricle volume, this effect is more likely due to the differences in total brain volume in these mice. It is notable that other areas containing cerebral spinal fluid (CSF), such as the 4th ventricle and the cerebral aqueduct, may be affected by these models' treatments and age; further evaluations of these areas are warranted as they may contribute to structural changes in gray/white matter (Preul et al., 2006; Resnick et al., 2000; Scahill et al., 2003).

Regional alterations in gray matter were also apparent within these GWI models over time. In the PB/PM model there were decreases in cortical volume beginning at 6 months that persisted to 12 months. These findings align with the increased lateral ventricle volume and suggest cortical thinning, which may explain the cognitive aberrations seen in this model (Carpenter et al., 2021; Zakirova et al., 2016; Zakirova et al., 2015) and GWI veterans. Similar results, although less pronounced, were observed in the PB/DEET/ CORT/DFP model, in which there was a slight decrease in cortical volume at month 9 in

GWI treated mice that was significantly different from the control. Further, in both GWI models, hippocampal volumes decreased over time and in all treatment groups, suggestive of an age-related volume reduction. In the PB/PM model, both GWI and control groups decreased at similar rates at 6 and 12 months. However, in the PB/DEET/CORT/DFP model this reduction was observed at 9 months only in the GWI treated group, indicating that this prior GWI exposure impacts this measure earlier. These data are in line with findings from GWI studies depicting volume reductions within rats (Wu et al., 2021) and the GWI veteran population (Chao et al., 2010). Moreover, these decreases in hippocampal volume are in line with observed cognitive and memory deficits at similar time points in previous studies utilizing the PB/PM (Carpenter et al., 2021) and PB/DEET/CORT/DFP (Chapter 5) models.

Hindbrain volumes were also impacted over the course of this study, and these effects were model dependent. In the cerebellum, In the PB/DEET/CORT/DFP model, GWI mice had significantly less cerebellar volume than control at each time point, although over time, both groups' volumes slightly increased. In the PB/PM model, there was a transient, significant reduction at 9 months in cerebellar volume that was not apparent at 12 months. As discussed earlier, these effects at 12 months may be due to increased water compensation and warrant further investigation. Nevertheless, these earlier and treatment-dependent decreases in volumes mirror the clinical observations of cerebellar atrophy in GWI veterans (Christova et al., 2017) and may explain certain dysfunctions in motor control (Carpenter et al., 2021). Additionally, consistent with GWI veteran studies (Christova et al., 2017; Zhang et al., 2020; Zhang et al., 2021), significant decreases in brainstem volume were observed with PB/DEET/CORT/DFP, but not PB/PM treatment

over time. Similar to the ventricular analysis, the brainstem was delineated into the medulla and pons for further volumetric characterization. In both models, medulla volumes decreased over time, whereas the pons increased. Within the pons, GWI treatment differences were observed as increases in the PB/PM model but decreases in the PB/DEET/CORT/DFP model. The brainstem is an important regulatory area for vital functions such as respiration and sleep (Moini and Piran, 2020); thus, the GWI observations here suggest these are areas worth further investigation.

Overall, this study provides insight into the progressive impact of GWI chemical exposures on brain structures that may be associated with previously reported behavioral and neurological effects observed in these models (Brown et al., 2021a; Carpenter et al., 2021; Zakirova et al., 2016). As GWI has heterogeneous symptomatology among veterans, this study provides valuable insights into structural differences between distinct chemical exposures, such as the earlier PB/PM hippocampal and PB/DEET/CORT/DFP brainstem deficits, that may benefit future investigations into targeted neuroprotective interventions.

Acknowledgements

This research was supported by Department of Defense grant numbers W81XWH1610586 and W81XWH2110661 to NMF and the Franklin Foundation Imaging Award to JMC. We would like to extend a special thanks to Kim Mason and Dr. William Oliver at the University of Georgia's Bio-Imaging Research Center for their assistance in this study. Additionally, we thank members of the Filipov Lab, Danielle Ludwig and Alexandria Goodyear, for their assistance in transporting mice to the imaging facility.

Author Contributions

JMC and NMF conceived and designed the study. JMC and NMF assisted in investigation and sample collection. JMC and SN performed sample and data analysis. JMC and NMF wrote the manuscript. All authors read or contributed editorially to the final manuscript version.

Conflict of Interest

The authors declare no conflicts of interest.

References

Breland, J.Y., Phibbs, C.S., Hoggatt, K.J., Washington, D.L., Lee, J., Haskell, S., Uchendu, U.S., Saechao, F.S., Zephyrin, L.C., Frayne, S.M., 2017. The Obesity Epidemic in the Veterans Health Administration: Prevalence Among Key Populations of Women and Men Veterans. J Gen Intern Med 32(Suppl 1), 11-17.

Brown, K.A., Carpenter, J.M., Preston, C.J., Ludwig, H.D., Clay, K.B., Harn, D.A., Norberg, T., Wagner, J.J., Filipov, N.M., 2021a. Lacto-N-fucopentaose-III ameliorates acute and persisting hippocampal synaptic plasticity and transmission deficits in a Gulf War Illness mouse model. Life Sci 279, 119707.

Brown, K.A., Preston, C.J., Carpenter, J.M., Ludwig, H.D., Norberg, T., Harn, D.A., Filipov, N.M., Wagner, J.J., 2021b. Lacto-N-fucopentaose-III (LNFPIII) ameliorates acute aberrations in hippocampal synaptic transmission in a Gulf War Illness animal model. Brain Res 1766, 147513.

Calley, C.S., Kraut, M.A., Spence, J.S., Briggs, R.W., Haley, R.W., Hart, J., 2010. The neuroanatomic correlates of semantic memory deficits in patients with Gulf War illnesses: a pilot study. Brain Imaging and Behavior 4(3), 248-255.

Carmichael, O.T., Kuller, L.H., Lopez, O.L., Thompson, P.M., Dutton, R.A., Lu, A., Lee, S.E., Lee, J.Y., Aizenstein, H.J., Meltzer, C.C., Liu, Y., Toga, A.W., Becker, J.T., 2007a. Cerebral ventricular changes associated with transitions between normal cognitive function, mild cognitive impairment, and dementia. Alzheimer Dis Assoc Disord 21(1), 14-24.

Carmichael, O.T., Kuller, L.H., Lopez, O.L., Thompson, P.M., Dutton, R.A., Lu, A., Lee, S.E., Lee, J.Y., Aizenstein, H.J., Meltzer, C.C., Liu, Y., Toga, A.W., Becker, J.T., 2007b. Ventricular volume and dementia progression in the Cardiovascular Health Study. Neurobiol Aging 28(3), 389-397.

Carpenter, J.M., Brown, K.A., Diaz, A.N., Dockman, R.L., Benbow, R.A., Harn, D.A., Norberg, T., Wagner, J.J., Filipov, N.M., 2021. Delayed treatment with the

immunotherapeutic LNFPIII ameliorates multiple neurological deficits in a pesticide-nerve agent prophylactic mouse model of Gulf War Illness. Neurotoxicol Teratol 87, 107012.

Carpenter, J.M., Gordon, H.E., Ludwig, H.D., Wagner, J.J., Harn, D.A., Norberg, T., Filipov, N.M., 2020. Neurochemical and neuroinflammatory perturbations in two Gulf War Illness models: Modulation by the immunotherapeutic LNFPIII. NeuroToxicology 77, 40-50.

Chad, J.A., Pasternak, O., Salat, D.H., Chen, J.J., 2018. Re-examining age-related differences in white matter microstructure with free-water corrected diffusion tensor imaging. Neurobiol Aging 71, 161-170.

Chao, L.L., 2020. The Prevalence of Mild Cognitive Impairment in a Convenience Sample of 202 Gulf War Veterans. International Journal of Environmental Research and Public Health 17(19), 7158.

Chao, L.L., Abadjian, L., Hlavin, J., Meyerhoff, D.J., Weiner, M.W., 2011. Effects of low-level sarin and cyclosarin exposure and Gulf War Illness on Brain Structure and Function: A study at 4T. NeuroToxicology 32(6), 814-822.

Chao, L.L., Rothlind, J.C., Cardenas, V.A., Meyerhoff, D.J., Weiner, M.W., 2010. Effects of low-level exposure to sarin and cyclosarin during the 1991 Gulf War on brain function and brain structure in US veterans. Neurotoxicology 31(5), 493-501.

Chao, L.L., Zhang, Y., Buckley, S., 2015. Effects of low-level sarin and cyclosarin exposure on white matter integrity in Gulf War Veterans. Neurotoxicology 48, 239-248.

Christova, P., James, L.M., Engdahl, B.E., Lewis, S.M., Carpenter, A.F., Georgopoulos, A.P., 2017. Subcortical brain atrophy in Gulf War Illness. Exp Brain Res 235(9), 2777-2786.

Clarke, T., Jamieson, J.D., Malone, P., Rayhan, R.U., Washington, S., VanMeter, J.W., Baraniuk, J.N., 2019. Connectivity differences between Gulf War Illness (GWI) phenotypes during a test of attention. PLoS One 14(12), e0226481-e0226481.

Cooper, C.M., Briggs, R.W., Farris, E.A., Bartlett, J., Haley, R.W., Odegard, T.N., 2016. Memory and functional brain differences in a national sample of U.S. veterans with Gulf War Illness. Psychiatry Research: Neuroimaging 250, 33-41.

Coughlin, S.S., Kang, H.K., Mahan, C.M., 2011. Selected Health Conditions Among Overweight, Obese, and Non-Obese Veterans of the 1991 Gulf War: Results from a Survey Conducted in 2003-2005. Open Epidemiol J 4, 140-146.

Dickey, B., Madhu, L.N., Shetty, A.K., 2021. Gulf War Illness: Mechanisms Underlying Brain Dysfunction and Promising Therapeutic Strategies. Pharmacology & Therapeutics 220, 107716.

Gopinath, K., Gandhi, P., Goyal, A., Jiang, L., Fang, Y., Ouyang, L., Ganji, S., Buhner, D., Ringe, W., Spence, J., Biggs, M., Briggs, R., Haley, R., 2012. FMRI reveals abnormal central processing of sensory and pain stimuli in ill Gulf War veterans. Neurotoxicology 33(3), 261-271.

Grant, M.K., Bobilev, A.M., Rasys, A.M., Branson Byers, J., Schriever, H.C., Hekmatyar, K., Lauderdale, J.D., 2020. Global and age-related neuroanatomical abnormalities in a Pax6-deficient mouse model of aniridia suggests a role for Pax6 in adult structural neuroplasticity. Brain Research 1732, 146698.

Gullett, J.M., O'Shea, A., Lamb, D.G., Porges, E.C., O'Shea, D.M., Pasternak, O., Cohen, R.A., Woods, A.J., 2020. The association of white matter free water with cognition in older adults. NeuroImage 219, 117040.

Gur, R.C., Mozley, P.D., Resnick, S.M., Gottlieb, G.L., Kohn, M., Zimmerman, R., Herman, G., Atlas, S., Grossman, R., Berretta, D., 1991. Gender differences in age effect on brain atrophy measured by magnetic resonance imaging. Proceedings of the National Academy of Sciences 88(7), 2845-2849.

Haley, R.W., Fleckenstein, J.L., Marshall, W.W., McDonald, G.G., Kramer, G.L., Petty, F., 2000. Effect of Basal Ganglia Injury on Central Dopamine Activity in Gulf War Syndrome: Correlation of Proton Magnetic Resonance Spectroscopy and Plasma Homovanillic Acid Levels. Archives of Neurology 57(9), 1280-1285.

Hubbard, N.A., Hutchison, J.L., Motes, M.A., Shokri-Kojori, E., Bennett, I.J., Brigante, R.M., Haley, R.W., Rypma, B., 2014. Central Executive Dysfunction and Deferred Prefrontal Processing in Veterans with Gulf War Illness. Clin Psychol Sci 2(3), 319-327.

James, L.M., Christova, P., Engdahl, B.E., Lewis, S.M., Carpenter, A.F., Georgopoulos, A.P., 2017. Human Leukocyte Antigen (HLA) and Gulf War Illness (GWI): HLA-DRB1*13:02 Spares Subcortical Atrophy in Gulf War Veterans. EBioMedicine 26, 126-131.

Koo, B.-B., Michalovicz, L.T., Calderazzo, S., Kelly, K.A., Sullivan, K., Killiany, R.J., O'Callaghan, J.P., 2018. Corticosterone potentiates DFP-induced neuroinflammation and affects high-order diffusion imaging in a rat model of Gulf War Illness. Brain, behavior, and immunity 67, 42-46.

Li, X., Spence, J.S., Buhner, D.M., Hart, J., Jr., Cullum, C.M., Biggs, M.M., Hester, A.L., Odegard, T.N., Carmack, P.S., Briggs, R.W., Haley, R.W., 2011. Hippocampal dysfunction in Gulf War veterans: investigation with ASL perfusion MR imaging and physostigmine challenge. Radiology 261(1), 218-225.

Macht, V.A., Woodruff, J.L., Maissy, E.S., Grillo, C.A., Wilson, M.A., Fadel, J.R., Reagan, L.P., 2019. Pyridostigmine bromide and stress interact to impact immune function, cholinergic neurochemistry and behavior in a rat model of Gulf War Illness. Brain, Behavior, and Immunity.

Maier-Hein, K.H., Westin, C.F., Shenton, M.E., Weiner, M.W., Raj, A., Thomann, P., Kikinis, R., Stieltjes, B., Pasternak, O., 2015. Widespread white matter

degeneration preceding the onset of dementia. Alzheimers Dement 11(5), 485-493.e482.

Megahed, T., Hattiangady, B., Shuai, B., Shetty, A.K., 2014. Parvalbumin and neuropeptide Y expressing hippocampal GABA-ergic inhibitory interneuron numbers decline in a model of Gulf War illness. Front Cell Neurosci 8, 447.

Miller, J.V., LeBouf, R.F., Kelly, K.A., Michalovicz, L.T., Ranpara, A., Locker, A.R., Miller, D.B., O'Callaghan, J.P., 2018. The Neuroinflammatory Phenotype in a Mouse Model of Gulf War Illness is Unrelated to Brain Regional Levels of Acetylcholine as Measured by Quantitative HILIC-UPLC-MS/MS. Toxicological Sciences 165(2), 302-313.

Minkeviciene, R., Hlushchenko, I., Virenque, A., Lahti, L., Khanal, P., Rauramaa, T., Koistinen, A., Leinonen, V., Noe, F.M., Hotulainen, P., 2019. MIM-Deficient Mice Exhibit Anatomical Changes in Dendritic Spines, Cortex Volume and Brain Ventricles, and Functional Changes in Motor Coordination and Learning. Frontiers in Molecular Neuroscience 12.

Moini, J., Piran, P., 2020. Chapter 9 - Brainstem, in: Moini, J., Piran, P. (Eds.), Functional and Clinical Neuroanatomy. Academic Press, pp. 293-317.

Murphy, D.G.M., DeCarli, C., Schapiro, M.B., Rapoport, S.I., Horwitz, B., 1992. Age-Related Differences in Volumes of Subcortical Nuclei, Brain Matter, and Cerebrospinal Fluid in Healthy Men as Measured With Magnetic Resonance Imaging. Archives of Neurology 49(8), 839-845.

Novelli, E.L., Diniz, Y.S., Galhardi, C.M., Ebaid, G.M., Rodrigues, H.G., Mani, F., Fernandes, A.A., Cicogna, A.C., Novelli Filho, J.L., 2007. Anthropometrical parameters and markers of obesity in rats. Lab Anim 41(1), 111-119.

O'Brien, P.D., Hinder, L.M., Callaghan, B.C., Feldman, E.L., 2017. Neurological consequences of obesity. Lancet Neurol 16(6), 465-477.

O'Callaghan, J.P., Kelly, K.A., Locker, A.R., Miller, D.B., Lasley, S.M., 2015. Corticosterone primes the neuroinflammatory response to DFP in mice: potential animal model of Gulf War Illness. J Neurochem 133(5), 708-721.

Ofori, E., Pasternak, O., Planetta, P.J., Li, H., Burciu, R.G., Snyder, A.F., Lai, S., Okun, M.S., Vaillancourt, D.E., 2015. Longitudinal changes in free-water within the substantia nigra of Parkinson's disease. Brain 138(8), 2322-2331.

Parihar, V.K., Hattiangady, B., Shuai, B., Shetty, A.K., 2013. Mood and memory deficits in a model of Gulf War illness are linked with reduced neurogenesis, partial neuron loss, and mild inflammation in the hippocampus. Neuropsychopharmacology 38(12), 2348-2362.

Preul, C., Hund-Georgiadis, M., Forstmann, B.U., Lohmann, G., 2006. Characterization of cortical thickness and ventricular width in normal aging: A morphometric study at 3 Tesla. Journal of Magnetic Resonance Imaging 24(3), 513-519.

Rayhan, R.U., Stevens, B.W., Timbol, C.R., Adewuyi, O., Walitt, B., VanMeter, J.W., Baraniuk, J.N., 2013. Increased brain white matter axial diffusivity associated with fatigue, pain and hyperalgesia in Gulf War illness. PLoS One 8(3), e58493.

Resnick, S.M., Goldszal, A.F., Davatzikos, C., Golski, S., Kraut, M.A., Metter, E.J., Bryan, R.N., Zonderman, A.B., 2000. One-year Age Changes in MRI Brain Volumes in Older Adults. Cerebral Cortex 10(5), 464-472.

Ribeiro, A.C.R., Deshpande, L.S., 2021. A review of pre-clinical models for Gulf War Illness. Pharmacology & Therapeutics 228, 107936.

Scahill, R.I., Frost, C., Jenkins, R., Whitwell, J.L., Rossor, M.N., Fox, N.C., 2003. A longitudinal study of brain volume changes in normal aging using serial registered magnetic resonance imaging. Arch Neurol 60(7), 989-994.

Van Riper, S.M., Alexander, A.L., Koltyn, K.F., Stegner, A.J., Ellingson, L.D., Destiche, D.J., Dougherty, R.J., Lindheimer, J.B., Cook, D.B., 2017. Cerebral white matter

structure is disrupted in Gulf War Veterans with chronic musculoskeletal pain. PAIN 158(12).

Ward, M.A., Carlsson, C.M., Trivedi, M.A., Sager, M.A., Johnson, S.C., 2005. The effect of body mass index on global brain volume in middle-aged adults: a cross sectional study. BMC Neurol 5, 23.

Washington, S.D., Rayhan, R.U., Garner, R., Provenzano, D., Zajur, K., Addiego, F.M., VanMeter, J.W., Baraniuk, J.N., 2020. Exercise alters cerebellar and cortical activity related to working memory in phenotypes of Gulf War Illness. Brain Communications 2(1).

White, R.F., Steele, L., O'Callaghan, J.P., Sullivan, K., Binns, J.H., Golomb, B.A., Bloom, F.E., Bunker, J.A., Crawford, F., Graves, J.C., Hardie, A., Klimas, N., Knox, M., Meggs, W.J., Melling, J., Philbert, M.A., Grashow, R., 2016. Recent research on Gulf War illness and other health problems in veterans of the 1991 Gulf War: Effects of toxicant exposures during deployment. Cortex 74, 449-475.

Whitmer, R.A., Gustafson, D.R., Barrett-Connor, E., Haan, M.N., Gunderson, E.P., Yaffe, K., 2008. Central obesity and increased risk of dementia more than three decades later. Neurology 71(14), 1057-1064.

Wu, X., Shetty, A.K., Reddy, D.S., 2021. Long-term changes in neuroimaging markers, cognitive function and psychiatric symptoms in an experimental model of Gulf War Illness. Life Sciences 285, 119971.

Wylie, G.R., Genova, H., Dobryakova, E., DeLuca, J., Chiaravalloti, N., Falvo, M., Cook, D., 2019. Fatigue in Gulf War Illness is associated with tonically high activation in the executive control network. Neuroimage Clin 21, 101641-101641.

Zakirova, Z., Crynen, G., Hassan, S., Abdullah, L., Horne, L., Mathura, V., Crawford, F., Ait-Ghezala, G., 2016. A Chronic Longitudinal Characterization of Neurobehavioral and Neuropathological Cognitive Impairment in a Mouse Model of Gulf War Agent Exposure. Front Integr Neurosci 9, 71-71.

Zakirova, Z., Tweed, M., Crynen, G., Reed, J., Abdullah, L., Nissanka, N., Mullan, M., Mullan, M.J., Mathura, V., Crawford, F., Ait-Ghezala, G., 2015. Gulf War agent exposure causes impairment of long-term memory formation and neuropathological changes in a mouse model of Gulf War Illness. PLoS One 10(3), e0119579-e0119579.

Zhang, Y., Avery, T., Vakhtin, A.A., Mathersul, D.C., Tranvinh, E., Wintermark, M., Massaband, P., Ashford, J.W., Bayley, P.J., Furst, A.J., 2020. Brainstem atrophy in Gulf War Illness. NeuroToxicology 78, 71-79.

Zhang, Y., Vakhtin, A.A., Dietch, J., Jennings, J.S., Yesavage, J.A., Clark, J.D., Bayley, P.J., Ashford, J.W., Furst, A.J., 2021. Brainstem damage is associated with poorer sleep quality and increased pain in gulf war illness veterans. Life Sciences 280, 119724.

Figures

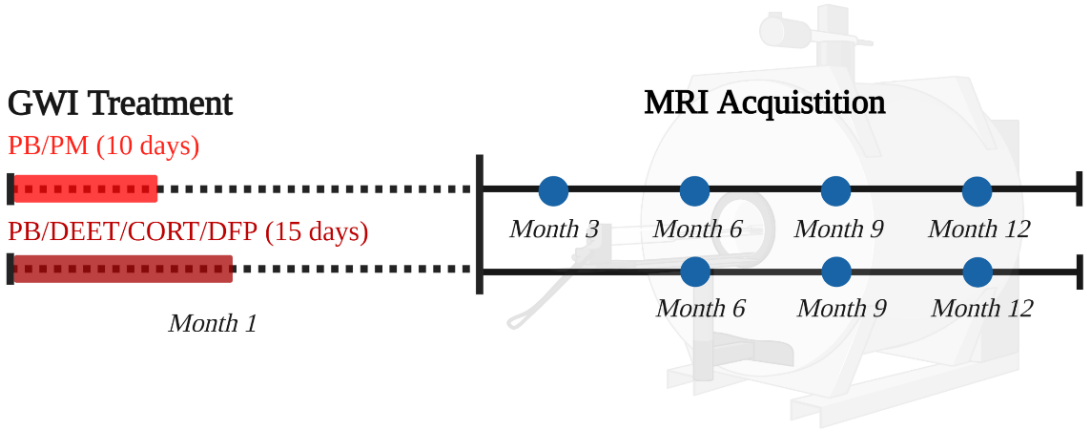

Figure 6.1. Experimental Timeline and Image Analysis. Shown is the experimental timeline for this study in which two GWI exposure paradigms were utilized (PB/PM: 10 days; PB/DEET/CORT/DFP: 15 days). MRI was conducted on mice 3 (PB/PM only), 6, 9, and 12 months post GWI exposure. Abbreviations: CORT: corticosterone; DEET: N,N-diethyl-meta-toluamide; DFP: diisopropylfluorophosphate; GWI: Gulf War Illness; MRI: magnetic resonance imaging; PB: pyridostigmine bromide; PM: permethrin.

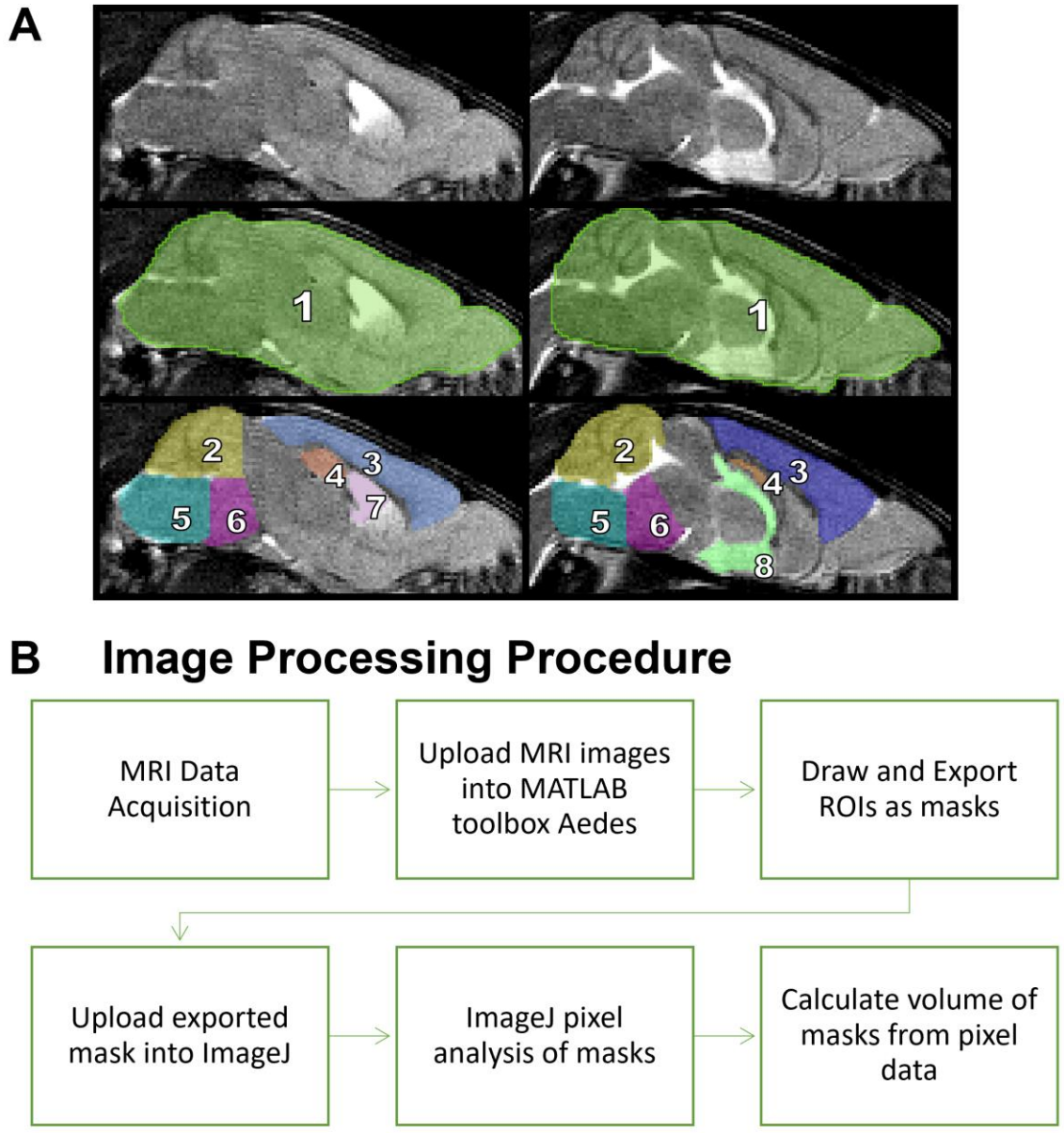

Figure 6.2. Brain masking for MRI image analysis. (A) Brain regions of interest (ROIs) were manually drawn using the MATLAB Aedes toolbox. Representative ROIs include: 1) total brain, 2) cerebellum, 3) cortex, 4) hippocampus, 5) medulla, 6) pons, 7) lateral ventricle, and 8) 3rd ventricle. **(B)** Imaging processing procedure.

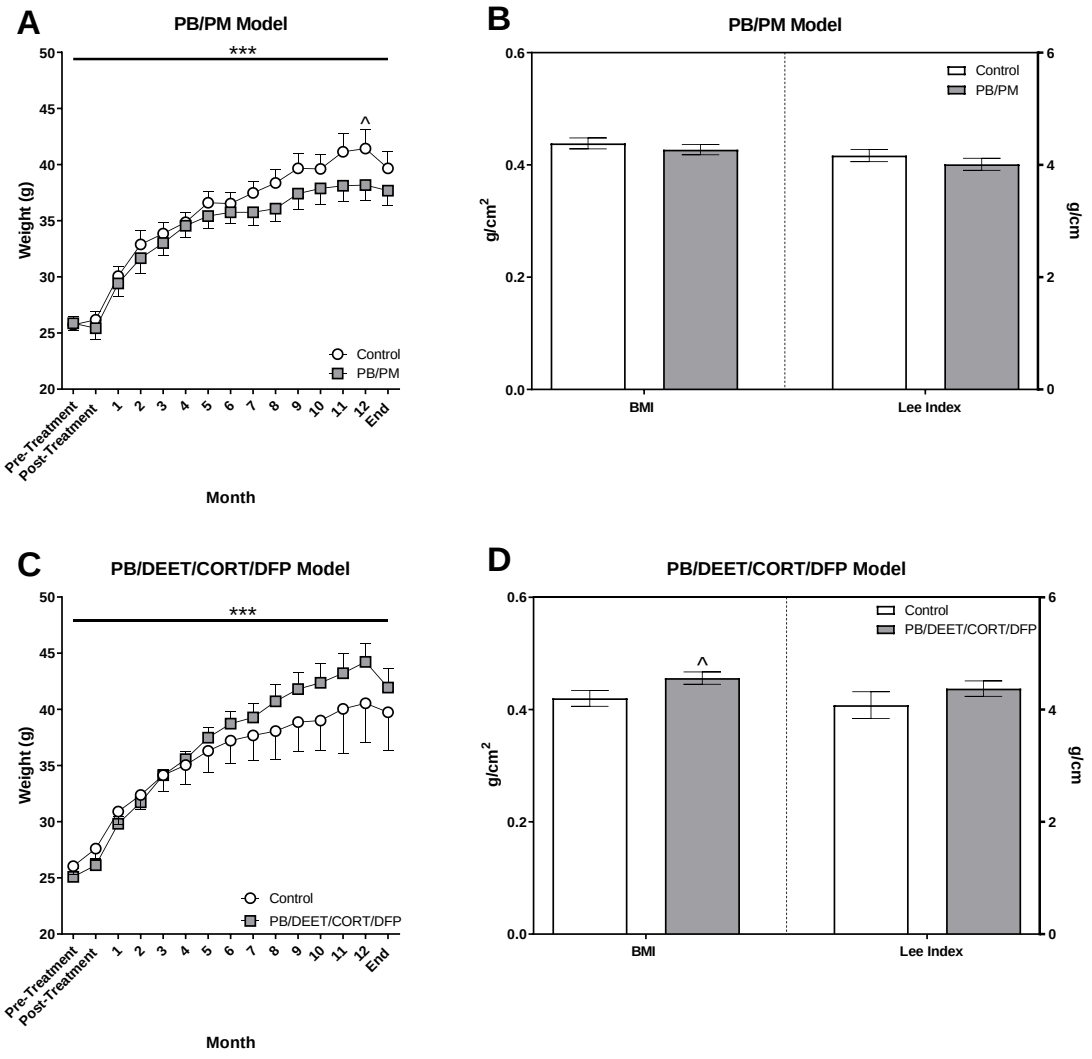
A
PB/PM Model
***
^
Weight (g)
Control
PB/PM
Pre-Treatment
Post-Treatment
Month
B
PB/PM Model
Control
PB/PM
g/cm2
g/cm
BMI
Lee Index
C
PB/DEET/CORT/DFP Model
***
Weight (g)
Control
PB/DEET/CORT/DFP
Pre-Treatment
Post-Treatment
Month
D
PB/DEET/CORT/DFP Model
^
Control
PB/DEET/CORT/DFP
g/cm2
g/cm
BMI
Lee Index

Figure 6.3. Monthly Weights and Calculated Anthropometrical Parameters. (A,C) Weights were monitored and are presented for the start of the study (pre-treatment), directly after treatment administration cessation (PB/PM: 10 days; PB/DEET/CORT/DFP: 15 days), and monthly until the end of the study at 13.5 months. **(B,D)** Anthropometrical parameters were evaluated by calculating the body mass index (BMI; [Body weight (g)/length^2 (cm^2]) and the Lee index [body weight (g)/length(cm)]. Data are presented at ± SEM. Sample sizes were: PB/PM model, n=6/group/timepoint; PB/DEET/CORT/DFP model, n=5-6/group/timepoint. *** indicates a significant effect of time, $p \leq 0.001$. $^{\wedge}$ indicates a trending effect of treatment, $p \leq 0.10$. Abbreviations: g: grams; CORT: corticosterone; DEET: N,N-diethyl-meta-toluamide; DFP: diisopropylfluorophosphate; PB: pyridostigmine bromide; PM: permethrin.

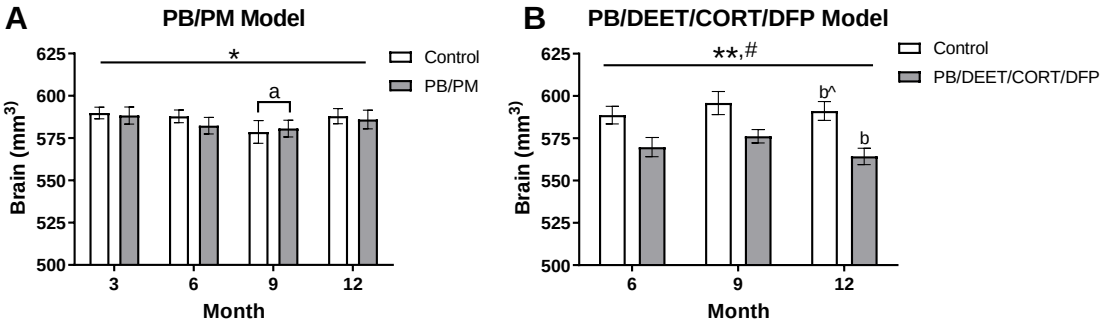

Figure 6.4. Longitudinal Brain Volumes in Two Models of Gulf War Illness. Longitudinal measurement of total brain volume in **(A)** PB/PM and **(B)** PB/DEET/CORT/DFP models of GWI. Data are presented as mean ± SEM. Sample sizes were: PB/PM model, n=6/group/timepoint; PB/DEET/CORT/DFP model, n=5-6/group/timepoint. * and ** indicate significant main effect of time where $p \leq 0.05$ or 0.01, respectively. $^{\#}$ indicates significant main effect of treatment, $p \leq 0.05$. ^{a} denotes a significant pairwise comparison from the 3 month time point, $p \leq 0.05$. ^{b} and $^{b\wedge}$ denote a significant ($p \leq 0.05$) and trending ($p \leq 0.10$) pairwise comparison from the 9 month time point. Abbreviations: CORT: corticosterone; DEET: N,N-diethyl-meta-toluamide; DFP: diisopropylfluorophosphate; PB: pyridostigmine bromide; PM: permethrin.

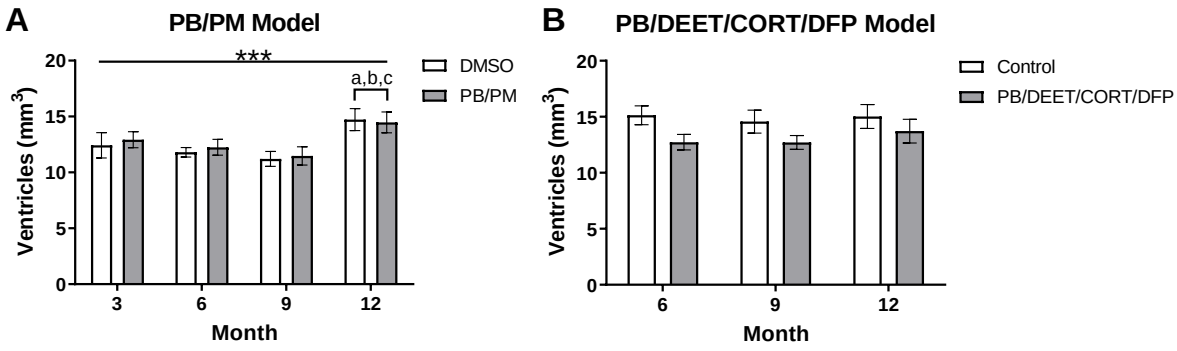

Figure 6.5. Longitudinal MRI Analysis of Ventricular Volume in Two Models of Gulf War Illness. Longitudinal measurement of total ventricular volume in **(A)** PB/PM (n=6/group) and **(B)** PB/DEET/CORT/DFP (n=5-6/group) models of GWI. Data are presented as mean ± SEM. Sample sizes were: PB/PM model, n=6/group/timepoint; PB/DEET/CORT/DFP model, n=5-6/group/timepoint. * and *** indicate significant main effect of time where $p \leq 0.05$ or 0.001, respectively. ^{a,b,} and ^{c} denote a significant pairwise comparison from the 3,6, and 9 month time point, respectively, $p \leq 0.05$. Abbreviations: CORT: corticosterone; DEET: N,N-diethyl-meta-toluamide; DFP: diisopropylfluorophos-phate; PB: pyridostigmine bromide; PM: permethrin.

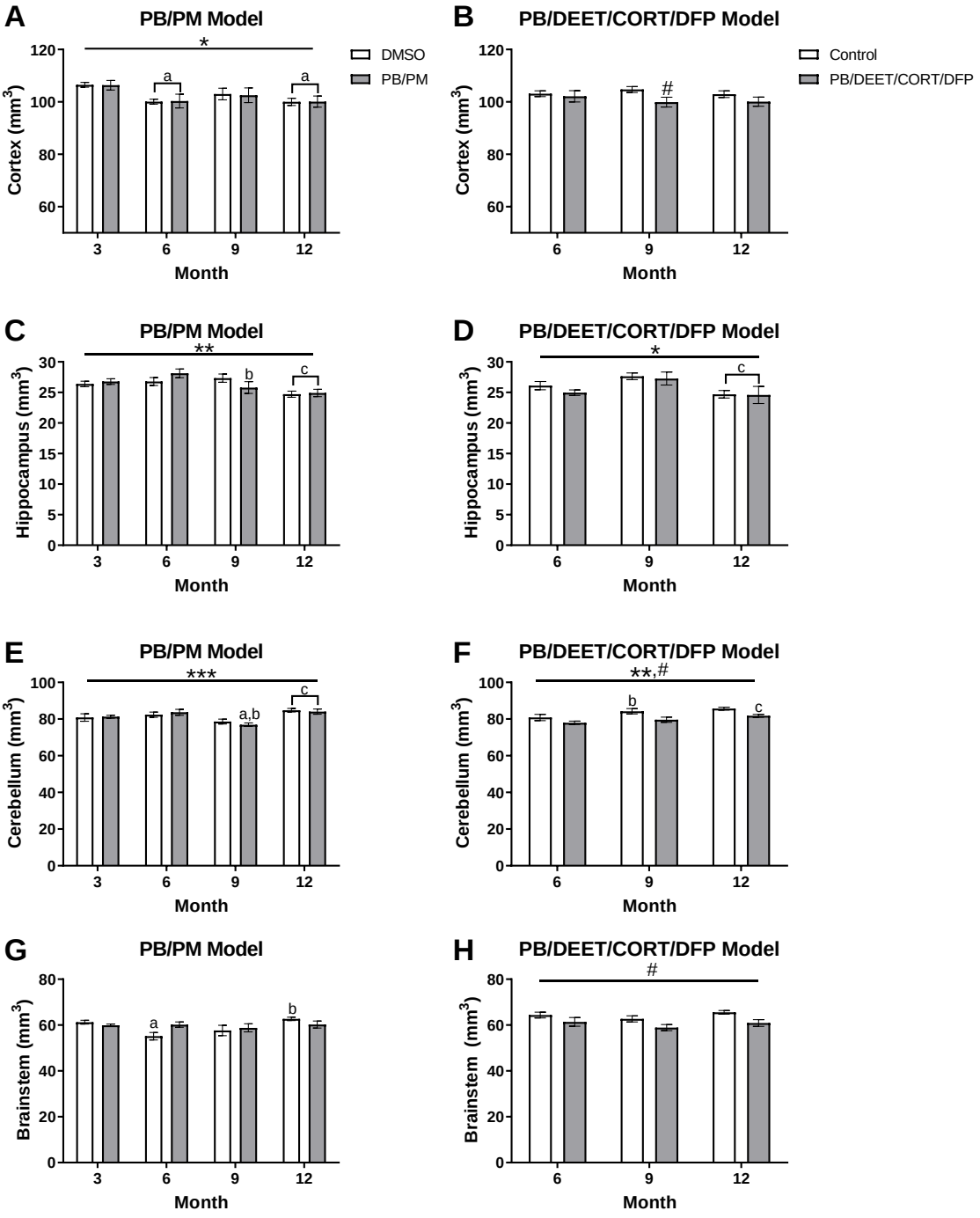
A
PB/PM Model
DMSO
PB/PM
Cortex (mm3)
Month
B
PB/DEET/CORT/DFP Model
Control
PB/DEET/CORT/DFP
C
PB/PM Model
Hippocampus (mm3)
D
PB/DEET/CORT/DFP Model
E
PB/PM Model
Cerebellum (mm3)
F
PB/DEET/CORT/DFP Model
G
PB/PM Model
Brainstem (mm3)
H
PB/DEET/CORT/DFP Model

Figure 6.6. Longitudinal MRI Analysis of Ventricular Volume in Two Models of Gulf War Illness. Longitudinal measurement of (A,B) cortical, (C,D) hippocampus, (E,F) cerebellar, and (G,H) brainstem volumes in the PB/PM (left) and PB/DEET/CORT/DFP (right) models of GWI. Data are presented as mean ± SEM. Sample sizes were: PB/PM model, n=6/group/timepoint; PB/DEET/CORT/DFP model, n=5-6/group/timepoint. *,**, and ** indicate significant main effect of time where $p \leq 0.05$, 0.01 or 0.001, respectively. $^{\#}$ indicates significant effect of treatment, $p \leq 0.05$. ^{a,b,c} denotes a significant pairwise comparison from the 3,6, and 9 month time points, respectively, $p \leq 0.05$Abbreviations: CORT: corticosterone; DEET: N,N-diethyl-meta-toluamide; DFP: diisopropylfluorophos-phate; PB: pyridostigmine bromide; PM: permethrin.

Table 1. Longitudinal MRI Assessment of Brain Area Volumes in the PB/PM Model of Gulf War Illness			
Brain Region	**Time Point**	**PB/PM Model** **Control**	**PB/PM**
Lateral Ventricle **	3	7.84 ± 0.80	7.76 ± 0.61
	6	7.33 ± 0.65	7.57 ± 0.64
	9	7.32 ± .57	7.36 ± 0.35
	12	9.10 ± 0.89 [a,b,c]	9.27 ± 0.84 [a,b,c]
3rd Ventricle *	3	4.55 ± 1.53	5.21 ± 0.29
	6	4.47 ± 1.00	4.68 ± 0.54
	9	3.89 ± 2.03	4.11 ± 1.32
	12	5.62 ± 0.30	5.22 ± 0.58
Medulla *	3	36.99 ± 2.45	35.68 ± 1.02
	6	31.30 ± 2.73 [a,#]	34.91 ± 2.11
	9	35.49 ± 3.49	35.41 ± 2.75
	12	34.49 ± 1.60	32.61 ± 2.14
Pons * #^**	3	21.89 ± 0.54	22.02 ± 0.89
	6	21.96 ± 2.04	23.44 ± 2.11
	9	19.07 ± 1.48 [a]	20.78 ± 1.83 [a]
	12	25.15 ± 1.16 [a]	24.74 ± 2.24 [a]

Table 6.1. Longitudinal MRI Assessment of Brain Area Volumes in the PB/PM Model of Gulf War Illness. This table depicts the longitudinal measurement (3, 6, 9 and 12 months post-PB/PM treatment) of volume in the following brain areas: lateral ventricle, 3rd ventricle, 4th ventricle, medulla, and pons. Sample sizes were n=6/group/time point. Data are presented as mean ± SEM. [*,**,] and [***] indicate significant main effect of time where $p \leq 0.05$, 0.01 and 0.001, respectively. [a,b,] and [c] denote a significant pairwise comparison from the 3,6, and 9 month time point, respectively, $p \leq 0.05$. [#^] and [#] and denotes a trending ($p \leq 0.10$) or significant ($p \leq 0.05$) treatment difference., respectively. Abbreviations: CORT: corticosterone; DEET: N,N-diethyl-meta-toluamide; DFP: diisopropylfluoro-phosphate; MRI: magnetic resonance imaging; PB: pyridostigmine bromide; PM: permethrin.

Table 2. Longitudinal MRI Assessment of Brain Area Volumes in the PB/DEET/CORT/DFP Model of Gulf War Illness			
Brain Region	**Time Point**	**PB/DEET/CORT/DFP Model**	
		Control	**PB/DEET/CORT/DFP**
Lateral Ventricle #	6	9.77 ± 1.95	7.84 ± 1.26
	9	9.82 ± 1.74	7.79 ± 0.95
	12	10.43 ± 1.76	8.00 ± 1.25
3rd Ventricle	6	5.37 ± 0.13	4.89 ± 0.29
	9	4.75 ± 0.61	4.92 ± 0.30
	12	4.98 ± 0.80	5.72 ± 0.58
Medulla * **	6	39.22 ± 2.40	38.44 ± 2.58
	9	37.35 ± 1.84	35.44 ± 2.33 [a]
	12	35.59 ± 1.36 [a]	33.99 ± 2.48
Pons * #**	6	21.57 ± 1.57	19.66 ± 2.52
	9	23.22 ± 1.68	21.41 ± 1.81
	12	25.96 ± 0.99 [a]	24.04 ± 3.17 [a]

Table 6.2. Longitudinal MRI Assessment of Brain Area Volumes in the PB/DEET/CORT/DFP Model of Gulf War Illness. This table depicts the longitudinal measurement (6, 9 and 12 months post-PB/DEET/CORT/DFP treatment) of volume in the following brain areas: lateral ventricle, 3rd ventricle, 4th ventricle, medulla, and pons. Sample sizes were n=5-6/group/time point. Data are presented as mean ± SEM. *** indicates a significant main effect of time where $p \leq 0.001$. [a] and [b] denote a significant pairwise comparison from the 6 and 9 month time point, respectively, $p \leq 0.05$. # and denotes a significant ($p \leq 0.05$) main effect of treatment. Abbreviations: CORT: corticosterone; DEET: N,N-diethyl-meta-toluamide; DFP: diisopropylfluorophosphate; MRI: magnetic resonance imaging; PB: pyridostigmine bromide; PM: permethrin

CHAPTER 7

SUMMARY AND CONCLUSIONS

1. Overview

More than 30 years after the Gulf War (GW), veterans continue to experience numerous, debilitating symptoms of Gulf War Illness (GWI) that include nervous and immune system deficits. Investigations into the etiopathogenesis of GWI are still ongoing, but suspected causes include the in-theater overexposures to neurotoxicants, such as pesticides, the prophylactic pyridostigmine bromide (PB), and in some veterans, chemical nerve agents. Unfortunately, a cure-all treatment does not exist for GWI, and therapeutics currently implored only manage individual or a few symptoms. As GWI veterans age, there appears to a rise in symptom severity and increased risk of age-related co-morbidities, such as neurodegenerative diseases of the aged. Thus, understanding the progressive pathobiology of GWI and developing neuroprotective therapeutics is imperative.

The goal of this dissertation work was to investigate GWI-specific progressive neurological and pathological effects within two, chemically distinct models of this disease and evaluate the beneficial effects of a novel immunotherapeutic, Lacto-N-fucopentaose III (LNFPIII). Here, we utilized the pyridostigmine bromide/permethrin (PB/PM) and PB/N-Diethyl-3-methylbenzamide/corticosterone/diisopropylfluorophosphate (PB/DEET/CORT/DFP) murine GWI models to characterize the acute and long-term effects of these GW relevant exposures on neurological measures. The following chapter will summarize

the findings and limitations of these studies, as well as provide insight into future research directions.

2. Summaries of Conducted Studies

Given the lack of detailed neurochemical characterization of accepted GWI models and the modulatory effects that inflammation plays on neurotransmitter homeostasis, Chapter Two sought to characterize the neurochemical monoamine and neuroinflammatory phenotypes after PB/PM and PB/DEET/CORT/DFP acute exposure (10 and 15 days, respectively). Additionally, LNFPIII was co-administered with GWI exposure to examine the potential modulatory effects of this treatment. In the brain of both models, serotonergic and dopaminergic dyshomeostasis was present in multiple regions, including the striatum, amygdala, and hippocampus. The observed effects varied between models and were more pronounced with PB/PM exposure. Peripherally, splenic 5-HT and NE were altered by GWI chemicals, primarily in the PB/DEET/CORT/DFP model. Further, GWI chemicals in both models produced some shared (IL-1β, CCL-2, TNFα and YM-1) and model specific elevations in hippocampal inflammatory markers, with the effects being more pronounced in the PB/DEET/CORT/DFP model. Notably, LNFPIII treatment modulated many of these acute effects, especially on brain neurochemistry and neuroinflammation. The data within this study expanded the characterizations of these models immediately after GWI relevant exposures. The acute effects observed within this study were notable, considering persistent and sustained monoaminergic disbalance and inflammation could influence GWI symptom presentation and severity long-term.

Due to the widespread acute neurochemical disbalance and neuroinflammation observed in these models, their long-term neurological characterizations were of interest.

Thus, further long-term investigations with these models were conducted to determine the neurobehavioral phenotypes and chronic pathology (i.e., neuroinflammation), as well as evaluate delayed LNFPIII treatment on these measures. In Chapter Three, a battery of behavioral tests and neurobiological evaluations were conducted 6-9 months post PB/PM exposures; LNFPIII treatment was initiated 1 month prior to behavioral testing (5 months after PB/PM). Prior PB/PM exposure led to multiple motor related dysfunctions such as decreases in locomotion, neuromuscular function, sensorimotor function. Additionally, increases in anxiety-like, but not depressive-like behavior were observed with prior PB/PM treatment. Moreover, PB/PM exposed mice learned at a slower rate in tests of cognition/memory and had impaired short-term recognition memory. LNFPIII treatment resolved and improved many of these behavioral deficits, particularly in the motor and cognition/memory domains. To further understand the aberrations observed within these two behavioral domains, striatal and hippocampal neuropathology was examined. Immunohistochemical analysis of tyrosine hydroxylase (TH), a dopaminergic marker, did not reveal any major PB/PM induced alterations in the striatum; however, there were increases in neuroinflammatory (astrocytes and microglia) cells in the hippocampus. Moreover, modest deficits in basal synaptic transmission and long term potentiation (LTP) were observed in the hippocampus. LNFPIII treatment minimized hippocampal inflammation, improved synaptic transmission and LTP, and increased striatal TH. The behavioral and biological parameters evaluated in this study provide additional data ion progression of GWI within this model and how immunomodulatory compounds (e.g., LNFPIII) could aid symptom management.

As GWI veterans exhibit a number of gastrointestinal complaints, investigation into gut health was warranted. In fact, in addition to the neurological effects of PB/PM exposures, it has been shown that this model produces changes in the gut microbiome; however, it was only examined at an acute time point. Thus, Chapter 4 sought to evaluate the acute and long-term peripheral effects of PB/PM exposure on the gut microbiota and health, and whether LNFPIII would modulate these effects. Using fecal 16S rRNA sequencing, we found that PB/PM altered specific taxa both acutely and long-term; PB/PM elicited more prominent long-term effects, notably, on the abundances of bacteria belonging *Lachnospiraceae* and *Ruminococcaceae* families and the genus *Allobaculum*. Further, LNFPIII improved a marker of gut health (i.e., decreased lipocalin-2) independent of GWI and, importantly, increased butyrate producers (e.g., *Butyricoccus*, *Ruminococcous*) in PB/PM-treated mice. Additionally, multiple operational taxonomic units correlated with aberrant behavior and lipocalin-2 in PB/PM samples; LNFPIII was modulatory. This suggests that the PB/PM induced changes in the gut microbiota may impact the neurological abnormalities observed in Chapter 3. The novel work within Chapter 4 highlights the unknown, chronic interactions between the microbiome and gut health in a GWI context and provides additional support for LNFPIII's beneficial effects on health.

Similar to Chapter 3, Chapter Five investigated the neurobehavioral and neurobiological effects of PB/DEET/CORT/DFP treatment 8-11 months post exposure to characterize the long-term phenotypes of this GWI model; LNFPIII treatment began 1 month prior to behavioral testing (7 months post GWI treatment) and continued until the study completion. Within tests of motor function, prior GW chemical exposure led to

hyperactivity and impaired sensorimotor function. Similar to the PB/PM model, PB/DEET/CORT/DFP led to increases in anxiety-like behavior and impaired short-term recognition memory. LNFPIII attenuated the motor-related deficits, reduced anxiety-like behavior, and improved overall grip strength and short-term memory. Prior exposure to PB/DEET/CORT/DFP also led to increases in glial markers and inflammatory factors (IL-6; Appendix A); LNFPIII reduced this neuroinflammation. Further, prior PB/DEET/CORT/DFP exposure decreased hippocampal basal synaptic transmission and long-term potentiation (LTP) that were recovered by the delayed LNFPIII treatment (Appendix A). The results uncovered here shed light on the previously unknown chronic effects of this treatment paradigm on neurological health. Moreover, they provide supplementary evidence that LNFPIII has positive modulating effects across multiple chemically-induced models of GWI.

Over the past 30 years, numerous clinical imaging studies have revealed alterations in brain structure and function that correspond to behavioral symptoms experienced by GWI veterans that may worsen with age. However, such studies in preclinical settings are limited. Thus, Chapter Six assessed the longitudinal structural brain alterations over the course of 12 months following GW chemicals exposures in both the PB/PM and PB/DEET/CORT/DFP models. Using a Varian 7T MRI System, structural scans were performed at 3, 6, 9, and 12 months post GWI exposures and volumetric analysis within the total brain, ventricles, cortex, hippocampus, cerebellum, and brainstem was conducted. The results of this study provide novel comparative similarities and distinctions between these exposure paradigms and aid in the understanding of GWI pathogenesis. Major similarities among the models included ventricular enlargement, alterations in cerebellar

volumes, and reductions in global brain and hippocampal volumes over time. Key differences were model specific, in which the PB/DEET/CORT/DFP model led to reduced brainstem volumes, while the PB/PM model produced cortical decreases over time. These effects align with previously observed behavioral deficits in these models such as reduced cognitive and motor performance (Chapters 3 and 5). Overall, the effects seen here add translational validity to these models and its utility for evaluation of future GWI neuroprotective interventions, such as LNFPIII.

3. Limitations of Current Studies

While these studies pointed at important new translational nuances across these GWI models, it is imperative to discuss the limitations of the current work. One shortcoming of these studies is all the subjects were male. While the majority of GW soldiers were male, females were also present in theater. In fact, clinical research has shown that female GWI veterans experience heightened symptoms in comparison to their counterparts. Thus, for future investigations, it is essential to evaluate female specific effects, as well as the sex-related differences in GWI.

Another limitation of the long-term studies (Chapters 3 and 5) is the possibility of confounding effects of rigorous behavioral testing. While the battery of testing encompassed many domains (i.e., cognition/memory, mood, and motor), carry over effects, such as stress, may have influenced behavioral results. The behavioral results observed were modest in both models, except for a few measures (i.e., sensorimotor function and cognition/memory). Future investigations utilizing these models should carefully consider reducing the number of behavioral assays and use those in which GWI effects were consistent and/or model-specific.

Moreover, while one of the aims of this dissertation was to evaluate behavioral alterations at a specific time point (e.g., PB/PM 6-8 and PB/DEET/CORT/DFP 8-10 months) post exposure, it would be beneficial, particularly for the PB/DEET/CORT/DFP model, to evaluate the progressive nature of behavioral alterations. This may introduce specific testing confounds, such as decreased sensitivity to a particular assay, but it could provide valuable time-course data for the appearance of certain behavioral aberrations. Utilizing certain behavioral assays, such as the open field which is minimally invasive and measures multiple parameters (e.g., locomotion and mood), at each of the timepoints in Chapter Six would have been beneficial as behavioral alterations over time could have been correlated to changing brain architecture.

Another area that needs addressing is the long-term characterization of the neurochemical and neuroinflammatory profile within the brain. While the acute neurochemical profiles were determined for both models across multiple brain regions, the only long-term monoaminergic characterization was on striatal dopamine in the long term PB/PM study. It would be of great interest to evaluate via HPLC neurochemistry (monoamines and amino acids), in brain regions that govern the behavioral alterations observed in these studies, such as the prefrontal cortex, motor cortex, and amygdala. Additionally, evaluations into the long-term neuroinflammatory profile in brain regions other than the hippocampus could benefit the results of the behavioral and structural data observed within these studies.

While the work in Chapter 4 provided valuable data on the consequences of PB/PM exposure on the host gut microbiota and health, these effects remain unknown within the PB/DEET/CORT/DFP model both acutely and chronically. Given similarities in these

models producing neuroinflammatory and behavioral alterations, it is postulated that the PB/DEET/CORT/DFP model would also elicit increases in gut pathological bacteria and inflammation; however, this warrants future investigation. As gastrointestinal complaints are high among GWI veterans, this data would provide important characterization and distinctions among these exposure paradigms, that would aid in targeted therapeutic development.

Finally, a large number of the LNFPIII effects observed within these studies were modest in nature and failed to reach statistical significance, which suggests that a higher dose may produce a more therapeutic advantage in modulating GWI induced effects. Albeit time consuming, utilizing varying concentrations of LNFPIII in these studies may have provided additional insights to the beneficial properties of this treatment. Future studies should consider adopting low and high LNFPIII concentrations (35 or 50 μg) to the study design to address this limitation. Additionally, all doses of LNFPIII were administered subcutaneously to mice. It would be valuable to evaluate a more minimally invasive route of administration (i.e., intranasal) for, ultimately, future use by GWI veterans.

4. Conclusions

GWI remains a progressive, persistent illness among GW veterans characterized by a number of neurological aberrations and without long-term efficacious treatment options (White et al., 2016; Zundel et al., 2019). Thus, understanding the heterogenous neurological pathology and its mechanisms for a targeted therapeutic approach is imperative. The research summarized here showcases the acute and chronic similarities and differences among the PB/PM and PB/DEET/CORT/DFP preclinical GWI models, all while providing highly translational data (e.g., neurobehavioral alterations,

neuroinflammation, and brain structural changes) to the human disease (Alshelh et al., 2020; Chao et al., 2011; Chao et al., 2016; Chao et al., 2010; Chao et al., 2015; White et al., 2016) . It addressed substantial knowledge gaps among these models, such as the acute neurochemical and neuroinflammatory profile in multiple brain regions, chronic effects of GWI exposures on behavior, neuroinflammation, and gut health, as well as characterizing the longitudinal alterations in brain architecture. Further, these findings demonstrate the beneficial effects of LNFPIII treatment on these measures and indicate it could be a potential GWI therapeutic in a clinical setting. However, as mentioned earlier, future investigations into these models are warranted to characterize other progressive clinical GWI symptoms, such as gastrointestinal disturbances that may influence neurological parameters. Additionally, further evaluation of LNFPIII is warranted, as an increased concentration of this treatment may substantially reduce GWI impairments in these models. Collectively, the work described herein highlights the complex pathology and behavioral phenotypes produced by two, chemically distinct preclinical GWI models at varying stages of life, and how in numerous measures, the immunotherapeutic LNFPIII ameliorated GWI induced neuropathology.

References

Alshelh, Z., Albrecht, D.S., Bergan, C., Akeju, O., Clauw, D.J., Conboy, L., Edwards, R.R., Kim, M., Lee, Y.C., Protsenko, E., Napadow, V., Sullivan, K., Loggia, M.L., 2020. In-vivo imaging of neuroinflammation in veterans with Gulf War illness. Brain, Behavior, and Immunity 87, 498-507.

Chao, L.L., Abadjian, L., Hlavin, J., Meyerhoff, D.J., Weiner, M.W., 2011. Effects of low-level sarin and cyclosarin exposure and Gulf War Illness on Brain Structure and Function: A study at 4T. NeuroToxicology 32(6), 814-822.

Chao, L.L., Reeb, R., Esparza, I.L., Abadjian, L.R., 2016. Associations between the self-reported frequency of hearing chemical alarms in theater and regional brain volume in Gulf War Veterans. Neurotoxicology 53, 246-256.

Chao, L.L., Rothlind, J.C., Cardenas, V.A., Meyerhoff, D.J., Weiner, M.W., 2010. Effects of low-level exposure to sarin and cyclosarin during the 1991 Gulf War on brain function and brain structure in US veterans. Neurotoxicology 31(5), 493-501.

Chao, L.L., Zhang, Y., Buckley, S., 2015. Effects of low-level sarin and cyclosarin exposure on white matter integrity in Gulf War Veterans. Neurotoxicology 48, 239-248.

White, R.F., Steele, L., O'Callaghan, J.P., Sullivan, K., Binns, J.H., Golomb, B.A., Bloom, F.E., Bunker, J.A., Crawford, F., Graves, J.C., Hardie, A., Klimas, N., Knox, M., Meggs, W.J., Melling, J., Philbert, M.A., Grashow, R., 2016. Recent research on Gulf War illness and other health problems in veterans of the 1991 Gulf War: Effects of toxicant exposures during deployment. Cortex 74, 449-475.

Zundel, C.G., Krengel, M.H., Heeren, T., Yee, M.K., Grasso, C.M., Janulewicz Lloyd, P.A., Coughlin, S.S., Sullivan, K., 2019. Rates of Chronic Medical Conditions in 1991 Gulf War Veterans Compared to the General Population. Int J Environ Res Public Health 16(6).

APPENDIX A

LACTO-N-FUCOPENTAOSE-III AMELIORATES ACUTE AND PERSISTING HIPPOCAMPAL SYNAPTIC PLASTICITY AND TRANSMISSION DEFICITS IN A GULF WAR ILLNESS MOUSE MODEL

Kyle A. Brown, Jessica M. Carpenter, Collin J. Preston, Helaina D. Ludwig, Kendall B. Clay, Donald A. Harn, Thomas Norberg, John J. Wagner, Nikolay M. Filipov
Published in *Life Sciences* 2021.
Reprinted here with the permission of publisher.

Abstract

Aims

The present study investigated if treatment with the immunotherapeutic, Lacto-N-fucopentaose-III (LNFPIII), resulted in amelioration of acute and persisting deficits in synaptic plasticity and transmission as well as trophic factor expression along the hippocampal dorsoventral axis in a mouse model of Gulf War Illness (GWI).

Main methods

Mice received either coadministered or delayed LNFPIII treatment throughout or following, respectively, exposure to a 15-day GWI induction paradigm. Subsets of animals were subsequently sacrificed 48 h, seven months, or 11 months post GWI-related (GWIR) exposure for hippocampal qPCR or in vitro electrophysiology experiments.

Key findings

Progressively worsened impairments in hippocampal synaptic plasticity, as well as a biphasic effect on hippocampal synaptic transmission, were detected in GWIR-exposed animals. Dorsoventral-specific impairments in hippocampal synaptic responses became more pronounced over time, particularly in the dorsal hippocampus. Notably, delayed LNFPIII treatment ameliorated GWI-related aberrations in hippocampal synaptic plasticity and transmission seven and 11 months post-exposure, an effect that was consistent with enhanced hippocampal trophic factor expression and absence of increased interleukin 6 (IL-6) in animals treated with LNFPIII.

Significance

Approximately a third of Gulf War Veterans have GWI; however, GWI therapeutics are presently limited to targeted and symptomatic treatments. As increasing evidence

underscores the substantial role of persisting neuroimmune dysfunction in GWI, efficacious neuroactive immunotherapeutics hold substantial promise in yielding GWI remission. The findings in the present report indicate that LNFPIII may be an efficacious candidate for ameliorating persisting neurological abnormalities presented in GWI.

Abbreviations: ACSF, artificial cerebrospinal fluid; BDNF, brain-derived neurotrophic factor; CNTF, ciliary neurotrophic factor; DEET, N,N-diethyl-meta-tolua-mide; DFP, diisopropylfluorophosphate; dH, dorsal hippocampus; ERK-1/2, extracellular signal-regulated kinase-1/2; fEPSP, field excitatory postsynaptic potential; GWI, Gulf War Illness; GWIR, Gulf War Illness-related; GWV, Gulf War Veterans; IL-6, interleukin 6; IL-1β, interleukin-1 beta; LNFPIII, Lacto-N-fucopentaose-III; LTP, long-term potentiation; NGF, nerve growth factor; PB, pyridostigmine bromide; PPF, paired-pulse facilitation; SYP, synaptophysin; TNFα, tumor necrosis factor alpha; vH, ventral hippocampus

Keywords

Hippocampus, Electrophysiology, Gulf War Illness, Synaptic plasticity, Synaptic transmission, Diisopropylfluorophosphate (DFP), Pyridostigmine bromide (PB), DEET, Lacto-N-fucopentaose-III (LNFPIIII), Growth factors

1. Introduction

Gulf War Illness (GWI) is a chronic multisymptom condition that affects approximately one-third of the 700,000 U.S. military personnel deployed in the 1990–1991 Gulf War [1]. Neurological (i.e., cognitive) and immunological (i.e., inflammation) deficits feature in GWI prominently [1]. Although the etiology of GWI is unknown, overexposures to neurotoxic pesticides, organophosphate (OP) nerve agents, nerve agent prophylactics, and wartime stress have been associated with GWI symptoms [[2], [3], [4]]. GWI symptom severity is correlated to the degree, duration, and type of GWI-related (GWIR) exposures [2,5]. Notably, the reported incidence [6] and symptom severity [7,8] of GWI have increased over time, suggesting disease progression. This underscores the critical need to employ GWI animal models reflecting the progressive nature of the disease and use such models for identifying efficacious GWI therapeutics.

GWI models have been established in the mouse [9,10]. These models recapitulate GWI by utilizing GWIR chemical exposures that, in some models, are interfaced with modeling of stress-like conditions, i.e., by administering glucocorticoids such as corticosterone (Cort) [10]. GWIR chemicals used to recapitulate GWI include pesticides such as N,N-diethyl-meta-toluamide (DEET), nerve agent prophylactics such as pyridostigmine bromide (PB), and a nerve agent surrogate, diisopropylfluorophosphate (DFP) [10]. DEET preferentially targets insect olfactory receptors; however, reports have indicated that overexposures may produce mammalian toxicity [11]. The carbamate PB, a reversible acetylcholinesterase (AChE) inhibitor, functions as a nerve agent prophylactic in the absence of stress; however, during chronic stress, PB might cross the blood-brain barrier and be neurotoxic [12,13]. Military operations during the GW exposed thousands

of U.S. personnel to low levels of OP nerve agent, making the incorporation of a relatively less volatile OP like DFP an appropriate component of recapitulating GWIR exposures [14,15].

While a number of preclinical and clinical studies have evaluated potential GWI therapeutics (Reviewed in: [16,17]), only symptomatic treatments are available. Increasing evidence indicates that prolonged symptoms of GWI are a result of neuroimmune dysfunction [[18], [19], [20]]. Inhibition of pro-inflammatory cytokines is a strategy that holds potential for extended remission of GWI [21]; however, studies employing immunotherapeutics to target persisting GWI-induced immune system dysregulation are limited. We previously demonstrated that the neoglycoconjugate Lacto-N-fucopentaose-III (LNFPIII) is a safe and efficacious agent for restoring central and peripheral immune function in disease states [[22], [23], [24]]. This neoglycoconjugate induces therapeutic effects, in part, by rebalancing the anti-inflammatory: inflammatory cytokine milieu, but it also directly stimulates the mitogen-activated protein kinase ERK-1/2 [23]. Importantly, we reported recently that LNFPIII rebalanced short-term neurochemical and inflammatory-related aberrations in two GWI models [25] and it ameliorated gut dysbiosis and inflammation when treatment was initiated months after GWIR exposures [26]. However, LNFPIII's efficacy in a progressive model of GWI is unknown.

Reports of impaired hippocampal-dependent behavior in GWI animal models [[27], [28], [29]] and GW veterans [5,30,31] are abundant. Persisting hippocampal structural abnormalities have been documented in clinical GWI studies [[31], [32], [33]]. Loss of hippocampal principal cells and interneurons [27,34,35] and aberrant glial activity [34,36,37] in GWI models have also been characterized. Electrophysiological studies

describing alterations in hippocampal synaptic plasticity or transmission in GWI models are sparse. The available preclinical reports indicate that glutamatergic, GABAergic, and dopaminergic synaptic plasticity and transmission are impaired in GWI [27,38]. Yet, studies accounting for the progressive nature of GWI that are focused on hippocampal neurophysiology are critically needed but unavailable. Accordingly, we evaluated the efficacy of LNFPIII in ameliorating acute and persisting electrophysiological, trophic factor, and cytokine aberrations presented in the well-established PB/DEET/CORT/DFP GWI model [10].

2. Materials and methods

2.1. Animal maintenance

Male C57BL/6J (Jackson Laboratory, Bar Harbor, ME) mice, aged eight-nine weeks, were housed in groups of five. Animals were acclimated to their home cages for at least one week after arrival and were maintained on a 12 h light/dark cycle (lights on from 0700 to 1900 h). Food and water were provided ad libitum. Following acclimation, animals were randomly assigned to one of four treatment groups: vehicle-vehicle, vehicle-LNFPIII, GWI-vehicle, and GWI-LNFPIII groups. All experiments were approved in advance by the University of Georgia Animal Care and Use Committee and were in accordance with the latest NIH and ARRIVE guidelines.

2.2. Materials

The following chemicals were used for animal treatments: corticosterone (Cort; Steraloids, Newport, RI), N,N-diethyl-meta-toluamide (DEET; Sigma Aldrich, St. Louis, MO), diisopropylfluorophosphate (DFP; Sigma Aldrich), and pyridostigmine bromide (PB; Sigma Aldrich). Lacto-N-fucopentaose-III (LNFPIII) dextran conjugate was

produced as previously described [23]. All additional chemicals and reagents used in this study, unless otherwise noted, were of analytical or higher grade and were obtained from Sigma Aldrich or Fisher Scientific (Hampton, NH).

2.3. GWI exposure protocol

The exposure protocol has been previously described [10,25] and is presented in Fig. 1A. Briefly, mice from the GWI-vehicle and GWI-LNFPIII groups were treated with a combination of PB (2 mg/kg, subcutaneous [s.c.]) and DEET (30 mg/kg, s.c.) daily for 14 days. PB and DEET were both delivered in 0.9% saline. Home cage drinking water of GWI-vehicle and GWI-LNFPIII groups was supplemented with Cort (200 mg/L in 1.2% ethanol [EtOH]) on days 8–14 to emulate combat-related stress. Following the same timeline as described for GWI-vehicle and GWI-LNFPIII treatment groups, vehicle-vehicle and vehicle-LNFPIII treated animals received saline vehicle injections and 1.2% EtOH/water. On day 15, animals from the GWI-vehicle and GWI-LNFPIII groups received a single injection of DFP (3.75 mg/kg, intraperitoneal [i.p.] in sterile saline). Vehicle-vehicle and vehicle-LNFPIII treated animals were treated with the saline vehicle (i.p.). The LNFPIII dosage used in the present report was selected based on our previous studies [[22], [23], [24], [25], [26],39,40]. Animals received vehicle carrier or LNFPIII treatment based on the following timelines:

2.4. Acute effects time point

The exposure protocol and electrophysiology schedule are presented in Fig. 1A. A subset of animals was selected to evaluate the acute effects of GWIR exposure, as well as the efficacy of LNFPIII coadministration in ameliorating GWIR exposure effects. On days 1–14, mice from the vehicle-LNFPIII and GWI-LNFPIII groups received daily treatments

of LNFPIII (35 μg/mouse, s.c.) whereas mice from the vehicle-vehicle and GWI-vehicle groups received equivalent amounts of the dextran vehicle carrier (35 μg/mouse, s.c.) diluted in sterile saline. Animals were sacrificed for experiments 48 h post GWIR exposure ± LNFPIII treatment. The bodyweight of animals sacrificed at the acute time point was monitored daily for the duration of the study as well as immediately prior to sacrifice for electrophysiology experiments.

2.5. Early persisting time point

The exposure protocol and electrophysiology schedule are presented in Fig. 2A. A subset of animals was utilized to evaluate the early persisting effects of GWIR exposure, as well as the efficacy of delayed LNFPIII treatment in ameliorating GWIR exposure-induced abnormalities seven months after exposure termination. Notably, these animals did not receive vehicle or LNFPIII during the GWIR exposure duration. Vehicle or LNFPIII treatment (35 μg/mouse, s.c.) began four months after GWIR exposure termination and continued twice per week until the animals were sacrificed for electrophysiology experiments three months later (seven months post GWIR exposure).

2.6. Late persisting time point

The exposure protocol and electrophysiology schedule are presented in Fig. 3A. A subset of animals was used to evaluate the late persisting effects of GWIR exposure and the efficacy of delayed LNFPIII treatment in ameliorating GWIR exposure-induced abnormalities 11 months after exposure. Mice began receiving vehicle or LNFPIII treatment eight months post GWIR exposure, which continued twice per week until the animals were sacrificed for electrophysiology experiments three months later (11 months post GWIR exposure termination).

Bodyweight of the animals used for the early and late persisting time points was recorded every other week for the duration of the study, as well as immediately before sacrifice for electrophysiology experiments.

2.7. Slice preparation and electrophysiology

Hippocampal slice preparation and electrophysiology experiments were conducted as previously described [41,42]. Briefly, mice were sacrificed following deep anesthetization with 2-bromo-2-chloro-1,1,1-trifluoroethane (halothane). Brains were removed and quickly submerged in oxygenated (95% O_2/5% CO_2), ice-cold dissection artificial cerebrospinal fluid (dACSF; 120 mM NaCl, 3 mM KCl, 4 mM $MgCl_2$, 1 mM NaH_2PO_4, 26 mM $NaHCO_3$, and 10 mM glucose). A mid-sagittal cut was made, and half of the brain was mounted on its caudal pole and sectioned along the horizontal plane with a vibratome to obtain 400 μm slices containing the dorsal hippocampus. The other half of the brain was mounted on its rostral pole and sectioned along the horizontal plane with a vibratome to acquire 400 μm slices containing the ventral hippocampus. The dorsal hippocampus and ventral hippocampus were subdissected free from the rest of the slice and the CA3 subfield was removed. These slices were then quickly placed in a submersion-type chamber and perfused with oxygenated (95% O_2/5% CO_2) ACSF (120 mM NaCl, 3 mM KCl, 1.5 mM $MgCl_2$, 1 mM NaH_2PO_4, 2.5 mM $CaCl_2$, 26 mM $NaHCO_3$, and 10 mM glucose). Slices were continuously perfused with ACSF (one mL/min) during a 45 min recovery period at room temperature followed by a 45 min recovery period at the recording temperature of 30 °C. Schaffer collateral fibers were stimulated by placing a bipolar electrode (Kopf Instruments, Tujunga, CA) in the stratum radiatum of the CA1 subfield; a 1.0 MΩ tungsten recording microelectrode (World Precision Instruments, Sarasota, FL)

was inserted in the same layer of CA1. During recording experiments, a stimulus pulse was applied once every minute to elicit responses from Schaffer collateral-CA1 synapses.

An input-output curve (I/O curve) was acquired at the beginning of each experiment by incrementally applying individual 15 μA stimulus pulses from 45 to 180 μA in intensity. The fEPSP slope (mV/ms) was measured in a one ms interval immediately following the fiber volley. After recording the I/O curve, the stimulus intensity was modified to elicit 35% of the maximal fEPSP slope and paired-pulse fEPSPs (50 ms interpulse interval) were recorded each minute for 5 min. Individual stimulus pulses were then applied each min for 30 min and baseline fEPSP responses were monitored. After recording baseline responses for 30 min, a high-frequency stimulation (HFS) protocol (three × 100 Hz/one-*sec* train at 20-s intervals) was utilized to induce long-term potentiation (LTP) and fEPSP responses were monitored for the subsequent 60 min. fEPSP responses were normalized to the average fEPSP slope value recorded during 26–30 min of baseline recording. LTP magnitude was calculated by averaging the normalized fEPSP slope values from 56 to 60 min post-HFS.

2.8. Quantitative PCR (qPCR) analysis

Analyses were completed on brain tissue (48 h: ventral hippocampus; 11 months: dorsal hippocampus and ventral hippocampus) as described in [25]. Briefly, total RNA from a single hippocampal brain punch (1.5 mm diameter, 500 μm thick section) was isolated by an E.Z.N.A total RNA isolation kit (Omega Bio-Tek, Norcross, GA) according to the manufacturer's directions. RNA was quantified with a Take3 micro-volume plate and Epoch microplate spectrophotometer (BioTek, Winooski, VT). Seventy-five ng RNA/sample was used to synthesize cDNA with a Maxima first-strand cDNA synthesis kit

for RT-qPCR (Thermo Fisher Scientific, Waltham, MA) and a PTC-200 Peltier thermal cycler (Bio-Rad, Hercules, CA; 10 min at 25 °C, 15 min at 50 °C, 5 min at 85 °C). Using one or two ng of cDNA per sample, expression of various inflammatory genes and growth factors was determined by a qPCR with mouse-specific primers (RealTimePrimers, Elkins Park, PA) and Maxima SYBR Green/lowRox qPCR Master Mix (2×) (Thermo Fisher Scientific, Waltham, MA). Amplifications were performed on Mx3005 P qPCR machine (Stratagene, San Diego, CA) programed for initial warming cycle (95 °C, 10 min) followed by 45 cycles (95 °C, 15 s, 60 °C, 1 min) with each sample run in duplicate. Primer sequences are listed in Table 1.

2.9. Data analysis

Electrophysiology data was digitized at 10 kHz, low-pass filtered at 1 kHz, and analyzed with pCLAMP 10.2 software (Axon Instruments, Sunnyvale, CA). Electrophysiology statistical analysis was completed using R version 4.0.2 (The R Foundation for Statistical Computing, Vienna, Austria). For electrophysiology data, statistical analysis was completed by using the aov() function for analysis of variance (ANOVA), the PostHocTest() function under the DescTools package (version 0.99.38) for Student-Newman-Keuls post hoc test, and the t.test function for preplanned Student's *t*-tests. Graphic production was completed using GraphPad Prism 8.0 (GraphPad Software Inc., San Diego, CA). Electrophysiology data were analyzed via two-way ANOVA with factor A being GWI treatment (vehicle or GWIR treatment) and factor B being LNFPIII treatment (vehicle or LNFPIII treatment). If a two-way ANOVA was significant ($p \leq 0.05$), treatment means were separated via Student-Newman-Keuls post hoc test or pairwise comparisons (as appropriate). An α level of 0.05 was used as the criterion for statistical

significance. Reported n-values (x(y)) indicate the number of slices (x) and the number of mice (y) assessed. All data are presented as mean ± SEM. Treatment differences detected in qPCR data were calculated using the $^{\Delta\Delta}$Ct method, analyzed and presented as a fold change normalized to 18S as the housekeeping gene, as described previously [25,43,44].

3. Results

3.1. Coadministration of LNFPIII enhanced LTP magnitude whereas both GWIR exposure and LNFPIII treatment increased hippocampal basal synaptic transmission 48 h post-exposure

The GWIR exposure ± LNFPIII coadministration timeline is represented in Fig. 1A. No significant main effect of GWIR exposure on LTP was observed 48 h post-exposure ($p = 0.80$; Fig. 1B, C, D). Coadministration of LNFPIII resulted in a significant main effect of LNFPIII on LTP magnitude 48 h post GWIR/LNFPIII treatments ($p = 0.018$; Fig. 1B, C, D). An interaction effect between GWIR X LNFPIII on LTP magnitude approached significance ($p = 0.077$). A post hoc comparison revealed a significant LTP enhancement in vehicle-LNFPIII animals compared to vehicle-vehicle animals ($p = 0.006$; Fig. 1D).

Significant main GWIR (p's < 0.05; stimulus intensities: 45–180 μA) and LNFPIII (p's = 0.05; stimulus intensities: 105–180 μA) effects on basal synaptic transmission were detected, resulting in increased basal synaptic activity 48 h post-exposure (Fig. 1E). A main effect of LNFPIII treatment on basal synaptic transmission approached significance at stimulus intensities of 75 and 90 μA ($p < 0.1$). A post hoc analysis showed significant ($p < 0.05$) increases in basal synaptic transmission in GWI-vehicle mice compared to vehicle-vehicle mice at 60, 75, 90, 105, 120, 135, 150, 165, and 180 μA stimulus

intensities. Additionally, significant increases in basal synaptic transmission in GWI-LNFPIII mice compared to GWI-vehicle mice at stimulus intensities of 45, 120, 135, 150, 165, and 180 μA were observed ($p < 0.05$). Finally, basal synaptic transmission in vehicle-LNFPIII mice compared to vehicle-vehicle mice was increased at stimulus intensities of 105, 120, 135, 150, 165, and 180 μA ($p < 0.05$). Neither GWIR exposure ($p = 0.67$) nor LNFPIII treatment ($p = 0.27$) had a significant main effect on paired-pulse facilitation (PPF; Fig. 1F).

3.2. LTP magnitude is reduced seven months after GWIR exposure, a reduction that is ameliorated by LNFPIII treatment initiated four months after GWIR exposure termination

Four months after GWIR exposure termination, a subset of animals began receiving vehicle or LNFPIII treatment twice per week until the animals were sacrificed for electrophysiology experiments (Fig. 2A). Following three months of vehicle or LNFPIII treatment (seven months post GWIR exposure termination), we found a significant effect of LNFPIII treatment on LTP magnitude in GWIR exposed animals ($p = 0.027$), resulting in a trending main effect of LNFPIII on LTP ($p = 0.09$; Fig. 2B, C, D). Specifically, a trend of a significant difference in LTP magnitude between vehicle-vehicle and GWI-vehicle animals was observed ($p = 0.063$), whereas a significant decrease in LTP magnitude in GWI-vehicle animals compared to GWI-LNFPIII animals was detected ($p = 0.013$; Fig. 2D). No significant differences in LTP magnitude between vehicle-vehicle, vehicle-LNFPIII, and GWI-LNFPIII animals were revealed ($p's \geq 0.34$).

Interestingly, no significant main effects of GWIR exposure or LNFPIII treatment on basal synaptic transmission were detected at any assessed stimulation intensity

(p's ≥ 0.17; Fig. 2E). Similar to the 48 h time point, no significant main effects of GWIR exposure ($p = 0.44$) or LNFPIII treatment ($p = 0.80$) on PPF were found (Fig. 2F).

3.3. Dorsal hippocampal LTP magnitude and basal synaptic transmission is reduced 11 months after GWIR exposure, an effect that is ameliorated by delayed LNFPIII treatment

Eight months after GWIR exposure termination, a subset of animals began receiving LNFPIII or vehicle treatment twice per week until the end of the study (Fig. 3A). Following three months of LNFPIII or vehicle treatment (11 months post GWIR exposure), a significant main effect of GWIR exposure, driven by the decrease in the GWI-vehicle group, on dorsal hippocampal (dH) LTP magnitude was revealed ($p = 0.029$; Fig. 3B, C, D). A trend of a significant LNFPIII main effect on dH LTP magnitude was also observed ($p = 0.076$) and it was due to the LNFPIII's ability to ameliorate the effect of GWIR exposure (Fig. 3D). There was a trend for an interaction effect between GWIR X LNFPIII on LTP magnitude as well ($p = 0.096$). A post hoc comparison revealed that the decrease in dH LTP magnitude of GWI-vehicle animals compared to vehicle-vehicle animals was significant ($p = 0.003$). Importantly, dH LTP magnitude of GWI-LNFPIII animals was significantly greater compared to the dH LTP magnitude of GWI-vehicle animals ($p = 0.016$; Fig. 3C, D). No significant differences in LTP magnitude between vehicle-vehicle, vehicle-LNFPIII, and GWI-LNFPIII animals were observed in the dH (p's ≥ 0.47).

In contrast to our findings 48 h and seven months post GWIR exposure, a significant reduction in dH basal synaptic transmission was detected 11 months post-exposure (Fig. 3E). Specifically, a significant main effect of GWIR exposure on dH basal synaptic transmission was found at stimulation intensities of 75–180 μA (p's < 0.05);

60 μA, the GWIR exposure effect was only a trend ($p < 0.1$). A post hoc analysis indicated that the decreases in dH basal synaptic transmission in GWI-vehicle mice compared to vehicle-vehicle mice at stimulus intensities of 60, 75, 90, 105, 120, 135, 150, 165, and 180 μA were significant ($p < 0.05$). Moreover, a significant increase in dH basal synaptic transmission in GWI-LNFPIII mice compared to GWI-vehicle mice was displayed at stimulus intensities of 120, 135, and 180 μA ($p < 0.05$); at 165 μA stimulus intensity, this effect was trending ($p < 0.1$). No significant difference in dH basal synaptic transmission between vehicle-vehicle and vehicle-LNFPIII-treated animals was detected ($p > 0.05$). Similar to the other time points, there were no significant main effects of GWIR exposure ($p = 0.31$) or LNFPIII treatment ($p = 0.75$) on PPF in the dH (Fig. 3F).

3.4. Ventral hippocampal basal synaptic transmission is reduced 11 months after GWIR exposure, an effect that is ameliorated by delayed LNFPIII treatment

Interestingly, there was no significant main effect of GWIR exposure on ventral hippocampal (vH) LTP magnitude ($p = 0.75$); however, a significant main effect of LNFPIII led to an increase in vH LTP magnitude ($p = 0.019$; Fig. 4A, B, C). Notably, due to a numeric decrease in GWI-vehicle and an increase in GWI-LNFPIII animals, vH LTP magnitude of the GWI-LNFPIII group was significantly greater compared to GWI-vehicle animals ($p = 0.003$; Fig. 4C). No significant differences in LTP magnitude between vehicle-vehicle, vehicle-LNFPIII, GWI-LNFPIII animals were observed in the vH (p's ≥ 0.18).

Additionally, a significant main effect of GWIR exposure on basal synaptic transmission was found in the vH at stimulus intensities of 135–180 μA (p's < 0.05; Fig. 4D). There was not a significant main effect of GWIR exposure on basal synaptic

transmission at stimulus intensities of 105 and 120 μA, but it approached significance ($p < 0.1$). A post hoc analysis found a significant decrease in vH basal synaptic transmission in GWI-vehicle animals compared to vehicle-vehicle animals at stimulus intensities of 135, 150, 165, and 180 μA ($p < 0.01$). Compared to vehicle-vehicle animals, a trend of a decrease in vH basal synaptic transmission in GWI-vehicle animals that approached significance ($p = 0.055$) was detected at 120 μA. A significant increase in the maximal basal synaptic response elicited in the vH of GWI-LNFPIII mice compared to GWI-vehicle mice was also found ($p = 0.035$). No significant difference in vH basal synaptic transmission between vehicle-vehicle and vehicle-LNFPIII treated animals was present ($p > 0.05$). Similar to the dH, no significant main effects of GWIR exposure ($p = 0.81$) or LNFPIII treatment ($p = 0.22$) on PPF were detected in the vH (Fig. 4E).

3.5. Coadministration of LNFPIII with GWIR treatment or delayed LNFPIII treatment differentially enhanced the production of trophic factors along the hippocampal dorsoventral axis

The expression of key inflammatory mediators (caspase 1, IL-6, IL-1β, and TNFα) and trophic factors (brain-derived neurotrophic factor [BDNF], nerve growth factor [NGF], and ciliary neurotrophic factor [CNTF]) were assessed in the vH 48 h post GWIR exposure ± LNFPIII coadministration (Table 2). No significant effects of GWIR exposure or LNFPIII treatment on vH inflammatory markers were detected via qPCR, but there were numerical increases of IL-6, IL-1β and TNFα in the GWI-vehicle group at this time point ($p > 0.05$; Table 2). Interestingly, both BDNF and NGF expression increases were detected in GWI-LNFPIII animals compared to vehicle-vehicle animals 48 h post-exposures, with the effect on BDNF being significant ($p = 0.04$). While the NGF increase

in the GWI-LNFPIII group compared to the vehicle-vehicle was only numeric, there was a stronger trend for an elevation in vH NGF expression when GWI-LNFPIII NGF was compared to GWI-vehicle NGF 48 h post-exposure ($p = 0.08$).

Additionally, trophic factor and selected cytokine expression were evaluated in both the dH and the vH 11 months post GWIR exposure with LNFPIII treatment beginning eight months post-exposure (Table 3). A trend for a significant increase in dH BDNF expression in GWI-LNFPIII animals compared to vehicle-vehicle animals was revealed ($p = 0.10$). Importantly, there was a trend for enhancement of dH BDNF expression in GWI-LNFPIII animals compared to GWI-vehicle animals that approached significance ($p = 0.06$). Notably, significant elevations in dH NGF levels in vehicle-LNFPIII animals compared to vehicle-vehicle animals ($p = 0.03$) as well as in GWI-LNFPIII animals compared to vehicle-vehicle animals ($p = 0.001$) were observed. A trend of a significant increase in dH NGF levels was detected in GWI-vehicle animals compared to vehicle-vehicle animals ($p = 0.08$); this trend was stronger in GWI-LNFPIII animals compared to GWI-vehicle animals was present ($p = 0.06$). Further, there was a significant increase in dH IL-6 levels for GWI-vehicle animals compared to vehicle-vehicle animals ($p = 0.02$). In the vH, there were no significant differences in BDNF or NGF expression between treatment groups, although all three trophic factors were numerically reduced in GWI-vehicle animals compared to vehicle-vehicle animals, something not seen in the vH of the GWI-LNFPIII mice. Of the numeric decreases of vH trophic factors in the GWI-vehicle group, the decrease of CNTF was most pronounced ($p = 0.07$). There were no significant differences in IL-6 expression between treatment groups in the vH.

4. Discussion

GWI models have been developed in the mouse [9,10] and the rat [45,46]. Acute studies employing the model used in the present report (or a modification of it) described neurochemical abnormalities within 6 h after GWIR exposure such as dyshomeostasis of monoaminergic neurotransmitters in limbic structures [25] and notable reductions in brain AChE specific activity that led to enhanced brain ACh levels [47]. In general, cholinergic transmission is impacted by acute exposure to AChE inhibitors, such as PB and DFP, resulting in learning and memory modulation [48]. Acute PB and DEET exposure has also been shown to increase hippocampal pyramidal cell excitability, an effect attributed to enhanced cholinergic transmission [11,13]. Additionally, mice that received repeated exposure to chlorpyrifos, an OP that shares the same mechanism as DFP and has been implicated in GWI etiology, exhibited enhanced hippocampal basal synaptic transmission one-week post-chlorpyrifos exposure [49]. Chlorpyrifos exposure increased phosphorylation of extracellular signal-regulated kinase-1/2 (ERK-1/2) and enhanced the secretion of neurotrophic factors such as BDNF [50,51]. Phosphorylation of ERK-1/2 is essential for facilitating the signaling cascade that results in BDNF-induced increases in hippocampal spine density [52] and synaptic transmission [53]. The present report demonstrated a significant increase in hippocampal basal synaptic transmission 48 h post GWIR exposure, which is consistent with the aforementioned studies. We postulate that this increase in basal synaptic transmission is due to elevated cholinergic activity, enhanced ERK-1/2 activation, and increased hippocampal BDNF, all of which are supported by the observed numerical and significant enhancement of vH BDNF mRNA levels in GWI-LNFPIII and GWI-vehicle animals, respectively. The modest numerical increase in LTP

magnitude in GWI-vehicle and GWI-LNFPIII animals detected 48 h post-GWIR exposure is also consistent with an enhanced cholinergic tone as well as ERK-dependent BDNF expression.

Acute neuroimmune abnormalities induced by the GWI exposure model used in the present study have been characterized. Specifically, an increase of multiple inflammatory cytokines in the brain [54], detrimental effects on prefrontal cortex glia functionality [36], and neuroinflammatory-related structural anomalies in the hippocampus [55] are among these acute effects. These data are in line with acute neuroimmune dysfunction reported in other GWI animal models [[56], [57], [58]], consistent with the hypothesis of GWI being a neuroimmune disease [59]. Notably, some studies have found beneficial effects of immunoactive therapies on components of GWI [10,60]. The potential therapeutic, LNFPIII, investigated in the present study utilizes the CD14/TLR-MAPK (ERK) axis to induce anti-inflammatory chemokine and cytokine production, facilitating ERK-1/2 phosphorylation [23]. In the current report, we did not detect significant differences in key inflammatory markers in the vH 48 h post-exposure, a finding that is consistent with investigations demonstrating that inflammatory cytokine production peaks within 6 h after exposure and subsequently returns to baseline levels in this GWI model [10,25,61]. However, coadministration of LNFPIII throughout GWIR exposure resulted in a significant enhancement of synaptic transmission and LTP, which is in line with a direct [23], likely BDNF-mediated effect. These results would also be consistent with LNFPIII shaping synaptic plasticity via diffuse, anti-inflammatory effects [62]. Finally, as we found no changes in paired-pulse facilitation (PPF) at the acute time point, a postsynaptic mechanism was likely responsible for the observed enhancement. These

electrophysiological data are consistent with an increase in synaptic density, suggesting that LNFPIII-mediated enhancement of trophic factor production may also enhance synaptic transmission and LTP via modulation of structural plasticity 48 h post-exposure.

While our findings at the acute time point indicate LNFPIII can affect measures of synaptic plasticity and transmission and trophic factor levels, the results reported at the persisting time points underscore the potential therapeutic efficacy of LNFPIII for the treatment of GWI. Importantly, the 11-month duration of rodent aging between GWI induction and electrophysiology recordings recapitulates the aging process of GW veterans [63], suggesting translational relevance of our results. The acute neuroinflammatory response in GWI models is short-lived; however, months after exposure, re-emerging neuroinflammatory aberrations are present and associate with GWI symptomology [33,64]. Notably, a delayed progressive worsening of clinical GWI symptoms has been established [6,7] and it is attributed, at least in part, to neuroimmune dysfunction [59]. Indeed, preclinical evidence is consistent with this delayed temporal profile. For instance, a recent study using a different GWI animal model than the paradigm employed in the present investigation detected progressive impairments in hippocampal synaptic plasticity and transmission as well as learning and memory, findings that coincided with abnormal neuroimmune cell activity [27]. Collectively, these clinical and preclinical findings indicate that persisting aberrant activation of neuroglia (i.e., microglia and astrocytes) and accompanying dyshomeostasis of cytokine signaling may be a major component underlying GWI pathophysiology. Reports of delayed neuroimmune dysfunction in GWI [19] may be particularly relevant to hippocampal synaptic plasticity and transmission as aging alone leads to neuroinflammatory aberrations and reductions of hippocampal trophic

factor production [65,66], underscoring the necessity to evaluate GWI animal models and the efficacy of GWI therapeutics at clinically relevant time points.

In the present report, following an initial enhancement in basal synaptic transmission 48 h after GWIR exposure, no change was found seven months post-exposure, and a reduction was observed 11 months after exposure. This delayed reduction in hippocampal basal synaptic transmission is consistent with the expected synaptic effects induced by the aforementioned delayed GWIR exposure-induced neuroinflammatory phenotype. Indeed, we detected a persisting increase in the expression of the pro-inflammatory cytokine IL-6 in the dH 11 months after GWIR exposures. While elevated hippocampal IL-6 levels have been described in this animal model at acute time points [10,25], this is the first study using this model to demonstrate persisting IL-6 enhancements. These findings are particularly noteworthy as elevated hippocampal IL-6 levels have been linked to prolonged impairments of synaptic transmission and in learning and memory [67]. Our synaptic transmission results are also in line with a preclinical study demonstrating that exposure to an OP implicated in the etiology of GWI, chlorpyrifos, leads to an initial enhancement of hippocampal synaptic transmission followed by a reduction three months later [49]. This delayed reduction was attributed to a decrease in CA1 apical dendritic spine density. In addition, we found a delayed decrease in LTP magnitude 11 months post-GWIR exposure. As we did not detect any significant changes in PPF at any time point, a postsynaptic, structure-specific effect, such as decreased synaptic density following GWI exposure, is indicated. This is further supported by the apparent reduction in all trophic factors assessed in the vH of GWI-vehicle animals 11 months post-GWIR exposure. Taken together, the findings in the present study are

consistent with a GWIR exposure-induced delayed reduction in CA1 synaptic density, but this structural change has to be verified in the future.

Importantly, delayed LNFPIII treatment restored hippocampal synaptic transmission and LTP seven and 11 months after GWIR exposure. The prolonged impact of delayed LNFPIII treatment on microglia, astrocytes, and/or the CD14/TLR-MAPK (ERK) axis may be responsible for restoring hippocampal synaptic plasticity and transmission. This is supported by studies in which LNFPIII treatment reduced the severity of experimental autoimmune encephalomyelitis by modulating innate and T cell immune responses [24], which are both dysfunctional in GWI [19]. LNFPIII also enhanced IL-10 levels, mitigated chronic inflammation, and restored metabolic function associated with diet-induced obesity [22]. Recent reports by our group demonstrated that LNFPIII treatment rebalanced neurochemical and neuroimmune functionality in multiple GWI animal models, acutely and chronically [25,26]. Therefore, we postulate that one likely reason for the restoration of synaptic transmission and LTP months after GWIR exposure is a result of LNFPIII-mediated anti-inflammatory: inflammatory milieu rebalancing. This effect may be more prominent in the dH given the abrogation of the GWIR effect on IL-6 by LNFPIII in the current study.

We observed an enhancement of hippocampal BDNF and NGF expression in GWI-LNFPIII-treated animals, suggesting that recovery of synaptic transmission and LTP months after GWIR exposure may also be a result of a direct, LNFPIII-induced increase in trophic factor production. This interpretation is consistent with recent reports that also detected aberrant BDNF levels in different GWI models, indicating that trophic factor dysregulation may be a conserved mechanism underlying GWI-like symptoms across

animal models [68,69]. Most notably, the efficacy of delayed LNFPIII treatment on ameliorating GWIR exposure-induced aberrations in hippocampal synaptic measurements and trophic factor levels is particularly encouraging as potential clinical treatment of GWI with LNFPIII would also follow a delayed timeline (i.e., beginning LNFPIII treatment decades after exposure).

The dH and the vH have been increasingly appreciated as functionally distinct structures [70,71]. Monitoring the persisting/delayed dorsoventral-specific impact of neurotoxicant overexposures on measurements of hippocampal synaptic plasticity and transmission may be essential for interpreting subtle behavioral changes described in disease states, such as GWI, especially early in the course of the disease. We observed no distinct dorsoventral-specific effects of GWIR exposure on measurements of synaptic plasticity and transmission at the 48 h and seven-month time points; however, we detected differential responses at the 11-month time point. For instance, we found a significant main effect of GWIR exposure on LTP magnitude in the dH, but not in the vH, a differential response that may be related to the persisting increase in IL-6 levels detected in the dH but not in the vH. We also detected a differential impact of GWIR exposure on trophic factor production in the dH compared to the vH. These findings may provide insight into reports of impairments in dH-dependent spatial memory tasks [34,37,72,73]. Abnormal vH-dependent behavior (i.e., anxiety), while reported, might be less pronounced [34,72,74], at least in GWI models and veterans with GWI that have experienced GWIR exposures in line with the ones of the model used in the current study. Similar to the delayed effects we observed, clinical GWI learning and memory deficits appear to become more marked over time [6,7]. Studies describing hippocampal sector- and subfield-specific structural

abnormalities in GW veterans have also been reported [31,75,76]. As we detected biphasic impairments in synaptic plasticity and transmission that were differentially manifested along the hippocampal dorsoventral axis, accounting for such hippocampal sector-specific effects may be essential for interpreting subtle, progressive neurological alterations presented in GWI. Future studies investigating the beneficial effects of LNFPIII on hippocampal-dependent learning and memory months after GWIR exposure(s) are warranted.

5. Conclusion

Thirty years after the end of the Persian Gulf War, there are no approved neuroactive therapies available for GWI. As understanding persisting/delayed GWI-induced alterations in hippocampal synaptic plasticity and transmission are essential for identifying efficacious therapies to treat cognitive deficits presented in GWI, our findings address a substantial knowledge gap in the field of GWI research. Importantly, our data suggest that LNFPIII treatment, initiated months after exposure to GWIR chemicals and stress, may be an efficacious therapy for restoring cognitive function and mood disorders in GWI.

Funding & disclosures

This research was supported by the Department of Defense (CDMRP grant number W81XWH-16-1-0586) to NMF.

Acknowledgments

KAB, CJP, and HDL received partial support from the Interdisciplinary Toxicology Program and/or the Department of Physiology and Pharmacology of the University of Georgia. Support by the Sharma Distinguished Professorship in Toxicology endowment to NMF is also acknowledged.

References

[1] R.F. White, L. Steele, J.P. O'Callaghan, K. Sullivan, J.H. Binns, B.A. Golomb, F.E. Bloom, J.A. Bunker, F. Crawford, J.C. Graves. Recent research on Gulf War illness and other health problems in veterans of the 1991 Gulf War: effects of toxicant exposures during deployment. Cortex, 74 (2016), pp. 449-475

[2] L. Steele, A. Sastre, M.M. Gerkovich, M.R. Cook. Complex factors in the etiology of Gulf War illness: wartime exposures and risk factors in veteran subgroups. Environ. Health Perspect., 120 (1) (2012), pp. 112-118

[3] N. Cherry, F. Creed, A. Silman, G. Dunn, D. Baxter, J. Smedley, S. Taylor, G.J. MacFarlane. Health and exposures of United Kingdom Gulf war veterans. Part II: the relation of health to exposure. Occup. Environ. Med., 58 (5) (2001), pp. 299-306

[4] W. Winkenwerder. Environmental exposure report: pesticides final report. Department of Defense, Washington, D.C (2003)

[5] K. Sullivan, M. Krengel, W. Bradford, C. Stone, T.A. Thompson, T. Heeren, R.F. White. Neuropsychological functioning in military pesticide applicators from the Gulf War: effects on information processing speed, attention and visual memory. Neurotoxicol. Teratol., 65 (2018), pp. 1-13

[6] C.G. Zundel, M.H. Krengel, T. Heeren, M.K. Yee, C.M. Grasso, P.A. Janulewicz Lloyd, S.S. Coughlin, K. Sullivan. Rates of chronic medical conditions in 1991 gulf war veterans compared to the general population. Int. J. Environ. Res. Public Health, 16 (6) (2019), p. 949

[7] B. Porter, K. Long, R.P. Rull, E.K. Dursa, M.C.S. Team. Prevalence of chronic multisymptom illness/gulf war illness over time among millennium cohort participants, 2001 to 2016. J. Occup. Environ. Med., 62 (1) (2020), pp. 4-10

[8] C.G. Zundel, T. Heeren, C.M. Grasso, A. Spiro III, S.P. Proctor, K. Sullivan, M. Krengel. Changes in health status in the Ft. Devens Gulf War veterans cohort: 1997-2017. Neurosci. Insights, 15 (2020), pp. 1-7

[9] L. Abdullah, G. Crynen, J. Reed, A. Bishop, J. Phillips, S. Ferguson, B. Mouzon, M. Mullan, V. Mathura, M. Mullan. Proteomic CNS profile of delayed cognitive impairment in mice exposed to Gulf War agents. NeuroMolecular Med., 13 (4) (2011), pp. 275-288

[10] J.P. O'Callaghan, K.A. Kelly, A.R. Locker, D.B. Miller, S.M. Lasley. Corticosterone primes the neuroinflammatory response to DFP in mice: potential animal model of Gulf War Illness. J. Neurochem., 133 (5) (2015), pp. 708-721

[11] V. Corbel, M. Stankiewicz, C. Pennetier, D. Fournier, J. Stojan, E. Girard, M. Dimitrov, J. Molgó, J.-M. Hougard, B. Lapied. Evidence for inhibition of cholinesterases in insect and mammalian nervous systems by the insect repellent deet. BMC Biol., 7 (1) (2009), Article 47

[12] D.W. Blick, S.Z. Kerenyi, S. Miller, M.R. Murphy, G.C. Brown, S.L. Hartgraves. Behavioral toxicity of anticholinesterases in primates: chronic pyridostigmine and soman interactions. Pharmacol. Biochem. Behav., 38 (3) (1991), pp. 527-532

[13] A. Friedman, D. Kaufer, J. Shemer, I. Hendler, H. Soreq, I. Tur-Kaspa. Pyridostigmine brain penetration under stress enhances neuronal excitability and induces early immediate transcriptional response. Nat. Med., 2 (12) (1996), p. 1382

[14] R.W. Haley, J.J. Tuite. Epidemiologic evidence of health effects from long-distance transit of chemical weapons fallout from bombing early in the 1991 Persian Gulf War. Neuroepidemiology, 40 (3) (2013), pp. 178-189

[15] W. Winkenwerder. US Demolition Operations at Khamisiyah. Final Report. U.S. Department of Defense, Washington, D.C (2002)

[16] B. Dickey, L.N. Madhu, A.K. Shetty. Gulf war illness: mechanisms underlying brain dysfunction and promising therapeutic strategies. Pharmacol. Ther., 220 (2020), Article 107716

[17] S.M. Nugent, M. Freeman, C.K. Ayers, K.A. Winchell, A.M. Press, M.E. O'Neil, R. Paynter, D. Kansagara. A systematic review of therapeutic interventions and management strategies for Gulf War Illness. Mil. Med., 186 (2020), pp. e169-e178

[18] A.P. Georgopoulos, L.M. James, A.F. Carpenter, B.E. Engdahl, A.C. Leuthold, S.M. Lewis. Gulf War illness (GWI) as a neuroimmune disease. Exp. Brain Res., 235 (10) (2017), pp. 3217-3225

[19] S.S. Coughlin. A neuroimmune model of Gulf War Illness. J. Environ. Health Sci. (2017), p. 3

[20] K.J. Trageser, M. Sebastian-Valverde, S.X. Naughton, G.M. Pasinetti. The innate immune system and inflammatory priming: potential mechanistic factors in mood disorders and gulf war illness. Front. Psychiatry, 11 (2020)

[21] T.J. Craddock, R.R. Del Rosario, M. Rice, J.P. Zysman, M.A. Fletcher, N.G. Klimas, G. Broderick. Achieving remission in Gulf War Illness: a simulation-based approach to treatment design. PLoS One, 10 (7) (2015), Article e0132774

[22] P. Bhargava, C. Li, K.J. Stanya, D. Jacobi, L. Dai, S. Liu, M.R. Gangl, D.A. Harn, C.-H. Lee. Immunomodulatory glycan LNFPIII alleviates hepatosteatosis and insulin resistance through direct and indirect control of metabolic pathways. Nat. Med., 18 (11) (2012), p. 1665

[23] S. Tundup, L. Srivastava, T. Norberg, W. Watford, D. Harn. A neoglycoconjugate containing the human milk sugar LNFPIII drives anti-inflammatory activation of antigen presenting cells in a CD14 dependent pathway. PLoS One, 10 (9) (2015), Article e0137495

[24] B. Zhu, S. Trikudanathan, A.L. Zozulya, C. Sandoval-Garcia, J.K. Kennedy, O. Atochina, T. Norberg, B. Castagner, P. Seeberger, Z. Fabry. Immune modulation by lacto-N-fucopentaose III in experimental autoimmune encephalomyelitis. Clin. Immunol., 142 (3) (2012), pp. 351-361

[25] J. Carpenter, H. Gordon, H. Ludwig, J. Wagner, D. Harn, T. Norberg, N. Filipov. Neurochemical and neuroinflammatory perturbations in two Gulf War Illness models: modulation by the immunotherapeutic LNFPIII. Neurotoxicology, 77 (2020), pp. 40-50

[26] R.S. Mote, J.M. Carpenter, R.L. Dockman, A.J. Steinberger, G. Suen, T. Norberg, D.A. Harn, J.J. Wagner, N.M. Filipov. Assessing the beneficial effects of the immunomodulatory glycan LNFPIII on gut microbiota and health in a mouse model of gulf war illness. Int. J. Environ. Res. Public Health, 17 (19) (2020), p. 7081

[27] X. Wang, Z. Xu, F. Zhao, K.J. Lin, J.B. Foster, T. Xiao, N. Kung, C.C. Askwith, J.P. Bruno, V. Valentini. Restoring tripartite glutamatergic synapses: a potential therapy for mood and cognitive deficits in Gulf War illness. Neurobiol. Stress (2020), p. 100240

[28] U. Joshi, J.E. Evans, A. Pearson, N. Saltiel, A. Cseresznye, T. Darcey, J. Ojo, A.P. Keegan, S. Oberlin, B. Mouzon. Targeting sirtuin activity with nicotinamide riboside reduces neuroinflammation in a GWI mouse model. NeuroToxicology, 89 (2020), pp. 281-290

[29] A.K. Shetty, S. Attaluri, M. Kodali, B. Shuai, G.A. Shetty, D. Upadhya, B. Hattiangady, L.N. Madhu, R. Upadhya, A. Bates. Monosodium luminol reinstates redox homeostasis, improves cognition, mood and neurogenesis, and alleviates neuro-and systemic inflammation in a model of Gulf War Illness. Redox Biol., 28 (2020), Article 101389

[30] T.N. Odegard, C.M. Cooper, E.A. Farris, J. Arduengo, J. Bartlett, R. Haley. Memory impairment exhibited by veterans with Gulf War Illness. Neurocase, 19 (4) (2013), pp. 316-327

[31] L.L. Chao, M.R. Raymond, C.K. Leo, L.R. Abadjian. Evidence of hippocampal structural alterations in gulf war veterans with predicted exposure to the Khamisiyah plume. J. Occup. Environ. Med., 59 (10) (2017), pp. 923-929

[32] X. Li, J.S. Spence, D.M. Buhner, J. Hart Jr., C.M. Cullum, M.M. Biggs, A.L. Hester, T.N. Odegard, P.S. Carmack, R.W. Briggs. Hippocampal dysfunction in Gulf War veterans: investigation with ASL perfusion MR imaging and physostigmine challenge. Radiology, 261 (1) (2011), pp. 218-225

[33] C.-H. Cheng, B.-B. Koo, S. Calderazzo, E. Quinn, K. Aenlle, L. Steele, N. Klimas, M. Krengel, P. Janulewicz, R. Toomey. Alterations in high-order diffusion imaging in veterans with Gulf War Illness is associated with chemical weapons exposure and mild traumatic brain injury. Brain Behav. Immun., 67 (2020), pp. 2107-2124

[34] V.K. Parihar, B. Hattiangady, B. Shuai, A.K. Shetty. Mood and memory deficits in a model of Gulf War illness are linked with reduced neurogenesis, partial neuron loss, and mild inflammation in the hippocampus. Neuropsychopharmacology, 38 (12) (2013), p. 2348

[35] T. Megahed, B. Hattiangady, B. Shuai, A.K. Shetty. Parvalbumin and neuropeptide Y expressing hippocampal GABA-ergic inhibitory interneuron numbers decline in a model of Gulf War illness. Front. Cell. Neurosci., 8 (2015), p. 447

[36] J. Belgrad, D.J. Dutta, S. Bromley-Coolidge, K.A. Kelly, L.T. Michalovicz, K.A. Sullivan, J.P. O'Callaghan, R.D. Fields. Oligodendrocyte involvement in Gulf War Illness. Glia, 67 (2019), pp. 2107-2124

[37] U. Joshi, J.E. Evans, R. Joseph, T. Emmerich, N. Saltiel, C. Lungmus, S. Oberlin, H. Langlois, J. Ojo, B. Mouzon. Oleoylethanolamide treatment reduces

neurobehavioral deficits and brain pathology in a mouse model of Gulf War Illness. Sci. Rep., 8 (1) (2018), Article 12921

[38] M.I. Torres-Altoro, B.N. Mathur, J.M. Drerup, R. Thomas, D.M. Lovinger, J.P. O'Callaghan, J.A. Bibb. Organophosphates dysregulate dopamine signaling, glutamatergic neurotransmission, and induce neuronal injury markers in striatum. J. Neurochem., 119 (2) (2011), pp. 303-313

[39] O. Atochina, A.A. Da'dara, M. Walker, D.A. Harn. The immunomodulatory glycan LNFPIII initiates alternative activation of murine macrophages in vivo. Immunology, 125 (1) (2008), pp. 111-121

[40] S. Tundup, L. Srivastava, J. Harn, A. Donald. Polarization of host immune responses by helminth-expressed glycans. Ann. N. Y. Acad. Sci., 1253 (1) (2012), pp. E1-E13

[41] C.J. Preston, K.A. Brown, J.J. Wagner. Cocaine conditioning induces persisting changes in ventral hippocampus synaptic transmission, long-term potentiation, and radial arm maze performance in the mouse. Neuropharmacology, 150 (2019), pp. 27-37

[42] M.M. Keralapurath, S.B. Briggs, J.J. Wagner. Cocaine self-administration induces changes in synaptic transmission and plasticity in ventral hippocampus. Addict. Biol., 22 (2) (2017), pp. 446-456

[43] S. Krishna, Z. Lin, B. Claire, J.J. Wagner, D.H. Harn, L.M. Pepples, D.M. Djani, M.T. Weber, L. Srivastava, N.M. Filipov. Time-dependent behavioral, neurochemical, and metabolic dysregulation in female C57BL/6 mice caused by chronic high-fat diet intake. Physiol. Behav., 157 (2016), pp. 196-208

[44] Z. Lin, C.A. Dodd, N.M. Filipov. Short-term atrazine exposure causes behavioral deficits and disrupts monoaminergic systems in male C57BL/6 mice. Neurotoxicol. Teratol., 39 (2013), pp. 26-35

[45] A. Abdel-Rahman, A.K. Shetty, M.B. Abou-Donia. Disruption of the blood–brain barrier and neuronal cell death in cingulate cortex, dentate gyrus, thalamus, and hypothalamus in a rat model of Gulf-War syndrome. Neurobiol. Dis., 10 (3) (2002), pp. 306-326

[46] V. Macht, J. Woodruff, C. Grillo, C. Wood, M. Wilson, L. Reagan. Pathophysiology in a model of Gulf War Illness: contributions of pyridostigmine bromide and stress. Psychoneuroendocrinology, 96 (2018), pp. 195-202

[47] A.R. Locker, L.T. Michalovicz, K.A. Kelly, J.V. Miller, D.B. Miller, J.P. O'Callaghan. Corticosterone primes the neuroinflammatory response to Gulf War Illness-relevant organophosphates independently of acetylcholinesterase inhibition. J. Neurochem., 142 (3) (2017), pp. 444-455

[48] M.E. Hasselmo. The role of acetylcholine in learning and memory. Curr. Opin. Neurobiol., 16 (6) (2006), pp. 710-715

[49] H.E. Speed, C.A. Blaiss, A. Kim, M.E. Haws, N.R. Melvin, M. Jennings, A.J. Eisch, C.M. Powell. Delayed reduction of hippocampal synaptic transmission and spines following exposure to repeated subclinical doses of organophosphorus pesticide in adult mice. Toxicol. Sci., 125 (1) (2011), pp. 196-208

[50] D.-H. Tan, S.-Q. Peng, Y.-L. Wu, Y.-M. Wang, C.-F. Lu, W. Ding, Q.-X. Wang, C.-H. Yan. Chlorpyrifos induces delayed cytotoxicity after withdrawal in primary hippocampal neurons through extracellular signal-regulated kinase inhibition. Biol. Pharm. Bull., 32 (10) (2009), pp. 1649-1655

[51] A.M. Betancourt, N.M. Filipov, R.L. Carr. Alteration of neurotrophins in the hippocampus and cerebral cortex of young rats exposed to chlorpyrifos and methyl parathion. Toxicol. Sci., 100 (2) (2007), pp. 445-455

[52] M. Alonso, J.H. Medina, L. Pozzo-Miller. ERK1/2 activation is necessary for BDNF to increase dendritic spine density in hippocampal CA1 pyramidal neurons. Learn. Mem., 11 (2) (2004), pp. 172-178

[53] H. Kang, E.M. Schuman. Long-lasting neurotrophin-induced enhancement of synaptic transmission in the adult hippocampus. Science, 267 (5204) (1995), pp. 1658-1662

[54] J.V. Miller, R.F. LeBouf, K.A. Kelly, L.T. Michalovicz, A. Ranpara, A.R. Locker, D.B. Miller, J.P. O'Callaghan. The neuroinflammatory phenotype in a mouse model of Gulf War Illness is unrelated to brain regional levels of acetylcholine as measured by quantitative HILIC-UPLC-MS/MS. Toxicol. Sci., 165 (2) (2018), pp. 302-313

[55] B.-B. Koo, L.T. Michalovicz, S. Calderazzo, K.A. Kelly, K. Sullivan, R.J. Killiany, J.P. O'Callaghan. Corticosterone potentiates DFP-induced neuroinflammation and affects high-order diffusion imaging in a rat model of Gulf War Illness. Brain Behav. Immun., 67 (2018), pp. 42-46

[56] Z. Zakirova, M. Tweed, G. Crynen, J. Reed, L. Abdullah, N. Nissanka, M. Mullan, M.J. Mullan, V. Mathura, F. Crawford. Gulf War agent exposure causes impairment of long-term memory formation and neuropathological changes in a mouse model of Gulf War Illness. PLoS One, 10 (3) (2015), Article e0119579

[57] J.O. Ojo, L. Abdullah, J. Evans, J.M. Reed, H. Montague, M.J. Mullan, F.C. Crawford. Exposure to an organophosphate pesticide, individually or in combination with other Gulf War agents, impairs synaptic integrity and neuronal differentiation, and is accompanied by subtle microvascular injury in a mouse model of Gulf War agent exposure. Neuropathology, 34 (2) (2014), pp. 109-127

[58] A. Abdel-Rahman, S.M. Abou-Donia, E.M. El-Masry, A.K. Shetty, M.B. Abou-Donia. Stress and combined exposure to low doses of pyridostigmine bromide, DEET, and permethrin produce neurochemical and neuropathological alterations in cerebral cortex, hippocampus, and cerebellum. J. Toxicol. Environ. Health Part A, 67 (2) (2004), pp. 163-192

[59] J.P. O'Callaghan, L.T. Michalovicz, K.A. Kelly. Supporting a neuroimmune basis of gulf war illness. EBioMedicine, 13 (2016), pp. 5-6

[60] J.A. Golier, K. Caramanica, A.C. Michaelides, I. Makotkine, J. Schmeidler, P.D. Harvey, R. Yehuda. A randomized, double-blind, placebo-controlled, crossover trial of mifepristone in Gulf War veterans with chronic multisymptom illness. Psychoneuroendocrinology, 64 (2016), pp. 22-30

[61] L.T. Michalovicz, A.R. Locker, K.A. Kelly, J.V. Miller, Z. Barnes, M.A. Fletcher, D.B. Miller, N.G. Klimas, M. Morris, S.M. Lasley. Corticosterone and pyridostigmine/DEET exposure attenuate peripheral cytokine expression: supporting a dominant role for neuroinflammation in a mouse model of Gulf War Illness. Neurotoxicology, 70 (2019), pp. 26-32

[62] G.A. Prieto, C.W. Cotman. Cytokines and cytokine networks target neurons to modulate long-term potentiation. Cytokine Growth Factor Rev., 34 (2017), pp. 27-33

[63] P. Sengupta. The laboratory rat: relating its age with human's. Int. J. Prev. Med., 4 (6) (2013), p. 624

[64] Z. Alshelh, D.S. Albrecht, C. Bergan, O. Akeju, D.J. Clauw, L. Conboy, R.R. Edwards, M. Kim, Y.C. Lee, E. Protsenko. In-vivo imaging of neuroinflammation in veterans with Gulf War illness. Brain Behav. Immun., 87 (2020), pp. 498-507

[65] R.J. Kelly, A.M. Minogue, A. Lyons, R.S. Jones, T.C. Browne, D.A. Costello, S. Denieffe, C. O'Sullivan, T.J. Connor, M.A. Lynch. Glial activation in AβPP/PS1 mice is associated with infiltration of IFNγ-producing cells. J. Alzheimers Dis., 37 (1) (2013), pp. 63-75

[66] A.M. Littlefield, S.E. Setti, C. Priester, R.A. Kohman. Voluntary exercise attenuates LPS-induced reductions in neurogenesis and increases microglia expression of a proneurogenic phenotype in aged mice. J. Neuroinflammation, 12 (1) (2015), Article 138

[67] D.L. Gruol. IL-6 regulation of synaptic function in the CNS. Neuropharmacology, 96 (2015), pp. 42-54

[68] A.C. Ribeiro, J. Zhu, M.M. Kronfol, F.M. Jahr, R.M. Younis, E. Hawkins, J.L. McClay, L.S. Deshpande. Molecular mechanisms for the antidepressant-like effects of a low-dose ketamine treatment in a DFP-based rat model for Gulf War Illness. NeuroToxicology, 15 (2020), pp. 1-15

[69] D. Kimono, D. Bose, R.K. Seth, A. Mondal, P. Saha, P. Janulewicz, K. Sullivan, S. Lasley, R. Horner, N. Klimas. Host Akkermansia muciniphila abundance correlates with gulf war illness symptom persistence via NLRP3-mediated neuroinflammation and decreased brain-derived neurotrophic factor. Neurosci. Insights, 15 (2020), Article 2633105520942480

[70] M.S. Fanselow, H.-W. Dong. Are the dorsal and ventral hippocampus functionally distinct structures? Neuron, 65 (1) (2010), pp. 7-19

[71] C. Papatheodoropoulos. Electrophysiological evidence for long-axis intrinsic diversification of the hippocampus. Front. Biosci. (Landmark Ed), 23 (2018), pp. 109-145

[72] B. Hattiangady, V. Mishra, M. Kodali, B. Shuai, X. Rao, A.K. Shetty. Object location and object recognition memory impairments, motivation deficits and depression in a model of Gulf War illness. Front. Behav. Neurosci., 8 (2014), p. 78

[73] L.N. Madhu, S. Attaluri, M. Kodali, B. Shuai, R. Upadhya, D. Gitai, A.K. Shetty. Neuroinflammation in gulf war illness is linked with HMGB1 and complement activation, which can be discerned from brain-derived extracellular vesicles in the blood. Brain Behav. Immun., 89 (2019), pp. 430-443

[74] Z. Zakirova, G. Crynen, S. Hassan, L. Abdullah, L. Horne, V. Mathura, F. Crawford, G. Ait-Ghezala. A chronic longitudinal characterization of neurobehavioral and neuropathological cognitive impairment in a mouse model of Gulf War agent exposure. Front. Integr. Neurosci., 9 (2016), p. 71

[75] M. Vythilingam, D.A. Luckenbaugh, T. Lam, C.A. Morgan III, D. Lipschitz, D.S. Charney, J.D. Bremner, S.M. Southwick. Smaller head of the hippocampus in Gulf

War-related posttraumatic stress disorder. Psychiatry Res. Neuroimaging, 139 (2) (2005), pp. 89-99

[76] L.L. Chao, S. Kriger, S. Buckley, P. Ng, S.G. Mueller. Effects of low-level sarin and cyclosarin exposure on hippocampal subfields in Gulf War Veterans. Neurotoxicology, 44 (2014), pp. 263-269

Figures.

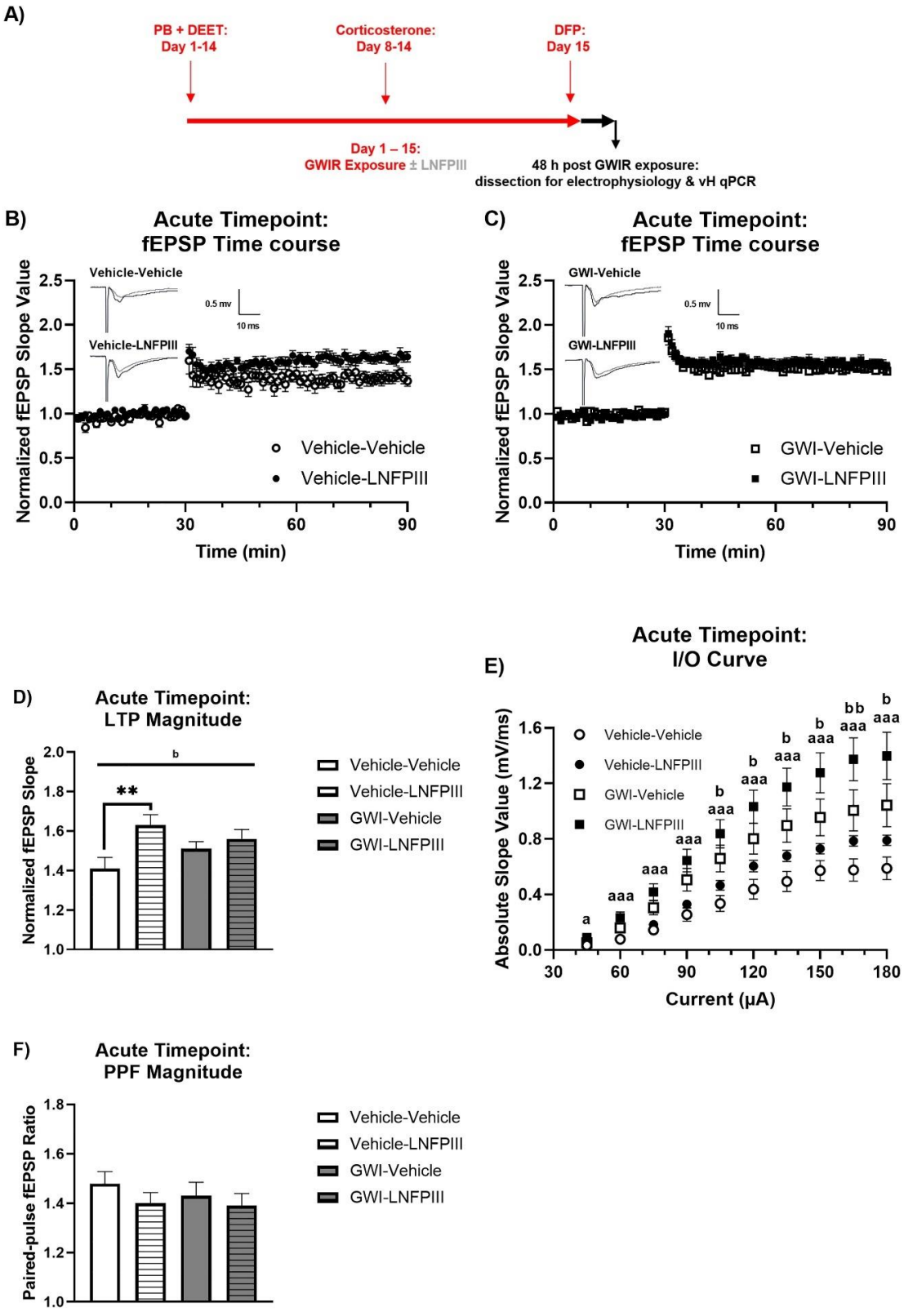
A)
PB + DEET:
Day 1-14
Corticosterone:
Day 8-14
DFP:
Day 15
Day 1 – 15:
GWIR Exposure ± LNFPIII
48 h post GWIR exposure:
dissection for electrophysiology & vH qPCR
B)
Acute Timepoint:
fEPSP Time course
Vehicle-Vehicle
Vehicle-LNFPIII
0.5 mv
10 ms
Normalized fEPSP Slope Value
Time (min)
C)
Acute Timepoint:
fEPSP Time course
GWI-Vehicle
GWI-LNFPIII
D)
Acute Timepoint:
LTP Magnitude
Normalized fEPSP Slope
E)
Acute Timepoint:
I/O Curve
Absolute Slope Value (mV/ms)
Current (µA)
F)
Acute Timepoint:
PPF Magnitude
Paired-pulse fEPSP Ratio

Fig. A.1. The effect of Gulf War Illness-related (GWIR) exposure ± LNFPIII coadministration on measurements of hippocampal synaptic plasticity and transmission 48 h post GWIR/LNFPIII treatment. A. Timeline of GWIR exposure and LNFPIII treatment for hippocampi that were dissected at the acute electrophysiological timepoint. B and C. Summary plots of normalized fEPSP values recorded from either vehicle-treated (B) or GWIR-exposed (C) animals 48 h post GWIR exposure. (B) compares Vehicle-Vehicle (○) and Vehicle-LNFPIII (●) treated mice whereas (C) compares GWI-Vehicle (□) and GWI-LNFPIII (■) treated mice. Insets show traces composed of average sweeps from 5 min pre-tetanus (grey) and 56–60 min post tetanus (black). D. Summary quantification of LTP magnitude recorded 48 h after GWIR exposure from Vehicle-Vehicle (1.41 ± 0.06, n = 11(4)), Vehicle-LNFPIII (1.63 ± 0.05, n = 18(4)), GWI-Vehicle (1.51 ± 0.04, n = 21(4)), and GWI-LNFPIII (1.56 ± 0.05, n = 17(4)) treated animals. E. Stimulus-response relationship of the average fEPSP slopes elicited by increasing stimulus intensities from Vehicle-Vehicle (○), Vehicle-LNFPIII (●), GWI-Vehicle (□), and GWI-LNFPIII (■) treatment groups recorded 48 h after GWIR exposure. F. The paired-pulse ratio for Vehicle-Vehicle (1.48 ± 0.05), Vehicle-LNFPIII (1.40 ± 0.04), GWI-Vehicle (1.43 ± 0.06), and GWI-LNFPIII (1.39 ± 0.05) treatment groups recorded 48 h after GWIR exposure (interpulse interval = 50 ms). ^{a} denotes main effect of GWIR exposure ($p < 0.05$, ^{aa} denotes $p < 0.01$, ^{aaa} denotes $p < 0.001$) whereas ^{b} denotes main effect of LNFPIII ($p < 0.05$, ^{bb} denotes $p < 0.01$, ^{bbb}). ** denotes $p < 0.01$ for treatment group differences. Data are expressed as mean ± SEM.

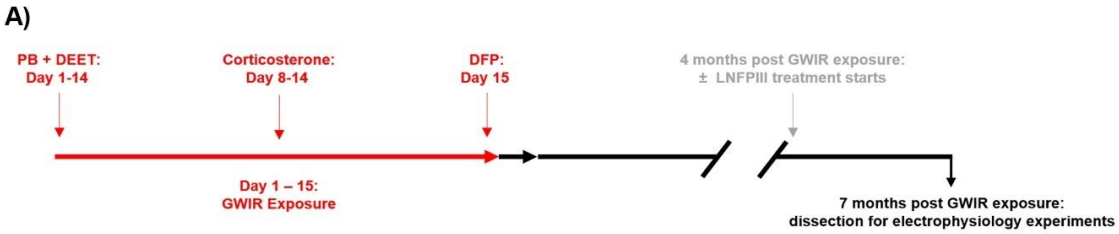
A)
PB + DEET:
Day 1-14
Corticosterone:
Day 8-14
DFP:
Day 15
4 months post GWIR exposure:
± LNFPIII treatment starts
Day 1 – 15:
GWIR Exposure
7 months post GWIR exposure:
dissection for electrophysiology experiments

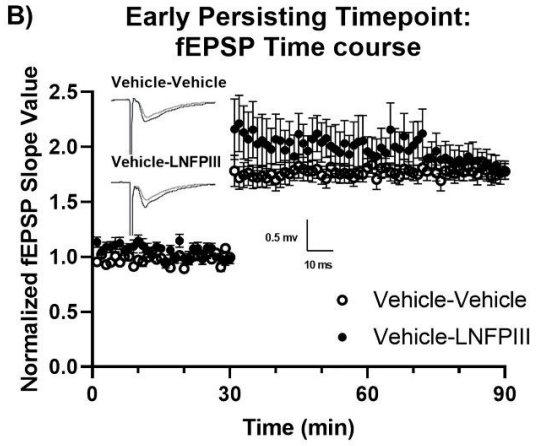
B)
Early Persisting Timepoint:
fEPSP Time course
Normalized fEPSP Slope Value
Time (min)
Vehicle-Vehicle
Vehicle-LNFPIII
0.5 mv
10 ms

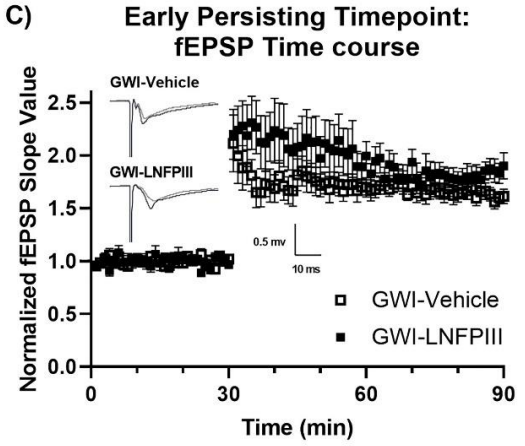
C)
Early Persisting Timepoint:
fEPSP Time course
Normalized fEPSP Slope Value
Time (min)
GWI-Vehicle
GWI-LNFPIII
0.5 mv
10 ms

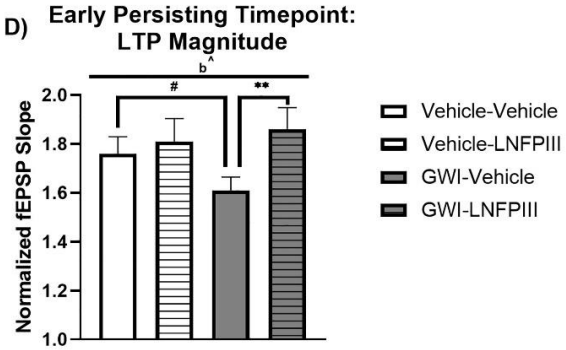
D)
Early Persisting Timepoint:
LTP Magnitude
Normalized fEPSP Slope
Vehicle-Vehicle
Vehicle-LNFPIII
GWI-Vehicle
GWI-LNFPIII

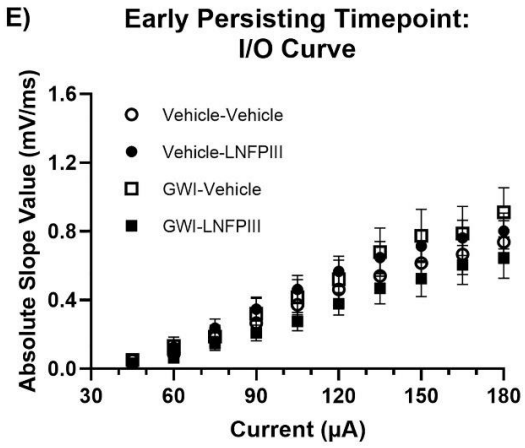
E)
Early Persisting Timepoint:
I/O Curve
Absolute Slope Value (mV/ms)
Current (μA)
Vehicle-Vehicle
Vehicle-LNFPIII
GWI-Vehicle
GWI-LNFPIII

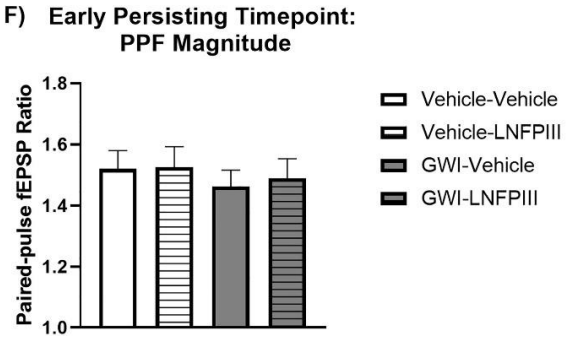
F)
Early Persisting Timepoint:
PPF Magnitude
Paired-pulse fEPSP Ratio
Vehicle-Vehicle
Vehicle-LNFPIII
GWI-Vehicle
GWI-LNFPIII

Fig. A.2. The effect of GWIR exposure ± delayed LNFPIII treatment on measurements of hippocampal synaptic plasticity and transmission 7 months post GWIR treatment. A. Timeline of GWIR exposure and LNFPIII treatment for hippocampi that were dissected at the early persisting electrophysiological timepoint. B and C. Summary plots of normalized fEPSP values recorded from either vehicle-treated (B) or GWIR-exposed (C) animals 7 months post GWIR exposure. (B) compares Vehicle-Vehicle (○) and Vehicle-LNFPIII (●) treated mice whereas (C) compares GWI-Vehicle (□) and GWI-LNFPIII (■) treated mice. Insets show traces composed of average sweeps from 5 min pre-tetanus (grey) and 56–60 min post tetanus (black). D. Summary quantification of LTP magnitude recorded 7 months after GWIR exposure from Vehicle-Vehicle (1.76 ± 0.07, n = 16(3)), Vehicle-LNFPIII (1.81 ± 0.10, n = 15(3)), GWI-Vehicle (1.61 ± 0.06, n = 14(3)), and GWI-LNFPIII (1.86 ± 0.09, n = 12(3)) treated animals. E. Stimulus-response relationship of the average fEPSP slopes elicited by increasing stimulus intensities from Vehicle-Vehicle (○), Vehicle-LNFPIII (●), GWI-Vehicle (□), and GWI-LNFPIII (■) treatment groups recorded 7 months after GWIR exposure. F. The paired-pulse ratio for Vehicle-Vehicle (1.52 ± 0.06), Vehicle-LNFPIII (1.53 ± 0.07), GWI-Vehicle (1.46 ± 0.05), and GWI-LNFPIII (1.49 ± 0.06) treatment groups recorded 7 months after GWIR exposure (interpulse interval = 50 ms). [a] denotes main effect of GWIR exposure ($p < 0.05$) whereas [b] denotes main effect of LNFPIII ($p < 0.05$, b^ denotes $p < 0.1$). [#] denotes $p < 0.1$; ** denotes $p < 0.01$ for treatment group differences. Data are expressed as mean ± SEM.

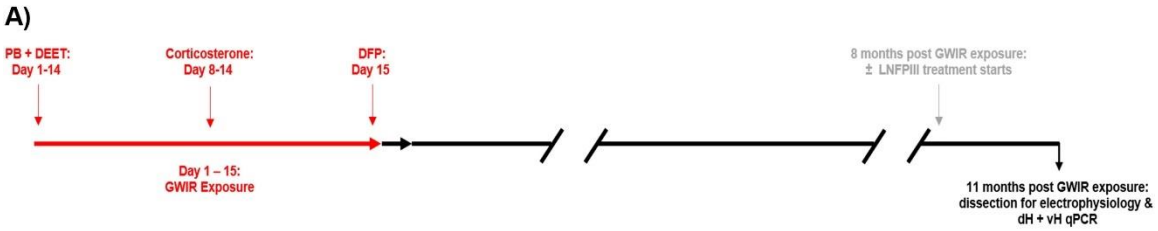
A)
PB + DEET:
Day 1-14
Corticosterone:
Day 8-14
DFP:
Day 15
8 months post GWIR exposure:
± LNFPIII treatment starts
Day 1 – 15:
GWIR Exposure
11 months post GWIR exposure:
dissection for electrophysiology &
dH + vH qPCR

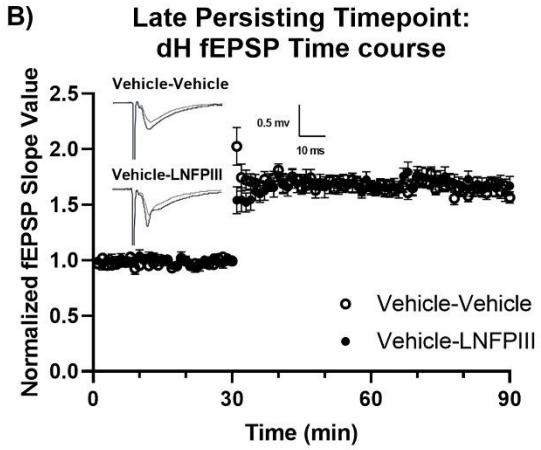
B)
Late Persisting Timepoint:
dH fEPSP Time course
Normalized fEPSP Slope Value
Vehicle-Vehicle
Vehicle-LNFPIII
0.5 mv
10 ms
Time (min)

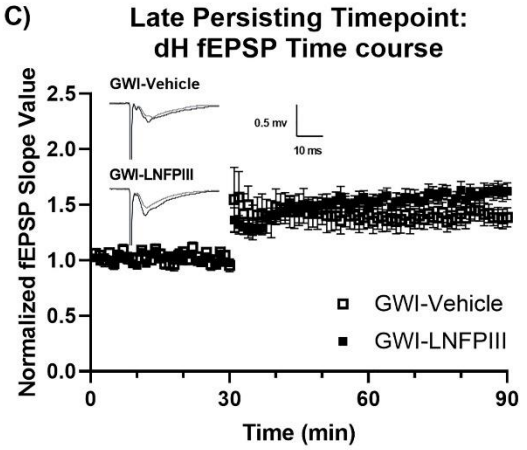
C)
Late Persisting Timepoint:
dH fEPSP Time course
Normalized fEPSP Slope Value
GWI-Vehicle
GWI-LNFPIII
0.5 mv
10 ms
Time (min)

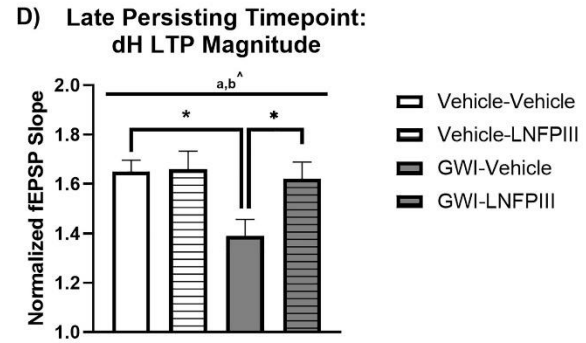
D)
Late Persisting Timepoint:
dH LTP Magnitude
Normalized fEPSP Slope
Vehicle-Vehicle
Vehicle-LNFPIII
GWI-Vehicle
GWI-LNFPIII

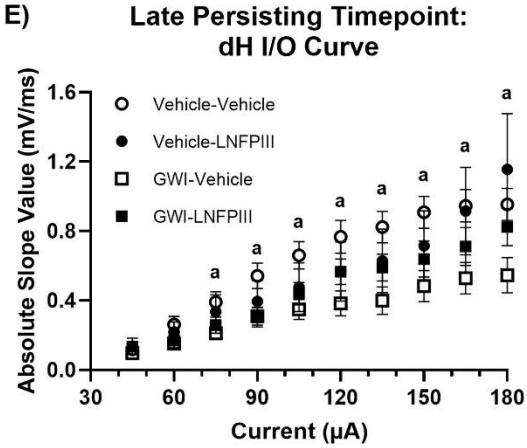
E)
Late Persisting Timepoint:
dH I/O Curve
Absolute Slope Value (mV/ms)
Vehicle-Vehicle
Vehicle-LNFPIII
GWI-Vehicle
GWI-LNFPIII
Current (µA)

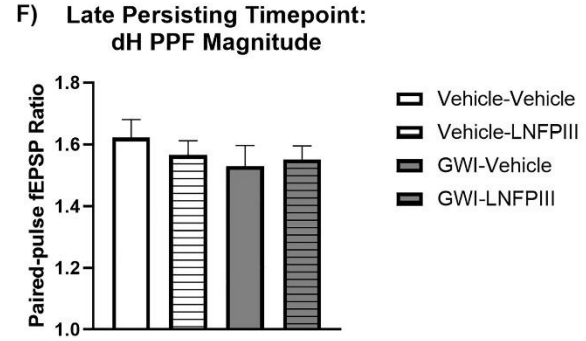
F)
Late Persisting Timepoint:
dH PPF Magnitude
Paired-pulse fEPSP Ratio
Vehicle-Vehicle
Vehicle-LNFPIII
GWI-Vehicle
GWI-LNFPIII

Fig. A.3. The effect of GWIR exposure ± delayed LNFPIII treatment on measurements of dorsal hippocampal (dH) synaptic plasticity and transmission 11 months post GWIR treatment. A. Timeline of GWIR exposure and LNFPIII treatment for hippocampi that were dissected at the late persisting electrophysiological timepoint. This timeline was also employed for the data presented in Fig. 4. B and C. Summary plots of normalized fEPSP values recorded in the dH from either vehicle-treated (B) or GWIR-exposed (C) animals 11 months post GWIR exposure. (B) compares Vehicle-Vehicle (○) and Vehicle-LNFPIII (●) treated mice whereas (C) compares GWI-Vehicle (□) and GWI-LNFPIII (■) treated mice. Insets show traces composed of average sweeps from 5 min pre-tetanus (grey) and 56–60 min post tetanus (black). D. Summary quantification of LTP magnitude recorded in the dH 11 months after GWIR exposure from Vehicle-Vehicle (1.65 ± 0.05, n = 15(7)), Vehicle-LNFPIII (1.66 ± 0.07, *n* = 13(5)), GWI-Vehicle (1.39 ± 0.07, n = 14(6)), and GWI-LNFPIII (1.62 ± 0.07, n = 14(5)) treated animals. E. Stimulus-response relationship of the average dH fEPSP slopes elicited by increasing stimulus intensities from Vehicle-Vehicle (●), Vehicle-LNFPIII (■), GWI-Vehicle (○), and GWI-LNFPIII (□) treatment groups recorded in the dH 11 months after GWIR exposure. F. The paired-pulse ratio for Vehicle-Vehicle (1.62 ± 0.06), Vehicle-LNFPIII (1.57 ± 0.05), GWI-Vehicle (1.53 ± 0.07), and GWI-LNFPIII (1.55 ± 0.05) treatment groups recorded in the dH 11 months after GWIR exposure (interpulse interval = 50 ms). [a] denotes main effect of GWIR exposure ($p < 0.05$) whereas [b] denotes main effect of LNFPIII ($p < 0.05$, b^ denotes $p < 0.1$). * denotes $p < 0.05$ for treatment group differences. Data are expressed as mean ± SEM.

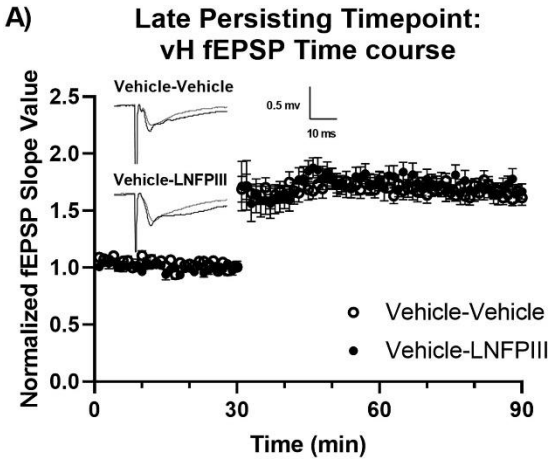
A)
Late Persisting Timepoint:
vH fEPSP Time course
Vehicle-Vehicle
Vehicle-LNFPIII
0.5 mv
10 ms
Normalized fEPSP Slope Value
Time (min)
Vehicle-Vehicle
Vehicle-LNFPIII

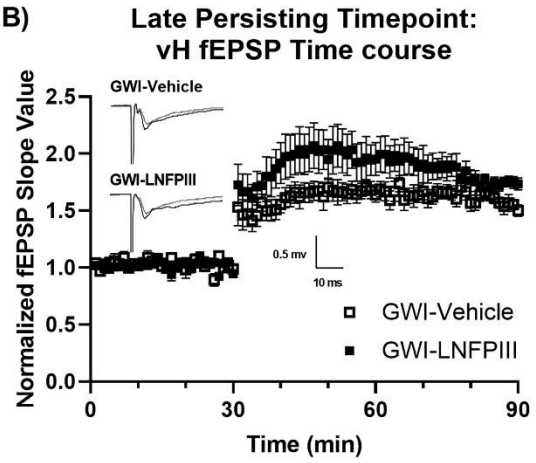
B)
Late Persisting Timepoint:
vH fEPSP Time course
GWI-Vehicle
GWI-LNFPIII
0.5 mv
10 ms
Normalized fEPSP Slope Value
Time (min)
GWI-Vehicle
GWI-LNFPIII

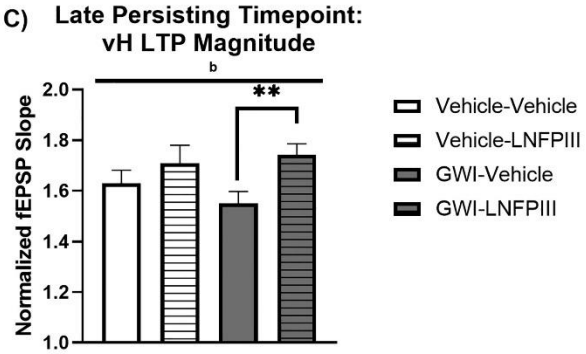
C)
Late Persisting Timepoint:
vH LTP Magnitude
b
**
Normalized fEPSP Slope
Vehicle-Vehicle
Vehicle-LNFPIII
GWI-Vehicle
GWI-LNFPIII

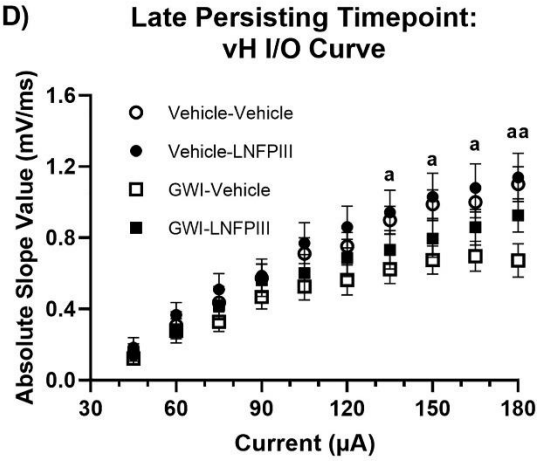
D)
Late Persisting Timepoint:
vH I/O Curve
Absolute Slope Value (mV/ms)
Current (µA)
Vehicle-Vehicle
Vehicle-LNFPIII
GWI-Vehicle
GWI-LNFPIII
a
a
a
aa

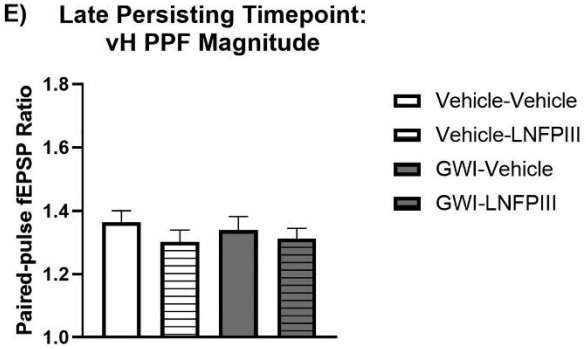
E)
Late Persisting Timepoint:
vH PPF Magnitude
Paired-pulse fEPSP Ratio
Vehicle-Vehicle
Vehicle-LNFPIII
GWI-Vehicle
GWI-LNFPIII

Fig. A.4. The effect of GWIR exposure ± delayed LNFPIII treatment on measurements of ventral hippocampal (vH) synaptic plasticity and transmission 11 months post GWIR treatment. A and B. Summary plots of normalized fEPSP values recorded in the vH from either vehicle-treated (A) or GWIR-exposed (B) animals 11 months post GWIR exposure. (A) compares Vehicle-Vehicle (○) and Vehicle-LNFPIII (●) treated mice whereas (B) compares GWI-Vehicle (□) and GWI-LNFPIII (■) treated mice. Insets show traces composed of average sweeps from 5 min pre-tetanus (grey) and 56–60 min post tetanus (black). C. Summary quantification of LTP magnitude recorded in the vH 11 months after GWIR exposure from Vehicle-Vehicle (1.63 ± 0.05, n = 15(7)), Vehicle-LNFPIII (1.71 ± 0.07, n = 14(5)), GWI-Vehicle (1.55 ± 0.05, n = 12(6)), and GWI-LNFPIII (1.74 ± 0.04, n = 12(5)) treated animals. D. Stimulus-response relationship of the average dH fEPSP slopes elicited by increasing stimulus intensities from Vehicle-Vehicle (●), Vehicle-LNFPIII (■), GWI-Vehicle (○), and GWI-LNFPIII (□) treatment groups recorded in the vH 11 months after GWIR exposure. E. The paired-pulse ratio for Vehicle-Vehicle (1.36 ± 0.04), Vehicle-LNFPIII (1.30 ± 0.04), GWI-Vehicle (1.34 ± 0.04), and GWI-LNFPIII (1.31 ± 0.03) treatment groups recorded in the vH 11 months after GWIR exposure (interpulse interval = 50 ms). [a] denotes main effect of GWIR exposure ($p < 0.05$, [aa] denotes $p < 0.01$), whereas [b] denotes main effect of LNFPIII ($p < 0.05$). ** denotes $p < 0.01$ for treatment group differences. Data are expressed as mean ± SEM.

Tables

Gene	Forward primer	Reverse primer
BDNF	CTGAGCGTGTGTGACAGTATTA	CTTTGGATACCGGGACTTTCTC
Casp1	GAGATGGTGAAAGAGGTGAA	GTGTTGAAGAGCAGAAAGCA
CNTF	ACAAGGTCTCCATAAGTGTCAGC	CTGCCATTGGTCCAGGATGA
IL-1β	GAGGACATGAGCACCTTCTTT	GCCTGTAGTGCAGTTGTCTAA
IL-6	ATGGATGCTACCAAACTGGAT	TGAAGGACTCTGGCTTTGTCT
NGF	CAGTGAGGTGCATAGCGTAAT	CTCCTTCTGGGACATTGCTATC
TNF-α	GCAGGTCTACTTTGGAGTCATTGC	TCCCTTTGCAGAACTCAGGAATGG

Table A.1. List of primers used in the quantitative PCR (qPCR) analysis. Gene abbreviations: IL-6, Interleukin 6; IL-1β, Interleukin 1 beta; TNFα, Tumor necrosis factor alpha; BDNF, Brain-derived neurotrophic factor; NGF, Nerve growth factor; CNTF, Ciliary neurotrophic factor.

Gene	Fold change			p-Values			
	Veh. – LNFPIII vs. control	GWI – Veh. vs. control	GWI – LNFPIII vs. control	Veh. – LNFPIII vs. control	GWI – Veh. vs. control	GWI – LNFPIII vs. control	GWI – Veh. vs. GWI – LNFPIII
Casp1	0.54 ± 0.04	0.70 ± 0.05	0.67 ± 0.05	0.21	0.28	0.19	0.93
IL-6	1.09 ± 0.13	1.19 ± 0.14	0.97 ± 0.12	0.86	0.52	0.93	0.52
IL-1β	0.50 ± 0.15	1.31 ± 0.41	0.64 ± 0.20	0.23	0.64	0.29	0.13
TNFα	1.32 ± 0.40	1.78 ± 0.54	0.94 ± 0.28	0.51	0.26	0.90	0.26
BDNF	0.88 ± 0.07	1.39 ± 0.11	1.87 ± 0.14	0.71	0.28	0.04	0.43
NGF	1.06 ± 0.14	0.92 ± 0.12	1.29 ± 0.17	0.90	0.80	0.39	0.08
CNTF	1.07 ± 0.04	0.92 ± 0.03	0.82 ± 0.03	0.83	0.73	0.12	0.66

Table A.2. qPCR assessment of cytokines and trophic factors in the ventral hippocampus 48 h post GWIR exposure. The effect of GWIR exposure ± LNFPIII on the expression of key inflammatory cytokines and growth factors in the ventral hippocampus (vH) measured by qPCR 48 h post GWIR exposure. vH samples from mice (n = 6 per treatment) were used for RNA isolation and subsequent qPCR analyses. Data were analyzed by the $2^{-\Delta\Delta Ct}$ method with 18S as the housekeeping gene and are expressed as a mean fold change from the Vehicle-Vehicle control ± SEM. Gene abbreviations: IL-6, Interleukin 6; IL-1β, Interleukin 1 beta; TNFα, Tumor necrosis factor alpha; BDNF, Brain-derived neurotrophic factor; NGF, Nerve growth factor; CNTF, Ciliary neurotrophic factor.

Region	Gene	Fold change			p-Values			
		Veh. – LNFPIII vs. control	**GWI – Veh. vs. control**	**GWI – LNFPIII vs. control**	**Veh. – LNFPIII vs. control**	**GWI – Veh. vs. control**	**GWI – LNFPIII vs. control**	**GWI – Veh. vs. GWI – LNFPIII**
dH	BDNF	0.67 ± 0.09	0.90 ± 0.12	1.55 ± 0.20	0.13	0.69	0.10	0.06
	NGF	1.48 ± 0.10	1.42 ± 0.09	2.18 ± 0.15	0.03	0.08	0.001	0.06
	CNTF	0.97 ± 0.05	0.98 ± 0.05	1.03 ± 0.05	0.84	0.93	0.74	0.84
	IL-6	0.90 ± 0.07	1.79 ± 0.15	1.29 ± 0.11	0.62	0.02	0.34	0.32
vH	BDNF	1.05 ± 0.07	0.87 ± 0.31	1.01 ± 0.07	0.82	0.54	0.95	0.56
	NGF	0.83 ± 0.08	0.67 ± 0.00	0.89 ± 0.09	0.48	0.11	0.61	0.19
	CNTF	0.79 ± 0.08	0.72 ± 0.09	0.96 ± 0.10	0.28	0.07	0.86	0.11
	IL-6	0.73 ± 0.09	0.79 ± 0.18	0.90 ± 0.11	0.33	0.51	0.67	0.71

Table A.3. qPCR assessment of trophic factors in the hippocampus 11 months post GWIR exposure. The effect of GWIR exposure ± LNFPIII on the expression of growth factors in the dorsal (dH) and ventral (vH) hippocampus measured by qPCR post GWIR exposure. dH and vH samples from mice (n = 7, 4, 7, 6, for the, respectively, Vehicle-Vehicle (Control), Vehicle-LNFPIII, GWI-Vehicle, GWI-LNFPIII groups) were used for RNA isolation and subsequent qPCR analyses. Data were analyzed by the $2^{-\Delta\Delta Ct}$ method with 18S as the housekeeping gene and are expressed as a mean fold change from the Vehicle-Vehicle control ± SEM. Gene abbreviations: BDNF, Brain-derived neurotrophic factor; NGF, Nerve growth factor; CNTF, Ciliary neurotrophic factor; IL-6, interleukin 6.

APPENDIX B

LACTO-N-FUCOPENTAOSE-III (LNFPIII) AMELIORATES ACUTE ABERRATIONS IN HIPPOCAMPAL SYNAPTIC TRANSMISSION IN A GULF WAR ILLNESS ANIMAL MODEL

Kyle A. Brown, Collin J. Preston, Jessica M. Carpenter, Helaina D. Ludwig, Donald A. Harn, Thomas Norberg, John J. Wagner, Nikolay M. Filipov
Published in *Brain Research* 2021.

Abstract

Approximately one-third of Persian Gulf War veterans are afflicted by Gulf War Illness (GWI), a chronic multisymptom condition that fundamentally presents with cognitive deficits (i.e., learning and memory impairments) and neuroimmune dysfunction (i.e., inflammation). Factors associated with GWI include overexposures to neurotoxic pesticides and nerve agent prophylactics such as permethrin (PM) and pyridostigmine bromide (PB), respectively. GWI-related neurological impairments associated with PB-PM overexposures have been recapitulated in animal models; however, there is a paucity of studies assessing PB-PM-related aberrations in hippocampal synaptic plasticity and transmission that may underlie behavioral impairments. Importantly, FDA-approved neuroactive treatments are currently unavailable for GWI. In the present study, we assessed the efficacy of an immunomodulatory therapeutic, lacto-N-fucopentaose-III (LNFPIII), on ameliorating acute effects of in vivo PB-PM exposure on synaptic plasticity and transmission as well as trophic factor/cytokine expression along the hippocampal dorsoventral axis. PB-PM exposure resulted in hippocampal synaptic transmission deficits 48 h post-exposure, a response that was ameliorated by LNFPIII coadministration, particularly in the dorsal hippocampus (dH). LNFPIII coadministration also enhanced synaptic transmission in the dH and the ventral hippocampus (vH). Notably, LNFPIII coadministration elevated long-term potentiation in the dH. Further, PB-PM exposure and LNFPIII coadministration uniquely altered key inflammatory cytokine and trophic factor production in the dH and the vH. Collectively, these findings demonstrate that PB-PM exposure impaired hippocampal synaptic responses 48 h post-exposure, impairments that differentially manifested along the dorsoventral axis. Importantly, LNFPIII ameliorated

GWI-related electrophysiological deficits, a beneficial effect indicating the potential efficacy of LNFPIII for treating GWI.

Abbreviations: BDNF, Brain-derived neurotrophic factor; CNTF, Ciliary neurotrophic factor; dH, Dorsal hippocampus; ERK, Extracellular signal-regulated kinase; fEPSP, field excitatory postsynaptic potential; GWI, Gulf war illness; IL-6, Interleukin 6; IL-1β, Interleukin 1 beta; LNFPIII, Lacto-N-fucopentaose-III; LTP, Long-term potentiation; NGF, Nerve growth factor; PB, Pyridostigmine bromide; PB-PM, Pyridostigmine bromide-permethrin; PM, Permethrin; PPF, Paired-pulse facilitation; SYP, Synaptophysin; TNFα, Tumor necrosis factor alpha; vH, Ventral hippocampus

Keywords: Hippocampus, Electrophysiology, Gulf War Illness, Permethrin, Pyridostigmine bromide, Lacto-N-fucopentaose-III (LNFPIIII)

1. Introduction

Gulf War Illness (GWI) is a chronic multisymptom condition that affects approximately a third of the 700,000 United States military forces that served in the 1990–1991 Persian Gulf War (White et al., 2016). Clinical symptoms of GWI include fatigue, cognitive deficits, and musculoskeletal pain, symptoms that progressively worsen over time and are likely related to neuroimmune dysfunction (Coughlin, 2017, Zundel et al., 2020). While the exact etiology of GWI is unknown, persistent wartime stress and excessive exposures to neurotoxic pesticides like permethrin (PM) and nerve agent prophylactics such as pyridostigmine bromide (PB) have been implicated in the pathogenesis of GWI (White et al., 2016). Currently, only symptomatic and targeted treatments of GWI are available with no approved neuroactive therapeutics.

Preclinical studies have characterized acute and persisting pyridostigmine bromide-permethrin (PB-PM)-induced neurological aberrations at the molecular, cellular, and behavioral levels in an established GWI model (Carpenter et al., 2020, Joshi et al., 2018, Zakirova et al., 2015). These neurological aberrations specifically include dysregulation of cytokine expression and signaling, undesirable activation of glial cells (i.e., astrocytes and microglia), and cognitive deficits (Carpenter et al., 2020, Joshi et al., 2018, White et al., 2016, Zakirova et al., 2015). Notably, learning and memory impairments in GWI veterans (Jeffrey et al., 2019) have been recapitulated in animals exposed to PB-PM (White et al., 2016), impairments that may be related to neuroimmune dysfunction (Trageser et al., 2020). Specifically, dorsal hippocampal (dH)-dependent learning and memory deficits (Joshi et al., 2018, Zakirova et al., 2015), as well as ventral hippocampal (vH)-related behavioral aberrations (i.e., abnormal anxiety-like behavior; Joshi et al., 2018) after PB-

PM exposure were reported. As increasing evidence suggests the dH and the vH are functionally distinct structures (Papatheodoropoulos, 2018), monitoring dorsoventral-specific effects of PB-PM exposure on hippocampal-dependent behavioral abnormalities may be crucial for interpreting abnormalities in synaptic plasticity and transmission along the hippocampal dorsoventral axis. However, reports evaluating the impact of PB-PM exposure on synaptic plasticity and transmission are unavailable. There is an additional paucity of investigations assessing the benefits of any therapeutic on GWI-related electrophysiological impairments. Given the emerging evidence of the substantial role neuroimmune dysfunction plays in GWI symptomology (Coughlin, 2017, Georgopoulos et al., 2017, Michalovicz et al., 2020, O'Callaghan et al., 2016), testing an immunotherapeutic for ameliorating PB-PM-induced abnormalities in hippocampal synaptic plasticity and transmission would address a substantial knowledge gap in the field of GWI research.

Recent reviews highlight the potential efficacy of a number of GWI therapeutics (Reviewed in: Dickey et al., 2020, Nugent et al., 2020), yet targeted and symptomatic treatments are available. Neuroimmune dysfunction is increasingly associated with the underlying pathobiology of GWI (Coughlin, 2017, Georgopoulos et al., 2017, Trageser et al., 2020). A particular approach that holds potential for extended remission of GWI is rebalancing inflammatory cytokines (Craddock et al., 2015); however, investigations utilizing immunotherapeutics to target GWI-induced immune system dysregulation are limited. The neoglycoconjugate lacto-N-fucopentaose-III (LNFPIII) was previously shown by our group to be a safe and efficacious agent for restoring central and peripheral immune function in disease states (Bhargava et al., 2012, Tundup et al., 2015, Zhu et al., 2012).

LNFPIII induces therapeutic effects by rebalancing the anti-inflammatory: inflammatory cytokine population as well as direct stimulation of kinases involved in trophic factor production such as the mitogen-activated protein kinase ERK-1/2 (Tundup et al., 2015). Importantly, recent work by our group demonstrated that LNFPIII coadministration ameliorated short-term neuroinflammatory and neurochemical-related aberrations in multiple GWI models (Carpenter et al., 2020) and it rebalanced persisting pathology such as gastrointestinal dysbiosis and inflammation when treatment was initiated months after GWI-related exposures (Mote et al., 2020). However, LNFPIII's efficacy in ameliorating hippocampal synaptic plasticity and transmission in a model of GWI is unknown. Accordingly, the present study investigated the efficacy of LNFPIII in ameliorating short-term PB-PM-induced deficits in dH and vH synaptic plasticity and transmission. We hypothesized that synaptic responses in the dH and the vH would be impaired 48 h post-PB-PM exposure and that LNFPIII coadministration would ameliorate synaptic activity in these sectors while also enhancing trophic factor production.

2. Results

2.1. LNFPIII coadministration ameliorated PB-PM-induced impairments in hippocampal basal synaptic transmission, particularly in the dorsal hippocampus

A significant reduction by PB-PM was detected in dH basal synaptic transmission at stimulus intensities of 120,135,150,165, and 180 μA when compared to vehicle-vehicle mice (p's ≤ 0.05; Fig. 1B). LNFPIII administration resulted in enhanced dH basal synaptic transmission compared to non-LNFPIII-treated groups at stimulation intensities of 150,165, and 180 μA (main effect: p's ≤ 0.05) as well as 135 μA (main effect: $p \leq 0.1$). Notably, LNFPIII treatment ameliorated the PB-PM reduction of dH basal synaptic

transmission by elevating activity in PB-PM-LNFPIII mice at stimulus intensities of 45,135,150,165, and 180 μA (p's ≤ 0.05). In the vH, a two-way ANOVA revealed an effect of PB-PM exposure on basal synaptic transmission at stimulation intensities of 105,150,165, and 180 μA (main effect: p's ≤ 0.05) as well as 45,90,120, and 135 μA (main effect: p's ≤ 0.1; Fig. 1C). This effect was driven mostly by a large, stimulus intensity-independent increase in basal synaptic activity in vehicle mice treated with LNFPIII, decreasing vH basal synaptic activity. LNFPIII treatment elevated vH basal synaptic transmission at stimulus intensities of 90 μA ($p < 0.05$) as well as 105 and 120 μA (p's $\leq$ 0.1) in vehicle-LNFPIII mice compared to vehicle-vehicle mice.

2.2. LNFPIII coadministered to PB-PM-exposed animals enhanced dorsal hippocampal long-term potentiation

A two-way ANOVA revealed a PB-PM × LNFPIII interaction effect ($p = 0.05$) on dH long-term potentiation (LTP) magnitude after PB-PM exposure; concurrent PB-PM exposure and LNFPIII treatment led to an increase in dH LTP magnitude compared to the PB-PM-vehicle group ($p \leq 0.05$, preplanned Student's t-test; Fig. 2A-2C). No significant main effects of PB-PM exposure or LNFPIII treatment were observed on dH paired-pulse facilitation (PPF) magnitude (Fig. 2D). There were no significant main effects of PB-PM or LNFPIII on LTP magnitude in the ventral hippocampus (vH) post-PB-PM exposure (Fig. 3A-3C). Additionally, there were no significant main effects of PB-PM exposure or LNFPIII treatment on vH PPF magnitude (Fig. 3D).

2.3. The effect of PB-PM exposure ± LNFPIII coadministration on the expression of key inflammatory cytokines and trophic factors along the hippocampal dorsoventral axis

A significant increase in the expression of dH inflammatory cytokine IL-6 was detected in PB-PM-Vehicle animals 48 h post-exposure ($p \leq 0.05$; Table 1). Increased expression of dH IL-1β in PB-PM-Vehicle mice also approached significance ($p < 0.1$). The magnitude of increased IL-6 and IL-1β dH expression was reduced when LNFPIII was coadministered to PB-PM-exposed animals. Other key inflammatory markers in the dH such as TNFα were not significantly altered as a result of PB-PM exposure or LNFPIII treatment. Additionally, a significant increase in dH brain-derived neurotrophic factor (BDNF) expression was observed in PB-PM vehicle mice ($p \leq 0.05$), a response that was not observed in animals that were coadministered LNFPIII.

In the vH, there were no significant effects of PB-PM exposure or LNFPIII treatment on the expression of inflammatory markers IL-6, IL-1β, or TNF-α 48 h post-exposure (Table 2). Further, no significant effects of PB-PM exposure or LNFPIII treatment on vH trophic factors were detected; however, LNFPIII treatment numerically enhanced BDNF. The trend was most pronounced in the PB-PM-LNFPIII group ($p < 0.08$).

3. Discussion

Presentation of pathology related to neuroimmune dysfunction has been consistently reported in the PB-PM GWI animal model (Joshi et al., 2018, Zakirova et al., 2015), which is in line with clinical reports indicating GWI is a neuroimmune disease (Coughlin, 2017). Elimination of PB and PM occurs rapidly (Anadon et al., 1991, Aquilonius et al., 1980) and results in direct PB-PM-induced enhancement of hippocampal

pro-inflammatory expression six h (Carpenter et al., 2020) but not 48 h post-exposure in the vH as shown here, a response that yields indirect, persisting, GWI-specific neuroinflammation (O'Callaghan et al., 2016). Interestingly, we detected significantly increased dH pro-inflammatory cytokine expression (i.e., IL-6) in PB-PM-Vehicle mice, which is in line with reports of differential susceptibility to pro-inflammatory stress along the hippocampal dorsoventral axis (Gulyaeva, 2019). To the best of our knowledge, this transient enhancement in hippocampal inflammatory cytokine expression following GWI-related exposures has been described in a different GWI model in a non-sector-specific manner (Michalovicz et al., 2019, O'Callaghan et al., 2015). In the PB-PM model, we have characterized the inflammatory cytokine profile only in the vH and only six h after exposure (Carpenter et al., 2020). The 48 h post-PB-PM data from both the dH and the vH shown here addresses a knowledge gap related to the temporal progression of GWI-related neuroinflammation in this model. Additionally, acute enhancement of inflammatory cytokines in the brain (i.e., IL-6 as observed in the dH) leads to/is associated with aberrant activation of microglia and astrocytes, which, while transient, has lasting effects on glial homeostasis, bringing forth impaired hippocampal synaptic plasticity and transmission in a temporal-specific manner along the dorsoventral axis (Onufriev et al., 2018, Prieto and Cotman, 2017). While it is unknown if the PB-PM-induced elevations in IL-6 expression found here coincide with abnormal neuroglia activation, irregular microglia stimulation facilitates an immune system response that produces undesirable activation of astrocytes (Ramesh et al., 2013), enabling secretion of inflammatory cytokines that impair hippocampal synaptic transmission (Prieto and Cotman, 2017). Furthermore, enhanced expression of pro-inflammatory cytokines may modulate the secretion of critical trophic

factors involved in hippocampal synaptic transmission such as BDNF (Barrientos et al., 2004, Kang and Schuman, 1995). Increased activation of hippocampal microglia following PB-PM exposure has been described (Abdullah et al., 2016, Joshi et al., 2018). Reports using the PB-PM GWI model also observed astrocyte activation, particularly in the hippocampus (Abdullah et al., 2011, Joshi et al., 2018, Zakirova et al., 2015). Additionally, elevated central and peripheral pro-inflammatory cytokine expression were found both six h and months after PB-PM exposure (Carpenter et al., 2020, Joshi et al., 2018, Mote et al., 2020).

In the present study, we observed reduced dH and vH basal synaptic transmission 48 h post-PB-PM exposure, an effect that was quantitatively greater in the dH compared to the vH. This observation is consistent with increased dH, but not vH, pro-inflammatory cytokines observed here as well as aforementioned investigations describing a PB-PM-induced neuroinflammatory phenotype that consequently leads to detrimental microglia and astrocyte activation, which may drive impairments in hippocampal synaptic transmission. Moreover, we assessed hippocampal LTP, a well-established synaptic substrate for learning and memory (Whitlock et al., 2006), to determine if PB-PM exposure adversely impacted hippocampal synaptic plasticity. Interestingly, we did not observe PB-PM-induced impairments in dH or vH LTP magnitude. An investigation by Onufriev et al. (2018) detected rapid production of pro-inflammatory cytokines as well as time-matched impairments in dH synaptic plasticity but a slower response in the vH following acute proinflammatory stress. Those results are in line with the current findings of a more substantial PB-PM-induced effect on dH synaptic measurements shortly after exposure and not yet evident on vH synaptic responses. These sector-specific effects may be of particular

interest as a GWI-relevant chemical was recently shown to induce differential acute effects on synaptic transmission along the hippocampal dorsoventral axis (Brown et al., 2020). Further, while there is a lack of information regarding PB-PM-induced modulations in hippocampal synaptic plasticity and transmission, studies assessing the PB-PM GWI animal model have found modulations in hippocampal presynaptic protein levels. For instance, a reduction in hippocampal synaptophysin (SYP) levels, a marker for presynaptic vesicles, was reported from two-three weeks and up to five months following PB-PM exposure (Zakirova et al., 2015); however, SYP knockout mice do not exhibit changes in PPF magnitude, a measurement indicative of presynaptic-mediated alterations in synaptic plasticity (Janz et al., 1999). Moreover, SYP knockout did not impact hippocampal LTP magnitude in this study. These results are consistent with our findings in the dH and the vH, where we did not observe PB-PM-induced variations of PPF or LTP magnitude. Coupled with the acute PB-PM-mediated impairment of dH and vH synaptic transmission, the lack of abnormalities in PPF magnitude between treatment groups is consistent with an interpretation indicating a decrease in the density of synapses in the CA1 subfield. This interpretation is in line with preclinical studies that observed reduced hippocampal CA1 apical dendritic spine density (Speed et al., 2011) and hippocampal neurogenesis (Parihar et al., 2013, Shetty et al., 2020, Wang et al., 2020) in GWI animal models that included PB and PM in the exposure protocol as well as exposure to another GWI-relevant pesticide.

We previously demonstrated that LNFPIII rebalanced central and peripheral immune function in immunological disease states such as experimental autoimmune encephalomyelitis (Zhu et al., 2012) as well as GWI (Carpenter et al., 2020, Mote et al., 2020). LNFPIII induces anti-inflammatory chemokine and cytokine production via the

CD14/TLR-MAPK (ERK) axis (Tundup et al., 2015). ERK is a kinase critical for the production of trophic factors, such as BDNF (Alonso et al., 2004). ERK-1/2 phosphorylation is also essential for the expression of late-LTP (English and Sweatt, 1997), a form of LTP that is dependent upon de novo protein synthesis and trophic factor production (Bekinschtein et al., 2007). Notably, studies investigating GWI animal models found decreased cortical (Kimono et al., 2020) and hippocampal BDNF levels (Ribeiro et al., 2020) as well as reduced tropomyosin receptor kinase B density in the hippocampus (Carreras et al., 2018), a receptor fundamentally involved in facilitating the actions of BDNF (Minichiello, 2009). Those findings indicate that GWI-related chemical exposures may impact secretion of the trophic factor in addition to its signaling activity. In the present study, LNFPIII treatment recovered dH basal synaptic transmission in PB-PM treated animals, an effect that may be attributed to either LNFPIII-mediated rebalancing of anti-inflammatory cytokine production (Carpenter et al., 2020, Mote et al., 2020) or LNFPIII-mediated effects on ERK (Tundup et al., 2015). Interestingly, we detected a significant increase in dH BDNF expression in PB-PM-Vehicle animals. Hippocampal BDNF overexpression has been associated with deficits in electrophysiological responses, hippocampal-dependent learning and memory, as well as other neurological aberrations (Croll et al., 1999, Cunha et al., 2009, Papaleo et al., 2011). Within the context of GWI-relevant exposures, our finding is consistent with a report describing neurotoxic responses that coincided with increased immediate early gene and BDNF expression shortly after exposure to pyrethroids similar to the pyrethroid used in the present study, PM (Özdemir et al., 2018). Simultaneous PB and stress exposure have also been shown to enhance hippocampal BDNF expression one h later (Barbier et al., 2009). We did not observe

altered dH BDNF expression in PB-PM-LNFPIII animals, a result that may be due to LNFPIII-mediated rebalancing of ERK activity. Accordingly, we speculate that rebalancing of cytokine and ERK-dependent trophic factor expression may, in part, underlie the ameliorative effects of the immunotherapeutic on dH basal synaptic transmission in PB-PM-LNFPIII mice. The lack of a statistically significant alteration in vH trophic factor expression in PB-PM-Vehicle animals is also in line with the dH and the vH being functionally distinct. For instance, differences in trophic factor expression in the dH compared to the vH following PB-PM exposure may be related to differential basal expression of hippocampal trophic factors such as BDNF (Zhu et al., 2006). As significant alterations in trophic factor expression were detected 48 h, but not six h (Carpenter et al., 2020), following PB-PM exposure and/or LNFPIII treatment, additional investigations into temporal-specific modulations in trophic factor expression along the hippocampal dorsoventral axis in this and other GWI animal models are warranted. Further, LNFPIII only enhanced vH basal synaptic transmission in vehicle animals, a response that we speculate may be attributed to the observed trending LNFPIII effect on vH BDNF secretion or differential baseline activity of immune mediators such as microglia and astrocytes along the hippocampal dorsoventral axis (Jinno et al., 2007, Ogata and Kosaka, 2002). Regarding synaptic plasticity, we did not observe an enhancement of dH LTP magnitude in vehicle-LNFPIII-treated animals, indicating that underlying non-measurable effects of PB-PM are needed for LNFPIII to exhibit this effect.

4. Conclusion

These findings indicate that exposure to a well-established GWI animal model consisting of PB-PM exposures resulted in impairments in hippocampal synaptic plasticity

and transmission 48 h post-exposure. These synaptic aberrations differentially manifested along the hippocampal dorsoventral axis, a novel finding that may provide insight into complex cognitive deficits presented in GWI. Importantly, LNFPIII coadministration ameliorated or enhanced several synaptic and trophic factor responses in animals exposed to PB-PM, indicating the immunotherapeutic may be an efficacious treatment for short-term GWI-related synaptic aberrations. Investigations assessing the efficacy of LNFPIII in treating persisting hippocampal synaptic plasticity and transmission abnormalities presented in multiple GWI animal models are currently being conducted.

5. Methods

5.1. Materials

Animals were exposed to pyridostigmine bromide (PB; ≥ 98% purity; Sigma Aldrich, St. Louis, MO) and permethrin (PM; 29.5% cis/69.5% trans isomer; 99% purity; Chem Service Inc., West Chester, PA). Production of the LNFPIII dextran conjugate was described in Tundup et al. (2015). Unless specifically indicated, all other chemicals and reagents used in this study were acquired from Sigma Aldrich or Fisher Scientific (Hampton, NH).

5.2. Animals

Eight to nine-week-old male C57BL/6J mice (Jackson Laboratories, Bar Harbor, ME) were housed in groups of four in an environmentally controlled room (22–24 °C), were maintained on a 12 h light/dark cycle (0700–1900 lights on) and received food and water access ad libitum. Animals underwent one week of acclimation and were then handled daily for one week before the start of the study. All procedures were in accordance

with the latest National Institutes of Health guidelines and were approved in advance by the University of Georgia Institutional Animal Care and Use Committee.

5.3. GWI model

Mice (n = 23; weight: 24.4 ± 0.19 g [mean ± SEM]) were randomly divided via random number generator into GWI (PB-PM) and vehicle (DMSO) treatment groups as follows: Vehicle-Vehicle (DMSO-Dextran), Vehicle-LNFPIII (DMSO-LNFPIII), PB-PM-Vehicle (PB-PM-Dextran), and PB-PM-LNFPIII. The body weight of randomized treatment groups did not significantly differ from one another. Mice then received 10 days of concurrent PB-PM exposure and LNFPIII treatment as described in Fig. 1A and Carpenter et al. (2020). Briefly, mice received daily treatment for 10 days with a combination of PB and PM (0.7 and 200 mg/kg, respectively, intraperitoneal [i.p.]) or DMSO vehicle (i.p.), immediately followed by an injection of LNFPIII or dextran vehicle (both 35 μg/mouse, subcutaneous) diluted in sterile saline. Body weights were monitored daily during PB-PM exposure until study completion. Forty-eight h after the last exposure, dH and vH tissue were collected for qPCR analysis, and electrophysiology experiments were conducted on dH and vH tissues. Researchers were blinded to treatment groups throughout qPCR analysis, electrophysiology experiments, and subsequent data analysis.

5.4. Quantitative PCR (qPCR) analysis

qPCR was completed on dH and vH tissue for key inflammatory cytokines (IL-6, IL-1β, and TNFα) and growth factors (brain-derived neurotrophic factor, nerve growth factor, and ciliary neurotrophic factor) as described in Carpenter et al. (2020) with additional details provided in Table 1, Table 2. Briefly, total RNA from a single dH or vH brain punch (1.5 mm diameter, 500 μm thick section) was isolated by an E.Z.N.A total

RNA isolation kit (Omega Bio-Tek, Norcross, GA) according to the manufacturer's directions. RNA was quantified with a Take3 micro-volume plate and Epoch microplate spectrophotometer (BioTek, Winooski, VT). Seventy-five ng RNA/sample was used to synthesize cDNA with a Maxima first-strand cDNA synthesis kit for RT-qPCR (Thermo Scientific, Waltham, MA) and a Peltier thermal cycler (Bio-Rad, Hercules, CA; 10 min at 25 ℃, 15 min at 50 ℃, 5 min at 85 ℃). Using 1 or 2 ng of cDNA per sample, expression of various inflammatory genes and the growth factors (Table 1, Table 2) were determined by a qPCR with mouse-specific primers (RealTimePrimers, Elkins Park, PA) and Maxima SYBR Green/lowRox qPCR Master Mix (2x) (Thermo Scientific). Amplifications were performed on Mx3005 P qPCR machine (Stratagene, San Diego, CA) and treatment differences were calculated as a fold change by the ΔΔ Ct method with 18S as the house keeping gene, as described previously (Krishna et al., 2016, Lin et al., 2013).

5.5. Slice preparation and electrophysiology

Brain dissection and hippocampal slice recovery were completed as described in Brown et al. (2020). Briefly, mice were sacrificed following deep anesthetization with 2-bromo-2-chloro-1,1,1-trifluoroethane (halothane). Brains were removed and quickly submerged in oxygenated (95% O2 / 5% CO2), ice-cold dissection artificial cerebrospinal fluid (dACSF; 120 mM NaCl, 3 mM KCl, 4 mM MgCl2, 1 mM NaH2PO4, 26 mM NaHCO3, and 10 mM glucose). A mid-sagittal cut was made, and half of the brain was mounted on its caudal pole and sectioned along the horizontal plane with a vibratome to obtain 400 µm slices containing the dorsal hippocampus. The other half of the brain was mounted on its rostral pole and sectioned along the horizontal plane with a vibratome to obtain 400 µm slices containing the ventral hippocampus. The dorsal hippocampus and

ventral hippocampus were subdissected free from the rest of the slice and the CA3 subfield was removed. These slices were then quickly placed in a submersion-type chamber and perfused with oxygenated (95% O2 / 5% CO2) ACSF (120 mM NaCl, 3 mM KCl, 1.5 mM MgCl2, 1 mM NaH2PO4, 2.5 mM CaCl2, 26 mM NaHCO3, and 10 mM glucose). Slices were continuously perfused with ACSF (one mL/min) during a 45 min recovery period at room temperature followed by a 45 min recovery period at the recording temperature of 30 °C. Schaffer collateral fibers were stimulated in the stratum radiatum of the CA1 subfield via a bipolar stimulating electrode (Kopf Instruments, Tujunga, CA) whereas recording was conducted via a 1.0 MΩ tungsten microelectrode (World Precision Instruments, Sarasota, FL). A stimulus pulse was applied once every min to elicit field excitatory postsynaptic potentials (fEPSPs) at Schaffer collateral-CA1 synapses.

An input–output curve (I/O curve) was generated at the beginning of each experiment by incrementally introducing individual 15 µA stimulus pulses from 45 to 180 µA in intensity. The fEPSP slope (mV/ms) was monitored in a one ms interval immediately following the fiber volley. The stimulus intensity was modified to elicit 35% of the maximal fEPSP slope and paired-pulse fEPSPs (50 ms interpulse interval) were recorded each minute for five min after recording the I/O curve. A stimulus pulse was then applied every min for 30 min to assess the baseline fEPSP response. After establishing the baseline fEPSP response, a high-frequency stimulation (HFS) protocol (three × 100 Hz/one-sec train at 20-sec intervals) was utilized to induce long-term potentiation (LTP) and fEPSP responses were monitored for the subsequent 60 min. fEPSP responses were normalized to the average fEPSP slope value recorded during 26–30 min of baseline recording. LTP

magnitude was calculated by averaging the normalized fEPSP slope values from 56 to 60 min post-HFS.

5.6. Statistical analysis

Two-way analysis of variance (ANOVA) was utilized to assess the effects of factor A (PB-PM) and factor B (LNFPIII) on electrophysiology response variables. Pairwise comparisons were conducted by Student-Newman-Keuls post hoc test or planned pairwise comparisons (Student's t-test, as appropriate) in the case of a significant main or interaction effect. qPCR statistical analysis was conducted as described in section 5.4. Statistical analysis was completed using R version 4.0.2 (The R Foundation for Statistical Computing, Vienna, Austria) and figures were generated using GraphPad Prism 5 (San Diego, CA).

CRediT authorship contribution statement

Kyle A. Brown: Data curation, Formal analysis, Investigation, Methodology, Validation, Visualization, Writing - original draft, Writing - review & editing. Collin J. Preston: Investigation, Data curation, Formal analysis, Writing - review & editing. Jessica M. Carpenter: Investigation, Data curation, Formal analysis, Writing - review & editing. Helaina D. Ludwig: Investigation, Data curation, Formal analysis, Writing - review & editing. Thomas Norberg: Funding acquisition, Resources. Donald A. Harn: Conceptualization, Funding acquisition, Resources. Nikolay M. Filipov: Conceptualization, Funding acquisition, Investigation, Methodology, Project administration, Resources, Supervision, Validation, Writing - review & editing. John J. Wagner: Conceptualization, Funding acquisition, Methodology, Project Administration, Resources, Supervision, Validation, Writing - review & editing.

Declaration of Competing Interest

The authors declare that they have no known competing financial interests or personal relationships that could have appeared to influence the work reported in this paper.

Acknowledgments

We thank Caroline Grant for the anatomical illustration of the hippocampus in Fig. 1.

Funding & disclosures

This research was supported by the Department of Defense (CDMRP grant number W81XWH-16-1-0586) to NMF. KAB and CJP received support from the Interdisciplinary Toxicology Program at the University of Georgia.

References

Abdullah, L., Crynen, G., Reed, J., Bishop, A., Phillips, J., Ferguson, S., Mouzon, B., Mullan, M., Mathura, V., Mullan, M., 2011. Proteomic CNS profile of delayed cognitive impairment in mice exposed to Gulf War agents. Neuromolecular Med. 13, 275–288.

Abdullah, L., Evans, J.E., Joshi, U., Crynen, G., Reed, J., Mouzon, B., Baumann, S., Montague, H., Zakirova, Z., Emmerich, T., 2016. Translational potential of long-term decreases in mitochondrial lipids in a mouse model of Gulf War Illness. Toxicology 372, 22–33.

Alonso, M., Medina, J.H., Pozzo-Miller, L., 2004. ERK1/2 activation is necessary for BDNF to increase dendritic spine density in hippocampal CA1 pyramidal neurons. Learn. Mem. 11, 172–178.

Anadon, A., Martinez-Larranaga, M., Diaz, M., Bringas, P., 1991. Toxicokinetics of permethrin in the rat. Toxicol. Appl. Pharmacol. 110, 1–8.

Aquilonius, S.-M., Eckern¨as, S.-Å., Hartvig, P., Lindstr¨om, B., Osterman, P., 1980. Pharmacokinetics and oral bioavailability of pyridostigmine in man. Eur. J. Clin. Pharmacol. 18, 423–428.

Barbier, L., Diserbo, M., Lamproglou, I., Amourette, C., Peinnequin, A., Fauquette, W., 2009. Repeated stress in combination with pyridostigmine: part II: changes in cerebral gene expression. Behav. Brain Res. 197, 292–300.

Barrientos, R.M., Sprunger, D.B., Campeau, S., Watkins, L.R., Rudy, J.W., Maier, S.F., 2004. BDNF mRNA expression in rat hippocampus following contextual learning is blocked by intrahippocampal IL-1β administration. J. Neuroimmunol. 155, 119–126.

Bekinschtein, P., Cammarota, M., Igaz, L.M., Bevilaqua, L.R., Izquierdo, I., Medina, J.H., 2007. Persistence of long-term memory storage requires a late protein synthesis- and BDNF-dependent phase in the hippocampus. Neuron 53, 261–277.

Bhargava, P., Li, C., Stanya, K.J., Jacobi, D., Dai, L., Liu, S., Gangl, M.R., Harn, D.A., Lee, C.-H., 2012. Immunomodulatory glycan LNFPIII alleviates hepatosteatosis and insulin resistance through direct and indirect control of metabolic pathways. Nat. Med. 18, 1665.

Brown, K.A., Filipov, N.M., Wagner, J.J., 2020. Dorsoventral-specific effects of a sarin surrogate, diisopropylfluorophosphate, on synaptic transmission in the mouse hippocampus. J. Pharmacol. Exp. Ther. 10–23.

Carpenter, J., Gordon, H., Ludwig, H., Wagner, J., Harn, D., Norberg, T., Filipov, N., 2020. Neurochemical and neuroinflammatory perturbations in two Gulf War Illness models: Modulation by the immunotherapeutic LNFPIII. Neurotoxicology 77, 40–50.

Carreras, I., Aytan, N., Mellott, T., Choi, J.-K., Lehar, M., Crabtree, L., Leite-Morris, K., Jenkins, B.G., Blusztajn, J.K., Dedeoglu, A., 2018. Anxiety, neuroinflammation, cholinergic and GABAergic abnormalities are early markers of Gulf War illness in a mouse model of the disease. Brain Res. 1681, 34–43.

Coughlin, S.S., 2017. A neuroimmune model of Gulf War Illness. J. Environ. Health Sci. 3.

Craddock, T.J., Del Rosario, R.R., Rice, M., Zysman, J.P., Fletcher, M.A., Klimas, N.G., Broderick, G., 2015. Achieving remission in Gulf War Illness: a simulation-based approach to treatment design. PLoS One 10, e0132774.

Croll, S., Suri, C., Compton, D., Simmons, M., Yancopoulos, G., Lindsay, R., Wiegand, S., Rudge, J., Scharfman, H., 1999. Brain-derived neurotrophic factor transgenic mice exhibit passive avoidance deficits, increased seizure severity and in vitro

hyperexcitability in the hippocampus and entorhinal cortex. Neuroscience 93, 1491–1506.

Cunha, C., Angelucci, A., D'Antoni, A., Dobrossy, M.D., Dunnett, S.B., Berardi, N., Brambilla, R., 2009. Brain-derived neurotrophic factor (BDNF) overexpression in the forebrain results in learning and memory impairments. Neurobiol. Dis. 33, 358–368.

Dickey, B., Madhu, L.N., Shetty, A.K., 2020. Gulf War Illness: Mechanisms Underlying Brain Dysfunction and Promising Therapeutic Strategies. Pharmacol. Ther. 107716.

English, J.D., Sweatt, J.D., 1997. A requirement for the mitogen-activated protein kinase cascade in hippocampal long term potentiation. J. Biol. Chem. 272, 19103–19106.

Georgopoulos, A.P., James, L.M., Carpenter, A.F., Engdahl, B.E., Leuthold, A.C., Lewis, S. M., 2017. Gulf War illness (GWI) as a neuroimmune disease. Exp. Brain Res. 235, 3217–3225.

Gulyaeva, N.V., 2019. Functional neurochemistry of the ventral and dorsal hippocampus: stress, depression, dementia and remote hippocampal damage. Neurochem. Res. 44, 1306–1322.

Janz, R., Südhof, T.C., Hammer, R.E., Unni, V., Siegelbaum, S.A., Bolshakov, V.Y., 1999. Essential roles in synaptic plasticity for synaptogyrin I and synaptophysin I. Neuron 24, 687–700.

Jeffrey, M.G., Krengel, M., Kibler, J., Zundel, C., Klimas, N.G., Sullivan, K., Craddock, T. J., 2019. Neuropsychological Findings in Gulf War Illness: A Review. Front. Psychol. 10, 2088.

Jinno, S., Fleischer, F., Eckel, S., Schmidt, V., Kosaka, T., 2007. Spatial arrangement of microglia in the mouse hippocampus: a stereological study in comparison with astrocytes. Glia. 55, 1334–1347.

Joshi, U., Evans, J.E., Joseph, R., Emmerich, T., Saltiel, N., Lungmus, C., Oberlin, S., Langlois, H., Ojo, J., Mouzon, B., 2018. Oleoylethanolamide treatment reduces neurobehavioral deficits and brain pathology in a mouse model of Gulf War Illness. Sci. Rep. 8, 12921.

Kang, H., Schuman, E.M., 1995. Long-lasting neurotrophin-induced enhancement of synaptic transmission in the adult hippocampus. Science 267, 1658–1662.

Kimono, D., Bose, D., Seth, R.K., Mondal, A., Saha, P., Janulewicz, P., Sullivan, K., Lasley, S., Horner, R., Klimas, N., 2020. Host Akkermansia muciniphila Abundance Correlates With Gulf War Illness Symptom Persistence via NLRP3-Mediated Neuroinflammation and Decreased Brain-Derived Neurotrophic Factor. Neurosci. Insights 15, 2633105520942480.

Krishna, S., Lin, Z., Claire, B., Wagner, J.J., Harn, D.H., Pepples, L.M., Djani, D.M., Weber, M.T., Srivastava, L., Filipov, N.M., 2016. Time-dependent behavioral, neurochemical, and metabolic dysregulation in female C57BL/6 mice caused by chronic high-fat diet intake. Physiol. Behav. 157, 196–208.

Lin, Z., Dodd, C.A., Filipov, N.M., 2013. Short-term atrazine exposure causes behavioral deficits and disrupts monoaminergic systems in male C57BL/6 mice. Neurotoxicol. Teratol. 39, 26–35.

Michalovicz, L.T., Locker, A.R., Kelly, K.A., Miller, J.V., Barnes, Z., Fletcher, M.A., Miller, D.B., Klimas, N.G., Morris, M., Lasley, S.M., 2019. Corticosterone and pyridostigmine/DEET exposure attenuate peripheral cytokine expression: Supporting a dominant role for neuroinflammation in a mouse model of Gulf War Illness. Neurotoxicology. 70, 26–32.

Michalovicz, L.T., Kelly, K.A., Sullivan, K., O'Callaghan, J.P., 2020. Acetylcholinesterase inhibitor exposures as an initiating factor in the development of Gulf War Illness, a chronic neuroimmune disorder in deployed veterans. Neuropharmacology 108073.

Minichiello, L., 2009. TrkB signalling pathways in LTP and learning. Nat. Rev. Neurosci. 10, 850.

Mote, R.S., Carpenter, J.M., Dockman, R.L., Steinberger, A.J., Suen, G., Norberg, T., Harn, D.A., Wagner, J.J., Filipov, N.M., 2020. Assessing the Beneficial Effects of the Immunomodulatory Glycan LNFPIII on Gut Microbiota and Health in a Mouse Model of Gulf War Illness. Int. J. Environ. Res. Public Health 17, 7081.

Nugent, S.M., Freeman, M., Ayers, C.K., Winchell, K.A., Press, A.M., O'Neil, M.E., Paynter, R., Kansagara, D., 2020. A Systematic Review of Therapeutic Interventions and Management Strategies for Gulf War Illness. Mil Med. O'Callaghan, J.P., Kelly, K.A., Locker, A.R., Miller, D.B., Lasley, S.M., 2015.

Corticosterone primes the neuroinflammatory response to DFP in mice: potential animal model of Gulf War Illness. J. Neurochem. 133, 708–721.

O'Callaghan, J.P., Michalovicz, L.T., Kelly, K.A., 2016. Supporting a neuroimmune basis of Gulf war illness. EBioMed. 13, 5–6.

Ogata, K., Kosaka, T., 2002. Structural and quantitative analysis of astrocytes in the mouse hippocampus. Neuroscience 113, 221–233.

Onufriev, M., Uzakov, S.S., Freiman, S., Stepanichev, M.Y., Moiseeva, Y.V., Lazareva, N., Markevich, V., Gulyaeva, N., 2018. The Dorsal and Ventral Hippocampus Have Different Reactivities to Proinflammatory Stress: Corticosterone Levels, Cytokine Expression, and Synaptic Plasticity. Neurosci. Behav. Physiol. 48, 1024–1031.

Özdemir, S., Altun, S., Özkaraca, M., Ghosi, A., Toraman, E., Arslan, H., 2018. Cypermethrin, chlorpyrifos, deltamethrin, and imidacloprid exposure up-regulates the mRNA and protein levels of bdnf and c-fos in the brain of adult zebrafish (Danio rerio). Chemosphere 203, 318–326.

Papaleo, F., Silverman, J.L., Aney, J., Tian, Q., Barkan, C.L., Chadman, K.K., Crawley, J. N., 2011. Working memory deficits, increased anxiety-like traits, and seizure susceptibility in BDNF overexpressing mice. Learn. Mem. 18, 534–544.

Papatheodoropoulos, C., 2018. Electrophysiological evidence for long-axis intrinsic diversification of the hippocampus. Front Biosci (Landmark Ed). 23, 109–145.

Parihar, V.K., Hattiangady, B., Shuai, B., Shetty, A.K., 2013. Mood and memory deficits in a model of Gulf War illness are linked with reduced neurogenesis, partial neuron loss, and mild inflammation in the hippocampus. Neuropsychopharmacology 38, 2348.

Prieto, G.A., Cotman, C.W., 2017. Cytokines and cytokine networks target neurons to modulate long-term potentiation. Cytokine Growth Factor Rev. 34, 27–33.

Ramesh, G., MacLean, A.G., Philipp, M.T., 2013. Cytokines and chemokines at the crossroads of neuroinflammation, neurodegeneration, and neuropathic pain. Mediat. Inflamm. 2013.

Ribeiro, A.C., Zhu, J., Kronfol, M.M., Jahr, F.M., Younis, R.M., Hawkins, E., McClay, J.L., Deshpande, L.S., 2020. Molecular mechanisms for the antidepressant-like effects of a low-dose ketamine treatment in a DFP-based rat model for Gulf War Illness. Neurotoxicology.

Shetty, A.K., Attaluri, S., Kodali, M., Shuai, B., Shetty, G.A., Upadhya, D., Hattiangady, B., Madhu, L.N., Upadhya, R., Bates, A., 2020. Monosodium luminol reinstates redox homeostasis, improves cognition, mood and neurogenesis, and alleviates neuro-and systemic inflammation in a model of Gulf War Illness. Redox Biol. 28, 101389.

Speed, H.E., Blaiss, C.A., Kim, A., Haws, M.E., Melvin, N.R., Jennings, M., Eisch, A.J., Powell, C.M., 2011. Delayed reduction of hippocampal synaptic transmission and spines following exposure to repeated subclinical doses of organophosphorus pesticide in adult mice. Toxicol. Sci. 125, 196–208.

Trageser, K.J., Sebastian-Valverde, M., Naughton, S.X., Pasinetti, G.M., 2020. The Innate Immune System and Inflammatory Priming: Potential Mechanistic Factors in Mood Disorders and Gulf War Illness. Front. Psychiatry 11.

Tundup, S., Srivastava, L., Norberg, T., Watford, W., Harn, D., 2015. A neoglycoconjugate containing the human milk sugar LNFPIII drives anti-inflammatory activation of antigen presenting cells in a CD14 dependent pathway. PLoS One 10, e0137495.

Wang, X., Xu, Z., Zhao, F., Lin, K.J., Foster, J.B., Xiao, T., Kung, N., Askwith, C.C., Bruno, J.P., Valentini, V., 2020. Restoring tripartite glutamatergic synapses: A potential therapy for mood and cognitive deficits in Gulf War illness. Neurobiol. Stress 100240.

White, R.F., Steele, L., O'Callaghan, J.P., Sullivan, K., Binns, J.H., Golomb, B.A., Bloom, F.E., Bunker, J.A., Crawford, F., Graves, J.C., 2016. Recent research on Gulf War illness and other health problems in veterans of the 1991 Gulf War: Effects of toxicant exposures during deployment. Cortex. 74, 449–475c.

Whitlock, J.R., Heynen, A.J., Shuler, M.G., Bear, M.F., 2006. Learning induces long-term potentiation in the hippocampus. Science 313, 1093–1097.

Zakirova, Z., Tweed, M., Crynen, G., Reed, J., Abdullah, L., Nissanka, N., Mullan, M., Mullan, M.J., Mathura, V., Crawford, F., 2015. Gulf War agent exposure causes impairment of long-term memory formation and neuropathological changes in a mouse model of Gulf War Illness. PLoS ONE 10, e0119579.

Zhu, B., Trikudanathan, S., Zozulya, A.L., Sandoval-Garcia, C., Kennedy, J.K., Atochina, O., Norberg, T., Castagner, B., Seeberger, P., Fabry, Z., 2012. Immune modulation by Lacto-N-fucopentaose III in experimental autoimmune encephalomyelitis. Clin. Immunol. 142, 351–361.

Zhu, S.-W., Yee, B.K., Nyffeler, M., Winblad, B., Feldon, J., Mohammed, A.H., 2006. Influence of differential housing on emotional behaviour and neurotrophin levels in mice. Behav. Brain Res. 169, 10–20.

Zundel, C.G., Heeren, T., Grasso, C.M., Spiro III, A., Proctor, S.P., Sullivan, K., Krengel, M., 2020. Changes in Health Status in the Ft. Devens Gulf War Veterans Cohort: 1997–2017. Neurosci. Insights 15, 1–7.

Figures

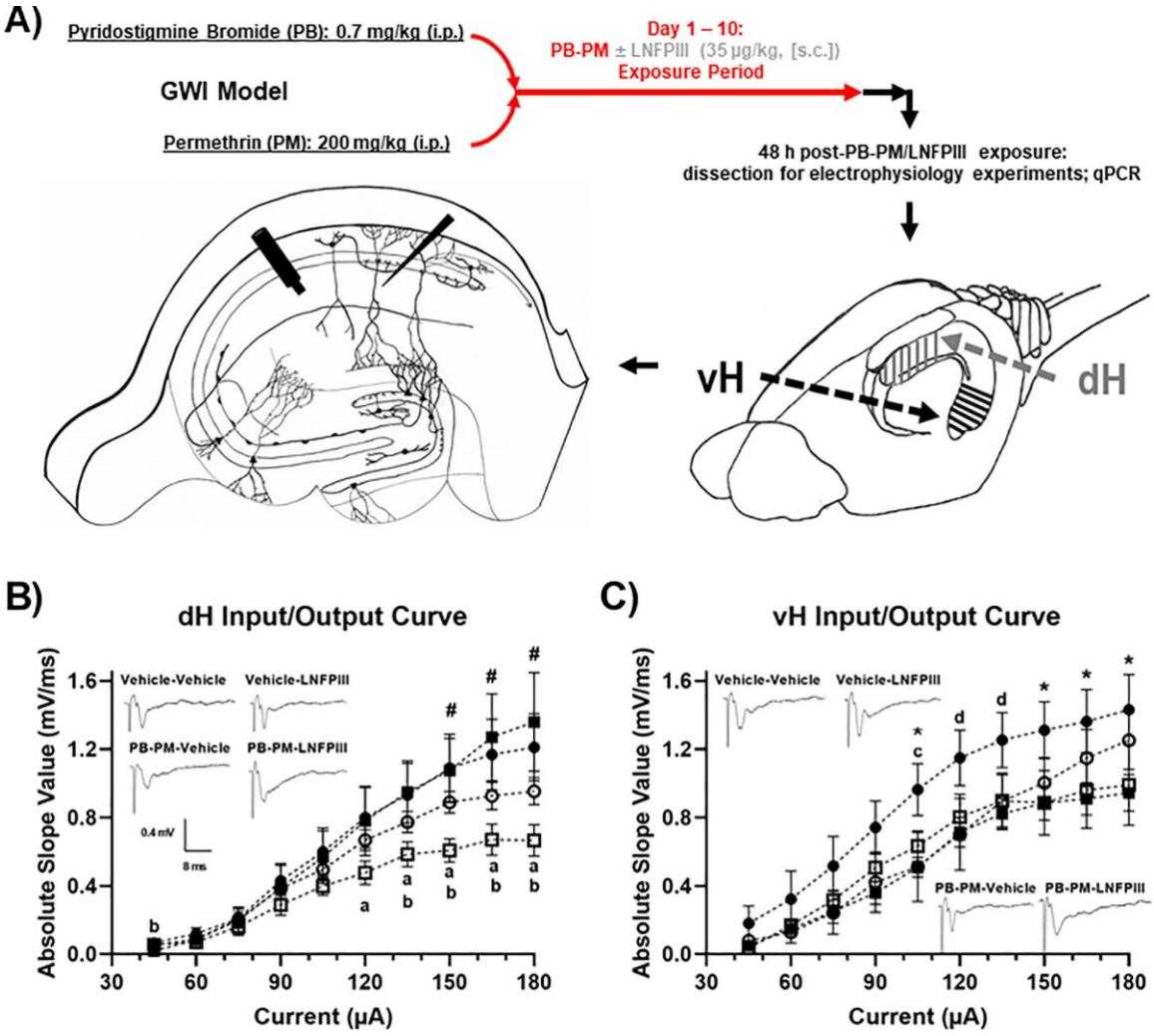
A)
Pyridostigmine Bromide (PB): 0.7 mg/kg (i.p.)
GWI Model
Permethrin (PM): 200 mg/kg (i.p.)
Day 1 – 10:
PB-PM ± LNFPIII (35 µg/kg, [s.c.])
Exposure Period
48 h post-PB-PM/LNFPIII exposure:
dissection for electrophysiology experiments; qPCR
vH
dH
B)
dH Input/Output Curve
Absolute Slope Value (mV/ms)
Current (µA)
Vehicle-Vehicle
Vehicle-LNFPIII
PB-PM-Vehicle
PB-PM-LNFPIII
0.4 mV
8 ms
C)
vH Input/Output Curve
Absolute Slope Value (mV/ms)
Current (µA)
Vehicle-Vehicle
Vehicle-LNFPIII
PB-PM-Vehicle
PB-PM-LNFPIII

Fig. B.1. Experimental design of pyridostigmine bromide-permethrin (PB-PM) exposure ± LNFPIII coadministration and their effect on dorsal (dH) and ventral (vH) hippocampal synaptic transmission 48 h post-exposure. A. Animals were randomly assigned to GWI (pyridostigmine bromide-permethrin; PB-PM) and vehicle (DMSO) treatment groups. Mice then received 10 days of daily exposure with a combination of PB and PM (0.7 and 200 mg/kg, respectively; i.p.) or DMSO (i.p.). Animals were also randomly selected to receive 10 days of concurrent daily treatment with either lacto-N-fucopentaose-III (LNFPIII) or dextran vehicle (both 35 µg/mouse; S.C., diluted in sterile saline). Electrophysiology and qPCR experiments were conducted 48 h following the last exposure. The cylinder found in the hippocampal slice represents a stimulating electrode along the Schaffer collateral-CA1 pathway found in the stratum radiatum whereas the triangle represents a recording electrode in the CA1 stratum radiatum. B. Stimulus-response relationship of the average fEPSP slopes elicited by increasing stimulus intensities from vehicle-vehicle (○; n = 9(3)), vehicle-LNFPIII (●; n = 9(4)), PB-PM-vehicle (□; n = 7(4)), and PB-PM-LNFPIII (■; n = 6(3)) treatment groups recorded from the dH 48 h after PB-PM exposure. C. Stimulus-response relationship of the average fEPSP slopes elicited by increasing stimulus intensities from vehicle-vehicle (○; n = 5(4)), vehicle-LNFPIII (●; n = 7(4)), PB-PM-vehicle (□; n = 8(4)), and PB-PM-LNFPIII (■; n = 12(3)) treatment groups recorded from the vH 48 h after PB-PM exposure. Insets show representative traces composed of average sweeps from 135 µA stimulation intensity. * denotes main effect of PB-PM ($p < 0.05$) whereas # denotes main effect of LNFPIII ($p < 0.05$). a compares vehicle-vehicle and PB-PM-vehicle; b compares PB-PM-vehicle and PB-PM-LNFPIII; c and d compare vehicle-vehicle and vehicle-LNFPIII groups. a, b, c indicates $p < 0.05$. d indicates $p < 0.1$. Data are expressed as mean ± SEM.

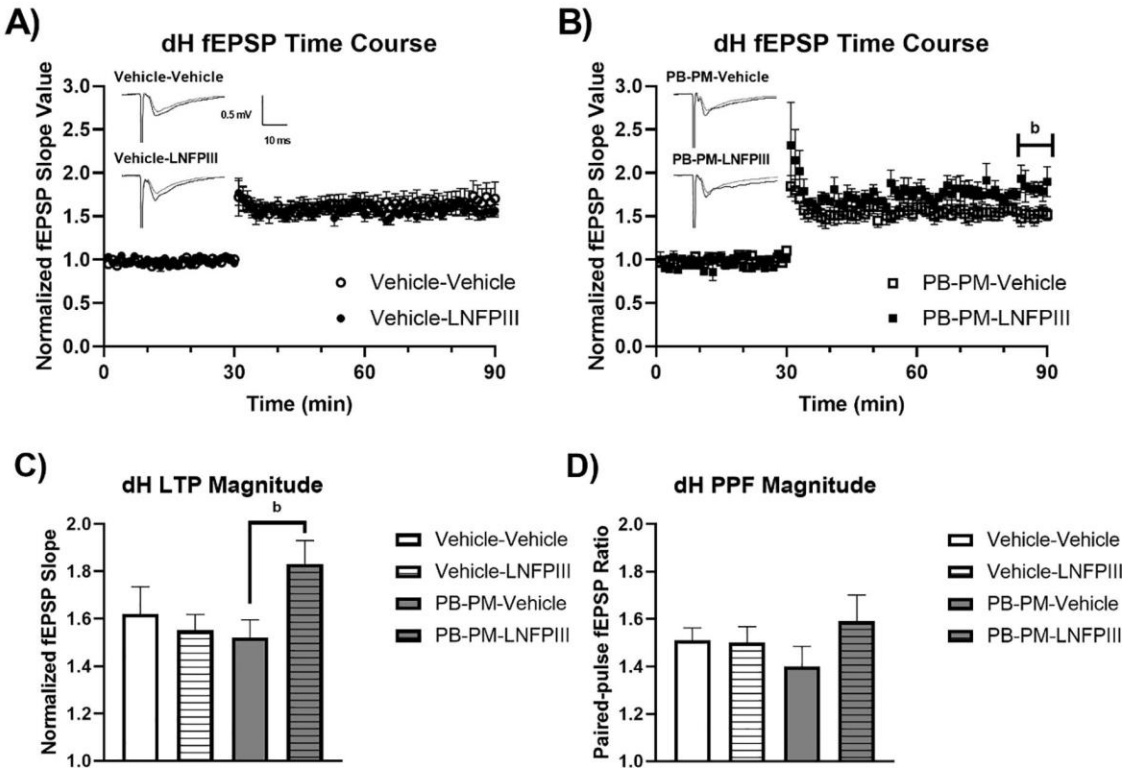
A)
dH fEPSP Time Course
Vehicle-Vehicle
0.5 mV
10 ms
Vehicle-LNFPIII
Normalized fEPSP Slope Value
Time (min)
Vehicle-Vehicle
Vehicle-LNFPIII
B)
dH fEPSP Time Course
PB-PM-Vehicle
PB-PM-LNFPIII
b
Normalized fEPSP Slope Value
Time (min)
PB-PM-Vehicle
PB-PM-LNFPIII
C)
dH LTP Magnitude
b
Normalized fEPSP Slope
Vehicle-Vehicle
Vehicle-LNFPIII
PB-PM-Vehicle
PB-PM-LNFPIII
D)
dH PPF Magnitude
Paired-pulse fEPSP Ratio
Vehicle-Vehicle
Vehicle-LNFPIII
PB-PM-Vehicle
PB-PM-LNFPIII

Fig. B.2. The effect of pyridostigmine bromide-permethrin (PB-PM) exposure ± LNFPIII coadministration on measurements of dorsal hippocampal (dH) synaptic plasticity 48 h post-PB-PM exposure. A and B. Summary plots of normalized fEPSP values recorded from the dH of vehicle-treated (A) or PB-PM exposed (B) animals 48 h post-PB-PM exposure. (A) compares vehicle-vehicle (○) and vehicle-LNFPIII (●) treated mice whereas (B) compares PB-PM-vehicle (□) and PB-PM-LNFPIII (■) treated mice. Insets show summary traces composed of average sweeps from 5 min pre-tetanus (grey) and 56–60 min post-tetanus (black). C. Summary quantification of dH LTP magnitude recorded 48 h after PB-PM exposure from vehicle-vehicle (1.62 ± 0.11, n = 9(3)), vehicle-LNFPIII (1.55 ± 0.07, n = 9(4)), PB-PM-vehicle (1.52 ± 0.08, n = 7(4)), and PB-PM-LNFPIII (1.83 ± 0.10, n = 6(3)) treated animals. D. The paired-pulse ratio for vehicle-vehicle (1.51 ± 0.05), vehicle-LNFPIII (1.50 ± 0.07), PB-PM-vehicle (1.40 ± 0.08), and PB-PM-LNFPIII (1.59 ± 0.11) treatment groups recorded from the dH 48 h after PB-PM exposure (interpulse interval = 50 ms). b compares PB-PM-vehicle and PB-PM-LNFPIII ($p < 0.05$ via preplanned Student's t-test). Data are expressed as mean ± SEM.

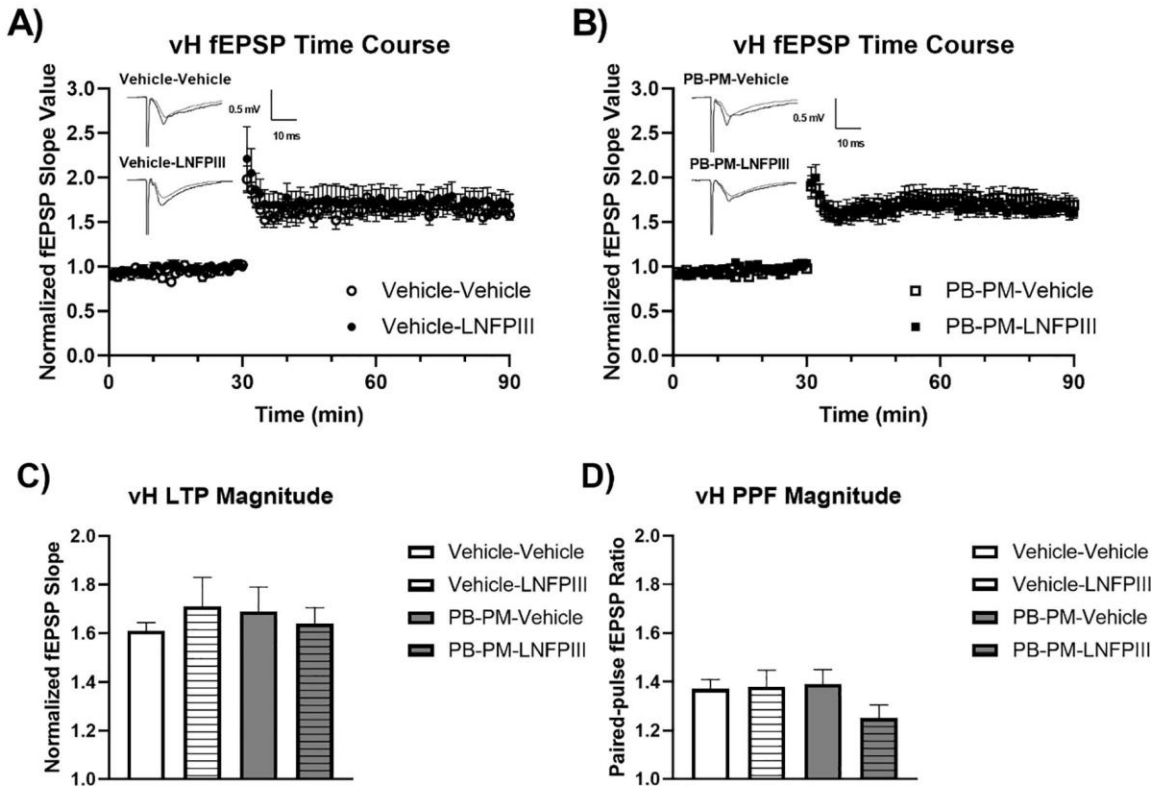
A)
vH fEPSP Time Course
Vehicle-Vehicle
Vehicle-LNFPIII
0.5 mV
10 ms
Normalized fEPSP Slope Value
Time (min)
Vehicle-Vehicle
Vehicle-LNFPIII
B)
vH fEPSP Time Course
PB-PM-Vehicle
PB-PM-LNFPIII
0.5 mV
10 ms
Normalized fEPSP Slope Value
Time (min)
PB-PM-Vehicle
PB-PM-LNFPIII
C)
vH LTP Magnitude
Normalized fEPSP Slope
Vehicle-Vehicle
Vehicle-LNFPIII
PB-PM-Vehicle
PB-PM-LNFPIII
D)
vH PPF Magnitude
Paired-pulse fEPSP Ratio
Vehicle-Vehicle
Vehicle-LNFPIII
PB-PM-Vehicle
PB-PM-LNFPIII

Fig. B.3. The effect of PB-PM exposure ± LNFPIII coadministration on measurements of ventral hippocampal (vH) synaptic plasticity 48 h post-PB-PM exposure. A and B. Summary plots of normalized fEPSP values recorded from the vH of vehicle-treated (A) or PB-PM exposed (B) animals 48 h post-PB-PM exposure. (A) compares vehicle-vehicle (○) and vehicle-LNFPIII (●) treated mice whereas (B) compares PB-PM-vehicle (□) and PB-PM-LNFPIII (■) treated mice. Insets show traces composed of average sweeps from 5 min pre-tetanus (grey) and 56–60 min post-tetanus (black). C. Summary quantification of vH LTP magnitude recorded 48 h after PB-PM exposure from vehicle-vehicle (1.61 ± 0.04, n = 5(4)), vehicle-LNFPIII (1.71 ± 0.12, n = 7(4)), PB-PM-vehicle (1.70 ± 0.10, n = 8(4)), and PB-PM-LNFPIII (1.64 ± 0.06, n = 12(3)) treated animals. D. The paired-pulse ratio for vehicle-vehicle (1.37 ± 0.04), vehicle-LNFPIII (1.38 ± 0.07), PB-PM-vehicle (1.39 ± 0.06), and PB-PM-LNFPIII (1.25 ± 0.06) treatment groups recorded from the vH 48 h after PB-PM exposure (interpulse interval = 50 ms). Data are expressed as mean ± SEM.

Tables

Gene	Treatment	p-value	Treatment	p-value	Treatment	p-value
	Vehicle-LNFPIII		PB-PM-Vehicle		PB-PM-LNFPIII	
IL-6	1.46 ± 0.255	0.258	**2.81 ± 0.491**	**0.002**	**2.23 ± 0.390**	**0.040**
IL-1β	0.95 ± 0.140	0.911	**2.15 ± 0.317**	**0.097**	**2.01 ± 0.296**	**0.063**
TNFα	0.98 ± 0.114	0.904	1.48 ± 0.174	0.117	1.23 ± 0.144	0.468
BDNF	1.36 ± 0.148	0.246	**2.26 ± 0.246**	**0.006**	1.33 ± 0.145	0.214
NGF	0.64 ± 0.174	0.195	0.88 ± 0.238	0.720	0.65 ± 0.175	0.304
CNTF	1.06 ± 0.173	0.777	0.88 ± 0.144	0.610	1.44 ± 0.234	0.138

Table B.1. The effect of PB-PM exposure ± LNFPIII coadministration (10 d) on the expression of key inflammatory cytokines and growth factors in the dorsal hippocampus (dH) measured by qPCR 48 h post-PB-PM exposure. dH samples from a separate cohort of mice (n = 5, 6, 6, 4, for the, respectively, Vehicle-Vehicle, Vehicle-LNFPIII, PB-PM-Vehicle, PB-PM-LNFPIII groups) treated identically to the cohort used for electrophysiology were used for RNA isolation and subsequent qPCR analyses. Data were analyzed by the $2^{-\Delta\Delta Ct}$ method with 18S as the housekeeping gene and are expressed as a mean fold change from the Vehicle-Vehicle control ± SEM. P-values reflect the comparison for each respective group compared to the Vehicle-Vehicle control. Gene abbreviations: IL-6, Interleukin 6; IL-1β, Interleukin 1 beta; TNFα, Tumor necrosis factor alpha; BDNF, Brain-derived neurotrophic factor; NGF, Nerve growth factor; CNTF, Ciliary neurotrophic factor.

Gene	Treatment	p-value	Treatment	p-value	Treatment	p-value
	Vehicle-LNFPIII		**PB-PM-Vehicle**		**PB-PM-LNFPIII**	
IL-6	0.93 ± 0.089	0.886	0.87 ± 0.083	0.624	0.89 ± 0.085	0.779
IL-1β	1.05 ± 0.402	0.941	0.89 ± 0.343	0.874	0.94 ± 0.362	0.94
TNFα	0.62 ± 0.209	0.249	0.72 ± 0.241	0.421	0.77 ± 0.259	0.494
BDNF	1.66 ± 0.415	0.227	1.37 ± 0.344	0.416	**2.50 ± 0.625**	**0.076**
NGF	0.95 ± 0.126	0.855	0.97 ± 0.129	0.902	1.14 ± 0.152	0.687
CNTF	0.80 ± 0.092	0.379	1.01 ± 0.117	0.963	1.16 ± 0.134	0.716

Table B.2. The effect of PB-PM exposure ± LNFPIII coadministration (10 d) on the expression of key inflammatory cytokines and growth factors in the ventral hippocampus (vH) measured by qPCR 48 h post-PB-PM exposure. vH samples from a separate cohort of mice (n = 5, 6, 6, 4, for the, respectively, Vehicle-Vehicle, Vehicle-LNFPIII, PB-PM-Vehicle, PB-PM-LNFPIII groups) treated identically to the cohort used for electrophysiology were used for RNA isolation and subsequent qPCR analyses. Data were analyzed by the $2^{-\Delta\Delta Ct}$ method with 18S as the housekeeping gene and are expressed as a mean fold change from the Vehicle-Vehicle control ± SEM. P-values reflect the comparison for each respective group compared to the Vehicle-Vehicle control. Gene abbreviations: IL-6, Interleukin 6; IL-1β, Interleukin 1 beta; TNFα, Tumor necrosis factor alpha; BDNF, Brain-derived neurotrophic factor; NGF, Nerve growth factor; CNTF, Ciliary neurotrophic factor.